2 THE CP-VIOLATING TWO-HIGGS DOUBLET MODEL

2.1 Theory review

Howard E. Haber and Maria Krawczyk

The Standard Model (SM) of electroweak physics is an $\mathrm{SU(2)_L}\times\mathrm{U(1)}$ gauge theory coupled to quarks, leptons and one complex hypercharge-one, $\mathrm{SU(2)_L}$ doublet of scalar fields. Due to the form of the scalar potential, one component of the complex scalar field acquires a vacuum expectation value, and the $\mathrm{SU(2)_L}\times\mathrm{U(1)}$ electroweak symmetry is spontaneously broken down to the $\mathrm{U(1)_{EM}}$ gauge symmetry of electromagnetism. Hermiticity requires that the parameters of the SM scalar potential are real. Consequently, the resulting bosonic sector of the electroweak theory is CP-conserving.

The SM, with its minimal Higgs structure, provides an extremely successful description of observed electroweak phenomena. Nevertheless, there are a number of motivations to extend the Higgs sector of this model by adding a second complex doublet of scalar fields [1–10]. Perhaps the best motivated of these extended models is the minimal supersymmetric extension of the Standard Model (MSSM) [11–13], which requires a second Higgs doublet (and its supersymmetric fermionic partners) in order to preserve the cancellation of gauge anomalies. The Higgs sector of the MSSM is a two-Higgs-doublet model (2HDM), which contains two chiral Higgs supermultiplets that are distinguished by the sign of their hypercharge. The theoretical structure of the MSSM Higgs sector is constrained by the supersymmetry, leading to numerous relations among Higgs masses and couplings. In particular, as in the case of the SM, the tree-level MSSM Higgs sector is CP-conserving. However, the supersymmetric relations among Higgs parameters are modified by loop-corrections due to the effects of supersymmetry-breaking that enter via the loops. Thus, the Higgs-sector of the (radiatively-corrected) MSSM can be described by an effective field theory consisting of the most general CP-violating two-Higgs-doublet model.

The 2HDM Lagrangian contains eight real scalar fields. After electroweak symmetry breaking, three Goldstone bosons ($G^\pm$ and G^0) are removed from the spectrum and provide the longitudinal modes of the massive $W^\pm$ and Z. Five physical Higgs particles remain: a charged Higgs pair ($H^\pm$) and three neutral Higgs bosons. If experimental data reveals the existence of a Higgs sector beyond that of the SM, it will be crucial to test whether the observed scalar spectrum is consistent with a 2HDM interpretation. In order to be completely general within this framework, one should allow for the most general CP-violating 2HDM when confronting the data. Any observed relations among the general 2HDM parameters would surely contribute to the search for a deeper theoretical understanding of the origin of electroweak symmetry breaking.

2.1.1 The general Two-Higgs-Doublet Model (2HDM)

The 2HDM is governed by the choice of the Higgs potential and the Yukawa couplings of the two scalar-doublets to the three generations of quarks and leptons. Let Φ_1 and Φ_2 denote two complex hypercharge-one, $\mathrm{SU(2)}_L$ doublet scalar fields. The most general gauge-invariant renormalizable Higgs scalar potential is given by

$$\begin{aligned}\mathcal{V} \;=\;& m_{11}^2\Phi_1^\dagger\Phi_1 + m_{22}^2\Phi_2^\dagger\Phi_2 - [m_{12}^2\Phi_1^\dagger\Phi_2 + \mathrm{h.c.}] \\ &+\tfrac{1}{2}\lambda_1(\Phi_1^\dagger\Phi_1)^2 + \tfrac{1}{2}\lambda_2(\Phi_2^\dagger\Phi_2)^2 + \lambda_3(\Phi_1^\dagger\Phi_1)(\Phi_2^\dagger\Phi_2) + \lambda_4(\Phi_1^\dagger\Phi_2)(\Phi_2^\dagger\Phi_1) \\ &+\left\{\tfrac{1}{2}\lambda_5(\Phi_1^\dagger\Phi_2)^2 + \left[\lambda_6(\Phi_1^\dagger\Phi_1) + \lambda_7(\Phi_2^\dagger\Phi_2)\right]\Phi_1^\dagger\Phi_2 + \mathrm{h.c.}\right\}, \end{aligned} \tag{2.1}$$

where m_{11}^2, m_{22}^2, and $\lambda_1,\cdots,\lambda_4$ are real parameters. In general, m_{12}^2, λ_5, λ_6 and λ_7 are complex.

2.1.1.1 Covariant notation with respect to scalar field redefinitions

In writing Eq. (2.1), we have implicitly chosen a basis in the two-dimensional "flavor" space of scalar fields. To allow for other basis choices, it will be convenient to rewrite Eq. (2.1) in a covariant form with respect to global U(2) transformations, $\Phi_a \to U_{a\bar{b}}\Phi_b$ (and $\Phi_{\bar{a}}^\dagger \to \Phi_{\bar{b}}^\dagger U_{b\bar{a}}^\dagger$), where the 2×2 unitary matrix U satisfies $U_{b\bar{a}}^\dagger U_{a\bar{c}} = \delta_{b\bar{c}}$. In our index conventions, replacing an unbarred index with a barred index is equivalent to complex conjugation (for further details see section 2.3). Thus, Eq. (2.1) can be expressed in U(2)-covariant form as [10, 14]:

$$\mathcal{V} = Y_{a\bar{b}}\Phi_{\bar{a}}^\dagger\Phi_b + \tfrac{1}{2}Z_{a\bar{b}c\bar{d}}(\Phi_{\bar{a}}^\dagger\Phi_b)(\Phi_{\bar{c}}^\dagger\Phi_d)\,, \tag{2.2}$$

where the indices a, $\bar{b}$, c and $\bar{d}$ run over the two-dimensional Higgs "flavor" space and $Z_{a\bar{b}c\bar{d}} = Z_{c\bar{d}a\bar{b}}$. Hermiticity of $\mathcal{V}$ implies that $Y_{a\bar{b}} = (Y_{b\bar{a}})^*$ and $Z_{a\bar{b}c\bar{d}} = (Z_{b\bar{a}d\bar{c}})^*$. Explicitly, the coefficients of the quadratic terms are

$$\begin{aligned} Y_{11} &= m_{11}^2\,, & Y_{12} &= -m_{12}^2\,,\\ Y_{21} &= -(m_{12}^2)^*\,, & Y_{22} &= m_{22}^2\,, \end{aligned} \tag{2.3}$$

and the coefficients of the quartic terms are

$$\begin{aligned} Z_{1111} &= \lambda_1\,, & Z_{2222} &= \lambda_2\,,\\ Z_{1122} &= Z_{2211} = \lambda_3\,, & Z_{1221} &= Z_{2112} = \lambda_4\,,\\ Z_{1212} &= \lambda_5\,, & Z_{2121} &= \lambda_5^*\,,\\ Z_{1112} &= Z_{1211} = \lambda_6\,, & Z_{1121} &= Z_{2111} = \lambda_6^*\,,\\ Z_{2212} &= Z_{1222} = \lambda_7\,, & Z_{2221} &= Z_{2122} = \lambda_7^*\,. \end{aligned} \tag{2.4}$$

Under the global U(2) transformation, the tensors Y and Z transform covariantly: $Y_{a\bar{b}} \to U_{a\bar{c}}Y_{c\bar{d}}U_{d\bar{b}}^\dagger$ and $Z_{a\bar{b}c\bar{d}} \to U_{a\bar{e}}U_{f\bar{b}}^\dagger U_{c\bar{g}}U_{h\bar{d}}^\dagger Z_{e\bar{f}g\bar{h}}$. Indices can only be summed over using the U(2)-invariant tensor $\delta_{a\bar{b}}$.

The advantage of introducing the U(2)-covariant notation is that one can immediately identify U(2)-invariant quantities as *basis-independent*; such quantities do not depend on the original choice of the Φ_1–Φ_2 basis. In particular, any physical observable must be independent of the basis choice and hence can be identified as some U(2)-invariant quantity. For example, the well-known $\tan\beta$ parameter of the general 2HDM is *not* a physical quantity [14–16].

2.1.1.2 Counting the degrees of freedom

The 2HDM scalar potential depends on six real parameters and four complex parameters, for a total of fourteen degrees of freedom. However, these parameters depend on the choice of the Φ_1–Φ_2 basis. In order to determine the number of physical degrees of freedom, one must take into account the possibility that unphysical degrees of freedom can be removed by redefining the scalar fields via the global U(2) "flavor" transformations. However, note that the global U(2) group can be decomposed as U(2) $\cong$ SU(2)$\times$U(1), where the global hypercharge U(1) transformation has *no* effect on the scalar potential parameters. In contrast, the scalar potential parameters will be modified by a general SU(2)-"flavor" transformation. Since an SU(2) transformation is specified by three parameters, three degrees of freedom can be removed by a redefinition of the scalar fields. Thus, the scalar potential provides eleven physical degrees of freedom that govern the properties of the 2HDM scalar sector [14, 15, 17].

2.1.1.3 Discrete symmetries and the 2HDM potential

The general 2HDM is not phenomenologically viable over most of its parameter space. In particular, if we allow for the most general Higgs-fermion Yukawa couplings, the model exhibits tree-level Higgs-mediated flavor-changing neutral currents (FCNCs), which may contradict the experimental bounds on

FCNCs. This can be ameliorated by either avoiding the untenable regions of parameter space or by introducing additional structure into the model. For example, in the Higgs sector of the MSSM, tree-level Higgs-mediated FCNCs are absent due to the supersymmetric structure of the Higgs-fermion Yukawa couplings. Tree-level Higgs-mediated FCNCs can also be eliminated by invoking appropriate discrete symmetries [18]. Here, we focus on discrete symmetries imposed on the scalar fields. Consider a discrete Z_2 symmetry realized for some choice of basis: $\Phi_1 \to \Phi_1$, $\Phi_2 \to -\Phi_2$. This discrete symmetry implies that $m_{12}^2 = \lambda_6 = \lambda_7 = 0$. A basis-independent characterization of this discrete symmetry has been given in [14, 19]. In practice, the discrete symmetry must also be extended to the fermion sector. By specifying the transformation properties of the fermions with respect to the discrete symmetry, one can constrain the form of the Higgs-fermion Yukawa interactions. In fact, removing the possibility of dangerous FCNC effects can also be achieved if the symmetry of the Z_2 discrete transformation of the Higgs potential is *softly* broken; *i.e.*, there exists a basis in which $\lambda_6 = \lambda_7 = 0$ but $m_{12}^2 \neq 0$ [15, 17]. A basis-independent characterization of the softly-broken discrete symmetry can also be given [14]. Finally, hard-breaking of the discrete Z_2 symmetry corresponds to the case in which no basis exists in which $\lambda_6 = \lambda_7 = 0$. Additional implications of the broken Z_2 symmetry can be found in section 2.4.

2.1.1.4 The scalar field vacuum expectation values

Electroweak symmetry breaking arises if the minimum of the scalar potential occurs for nonzero expectation values of the scalar fields. The condition for extrema of the scalar potential

$$\left.\frac{\partial \mathcal{V}}{\partial \Phi_1}\right|_{\substack{\Phi_1=\langle\Phi_1\rangle,\\ \Phi_2=\langle\Phi_2\rangle}} = 0, \qquad \left.\frac{\partial \mathcal{V}}{\partial \Phi_2}\right|_{\substack{\Phi_1=\langle\Phi_1\rangle,\\ \Phi_2=\langle\Phi_2\rangle}} = 0 \tag{2.5}$$

yields the vacuum expectation values (vevs) $\langle\Phi_{1,2}\rangle$. The scalar fields will develop non-zero vevs if the mass matrix constructed from the quadratic squared-mass parameters of the Higgs potential (m_{ij}^2) has at least one negative eigenvalue. By employing an appropriate weak isospin and $\mathrm{U}(1)_Y$ transformation, it is always possible to write the scalar field vevs in the following form

$$\langle\Phi_1\rangle = \frac{1}{\sqrt{2}}\begin{pmatrix} 0 \\ v_1 \end{pmatrix}, \qquad \langle\Phi_2\rangle = \frac{1}{\sqrt{2}}\begin{pmatrix} u \\ v_2 e^{i\xi} \end{pmatrix}, \tag{2.6}$$

where v_1 and v_2 are real and positive, and $0 \leq \xi < 2\pi$. Depending on the parameters of Higgs potential, the extremum for $u \neq 0$ describes either saddle point or a minimum of the potential, called the *charged vacuum*, where the $\mathrm{U}(1)_{\mathrm{EM}}$ symmetry is spontaneously broken [15, 20–22]. The vacuum solution with $u = 0$ preserves the $\mathrm{U}(1)_{\mathrm{EM}}$ symmetry; it corresponds to a local minimum of potential if its parameters are such that the physical Higgs squared-masses are non-negative. In this case, one can show that the energy of the charged vacuum is larger than energy of the $\mathrm{U}(1)_{\mathrm{EM}}$ preserving vacuum [20, 22].

Henceforth, we assume that the global minimum of the scalar potential respects the $\mathrm{U}(1)_{\mathrm{EM}}$ gauge symmetry. In this case $u = 0$ and it is convenient to write:

$$v_1 \equiv v\cos\beta\,, \qquad v_2 \equiv v\sin\beta\,, \tag{2.7}$$

where $v^2 \equiv v_1^2 + v_2^2 = (\sqrt{2}G_F)^{-1/2} = (246\ \mathrm{GeV})^2$ and $0 \leq \beta \leq \pi/2$.

One is always free to rephase Φ_2 in order to set $\xi = 0$. In the following, we shall always work in a basis in which the two neutral Higgs field vevs are real and positive (corresponding to a *real vacuum*). The scalar minimum conditions (2.5) then yield:

$$m_{11}^2 = m_{12}^2\, t_\beta - \tfrac{1}{2}v^2\left[\lambda_1 c_\beta^2 + (\lambda_3+\lambda_4+\lambda_5 s_\beta^2 + (2\lambda_6+\lambda_6^*)s_\beta c_\beta + \lambda_7 s_\beta^2 t_\beta\right] \tag{2.8}$$

$$m_{22}^2 = (m_{12}^2)^*\, t_\beta^{-1} - \tfrac{1}{2}v^2\left[\lambda_2 s_\beta^2 + (\lambda_3+\lambda_4+\lambda_5^* c_\beta^2 + \lambda_6^* c_\beta^2 t_\beta^{-1} + (\lambda_7 e^{i\xi} + 2\lambda_7^* e^{-i\xi})s_\beta c_\beta\right], \tag{2.9}$$

where $s_\beta = \sin\beta$, $c_\beta = \cos\beta$ and $t_\beta = \tan\beta$. Since m_{11}^2 and m_{22}^2 are both real, the imaginary part of either Eq. (2.8) or Eq. (2.9) yields one independent equation:

$$\mathrm{Im}\,(m_{12}^2) = \tfrac{1}{2}v^2\left[\,\mathrm{Im}\,(\lambda_5)s_\beta c_\beta + \,\mathrm{Im}\,(\lambda_6)c_\beta^2 + \,\mathrm{Im}\,(\lambda_7)s_\beta^2\right]. \tag{2.10}$$

The quantities

$$\delta \equiv \frac{\mathrm{Im}\,(m_{12}^2)}{v^2 s_\beta c_\beta}, \qquad \eta \equiv \frac{\mathrm{Re}\,(m_{12}^2)}{v^2 s_\beta c_\beta}, \tag{2.11}$$

will be useful in our discussion of the Higgs mass eigenstates and the mixing of CP-even and CP-odd states. Note that $\mathrm{Re}\,(m_{12}^2)$ is not determined by the scalar potential minimum conditions.

2.1.1.5 Theoretical constraints on the Higgs potential parameters

The parameters of Higgs potential are constrained by various conditions. To have a *stable vacuum*, the potential must be positive at large quasi–classical values of the magnitudes of the scalar fields for an arbitrary direction in the (Φ_1, Φ_2) plane. These are the *positivity constraints* [23–26]. The *minimum constraints* are the conditions ensuring that the extremum is a minimum for all directions in (Φ_1, Φ_2) space, except for the direction of the Goldstone modes. It is realized when the squared-masses of the five physical Higgs bosons are all positive.

The tree-level amplitudes for the scattering of longitudinal gauge bosons at high energy can be related via the equivalence theorem [27] to the corresponding amplitudes in which the longitudinal gauge bosons are replaced by Goldstone bosons. The latter can be computed in terms of quartic couplings λ_i that appear in the Higgs potential. By imposing *tree-level unitarity constraints* on these amplitudes, one can derive upper bounds on the values of certain combinations of Higgs quartic couplings [28–34].

The *perturbativity condition* for a validity of a tree approximation in the description of interactions of the lightest Higgs boson may be somewhat less restrictive than the unitarity constraints. For example, by requiring that one-loop corrections to Higgs self-couplings are small compared to tree-level couplings, one expects that $|\lambda_i|/16\pi^2 \ll 1$.

Unitarity constraints for the 2HDM were first derived for the potential without a hard violation of the discrete Z_2 symmetry and for the CP conserving case (*e.g.*, see [32]). Extension to the CP-violating case can be found in [33], and for the case of hard discrete Z_2 symmetry violation in [34].

2.1.2 Conditions for Higgs sector CP-violation

Higgs sector CP-violation may be either explicit or spontaneous. Explicit CP conservation[1] or violation refers respectively to the consistent or inconsistent CP transformation properties of the various terms that appear in the Lagrangian. If the scalar Lagrangian is explicitly CP-conserving, but the vacuum state of the theory violates CP, then one says that CP is spontaneously broken [1, 10, 35]. The observable consequences of Higgs sector CP-violation (either explicit or spontaneous) include the mixing of neutral Higgs states of opposite CP quantum numbers and/or the existence of (direct) CP-violating Higgs interactions.

The CP state mixing and the direct CP-violation in the gauge/Higgs interactions are determined by the properties of the scalar Lagrangian (and the corresponding vacuum state). These CP-violating effects are absent if and only if there exists a basis in which the two neutral Higgs vacuum expectation values and the scalar potential parameters are simultaneously real [36, 37]. Given an arbitrary potential, the existence or non-existence of such a basis may be difficult to determine directly. For this problem, the basis-independent methods are invaluable. In particular, a set of basis-independent conditions can be

[1] Since CP is violated in the SM via the CKM mixing of the quarks, it is generally unnatural to demand that the Higgs sector of the 2HDM explicitly conserve CP. Nevertheless, one can naturally impose a CP-conserving Higgs sector by employing an appropriate discrete symmetry. In the MSSM, the Higgs sector is CP-conserving at tree-level (due to the supersymmetry), although one finds CP-violation arising at one-loop due to supersymmetry-breaking effects.

found to test for the CP-invariance of the scalar sector. Following [38], we introduce three U(2)-invariant quantities [37]:

$$-\tfrac{1}{2}v^2 J_1 \equiv \widehat{v}_{\bar{a}}^* Y_{a\bar{b}} Z^{(1)}_{b\bar{d}} \widehat{v}_d \,, \tag{2.12}$$

$$\tfrac{1}{4}v^4 J_2 \equiv \widehat{v}_{\bar{b}}^* \widehat{v}_{\bar{c}}^* Y_{b\bar{e}} Y_{c\bar{f}} Z_{e\bar{a}f\bar{d}} \widehat{v}_a \widehat{v}_d \,, \tag{2.13}$$

$$J_3 \equiv \widehat{v}_{\bar{b}}^* \widehat{v}_{\bar{c}}^* Z^{(1)}_{b\bar{e}} Z^{(1)}_{c\bar{f}} Z_{e\bar{a}f\bar{d}} \widehat{v}_a \widehat{v}_d \,, \tag{2.14}$$

where $\langle \Phi_a^0 \rangle \equiv v\widehat{v}_a/\sqrt{2}$, and $\widehat{v}_a$ is a unit vector in the complex two-dimensional Higgs flavor space. Then, the scalar sector is CP-conserving (*i.e.*, no explicit nor spontaneous CP-violation is present) if J_1, J_2 and J_3 defined in Eqs. (2.12)–(2.14) are real.[2] If the scalar potential is CP-violating, then the CP state mixing depends only on $\mathrm{Im}\, J_2$ [16, 39], whereas CP-violation in the gauge/Higgs boson interactions is governed by all three quantities $\mathrm{Im}\, J_k$, $k = 1, 2, 3$.

2.1.2.1 Explicit CP-conservation

The general 2HDM scalar potential explicitly violates the CP symmetry. An explicitly CP-conserving scalar potential requires the existence of a Φ_1–Φ_2 basis in which all the Higgs potential parameters are real. Such a basis will henceforth be called a *real basis*. However, given an arbitrary potential, the existence or non-existence of a real basis may be difficult to discern, as already noted. In Ref. [37], the necessary and sufficient *basis-independent* conditions for an explicitly CP-conserving scalar potential have been established, in terms of the following four potentially complex invariants:

$$I_{Y3Z} \equiv \mathrm{Im}\,(Z^{(1)}_{a\bar{c}} Z^{(1)}_{e\bar{b}} Z_{b\bar{e}c\bar{d}} Y_{d\bar{a}}) \,, \tag{2.15}$$

$$I_{2Y2Z} \equiv \mathrm{Im}\,(Y_{a\bar{b}} Y_{c\bar{d}} Z_{b\bar{a}d\bar{f}} Z^{(1)}_{f\bar{c}}) \,, \tag{2.16}$$

$$I_{6Z} \equiv \mathrm{Im}\,(Z_{a\bar{b}c\bar{d}} Z^{(1)}_{b\bar{f}} Z^{(1)}_{d\bar{h}} Z_{f\bar{a}j\bar{k}} Z_{k\bar{j}m\bar{n}} Z_{n\bar{m}h\bar{c}}) \,, \tag{2.17}$$

$$I_{3Y3Z} \equiv \mathrm{Im}\,(Z_{a\bar{c}b\bar{d}} Z_{c\bar{e}d\bar{g}} Z_{e\bar{h}f\bar{q}} Y_{g\bar{a}} Y_{h\bar{b}} Y_{q\bar{f}}) \,, \tag{2.18}$$

where $Z^{(1)}_{a\bar{d}} \equiv \delta_{b\bar{c}} Z_{a\bar{b}c\bar{d}}$.

The conditions for a CP-conserving scalar potential depend on the invariant quantity [14, 19]:

$$Z \equiv 2\ \mathrm{Tr}\ [Z^{(1)}]^2 - (\mathrm{Tr}\ Z^{(1)})^2 = (\lambda_1 - \lambda_2)^2 + 4|\lambda_6 + \lambda_7|^2 \,, \tag{2.19}$$

Note that if Z vanishes, then Eq. (2.19) implies that $\lambda_1 = \lambda_2$ and $\lambda_7 = -\lambda_6$ for *all* basis choices. Two distinct cases are possible. If $Z \neq 0$, then the necessary and sufficient conditions for an explicitly CP-conserving 2HDM scalar potential are given by $I_{Y3Z} = I_{2Y2Z} = I_{6Z} = 0$. (A similar result has also been obtained in [40].) In this case $I_{3Y3Z} = 0$ is automatically satisfied. If $Z = 0$, then the aforementioned first three invariants automatically vanish, in which case the necessary and sufficient condition for an explicitly CP-conserving 2HDM scalar potential is given by $I_{3Y3Z} = 0$. Explicit expressions for the imaginary parts of the four CP-odd invariants above can be found in [37]. The significance of the four conditions above from a group-theoretical perspective has been recently discussed in [19, 41].

Finally, we note that the imposition of the discrete Z_2 symmetry $\Phi_1 \to \Phi_1$, $\Phi_2 \to -\Phi_2$ implies that the scalar potential is CP-conserving. Since λ_5 is the only nonzero complex parameter in the basis where the discrete symmetry is manifest, it is a simple matter to rephase one of the scalar doublets to render λ_5 real. Explicit CP-violation can arise if the $\Phi_1 \to \Phi_1$, $\Phi_2 \to -\Phi_2$ discrete Z_2 symmetry breaking is either hard or soft. In the latter case, *e.g.*, CP violation is a consequence of a nontrivial relative phase in the complex parameters m_{12}^2 and λ_5.

[2] One can show that the reality of the J_k is equivalent to the invariant conditions given in Eq. (2.75) of section 2.3 [14, 38].

2.1.2.2 Spontaneous CP-violation

If the scalar Lagrangian is explicitly CP-conserving but the Higgs vacuum is CP-violating, then CP is spontaneously broken. However, both spontaneous and explicit CP-violation yield similar CP-violating phenomenology. To distinguish between the two, one would need to discover CP-violation in the Higgs sector and prove that the fundamental scalar Lagrangian is CP-conserving. In principle, such a distinction is possible. For example, suppose one could verify that $I_{Y3Z} = I_{2Y2Z} = I_{6Z} = I_{3Y3Z} = 0$, whereas at least one of three invariants J_1, J_2 and J_3 possesses a non-zero imaginary part. In this case, the CP-symmetry in the Higgs sector is spontaneously broken.[3] In practice, distinguishing between explicit and spontaneous CP-violation by experimental observations and analysis seems extremely difficult.

Spontaneous CP-violation cannot arise in the presence of the $\Phi_1 \to \Phi_1$, $\Phi_2 \to -\Phi_2$ discrete Z_2 symmetry. In particular, in this case the scalar potential minimum condition implies that it is possible to transform to a real basis in which the two neutral vacuum expectation values are real.

2.1.3 The Higgs mass spectrum

2.1.3.1 CP violation and mixing of states

We introduce the following field decomposition

$$\Phi_1 = \begin{pmatrix} \varphi_1^+ \\ \dfrac{v_1 + \varphi_1 + i\chi_1}{\sqrt{2}} \end{pmatrix}, \qquad \Phi_2 = \begin{pmatrix} \varphi_2^+ \\ \dfrac{v_2 + \varphi_2 + i\chi_2}{\sqrt{2}} \end{pmatrix}. \tag{2.20}$$

Then the corresponding scalar squared-mass matrix can be transformed to the block diagonal form by a separation of the massless charged and neutral Goldstone boson fields, $G^\pm$ and G^0, and the charged Higgs boson fields $H^\pm$:

$$G^\pm = \cos\beta\,\varphi_1^\pm + \sin\beta\,\varphi_2^\pm\,, \tag{2.21}$$

$$G^0 = \cos\beta\;\chi_1 + \sin\beta\;\chi_2\,. \tag{2.22}$$

The physical charged Higgs boson is orthogonal to $G^\pm$:

$$H^\pm = -\sin\beta\,\varphi_1^\pm + \cos\beta\,\varphi_2^\pm\,. \tag{2.23}$$

The mass of the charged Higgs boson is easily obtained:

$$M_{H^\pm}^2 = \left[\eta - \frac{1}{2}(\lambda_4 + \operatorname{Re}\lambda_5 + \operatorname{Re}\lambda_{67})\right] v^2\,, \tag{2.24}$$

where $\lambda_{67} \equiv \lambda_6 \cot\beta + \lambda_7 \tan\beta$ and η is defined in Eq. (2.11). The physical neutral Higgs bosons are mixtures of the two CP-even fields φ_1, φ_2 and a CP-odd field

$$A = -\sin\beta\,\chi_1 + \cos\beta\,\chi_2\,, \tag{2.25}$$

that is orthogonal to G^0. Consequently, in the general 2HDM, the physical neutral Higgs bosons are states of indefinite CP.

In the $\{\varphi_1, \varphi_2, A\}$ basis, the real symmetric squared-mass matrix $\mathcal{M}^2$ for neutral sector is obtained:

$$\mathcal{M}^2 = \begin{pmatrix} M_{11}^2 & M_{12}^2 & M_{13}^2 \\ M_{12}^2 & M_{22}^2 & M_{23}^2 \\ M_{13}^2 & M_{23}^2 & M_{33}^2 \end{pmatrix}. \tag{2.26}$$

[3] One would also have to prove the absence of explicit CP-violation in the Higgs-fermion couplings. The relevant basis-independent conditions have been given in [10, 38].

Diagonalizing the matrix $\mathcal{M}^2$ by using an orthogonal transformation R we obtain the physical neutral states $h_{1,2,3}$, with corresponding squared-masses M_i^2 that are the eigenvalues of the matrix $\mathcal{M}^2$:

$$\begin{pmatrix} h_1 \\ h_2 \\ h_3 \end{pmatrix} = R \begin{pmatrix} \varphi_1 \\ \varphi_2 \\ A \end{pmatrix} , \quad \text{with} \quad R\mathcal{M}^2 R^T = \text{diag}(M_1^2,\, M_2^2,\, M_3^2)\,. \tag{2.27}$$

The diagonalizing matrix R can be written as a product of three rotation matrices R_i, corresponding to rotations by three angles $\alpha_i \in (0, \pi)$ about the z, y and x axes, respectively:

$$R = R_3 R_2 R_1 = \begin{pmatrix} c_1\, c_2 & c_2\, s_1 & s_2 \\ -c_1\, s_2\, s_3 - c_3\, s_1 & c_1\, c_3 - s_1\, s_2\, s_3 & c_2\, s_3 \\ -c_1\, c_3\, s_2 + s_1\, s_3 & -c_1\, s_3 - c_3\, s_1\, s_2 & c_2\, c_3 \end{pmatrix} . \tag{2.28}$$

Here, we define $c_i = \cos\alpha_i$, $s_i = \sin\alpha_i$ and adopt the convention for masses that $M_1 \le M_2 \le M_3$.

One can first diagonalize the upper left 2×2 block of the matrix $\mathcal{M}^2$. This partial diagonalization [15] results in the neutral, CP-even Higgs fields which we denote as h and $(-H)$,

$$H = \cos\alpha\, \varphi_1 + \sin\alpha\, \varphi_2, \qquad\qquad h = -\sin\alpha\, \varphi_1 + \cos\alpha\, \varphi_2\,, \tag{2.29}$$

where $\alpha \equiv \alpha_1 - \pi/2$ is the mixing angle that renders the 2×2 CP-even submatrix diagonal.[4] At this stage the CP–odd field A remains unmixed:

$$\begin{pmatrix} h \\ -H \\ A \end{pmatrix} = R_1 \begin{pmatrix} \varphi_1 \\ \varphi_2 \\ A \end{pmatrix} , \qquad \text{with} \quad R_1 \mathcal{M}^2 R_1^T = \mathcal{M}_1^2 \equiv \begin{pmatrix} M_h^2 & 0 & M_{13}'^2 \\ 0 & M_H^2 & M_{23}'^2 \\ M_{13}'^2 & M_{23}'^2 & M_A^2 \end{pmatrix} , \tag{2.30}$$

where

$$M_A^2 = \left[\eta - \text{Re}\,(\lambda_5 - \tfrac{1}{2}\lambda_{67})\right] v^2\,, \tag{2.31}$$

$$M_{h,H}^2 = \tfrac{1}{2}\left[M_{11} + M_{22} \mp \sqrt{(M_{11} - M_{22})^2 + 4M_{12}^2}\right] . \tag{2.32}$$

The off-diagonal squared-masses $M_{13}'^2$ and $M_{23}'^2$ are given by

$$M_{13}'^2 = c_1 M_{13}^2 + s_1 M_{23}^2 = -\tfrac{1}{2}\left[2\delta\cos(\beta+\alpha) - \text{Im}\,\tilde{\lambda}_{67}\cos(\beta-\alpha)\right] v^2, \tag{2.33}$$

$$M_{23}'^2 = -s_1 M_{13}^2 + c_1 M_{23}^2 = \tfrac{1}{2}\left[2\delta\sin(\beta+\alpha) + \text{Im}\,\tilde{\lambda}_{67}\sin(\beta-\alpha)\right] v^2\,, \tag{2.34}$$

where $\tilde{\lambda}_{67} \equiv \lambda_6 \cot\beta - \lambda_7 \tan\beta$ and δ is defined in Eq. (2.11).

In the general CP-violating 2HDM, the states h, H and A are useful intermediaries, which do not directly correspond to physical objects. In the case of CP conservation (realized for $M_{13}'^2 = M_{23}'^2 = 0$), the fields h, H and A represent physical Higgs bosons: $h_1 = h$, $h_2 = -H$, $h_3 = A$. If at least one of the off diagonal terms differs from zero, an additional diagonalization is necessary, and the mass eigenstates, which are now admixtures of CP–even and CP–odd states, violate the CP symmetry. In this case we express the physical Higgs boson states $h_{1,2,3}$ as linear combinations of h, H, A:

$$\begin{pmatrix} h_1 \\ h_2 \\ h_3 \end{pmatrix} = R_3 R_2 \begin{pmatrix} h \\ -H \\ A \end{pmatrix} \qquad \text{with} \quad R\,\mathcal{M}^2\,R^T = R_3 R_2 \mathcal{M}_1^2 R_2^T R_3^T = \begin{pmatrix} M_1^2 & 0 & 0 \\ 0 & M_2^2 & 0 \\ 0 & 0 & M_3^2 \end{pmatrix} . \tag{2.35}$$

[4] The appearance of the minus sign in $-H$ and the shift by $\pi/2$ in the definition of α is needed in order to match the standard convention used for CP-conserving case [8].

The following mass sum rule holds:

$$M_1^2 + M_2^2 + M_3^2 = M_h^2 + M_H^2 + M_A^2 = M_{11}^2 + M_{22}^2 + M_{33}^2 \,. \tag{2.36}$$

In general, the Higgs mass-eigenstates h_i [Eq. (2.27)] are not states of definite CP parity since they are mixtures of fields $\varphi_{1,2}$ and A, which possess opposite CP parities. Such CP-state mixing is absent if and only if $M_{13}^2 = M_{23}^2 = 0$. In particular, for $\sin 2\beta \neq 0$, the absence of CP-state mixing implies that $\mathrm{Im}\,\tilde{\lambda}_{67} = 0$ and $\delta \propto \mathrm{Im}\,(m_{12}^2) = 0$. In this latter case, h, H and A are the physical Higgs bosons, with masses given by eqs. (2.31) and (2.32), and $\alpha_2 = \alpha_3 = 0$.

2.1.3.2 Various cases of CP mixing

We consider a number of possible interesting patterns of CP-even/CP-odd scalar state mixing [15]:

• If $\boldsymbol{\varepsilon_{13} \equiv |M_{13}'^2/(M_A^2 - M_h^2)| \ll 1}$, then $\alpha_2 \approx 0$ and the Higgs boson h_1 practically coincides with the lighter CP-even state, h. In addition, the CP-violating couplings of h are very small, typically of $\mathcal{O}(\varepsilon_{13})$. The diagonalization of the residual $\langle 23\rangle$ corner of the squared-mass matrix (2.30) using the rotation matrix R_3 yields the mass eigenstates h_2 and h_3. These are superpositions of H and A with a potentially large mixing angle α_3:

$$\tan 2\alpha_3 \approx \frac{-2M_{23}'^2}{M_A^2 - M_H^2} \,. \tag{2.37}$$

If $M_A \approx M_H$, then the CP-violating state mixing can be strong even at small but nonzero $|M_{23}'^2|/v^2$. For large values of $M_H \approx M_A$ the proper widths of H and A become large and the H and A mass peaks strongly overlap. Here, one should include a (complex) matrix of Higgs polarization operators [42, 43].

• If $\boldsymbol{\varepsilon_{23} \equiv |M_{23}'^2/(M_A^2 - M_H^2)| \ll 1}$, then $\alpha_3 \approx 0$ and the Higgs boson h_2 practically coincides with the heavier CP-even state, $-H$. Similarly to the previous case, the diagonalization of the $\langle 13\rangle$ part of squared-mass matrix (2.30), using the rotation matrix R_2 yields the mass eigenstates h_1 and h_3. These are superpositions of h and A states, which can strongly mix with large mixing angle α_2:

$$\tan 2\alpha_2 \approx \frac{-2M_{13}'^2}{M_A^2 - M_h^2} \,. \tag{2.38}$$

As in the previous case, if $M_A \approx M_h$, the CP-violating state mixing can be strong even at small $M_{13}'^2/v^2$.

• The case of *weak CP-violating state mixing* combines both cases above. That is ε_{13}, $\varepsilon_{23} \ll 1$, which imply that α_2, $\alpha_3 \approx 0$, in which case the CP–even states h, H are weakly mixed with the CP–odd state A. The corresponding physical Higgs masses are given by

$$M_1^2 \simeq M_h^2 - s_2^2(M_A^2 - M_h^2), \qquad M_2^2 \simeq M_H^2 - s_3^2(M_A^2 - M_H^2), \tag{2.39}$$

with M_3^2 given by the sum rule (2.36) . In the particular case of *soft-violation of the discrete Z_2 symmetry* we also have

$$s_2 \simeq \delta\, \frac{\cos(\beta+\alpha)}{M_A^2 - M_h^2} v^2, \qquad s_3 \simeq -\delta\, \frac{\sin(\beta+\alpha)}{M_A^2 - M_H^2} v^2. \tag{2.40}$$

• The case of the *intense coupling regime* with $M_A \approx M_h \approx M_H$ [44] may also yield strong CP-violating state mixing even when both δ and $\mathrm{Im}\,\tilde{\lambda}_{67}$ are small.

2.1.4 Higgs boson couplings

In the investigation of phenomenological aspects of 2HDM it is useful to introduce *relative couplings*, defined as the couplings of each neutral Higgs boson h_i ($i = 1, 2, 3$) to gauge bosons W^+W^- or ZZ,

Higgs bosons H^+H^- and h_jh_k, quarks $\bar{q}q$ ($q = u, d$) and charged leptons $\ell^+\ell^-$, normalized to the corresponding couplings of the SM Higgs boson:

$$\chi^{(i)} = g_j^{(i)}/g_j^{\rm SM}\,, \qquad j = W^\pm, Z, H^\pm, u, d, \ell\ldots\,, \tag{2.41}$$

where $g_j^{(i)}$ denotes the jjh_i coupling. Note that for bosonic j, the relative couplings are real. In the case of neutral Higgs boson (h_i) couplings to fermions pairs $f\bar{f}$, the Yukawa couplings take the form

$$-\mathcal{L}_Y = \bar{f}(g_{Ri} + ig_{Ii}\gamma_5)f\,h_i = \bar{f}_L(g_{Ri} + ig_{Ii})f_R\,h_i + \text{h.c.}\,, \tag{2.42}$$

where the right and left-handed fermion fields are defined as usual: $f_R \equiv P_R f$ and $f_L \equiv P_L f$, with $P_{R,L} \equiv \frac{1}{2}(1 \pm \gamma_5)$. Hence, we shall compute the Higgs–fermion relative coupling in Eq. (2.41) by employing the *complex* couplings $g_i = g_{Ri} + ig_{Ii}$.

One can also make use of basis-independent techniques to obtain expressions for Higgs couplings to gauge bosons, Higgs bosons and fermions that are invariant under U(2) field redefinitions of the two complex scalar doublet fields [16]. Further details of this procedure and a complete collection of 2HDM couplings can be found in section 2.3.

2.1.4.1 Bosonic sector

The gauge bosons V (W and Z) couple only to the CP–even fields φ_1, φ_2. In terms of the relative couplings defined in Eq. (2.41), the couplings of gauge bosons to the physical Higgs bosons h_i are:

$$\chi_V^{(i)} = \cos\beta\, R_{i1} + \sin\beta\, R_{i2}, \qquad V = W \text{ or } Z. \tag{2.43}$$

In particular, in the case of weak CP-violating state mixing considered above, we obtain

$$\chi_V^{(1)} \simeq \sin(\beta-\alpha), \qquad \chi_V^{(2)} \simeq -\cos(\beta-\alpha), \qquad \chi_V^{(3)} \simeq -s_2\sin(\beta-\alpha) + s_3\cos(\beta-\alpha). \tag{2.44}$$

The cubic and quartic Higgs self-couplings as functions of the Higgs potential parameters and the elements of mixing matrix were obtained in [15, 16, 45–47]. In the case of soft Z_2 symmetry violation in the CP-conserving case, these latter results simplify. The Higgs self-couplings can be expressed in terms of the Higgs masses and the mixing angles α and β. Moreover, if the Higgs-fermion Yukawa interactions are of type-II [as defined below Eq. (2.46)], the trilinear couplings can be given in terms of the Higgs masses, the relative couplings to gauge bosons and quarks, and the parameter η [15]. As an important example, in the case of weak CP-violating state mixing and soft Z_2 symmetry-violation, the coupling of the neutral scalar h_i to a charged Higgs boson pair (normalized to $2M_{H^\pm}^2/v$) can be expressed in terms of the relative neutral Higgs couplings to the gauge bosons and fermions as follows:

$$\chi_{H^\pm}^{(i)} = \left(1 - \frac{M_i^2}{2M_{H^\pm}^2}\right)\chi_V^{(i)} + \frac{M_i^2 - \eta v^2}{2M_{H^\pm}^2}\,\text{Re}\,(\chi_u^{(i)} + \chi_d^{(i)}). \tag{2.45}$$

Deviations of the cubic Higgs boson self-couplings from the corresponding Standard Model value would also provide insight into the dynamics of the 2HDM. In particular, as emphasized in section 2.6, there is a strong correlation between the loop-corrected hhh coupling and successful electroweak baryogenesis (that makes critical use of the CP-violation from the Higgs sector).

2.1.4.2 Fermion–Higgs boson Yukawa couplings

The Higgs couplings to fermions are model dependent. The most general structure for the Higgs-fermion Yukawa couplings, often referred to as the type-III model [48, 49], is given in the generic basis by:

$$-\mathcal{L}_{\rm Y} = \overline{Q_L^0}\widetilde{\Phi}_1\Gamma_1 U_R^0 + \overline{Q_L^0}\Phi_1\Delta_1 D_R^0 + \overline{Q_L^0}\widetilde{\Phi}_2\Gamma_2 U_R^0 + \overline{Q_L^0}\Phi_2\Delta_2 D_R^0 + \text{h.c.}\,, \tag{2.46}$$

where $\widetilde{\Phi}_i \equiv i\sigma_2\Phi_i^*$, Q_L^0 is the weak isospin quark doublet, and U_R^0, D_R^0 are weak isospin quark singlets. Here, Q_L^0, U_R^0, D_R^0 denote the interaction basis states, which are vectors in the quark flavor space, and $\Gamma_1, \Gamma_2, \Delta_1, \Delta_2$ are Yukawa coupling matrices in quark flavor space.[5] We have omitted the leptonic couplings in Eq. (2.46); these follow the same pattern as the down-type quark couplings.

In some models, not all the terms in Eq. (2.46) are present at tree-level [50]. For example, in a type-I model (2HDM-I) [51], there exists a basis where $\Gamma_2 = \Delta_2 = 0$.[6] Similarly, in a type-II model (2HDM-II) [52], there exists a basis where $\Gamma_1 = \Delta_2 = 0$. The vanishing of certain Higgs-fermion couplings at tree-level can be enforced by imposing a discrete Z_2 symmetry under which $\Phi_1 \to \Phi_1$, $\Phi_2 \to -\Phi_2$, and the fermion fields are either invariant or change sign according to whether one wishes to preserve either the type-I or type-II Higgs-fermion couplings while eliminating the other possible terms in Eq. (2.46). Another well-known example is the MSSM Higgs sector, which exhibits a type-II Higgs-fermion coupling pattern that is enforced by supersymmetry.

The fermion–Higgs boson Yukawa couplings can be derived from Eq. (2.46) (see, *e.g.*, chapter 22 of [10]). Without loss of generality, we choose a basis corresponding to a real vacuum (*i.e.*, $\xi = 0$). The fermion mass eigenstates are related to the interaction eigenstates by bi-unitary transformations:

$$P_L U = V_L^U P_L U^0\,, \qquad P_R U = V_R^U P_R U^0\,, \qquad P_L D = V_L^D P_L D^0\,, \qquad P_R D = V_R^D P_R D^0\,, \tag{2.47}$$

and the Cabibbo-Kobayashi-Maskawa matrix is defined as $K \equiv V_L^U V_L^{D\,\dagger}$. It is also convenient to define "rotated" linear combinations of the Yukawa coupling matrices:

$$\kappa^U \equiv V_L^U(\Gamma_1 c_\beta + \Gamma_2 s_\beta)V_R^{U\,\dagger}\,, \qquad \rho^U \equiv V_L^U(-\Gamma_1 s_\beta + \Gamma_2 c_\beta)V_R^{U\,\dagger}\,, \tag{2.48}$$

$$\kappa^D \equiv V_L^D(\Delta_1 c_\beta + \Delta_2 s_\beta)V_R^{D\,\dagger}\,, \qquad \rho^D \equiv V_L^D(-\Delta_1 s_\beta + \Delta_2 c_\beta)V_R^{D\,\dagger}\,. \tag{2.49}$$

The quark mass terms are identified by replacing the scalar fields with their vacuum expectation values. The unitary matrices V_L^U, V_L^D, V_R^U and V_R^D are chosen so that κ^D and κ^U are diagonal with real non-negative entries. These quantities are proportional to the *diagonal* quark mass matrices:

$$M_D = \frac{v}{\sqrt{2}}\kappa^D\,, \qquad M_U = \frac{v}{\sqrt{2}}\kappa^U\,. \tag{2.50}$$

In a general model, the matrices ρ^D and ρ^U are independent *complex* non-diagonal matrices.

It is convenient to rewrite Eq. (2.46) in terms of the CP-even Higgs fields H and h and the CP-odd fields A (and the Goldstone boson G^0). The end result is:

$$\begin{aligned}
-\mathcal{L}_Y = {}& \frac{1}{v}\,\overline{D}\left[M_D s_{\beta-\alpha} + \frac{v}{\sqrt{2}}(\rho^D P_R + \rho^{D\dagger} P_L)c_{\beta-\alpha}\right] Dh + \frac{i}{v}\overline{D}M_D\gamma_5 DG^0 \\
& + \frac{1}{v}\,\overline{D}\left[M_D c_{\beta-\alpha} - \frac{v}{\sqrt{2}}(\rho^D P_R + \rho^{D\dagger} P_L)s_{\beta-\alpha}\right] DH + \frac{i}{\sqrt{2}}\overline{D}(\rho^D P_R - \rho^{D\dagger} P_L)DA \\
& + \frac{1}{v}\,\overline{U}\left[M_U s_{\beta-\alpha} + \frac{v}{\sqrt{2}}(\rho^U P_R + \rho^{U\dagger} P_L)c_{\beta-\alpha}\right] Uh - \frac{i}{v}\overline{U}M_D\gamma_5 UG^0 \\
& + \frac{1}{v}\,\overline{U}\left[M_U c_{\beta-\alpha} - \frac{v}{\sqrt{2}}(\rho^U P_R + \rho^{U\dagger} P_L)s_{\beta-\alpha}\right] UH - \frac{i}{\sqrt{2}}\overline{U}(\rho^U P_R - \rho^{U\dagger} P_L)UA \\
& + \left\{\overline{U}\left[K\rho^D P_R - \rho^{U\dagger} K P_L\right] DH^+ + \frac{\sqrt{2}}{v}\,\overline{U}\left[KM_D P_R - M_U K P_L\right] DG^+ + \text{h.c.}\right\}\,,
\end{aligned} \tag{2.51}$$

[5] We have reversed the lettering conventions for these coupling matrices as compared to [10] since Δ is more naturally associated with the coupling to down-type quarks.

[6] A type-I model can also be defined as a model in which $\Gamma_1 = \Delta_1 = 0$ in some basis. Clearly, the two definitions are equivalent, since the difference in the two conditions is simply an interchange of Φ_1 and Φ_2 which can be viewed as a change of basis.

where $s_{\beta-\alpha} = \sin(\beta-\alpha)$ and $c_{\beta-\alpha} = \cos(\beta-\alpha)$. In the most general CP-violating 2HDM, the physical Higgs fields are linear combinations of h, H and A. As advertised, since ρ^D and ρ^U are non-diagonal, Eq. (2.51) exhibits tree-level Higgs-mediated FCNCs.[7] See section 2.5 for a study of the implications of flavor-changing fermion–Higgs boson couplings for a variety of neutral current processes.

The fermion–Higgs boson Yukawa couplings simplify considerably in type-I and type-II models. In particular, ρ^D and ρ^U are no longer independent parameters. For example, in a one-generation type-II model, $\Gamma_1 = \Delta_2 = 0$, which implies that [14]

$$\tan\beta = \frac{-\rho^D}{\kappa^D} = \frac{\kappa^U}{\rho^U}\,. \tag{2.52}$$

These two equations are consistent, since the type-II condition is equivalent to $\kappa^U\kappa^D + \rho^U\rho^D = 0$. Moreover, using Eqs. (2.50) and (2.52), it follows that:

$$\rho^D = -\frac{\sqrt{2}m_d}{v}\tan\beta\,, \qquad \rho^U = \frac{\sqrt{2}m_u}{v}\cot\beta\,. \tag{2.53}$$

Inserting this result into Eq. (2.51) yields the well-known Feynman rules for the type-II Higgs-quark interactions. For example, in the case of weak CP-violating state mixing, one finds the expected form for the relative couplings of the neutral Higgs bosons to the up and down-type quarks:

$$\chi_d^{(1)} = -\frac{\sin\alpha}{\cos\beta} = s_{\beta-\alpha} - \tan\beta\, c_{\beta-\alpha}\,, \qquad \chi_u^{(1)} = \frac{\cos\alpha}{\sin\beta} = s_{\beta-\alpha} + \cot\beta\, c_{\beta-\alpha}\,, \tag{2.54}$$

$$-\chi_d^{(2)} = \frac{\cos\alpha}{\cos\beta} = c_{\beta-\alpha} + \tan\beta\, s_{\beta-\alpha}\,, \qquad -\chi_u^{(2)} = \frac{\sin\alpha}{\sin\beta} = c_{\beta-\alpha} - \cot\beta\, s_{\beta-\alpha}\,, \tag{2.55}$$

$$\chi_d^{(3)} = -i\tan\beta\,, \qquad \chi_u^{(3)} = -i\cot\beta\,. \tag{2.56}$$

Note the extra minus sign in $\chi_i^{(2)}$ which arises due to the identification of $h_2 \simeq -H$ in this limiting case.

A similar analysis can be given for models of type-I. In the same CP-conserving limiting case considered above, $\chi_u^{(i)}$ is identical to the corresponding type-II values given above, but $\chi_d^{(i)} = \chi_u^{(i)\,*}$.

2.1.4.3 The decoupling limit and implications for a SM-like Higgs boson

Suppose that all the coefficients of the quartic terms are held fixed [with values that are not allowed to exceed $\mathcal{O}(1)$]. Then, in the limit that $M_{H^\pm} \gg v = 246$ GeV, we find that one neutral Higgs boson has mass of $\mathcal{O}(v)$, while the other two neutral Higgs bosons have mass of $\mathcal{O}(M_{H^\pm})$. In this *decoupling limit*, one can formally integrate out the heavy Higgs states from the theory [53–58]. The resulting Higgs effective theory yields precisely the SM Higgs sector up to corrections of of $\mathcal{O}(v^2/M_{H^\pm}^2)$. Thus, the properties of the light neutral Higgs boson of the model, h_1, are nearly identical to those of the CP-even SM Higgs boson. Note that the CP-violating couplings of the lightest neutral Higgs boson to the fermions, gauge bosons and to itself are suppressed by a factor of $\mathcal{O}(v^2/M_{H^\pm}^2)$. In contrast, the two heavy neutral Higgs bosons will generally be significant admixtures of the CP-even and CP-odd states H and A.

In the approach to the decoupling limit, $c_{\beta-\alpha} \simeq \mathcal{O}(v^2/M_{H^\pm}^2)$ [58]. Then, Eqs. (2.44) and (2.54) yields $\chi_V^{(1)} \simeq \chi_d^{(1)} \simeq \chi_u^{(1)} \simeq 1$, as expected. The flavor structure of the Higgs-quark interactions in the decoupling limit is also noteworthy. Eq. (2.51) yields approximately flavor-diagonal $\overline{Q}Qh_1$ couplings, since the contribution of the non-diagonal ρ^Q is suppressed by $c_{\beta-\alpha}$. The heavier neutral Higgs bosons possess unsuppressed flavor non-diagonal Yukawa interactions, and thus can mediate FCNCs at tree-level. Of course, such FCNC effects would be suppressed by a factor of $\mathcal{O}(v^2/M_{H^\pm}^2)$ due to the heavy

[7] Note that even in the case of a CP-conserving Higgs potential, where h, H and A are physical mass eigenstates, Eq. (2.51) exhibits CP-violating Yukawa couplings proportional to the *complex* matrices ρ^D and ρ^U.

masses of the exchanged Higgs bosons. The existence of a decoupling limit depends on the possibility of taking $M^2_{H^\pm}$ arbitrarily large while holding the parameters λ_i fixed. Using Eq. (2.24), it follows that the approach to the decoupling limit corresponds to the region of 2HDM parameter space where $\eta \gg |\lambda_i|$. This implies that no decoupling limit exists in a 2HDM with an exact discrete Z_2 symmetry.

The presence of a SM-like Higgs boson (which is defined as a neutral scalar that possesses tree-level couplings which are nearly identical to those of the SM Higgs boson) is consistent with a 2HDM with parameters near the decoupling limit. However, a SM-Higgs boson can arise in non-decoupling regions of the 2HDM parameter space. As an example, in the CP-conserving limit with $c_{\beta-\alpha} \simeq 1$ and $\cot\beta\, s_{\beta-\alpha} \ll 1$, it follows that the heavier CP-even state H strongly resembles a SM-like Higgs boson. Other examples of a SM-like Higgs boson in a non-decoupling regime can be found in [58, 59].

The decoupling limit is also a regime in which all but the lightest Higgs boson are very heavy and nearly mass-degenerate. However, large Higgs masses (often with significant mass splittings) can also arise in a non-decoupling parameter regime in which the λ_i are large. In this case, the heavy Higgs boson masses are bounded from above by imposing unitarity constraints on the λ_i. These unitarity constraints, which have been obtained for the CP-conserving case in [32], can be more severe in the CP-violating case [33, 34]. For example, the unitarity limit constrains the parameter $|\lambda_5|$ while the Higgs mass formulae depend on $\mathrm{Re}\,\lambda_5$. In general, reasonably large H,$H^\pm$ and A masses (up to about 600 GeV), consistent with the unitarity constraints, can be obtained for very large or very small $\tan\beta$ and reasonably small values of $\eta \approx (M_h/v)^2$, as well as for $\tan\beta \approx 1$ with $\eta \approx 0$ [15].

Finally, we note that in a non-decoupling parameter regime, the loop effects due to virtual exchange of heavy Higgs boson states do not decouple. Thus, in this parameter regime, one can also deduce upper bounds for heavy Higgs masses (or equivalently a bound on the departure from the decoupling limit). As an example, the non-decoupling effects of charged and neutral Higgs boson one-loop contributions to leptonic τ-decays can yield an upper limit on the charged Higgs boson mass [60].

2.1.4.4 Pattern relations and sum rules

The orthogonality of the mixing matrix R allows one to obtain a number of relations [15, 61–63] among the relative couplings of neutral Higgs particles to the gauge bosons and fermions. For simplicity, we restrict the following analysis to the case of one generation of quarks (and leptons). Consider the following ratio of tree-level relative neutral Higgs couplings in the general CP-violating 2HDM:

$$\mathcal{R} \equiv \frac{\chi_V^{(i)} - \chi_d^{(i)\,*}}{\chi_u^{(i)} - \chi_V^{(i)}}\,, \tag{2.57}$$

where i labels the Higgs mass eigenstates. One can easily verify that Eq. (2.57) holds separately for each value of $i = 1, 2, 3$. Moreover, if the denominator of Eq. (2.57) vanishes, then the numerator must vanish as well and vice versa. The neutral Higgs boson relative couplings χ_j also satisfy a *vertical sum rule* [46, 64, 65]:

$$\sum_{i=1}^{3} (\chi_j^{(i)})^2 = 1 \qquad (j = V, d, u)\,. \tag{2.58}$$

Note that Eqs. (2.57) and (2.58) also holds for the corresponding relative couplings of the definite CP scalar states h, H and A.

In models with type-I and type-II Higgs–fermion Yukawa couplings, additional tree-level *pattern relations* and sum rules are respected. This is not surprising, given that the type-I and type-II conditions impose extra relations among the Higgs-fermion couplings. For example, Eq. (2.57) can be extended to the following result [15]:

$$\mathcal{R} = \frac{\chi_V^{(i)} - \chi_d^{(i)\,*}}{\chi_u^{(i)} - \chi_V^{(i)}} = \frac{1 - |\chi_d^{(i)}|^2}{|\chi_u^{(i)}|^2 - 1} = \frac{\mathrm{Im}\,\chi_d^{(i)}}{\mathrm{Im}\,\chi_u^{(i)}}\,, \tag{2.59}$$

where $\mathcal{R}$ is independent of the index i that labels the neutral Higgs state. A brief computation shows that in type-I models, $\mathcal{R} = -1$, whereas in type-II models, $\mathcal{R} = \tan^2\beta$. In writing Eq. (2.59), we implicitly assumed that the denominators do not vanish. For example, Eq. (2.59) can also be applied to the couplings of the neutral Higgs states of definite CP: h, H and A. However, in the CP-conserving limit, $\chi_u^{(i)}$ and $\chi_d^{(i)}$ are real for $i = h$ and H, so for these states the ratio of imaginary parts in Eq. (2.59) should be removed.

From Eq. (2.59), one can derive a *horizontal sum rule* for the neutral Higgs boson couplings [65]:

$$\mathcal{R}\,|\chi_u^{(i)}|^2 + |\chi_d^{(i)}|^2 = 1 + \mathcal{R}\,. \tag{2.60}$$

Taken together, the vertical and horizontal sum rules guarantee that the cross section to produce each neutral Higgs boson h_i (or h, H, A) of the 2HDM-I or 2HDM-II, in the processes involving the Yukawa interaction, cannot be lower than the corresponding cross section for the production of the SM Higgs boson with the same mass [65].

The following linear relation among neutral Higgs boson relative couplings [15] is also a consequence of Eq. (2.59)

$$(1+\mathcal{R})\chi_V^{(i)} = \chi_d^{(i)\,*} + \mathcal{R}\,\chi_u^{(i)}\,. \tag{2.61}$$

Models with type I and II Higgs-fermion Yukawa couplings can be distinguished by the following pattern relation, which only holds in the 2HDM-II: [62, 63]:

$$(\chi_u^{(i)} + \chi_d^{(i)})\chi_V^{(i)} - \chi_u^{(i)}\chi_d^{(i)} = 1\,. \tag{2.62}$$

Of course, Eqs. (2.60)–(2.62) can also be applied to the neutral Higgs states of definite CP: h, H and A.

2.2 Overview of phenomenology

Gérald Grenier, Howard E. Haber and Maria Krawczyk

We present a brief tour of the phenomenological and experimental investigations of the Higgs of the general 2HDM sector [9, 66, 67] at existing colliders (LEP[8] and TEVATRON), and at colliders now under construction (LHC) and under development (the ILC and the associated Photon Linear Collider (PLC) [68]). Results from the LHC and the ILC/PLC can provide useful synergies for CP studies of the general 2HDM, as discussed in [69, 70] and illustrated in section 2.14. The possibility of higher energy lepton colliders such as CLIC [71] and $\mu^+\mu^-$ collider [72, 73] have also been considered, and these facilities provide additional opportunities for CP studies of the Higgs sector.

2.2.1 Present limits on Higgs boson masses and couplings

Due to the complexity of the general 2HDM parameter space, there are no completely model-independent limits on Higgs boson masses and couplings. However, the absence of a Higgs boson discovery at LEP and the Tevatron places numerous constraints on the 2HDM parameters.

In the decoupling limit of the 2HDM (see section 2.1.4.3), where the properties of the lightest neutral Higgs boson approach those of the SM Higgs boson, the mass limits of the SM Higgs apply: $M_h > 114.4$ GeV [74]. Less definitive results exist away from the decoupling limit, where significant deviations of the properties of the lightest neutral Higgs boson from those of the SM Higgs boson can be realized [58, 63]. Within the context of the MSSM, numerous mass limits have been quoted depending on a number of underlying theoretical assumptions. Many of these limits are described in Section 3.2. Here, we briefly focus on some of the more model-independent limits that have been obtained at LEP.

[8] Although the LEP collider shut down in 2000, there are still ongoing analyses of data.

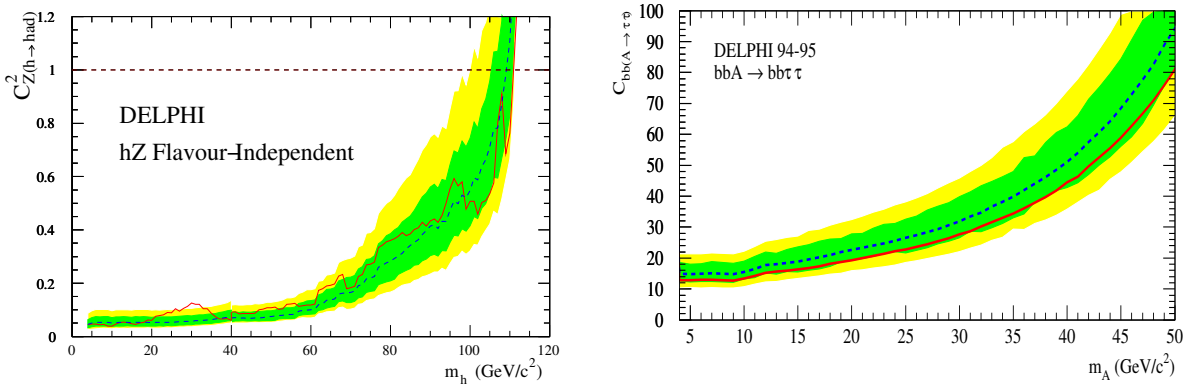

Fig. 2.1: Model independent upper limits for the CP-even and CP-odd Higgs boson masses as a function of their couplings to vector bosons and down-type fermions. The allowed parameter regimes (at 95% CL) lie below the solid lines. In the left panel, the squared relative coupling χ^2_V is shown as function of M_h [75]. In the right panel, the relative coupling χ_d is shown as function of M_A [76]. The relative couplings are defined in section 2.1.4 (note that the vertical axes employ different symbols for these relative couplings).

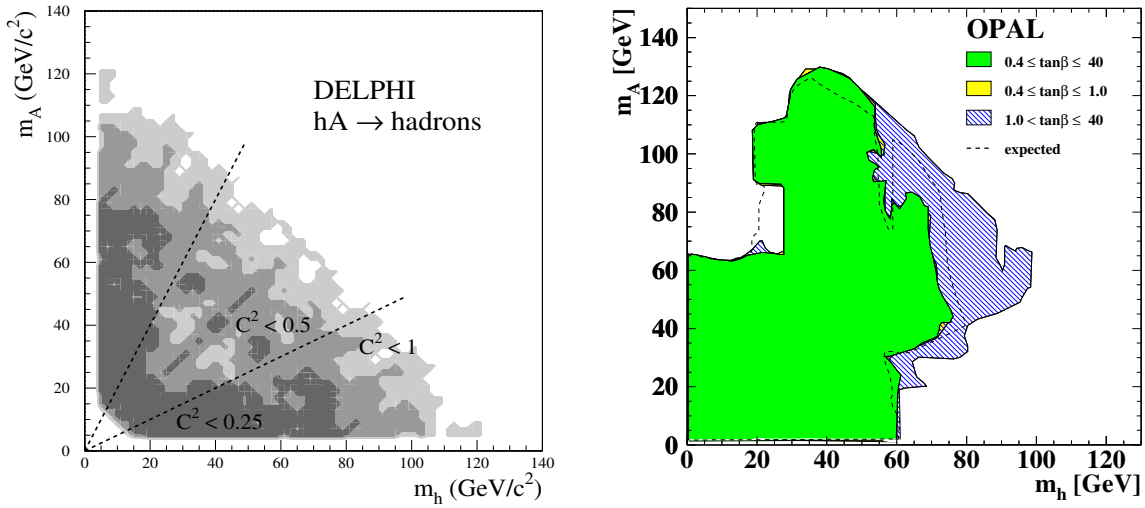

Fig. 2.2: In the left panel, constraints on the parameter $C^2 \equiv \cos^2(\beta-\alpha)$ are exhibited as a function of the Higgs masses M_h and M_A, based on the non-observation of $e^+e^- \to hA$ (assuming purely hadronic final states). Similar results are reinterpreted in the right panel in the CP conserving type-II 2HDM. The shaded area denotes the excluded regions of the (M_h, M_A) plane, independently of the CP-even neutral Higgs boson mixing angle [77,78].

If the neutral Higgs boson coupling to gauge bosons is suppressed, then $(\chi^h_V)^2 = \sin^2(\beta-\alpha) \ll 1$, and the upper bound on the Higgs mass (derived from the non-observation of $e^+e^- \to Zh$) is significantly reduced from the corresponding SM Higgs boson mass limit [75, 79], as shown in the left panel of Fig. 2.1. In the CP-conserving 2HDM, the cross section for $e^+e^- \to hA$ is proportional $\cos^2(\beta-\alpha)$ and depends on the corresponding masses M_h and M_A. The constraints on $\cos^2(\beta-\alpha)$ deduced from the non-observation of hA production at LEP yields an exclusion limit in the M_h–M_A plane shown in Fig. 2.2 [77, 78]. Note that these exclusion plots cannot exclude the possible existence of one very light neutral Higgs boson. For a CP-odd Higgs boson (which does not couple to gauge bosons at tree-level), important constraints on the Yukawa coupling χ_d as a function of the Higgs mass are derived from searches for $e^+e^- \to b\bar{b}A$ (where $A \to \tau^+\tau^-$). The absence of an observed $b\bar{b}\tau^+\tau^-$ signal above the SM background yields the exclusion plot shown in the right panel of Fig. 2.1 [76]. These limits depend

on the enhancement of the $b\bar{b}A$ coupling (which for type-II Yukawa couplings is proportional to $\tan\beta$). A similar search was also performed for four b final states resulting from $b\bar{b}A(\to b\bar{b})$ production and for four tau final states resulting from $\tau^+\tau^- A(\to \tau^+\tau^-)$. The same four-fermion signatures can also result from the production of the CP-even state h [76].

The phenomenology of the charged Higgs boson of the 2HDM depends on fewer model parameters compared to that of the neutral Higgs bosons. Mass limits (at 95% CL) exist for the CP-conserving 2HDM-I and 2HDM-II and are given by 78.6 GeV [80] and 76.7 GeV [81], respectively. These limits are independent of $\tan\beta$. All other limits involving the charged Higgs boson mass depend on $\tan\beta$. For example, the CDF Collaboration reports [82] no charged Higgs bosons have been observed in top quark decays at the Tevatron. This data excludes certain regions of the $M_{H^\pm}$–$\tan\beta$ plane.

Virtual charged Higgs exchange can affect low-energy processes and place constraints on the 2HDM parameters. The most powerful constraint of this type can be obtained from the observed rate for $b \to s\gamma$, which is consistent with the predictions of the Standard Model. Thus, the contributions via loops due to new physics must be rather small. In the 2HDM, there is an extra contribution due to a charged Higgs boson loop. The significance of this contribution depends on the structure of the Higgs-fermion couplings. For example, there is almost no constraint in the CP-conserving 2HDM-I. In contrast, in the 2HDM-II, the experimental observation of $b \to s\gamma$ implies a 95% CL lower limit of $M_{H^\pm} \gtrsim 320$ GeV [83,84]. However, such a limit must be interpreted with care, since virtual effects originating from other new physics sources can cancel the charged Higgs contribution, thereby significantly relaxing (or removing entirely) the charged Higgs mass limit.

A number of other observables can also provide useful constraints on 2HDM parameters. For example, a lower bound on $M_{h^\pm}/\tan\beta$ can be obtained in precision measurements of semi-leptonic b decays [85] and leptonic τ-decays [60] by constraining the size of the tree-level charged Higgs boson exchange contributions. Constraints on Higgs masses and couplings have been obtained for type-II [60, 86] and for type III Higgs-fermion couplings [87–89]. Additional examples of this type can be found in section 2.5. Global fits using different electroweak observables such as ρ, R_b and $b \to s\gamma$ [90] (and $(g-2)_\mu$ in [91]), have been made for the 2HDM-II, and these can significantly constrain the allowed regions of the parameter space.

2.2.2 Probing the CP nature of the neutral Higgs bosons

If phenomena consistent with the 2HDM are discovered, it will be important to discover the form of the 2HDM that is realized in nature. One critical step in this program is the determination of the CP-properties of the three neutral Higgs bosons. If CP is conserved, then one can associate definite CP-quantum numbers with the three states (*i.e*, the CP-even h and H and the CP-odd A). If CP is violated, there is mixing among these states of definite CP, the corresponding mass-eigenstates h_1, h_2 and h_3 are states of indefinite CP. In this latter case, one of the main tasks of the experimental Higgs studies is to confirm this mixing and determine the corresponding mixing angles. If the 2HDM parameters lie in the vicinity of the decoupling regime, then to a very good approximation $h_1 \simeq h$ is a SM-like CP-even Higgs boson. However, even in this case, there may be significant CP-violating effects involving the heavy neutral Higgs bosons, manifested by large mixing between the H and A. In the decoupling regime, the mass splitting between the heavy neutral Higgs states tends to be small (of order $M_Z^2/M_{H^\pm}^2$). Consequently, the mixing between H and A in the CP-violating case and the overlapping of the H and A resonances in the CP-conserving case can lead to similar phenomenological effects. Moreover, in the case of nearly mass-degenerate scalar states, one should include the effects of the non-zero width in scalar mass matrix [42, 43], leading to the phenomena of resonant Higgs bosons production. A study of this type is presented in Section 3.12.

In order to determine the CP-properties of the neutral scalar states, one must study the various Higgs couplings to gauge bosons and fermions that govern the Higgs production and decay processes. In general, the CP-indefinite neutral states h_i exhibit both scalar and pseudoscalar couplings to fermion

pairs. In contrast, W^+W^- and ZZ couple dominantly to the CP-even component of the neutral Higgs bosons. This latter coupling enters at tree-level, whereas the coupling to the CP-odd component is a one-loop generated effect [92]. Nevertheless, in a completely model-independent study of Higgs decay to massive vector boson pairs, one may wish to allow for the possibility of a non-negligible CP-odd component that couples to vector bosons, as in [93]. For example, Lorentz invariance dictates that the most general interaction vertex for the coupling of a neutral Higgs boson h_j to ZZ is given by [94–96]:

$$\Gamma_{\mu\nu}(k_1\,,\,k_2) = \frac{ig}{m_Z\cos\theta_W}\left[a_j m_Z^2 g_{\mu\nu} + b_j(k_{2\mu}k_{1\nu} - k_1\cdot k_2 g_{\mu\nu}) + c_j\epsilon_{\mu\nu\alpha\beta}k_1^\alpha k_2^\beta\right]\,, \qquad (2.63)$$

where the incoming momenta k_1 and k_2 correspond to the fields Z_μ and Z_ν, respectively, a_j and b_j are CP-even form factors and c_j is a CP-odd form factor. (We assume a convention where $\epsilon_{0123} = 1$.) The form factors depend on Lorentz invariant combinations of the external momenta. For the CP-violating 2HDM at tree level, $b_j = c_j = 0$ and $a_j = R_{j1}\cos\beta + R_{j2}\sin\beta$, where R is the mixing matrix defined in Eq. (2.27). The form factors b_j and c_j (and modifications of a_j) are generated by radiative loop corrections. These corrections can generate both dispersive (real) and absorptive (imaginary) contributions to the form factors (the latter corresponds to the possibility of on-shell intermediate states). Contributions to b_j and c_j can also be generated due to new physics at the TeV-scale. After integrating out the effects of the high-scale physics, effective local (dimension-five) operators of the form $Z_{\mu\nu}Z^{\mu\nu}h_j$ and $\epsilon_{\mu\nu\alpha\beta}Z^{\mu\nu}Z^{\alpha\beta}h_j$ can be generated in the low-energy effective Lagrangian that result in contributions to b_j and c_j, respectively [97,98], where $Z_{\mu\nu} \equiv \partial_\mu Z_\nu - \partial_\nu Z_\mu + ig\cos\theta_W(W_\mu^+W_\nu^- - W_\nu^+W_\mu^-)$ is the field strength tensor of the Z boson. The hermiticity of these two operators implies that the contributions of high-scale physics to the form factors must be real.

The discovery of a CP-violating signal in the ZZh_j interaction requires a detection of an interference effect between the CP-even and CP-odd form factors of Eq. (2.63). If the tree-level term a_j dominates, the direct observation of CP-violation will be difficult. In contrast, there are no tree-level couplings of the neutral Higgs bosons to gluon pairs or photon pairs, so that the loop coupling to the CP-even and CP-odd components of the neutral Higgs bosons can be competitive. One can also infer the existence of CP-violation indirectly (in the context of the 2HDM) if there is significant CP-mixing among the three neutral states. In this case, the observation of ZZh_j couplings for all three states h_j would provide strong evidence for the CP-mixing of the scalar states.

For a neutral Higgs boson with a mass below 140 GeV the most detailed information of its CP properties can be obtained from its decay into $\tau^+\tau^-$ [99–101] (a tool is provided in [102]). For larger Higgs masses, one must employ the decays into W^+W^- and/or ZZ [93], if the corresponding branching ratios are suitably large (in the decoupling regime only h_1 can have significant couplings to W^+W^- and ZZ). Finally, for Higgs masses above 350 GeV, one can employ the $t\bar{t}$ decay mode [103]. In each case, the CP properties can be determined by studying the angular distributions of the various final state decay products. Additional CP-odd observables can be constructed by considering the properties of the Higgs production process. The production of a neutral Higgs boson in association with hadronic jets (*e.g*, as in gauge boson fusion at the LHC [104]) or in association with $t\bar{t}$ [105, 106] have been investigated. We note that if Higgs production via diffractive processes is observable at the LHC, then the azimuthal angular distribution of the tagged protons can be used to study the CP-properties of the produced Higgs boson. For further details, see [107, 108] and Section 3.8.

At the ILC and CLIC, the Higgs bosons are produced in pairs or in association with other particles. At the PLC and at a $\mu^+\mu^-$ collider, one can produce a single neutral Higgs boson through a resonant s-channel process via $\gamma\gamma$ fusion and $\mu^+\mu^-$ annihilation, respectively. For example, in $\gamma\gamma$ fusion to a neutral Higgs boson, one can make use of the polarization of the photon beams to study in detail the CP-properties of the resonant neutral Higgs states [109]. The interference between a Higgs signal and the SM background can also provide information that enables one to determine the CP property of the Higgs boson. Specific examples will be cited below in the discussion of CP studies at the ILC and PLC.

2.2.3 SM-like Higgs boson scenario

The Higgs boson direct search limits and the global electroweak fits to the precision electroweak data from LEP, SLC and the Tevatron provides a strong hint for the existence of a SM-like Higgs boson with a mass in the range of 115 GeV—207 GeV [110]. Precision measurements of Higgs couplings and quantum numbers (spin and CP) at future colliders are needed to confirm the nature of such a particle. A SM-like Higgs boson can appear in both the CP-conserving and the CP-violating 2HDM in the decoupling regime as previously noted [58, 63]. In this case, the other Higgs boson masses of the model must be significantly larger than M_Z.

For special choices of the 2HDM parameters, a SM-like Higgs boson can also appear in a non-decoupling regime [58, 59, 90] of the model parameter space. In this latter case, a SM-like Higgs boson would possess tree-level couplings that approximately match those of the SM Higgs boson (although opposite to the SM signs of couplings are possible). However in contrast to the decoupling regime, the masses of the non-SM-like neutral and charged Higgs bosons in the non-decoupling regime need not be particularly heavy. It may be possible to distinguish a SM-like Higgs boson from the Higgs boson of the Standard Model due to the effects of one-loop induced couplings. For example, the couplings of a SM-like Higgs boson to two gluons and to two photons can deviate from those of the corresponding SM Higgs couplings, due to the contribution of a charged Higgs boson loop [59, 62].

In the non-decoupling scenario just considered, a very light h_1 may exist with suppressed couplings to gauge bosons, whereas the heavier H (in the CP-conserving model) or h_2 in the CP-violating model corresponds to a SM-like Higgs boson. In such a case, even a very light h or A (with the mass of the SM-like H above 114 GeV) is not excluded by LEP data in the CP conserving 2HDM-II as shown in section 2.2.1. In the MSSM with large loop-induced CP-violating Higgs Yukawa interactions, a benchmark scenario named CPX [111] has been provided for further studies of this scenario. The OPAL collaboration has reanalyzed its data in the light of the CPX scenario [112]. Combined LEP results and ATLAS prospects for this benchmark are provided in Sections 3.2 and 3.3.

In [113] very large non-decoupling effects were found in the CP conserving 2HDM due to loop corrections in Higgs self-couplings (for small η). These can yield deviations as large as 100% from the Standard Model prediction, even when all the other couplings of the lightest Higgs boson to gauge bosons and fermions are in good agreement with the Standard Model.

2.2.4 Tri-mixing scenarios

In some portion of the 2HDM parameter space, the three neutral Higgs bosons can be close in mass and have similar coupling strengths to the Z. This has been called the three-way mixing regime (in the CP-conserving case sometimes referred to as the intense coupling regime [44]).

A good experimental Higgs mass resolution is important to probe this scenario at the LHC. Here the mass resolution expected for the SM Higgs searches, which is between $\sim$ 300 MeV and 2 GeV [114, 115], should be sufficient. The total cross-section for Higgs production is divided up (roughly equally) among the three neutral Higgs bosons. One must check that the three h_iZZ couplings satisfy the vertical sum rule Eq. (2.58). This parameter regime seems very challenging at the Tevatron but might be easier to probe at the LHC. Detailed analyses of such scenarios were also performed for the ILC [116] and PLC [117]. A similar two-mixing scenario was considered in [43], for the PLC.

2.2.5 CP studies of the Higgs sector at the LHC

After the initial discovery of a (candidate) neutral Higgs boson at the LHC, it will be important to verify whether the properties of this state are consistent with those of the SM Higgs boson, or whether an extension of the SM Higgs sector is required. The CP properties can be determined at the LHC by studying angular distributions of the Higgs decay products. The $gg \to h_i \to f\bar{f}$ process has been considered for the $t\bar{t}$ final state in [103, 118] and analyses for $\tau^+\tau^-$ and $t\bar{t}$ final states are presented in

sections 2.7 and 2.8. The decay $h_i \to VV$ with $V = W^\pm$ or Z, followed by leptonic decays of the vector boson V has been considered in [93, 119]. The sensitivity of the four-lepton channel (for $h_i \to ZZ$) to CP-violating observables is examined in sections 2.12 and 2.11 and in section 2.13 for the $e^+e^-\mu^+\mu^-$ final states.

The CP properties can also be determined by studying angular distributions of particles produced in association with the h_i. The distribution of azimuthal angles of two light accompanying jets in h_ijj production via gluon-gluon and vector boson fusion are studied in section 2.10 as a probe for the CP properties of h_i. In the case of gluon fusion, this distribution might be diluted by higher order corrections [120]. In the $gg \to h_i t\bar{t}$ production, CP-sensitive variables can be build as studied in section 2.9. In this same production, certain weighted cross section integrals described in [121] can provide a determination of the CP nature of a light h_i. A similar study was performed in [122] for partonic processes involving gluons and light quarks accompanying by two jets, for neutral Higgs bosons lighter than 200 GeV.

Charged Higgs boson production and decays can also be useful for probing CP properties of the Higgs sector at LHC. The associated production of $H^\pm h_1$ with $H^\pm \to W^\pm h_1$ and $h_1 \to b\bar{b}$ yields events with four b-quarks, a charged lepton and missing transverse energy. There is virtually no Standard Model background, and the corresponding signal can be as large as 45 events for an integrated luminosity of 30 fb^{-1} at the LHC [123]. For $m_{H^\pm} < m_t$, the $t\bar{t}$ pair production, with one top quark decaying into $bH^\pm$ and $H^\pm \to W^\pm h_1 \to W^\pm b\bar{b}$ (and the other top quark decays into $bW^\pm$), yields a signal of four b quarks and two W bosons. It is relatively free of Standard Model background and can result in roughly 5000 events for a luminosity of 30 fb^{-1} at the LHC [124]. In some regions of the 2HDM parameter space, the study of $H^\pm W^\mp$ production might allow one to distinguish between Higgs sector of the MSSM and a general 2HDM [125]. Evidence for CP violation can be revealed in asymmetries in the associated production of a charged Higgs boson and the top quark [126]. Asymmetries in charged Higgs boson decay into $t\bar{b}, \bar{t}b$ can also be used to probe CP violation [127], whereas measuring the same asymmetries in $H^\pm \to \tau^\pm \nu_\tau$ decay is more challenging [128].

In a general 2HDM, one expects (at some level) the existence of FCNC processes and lepton-flavor-violating (LFV) processes in the leptonic sector, mediated by tree-level neutral Higgs boson exchange. For example, h_i can decay into 2 charged leptons of different flavors. Typical branching ratios compatible with current experimental data for LFV h_i decay can be found in [129]. The most promising decay is $h_1 \to \tau^\pm\mu^\mp$. Measurements of the muon anomalous magnetic moment [130] favor regions of the parameter space where the $h_1 \to \tau^\pm\mu^\mp$ decay can be seen at both the LHC and Tevatron [131].

2.2.6 CP studies of the Higgs sector at the ILC

We briefly survey some of the main aspects of the CP study at a high energy linear e^+e^- collider (ILC) with $\sqrt{s} = 500$—1000 GeV, assuming an integrated luminosity of 100 fb^{-1} and a longitudinally polarized electron beam (up to 90%). The main neutral Higgs production mechanisms at the ILC [132,133] are governed by the Higgs interaction with gauge bosons: $e^+e^- \to Zh_i$ via Higgs-strahlung, $e^+e^- \to \nu\bar{\nu}h_i$ via W^+W^- fusion and $e^+e^- \to e^+e^-h_i$ via ZZ-fusion. The gauge boson fusion processes become the dominant Higgs production processes at large $\sqrt{s}$. Neutral and charged Higgs bosons can also be produced in pairs: $e^+e^- \to h_ih_j$ $(i \neq j)$ via s-channel Z-exchange and $e^+e^- \to H^+H^-$ via s-channel γ and Z-exchange. Note that in the decoupling limit, the two heaviest neutral Higgs bosons (h_2 and h_3) and $H^\pm$ are heavy and roughly mass degenerate. Thus, the pair (or associated) production of a pair of heavy states is kinematically possible only if $\sqrt{s}$ is larger than twice the mass of the heavy Higgs states.

The Higgs-strahlung cross section $e^+e^- \to Zh_i$ depends on whether the h_i is CP-even, CP-odd, or a mixture [94, 95, 97, 134, 135]. For a CP-even (CP-odd) Higgs boson, the Z is longitudinally (transversally) polarized. The spin, parity and charge conjugation quantum numbers, J^{PC}, of the Higgs boson can potentially be determined independently of the model by studying the threshold dependence and angular distribution of the Higgs and Z boson [136]. The angular distribution of the fermions in the $Z \to f\bar{f}$ reflects the CP nature of the state h_i [95,97,134,135]. A full simulation was performed in [137]

for the TESLA design, with promising results. It should be noted that in the analyses cited above, generic CP-odd couplings of the Higgs boson to gauge boson pairs were assumed. In practice, such couplings are expected to be quite suppressed, as they are necessarily absent at tree-level and thus can only appear at one loop (in contrast to the tree-level CP-even couplings), as discussed in section 2.2.2.

The Yukawa couplings of the neutral Higgs bosons can be studied in the associated production processes $e^+e^- \to f\bar{f}h_i$, where $(f = b, t, \tau, \mu)$. The Yukawa process and the Higgs production processes $e^+e^- \to Zh_i$ and $e^+e^- \to h_ih_j$ $(i \neq j)$ are complementary in the search for at least one Higgs boson of the CP-violating 2HDM [65, 138]. In all these processes, correlations between the production and decay (with polarized initial beams) yield numerous observables that are sensitive to the spin and CP properties of the produced Higgs bosons. For example, the sensitivity to CP violation in the Yukawa coupling to b quarks, was studied in [139]. In this analysis the process $e^+e^- \to b\bar{b}\nu\bar{\nu}$ was considered for a Higgs boson with a mass of 120 GeV that decays primarily into $b\bar{b}$, and the interference between the Higgs signal and SM background was exploited to determine the CP properties of the Higgs boson. The process $e^+e^- \to t\bar{t}h_i$ alone may be sufficient to provide a reasonable determination of the $t\bar{t}$ and ZZ couplings and the CP-properties of the produced h_i [140]. The Yukawa interaction is also responsible for singly-produced charged Higgs bosons via $e^-e^+ \to b\bar{c}H^+$, $\tau\bar{\nu}H^+$. These production processes provide a test of the chirality of the charged Higgs boson Yukawa couplings [141].

The Higgs self-couplings are very difficult to ascertain at the LHC. At the ILC, these couplings can be measured with limited accuracy in the processes $e^+e^- \to Zh_ih_j$ and $e^+e^- \to \nu\bar{\nu}h_ih_j$ [113, 142, 143]. These processes depend both on the Higgs self couplings and the VVh_i and VVh_ih_j couplings.

2.2.7 CP studies of the Higgs sector at the PLC

By shining intense laser light on the electron (and positron) beam, one can convert the initial beam of the ILC into a photon beam via Compton backscattering. This provides a mechanism for using the ILC as an electron-photon or photon-photon collider. In the photon linear collider (PLC) mode of the ILC, the photon beams are produced with energies up to 80% of the electron-positron center-of-mass energy and with a luminosity similar to that of the original colliding e^+e^- beams. Moreover, it is possible to produce highly polarized photon beams (the degree of polarization depends on the polarization of the laser light employed in the Compton backscattering that produces the photon beam, and polarization of the electron beam). At the PLC, the neutral Higgs boson can be produced resonantly in the s-channel, leading to a higher mass reach than the parent e^+e^- collider. Moreover, the polarization of the photon beams can be selected to form an (approximately pure) CP-odd or CP-even initial state. This provides an ideal laboratory for studying the CP properties of the neutral Higgs boson. For example, CP-violating asymmetries in neutral Higgs boson processes can be constructed even without information on the final states.

The spin and parity of the Higgs boson can be measured in a model-independent way at the PLC using the $h_i \to ZZ$ (ZZ^*) decay channel [93], and the angular distributions of the fermions from the decays $Z \to f\bar{f}$. The detection of Higgs sector CP-violating effects can be ascertained by studying a variety of final states. By taking into account interference effects of the Higgs signal and background, one can extract both the Higgs partial width $\Gamma_{\gamma\gamma}$ and the phase of the Higgs amplitude, $\phi_{\gamma\gamma}$, for the W^+W^- final state [144] and for the $t\bar{t}$ final state [145]. Other analyses of CP violation in $\gamma\gamma \to h_i \to W^+W^-$ have been given in [146]; realistic simulations for the 2HDM with a SM-like Higgs boson and in a model independent approach were performed in [144, 147] and are discussed in section 2.14. In particular, the simultaneous simulation of ZZ and W^+W^- final states is crucial in determining the CP properties of the neutral Higgs bosons with masses in the range of 200—300 GeV. Various analyses related to heavy neutral Higgs boson production in $\gamma\gamma \to ZZ, ZH$, which also make use of the interference effects with the SM background, are given in [148]. The process $\gamma\gamma \to h_i \to t\bar{t}$ also provides an ideal setting for studying the CP properties of the neutral Higgs boson. Model independent studies of this channel are given in [145, 149–151].

Both linearly and circularly polarized photon beams are necessary in order to measure polarization asymmetries and to establish the CP property of the heavy h_i. Experimental signatures of CP-violating mixing of the heavy CP-even and CP-odd neutral Higgs states (H/A) at the PLC with (linear and circular) polarized beams were studied in [43] in the decoupling regime including effect of non-zero Higgs widths. Resonant loop-induced CP violation in Higgs-strahlung, in tri-mixing and two-mixing scenarios, was studied in [117]. The CP asymmetries in the production and decays of pairs of muons, taus, b and t quarks were used in this analysis. Although both analyses cited above were carried out for the case of the MSSM Higgs sector, the main results should hold for the more general (CP-violating) 2HDM.

The Yukawa couplings of the Higgs boson can be explored at the PLC by making use of another mechanism. The fermionic fusion, from the splitting of two photons into pairs of fermions, may lead to the production of neutral or charged Higgs bosons without strong suppression at high energies. This splitting leads to a collinear enhancement $\log(M_h/m_f)$ (where M_h is the mass of the produced Higgs boson), which can be interpreted as the generation of "partonic densities" in the photon. The $\tau\tau$ fusion was used e.g. in [152] as a method to determine the Yukawa coupling of neutral Higgs boson. Likewise, single charged Higgs boson production in $\gamma\gamma \to b\bar{c}H^+, \tau\bar{\nu}H^+$, via $\gamma \to c\bar{c}$ and $\gamma \to b\bar{b}$, may be useful to discriminate models [141]. It is possible to determine the chirality of Yukawa couplings $H^+bc, H^+\tau\nu$ by choosing the polarization of the colliding photon beams.

Finally, $\gamma\gamma \to h_ih_j$ (via box and triangle loops with gauge bosons and fermions) can be used to determine Higgs self-couplings [143], with larger sensitivity than in the "parent" e^+e^- collider.

2.2.8 CP studies of the Higgs sector at a multi-TeV lepton collider

In the decoupling limit, h_1 is nearly indistinguishable from the SM-Higgs boson. The heavier Higgs bosons h_2, h_3 and $H^\pm$ (which are degenerate in mass up to corrections of order $m_Z^2/m_{H^\pm}$) may be too heavy to be studied directly at the LHC and ILC. In this case, a multi-TeV lepton collider will be required to fully explore the Higgs sector and provide a comprehensive study of the heavy Higgs states, in particular of the Higgs sector CP-violation. Thus, we briefly survey the potential for CP studies at a high luminosity multi-TeV e^+e^- collider such as CLIC [71] and a $\mu^+\mu^-$ collider [72, 73].

At CLIC, the heavy Higgs states are produced in pairs via $e^+e^- \to h_ih_j$ ($j = 2, 3$) and $e^+e^- \to H^+H^-$ (note that single production of a heavy Higgs state: $e^+e^- \to h_1h_j$ ($j = 2, 3$) is suppressed in the decoupling limit [53, 58]). The dominant decay of the charged Higgs boson is $H^+ \to t\bar{b}$. An asymmetry between the H^+ and H^- partial decay rates into $t\bar{b}$ and $\bar{t}b$ would be a signal of CP-violation. A simulation performed in [153] suggests that a 10% asymmetry could be detected as a 3σ effect with $5\ \mathrm{ab}^{-1}$ of data at CLIC with $\sqrt{s} = 3$ TeV. No analogous study has yet been performed for the h_ih_j final state (see [154] for an analysis of the discovery potential for $e^+e^- \to HA$ at CLIC).

At a $\mu^+\mu^-$ collider, the s-channel single production of a heavy neutral Higgs boson [155, 156] provides a new discovery mode as compared to the e^+e^- colliders. This production mechanism is feasible at a $\mu^+\mu^-$ collider due to the mass enhancement in the Higgs coupling to $\mu^+\mu^-$ relative to e^+e^-. In addition, the charged Higgs boson can also be singly produced via $\mu^+\mu^- \to h_j \to H^\pm W^\mp$. The superb energy resolution of the $\mu^+\mu^-$ would permit the separation of the heavy neutral Higgs boson s-channel resonances, even though these states are nearly degenerate in mass. It is demonstrated in [157] that the s-channel production rates for the heavy neutral Higgs states and the transverse-polarization asymmetries are complementary in diagnosing Higgs sector CP-violation. Additional CP-violating observables can be studied by examining the heavy Higgs decays into a pair of third generation quarks or leptons [158]. The importance of the muon beam polarization for Higgs CP studies in $\mu^+\mu^- \to h_j$ ($j = 2, 3$) is emphasized in [159]. In singly produced charged Higgs bosons in association with the W, an asymmetry in the production rates for $H^\pm W^\mp$ also provides a signal of CP violation [160].

2.3 Basis-independent treatment of Higgs couplings in the CP-violating 2HDM

Howard E. Haber

In the most general two-Higgs-doublet model (2HDM), there is no distinction between the two complex hypercharge-one SU(2) doublet scalar fields, Φ_a ($a = 1, 2$). Thus, any two orthonormal linear combinations of these two fields can serve as a basis for the Lagrangian. All physical observables of the model must be basis-independent. For example, $\tan\beta \equiv v_2/v_1$ [see Eq. (2.7)] is basis-dependent and thus cannot be a physical parameter of the model [14–16]. Basis independent techniques have been exploited to great advantage in [14, 19, 37, 40, 41] in the study of the CP-violating structure of the 2HDM (and extend the results originally obtained in [38, 39].) In addition, the importance of the scalar-doublet field redefinitions (and rephasing transformations) have been emphasized, and some of their implications for 2HDM phenomenology have been explored in [15]. In this paper, we employ the basis-independent formalism to obtain an invariant description of all 2HDM couplings.

2.3.1 Basis-independent formalism for the 2HDM

The fields of the 2HDM consist of two identical complex hypercharge-one, SU(2) doublet scalar fields $\Phi_a(x) \equiv (\Phi_a^+(x)\,,\, \Phi_a^0(x))$, where $a = 1, 2$ can be considered a Higgs "flavor" index. The most general redefinition of the scalar fields (which leaves the form of the canonical kinetic energy terms invariant) corresponds to a global U(2) transformation, $\Phi_a \to U_{a\bar{b}}\Phi_b$ [and $\Phi_{\bar{a}}^\dagger \to \Phi_{\bar{b}}^\dagger U_{b\bar{a}}^\dagger$]. Here, it is convenient to introduce unbarred and barred indices with a summation convention in which only barred–unbarred index pairs of the same letter are summed. The basis-independent formalism consists of writing all equations involving the Higgs sector fields in a U(2)-covariant fashion. Basis-independent quantities can then be identified as invariant scalars under U(2). The U(2)-invariants are easily identified as products of tensor quantities with all barred and unbarred index pairs summed with no flavor indices left over.

The scalar potential can be written in U(2)-covariant form [10, 14] in terms of the tensors $Y_{a\bar{b}}$ and $Z_{a\bar{b}c\bar{d}}$ as shown in Eq. (2.2). The vacuum of the theory is assumed to respect the electromagnetic $\mathrm{U(1)_{EM}}$ gauge symmetry. The $\mathrm{U(1)_{EM}}$-conserving vacuum expectation value can be written as:

$$\langle\Phi_a\rangle = \frac{v}{\sqrt{2}}\begin{pmatrix} 0 \\ \widehat{v}_a \end{pmatrix}\,, \quad (a = 1, 2)\,, \quad \text{with} \qquad \widehat{v}_a \equiv e^{i\eta}\begin{pmatrix} c_\beta \\ s_\beta\, e^{i\xi} \end{pmatrix}\,, \tag{2.64}$$

where $v \equiv 2m_W/g = 246$ GeV, $c_\beta \equiv \cos\beta$, $s_\beta \equiv \sin\beta$ and $\widehat{v}_a$ is a vector of unit norm. The overall phase η is arbitrary. By convention, we take $0 \leq \beta \leq \pi/2$ and $0 \leq \xi < 2\pi$.

Under a U(2)-flavor transformation, $\widehat{v}_a \to U_{a\bar{b}}\widehat{v}_b$. The unit vector $\widehat{v}_a$ can also be considered to be an eigenvector of unit norm of the Hermitian matrix $V_{a\bar{b}} \equiv \widehat{v}_a\widehat{v}_{\bar{b}}^*$. Since V is Hermitian, it possesses a second eigenvector of unit norm that is orthogonal to $\widehat{v}_a$. We denote this eigenvector by $\widehat{w}_a$, which satisfies $\widehat{v}_{\bar{b}}^*\widehat{w}_b = 0$. The most general solution for $\widehat{w}_a$, up to an overall multiplicative phase factor, is:

$$\widehat{w}_b \equiv \widehat{v}_{\bar{a}}^*\,\epsilon_{ab} = e^{-i\eta}\begin{pmatrix} -s_\beta\, e^{-i\xi} \\ c_\beta \end{pmatrix}\,. \tag{2.65}$$

The inverse relation to Eq. (2.65) is easily obtained: $\widehat{v}_{\bar{a}}^* = \epsilon_{\bar{a}\bar{b}}\,\widehat{w}_b$. Above, we have introduced two Levi-Civita tensors with $\epsilon_{12} = -\epsilon_{21} = 1$ and $\epsilon_{11} = \epsilon_{22} = 0$. However, ϵ_{ab} and $\epsilon_{\bar{a}\bar{b}}$ are not proper tensors with respect to the full flavor-U(2) group (although these are invariant SU(2)-tensors). That is, $\widehat{w}_a$ does not transform covariantly with respect to the full flavor-U(2) group. If $U = e^{i\psi}\widehat{U}$, with $\det\widehat{U} = 1$ (and consequently $\det U = e^{2i\psi}$), it is simple to check that under a U(2) transformation

$$\widehat{v}_a \to U_{a\bar{b}}\widehat{v}_b \qquad \text{implies that} \qquad \widehat{w}_a \to (\det U)^{-1}\,U_{a\bar{b}}\,\widehat{w}_b\,. \tag{2.66}$$

Henceforth, we shall define a pseudotensor as a tensor that transform covariantly with respect to the flavor-SU(2) subgroup but whose transformation law with respect to the full flavor-U(2) group is

only covariant modulo an overall nontrivial phase equal to some integer power of $\det U$. Thus, $\widehat{w}_a$ is a pseudovector. However, we can use $\widehat{w}_a$ to construct proper tensors. For example, the Hermitian matrix $W_{a\bar{b}} \equiv \widehat{w}_a \widehat{w}^*_{\bar{b}} = \delta_{a\bar{b}} - V_{a\bar{b}}$ is a proper second-ranked tensor.

One can write a set of independent scalar quantities constructed out of $Y_{a\bar{b}}$, $Z_{a\bar{b}c\bar{d}}$, v_a and w_a. There are six independent invariant quantities:

$$\begin{aligned} Y_1 &\equiv \mathrm{Tr}\,(YV)\,, & Y_2 &\equiv \mathrm{Tr}\,(YW)\,, \\ Z_1 &\equiv Z_{a\bar{b}c\bar{d}} V_{b\bar{a}} V_{d\bar{c}}\,, & Z_2 &\equiv Z_{a\bar{b}c\bar{d}} W_{b\bar{a}} W_{d\bar{c}}\,, \\ Z_3 &\equiv Z_{a\bar{b}c\bar{d}} V_{b\bar{a}} W_{d\bar{c}}\,, & Z_4 &\equiv Z_{a\bar{b}c\bar{d}} V_{b\bar{c}} W_{d\bar{a}}\,, \end{aligned} \tag{2.67}$$

and four independent pseudo-invariant quantities:

$$\begin{aligned} Y_3 &\equiv Y_{a\bar{b}}\, \widehat{v}^*_{\bar{a}}\, \widehat{w}_b\,, & Z_5 &\equiv Z_{a\bar{b}c\bar{d}}\, \widehat{v}^*_{\bar{a}}\, \widehat{w}_b\, \widehat{v}^*_{\bar{c}}\, \widehat{w}_d\,, \\ Z_6 &\equiv Z_{a\bar{b}c\bar{d}}\, \widehat{v}^*_{\bar{a}}\, \widehat{v}_b\, \widehat{v}^*_{\bar{c}}\, \widehat{w}_d\,, & Z_7 &\equiv Z_{a\bar{b}c\bar{d}}\, \widehat{v}^*_{\bar{a}}\, \widehat{w}_b\, \widehat{w}^*_{\bar{c}}\, \widehat{w}_d\,, \end{aligned} \tag{2.68}$$

that depend linearly on Y and Z. Note that the invariants are manifestly real, whereas the pseudo-invariants are potentially complex. Using Eq. (2.66), it follows that under a flavor-U(2) transformation specified by U, the pseudo-invariants Y_3, Z_5, Z_6 and Z_7 transform as:

$$[Y_3, Z_6, Z_7] \to (\det U)^{-1} [Y_3, Z_6, Z_7] \qquad \text{and} \qquad Z_5 \to (\det U)^{-2} Z_5\,. \tag{2.69}$$

Thus, Eqs. (2.67) and (2.68) correspond to thirteen invariant real degrees of freedom (ten magnitudes and three relative phases) prior to imposing the scalar potential minimum conditions:

$$Y_1 = -\tfrac{1}{2} Z_1 v^2\,, \qquad\qquad Y_3 = -\tfrac{1}{2} Z_6 v^2\,. \tag{2.70}$$

This leaves eleven independent real degrees of freedom (one of which is the vacuum expectation value v) that specify the 2HDM parameter space.

2.3.2 (Pseudo)-invariants and the Higgs bases

Once the scalar potential minimum is determined, which defines $\widehat{v}_a$, one class of basis choices is uniquely selected. Suppose we begin in a generic Φ_1–Φ_2 basis. We define new Higgs doublet fields:

$$\boldsymbol{H}_1 = (H_1^+\,,\, H_1^0) \equiv \hat{v}^*_{\bar{a}} \Phi_a\,, \qquad\qquad \boldsymbol{H}_2 = (H_2^+\,,\, H_2^0) \equiv \hat{w}^*_{\bar{a}} \Phi_a = \epsilon_{\bar{b}\bar{a}} \widehat{v}_b \Phi_a\,. \tag{2.71}$$

With respect to U(2) transformations, $\boldsymbol{H}_1$ is an invariant field and $\boldsymbol{H}_2$ is a pseudo-invariant field that transforms as $\boldsymbol{H}_2 \to (\det U) \boldsymbol{H}_2$. The latter phase freedom defines a class of Higgs bases. The definitions of $\boldsymbol{H}_1$ and $\boldsymbol{H}_2$ imply that

$$\langle H_1^0 \rangle = v/\sqrt{2}\,, \qquad\qquad \langle H_2^0 \rangle = 0\,. \tag{2.72}$$

Hence, all Higgs bases are characterized by: $\widehat{v} = (1, 0)$ and $\widehat{w} = (0, 1)$. Using Eqs. (2.67) and (2.68), one identifies Y_1, Y_2, Y_3 and Z_1, Z_2,…,Z_7 as the coefficients of the 2HDM scalar potential in any Higgs basis.

Explicitly, the scalar field doublets in the Higgs basis can be parameterized as follows:

$$\boldsymbol{H}_1 = \begin{pmatrix} G^+ \\ \frac{1}{\sqrt{2}} \left(v + \phi_1^0 + i G^0 \right) \end{pmatrix}\,, \qquad \boldsymbol{H}_2 = \begin{pmatrix} H^+ \\ \frac{1}{\sqrt{2}} \left(\phi_2^0 + i a^0 \right) \end{pmatrix}\,, \tag{2.73}$$

where $G^\pm$ are the charged Goldstone bosons, G^0 is the CP-odd neutral Goldstone boson, and $H^\pm$ are the charged Higgs bosons with mass: $M^2_{H^\pm} = Y_2 + \frac{1}{2} Z_3 v^2$. Since $\widehat{v}$ is a vector and $\widehat{w}$ is a pseudovector, it follows that $G^\pm$ is an invariant field and $H^\pm$ is a pseudo-invariant field that transforms as:

$$H^\pm \to (\det U)^{\pm 1} H^\pm \tag{2.74}$$

with respect to flavor-U(2) transformations. The neutral Higgs mass-eigenstates are linear combinations of ϕ_1^0, ϕ_2^0 and a^0. CP-violation due to the mixing of neutral scalar CP-eigenstates and/or direct CP-violation in the bosonic interactions of the gauge/Higgs bosons are *absent* if and only if [14, 38, 39]:

$$\mathrm{Im}\,[Z_5^* Z_6^2] = \mathrm{Im}\,[Z_6 Z_7^*] = \mathrm{Im}\,[Z_5^*(Z_6+Z_7)^2] = 0\,. \tag{2.75}$$

2.3.3 The physical Higgs mass-eigenstates

It is simplest to perform the diagonalization of the neutral scalar squared-mass matrix in the Higgs basis. As in Section 2.1, we denote the neutral mass-eigenstate Higgs fields by h_1, h_2 and h_3. The angles θ_{ij} parameterize the rotation matrix that converts the neutral Higgs basis fields ϕ_1^0, ϕ_2^0 and a^0 into the mass-eigenstate fields h_k. Details of the diagonalization procedure can be found in [16].[9] The end result is:

$$\begin{pmatrix} h_1 \\ h_2 \\ h_3 \end{pmatrix} = \begin{pmatrix} q_{11} & \frac{1}{\sqrt{2}} q_{12}^* \, e^{i\theta_{23}} & \frac{1}{\sqrt{2}} q_{12} \, e^{-i\theta_{23}} \\ q_{21} & \frac{1}{\sqrt{2}} q_{22}^* \, e^{i\theta_{23}} & \frac{1}{\sqrt{2}} q_{22} \, e^{-i\theta_{23}} \\ q_{31} & \frac{1}{\sqrt{2}} q_{32}^* \, e^{i\theta_{23}} & \frac{1}{\sqrt{2}} q_{32} \, e^{-i\theta_{23}} \end{pmatrix} \begin{pmatrix} \sqrt{2}\,\mathrm{Re}\, H_1^0 - v \\ H_2^0 \\ H_2^{0\,\dagger} \end{pmatrix}, \tag{2.76}$$

where

$$\begin{aligned} q_{11} &= c_{13}c_{12}\,, & q_{21} &= c_{13}s_{12}\,, & q_{31} &= s_{13}\,, & q_{41} &= i\,, \\ q_{12} &= -s_{12} - ic_{12}s_{13}\,, & q_{22} &= c_{12} - is_{12}s_{13}\,, & q_{32} &= ic_{13}\,, & q_{42} &= 0\,, \end{aligned} \tag{2.77}$$

with $c_{ij} \equiv \cos\theta_{ij}$ and $s_{ij} \equiv \sin\theta_{ij}$. We have also defined $q_{4\ell}$ ($\ell = 1, 2$) for later use. In particular,

$$q_{k\ell} \to q_{k\ell}\,, \qquad \text{and} \qquad e^{i\theta_{23}} \to (\det U)^{-1} e^{i\theta_{23}}\,, \tag{2.78}$$

under a U(2) transformation. That is, the $q_{k\ell}$ are invariants, which implies that θ_{12} and θ_{13} are U(2)-invariant angles, whereas $e^{i\theta_{23}}$ is a pseudo-invariant. Note that since H_1 and $e^{i\theta_{23}} H_2$ are U(2)-invariant fields, it follows that the h_k are invariant fields, as expected. We shall also define $Z_5 \equiv |Z_5| e^{2i\theta_5}$ and $Z_{6,7} \equiv |Z_{6,7}| e^{i\theta_{6,7}}$, in which case the $\phi_n \equiv \theta_n - \theta_{23}$ ($n = 5, 6, 7$) are U(2)-invariant angles.

If $\mathrm{Im}\,(Z_5^* Z_6^2) = 0$, then the neutral scalar squared-mass matrix can be transformed into block diagonal form, which contains the squared-mass of a CP-odd neutral mass-eigenstate Higgs field A and a 2×2 sub-matrix that yields the squared-masses of two CP-even neutral mass-eigenstate Higgs fields h and H. The analytic form of this diagonalization is simple and yields the well-known results of the CP-conserving 2HDM . If $\mathrm{Im}\,(Z_5^* Z_6^2) \neq 0$, then the neutral scalar mass-eigenstates do not possess definite CP quantum numbers, and the three invariant mixing angles θ_{12}, θ_{13} and $\phi_6 \equiv \theta_6 - \theta_{23}$ are non-trivial.

The angles θ_{13} and ϕ_6 are determined modulo π from [16]:

$$\tan\theta_{13} = \frac{\mathrm{Im}\,(Z_5\, e^{-2i\theta_{23}})}{2\,\mathrm{Re}\,(Z_6\, e^{-i\theta_{23}})}\,, \qquad \tan 2\theta_{13} = \frac{2\,\mathrm{Im}\,(Z_6\, e^{-i\theta_{23}})}{Z_1 - A^2/v^2}\,, \tag{2.79}$$

where $A^2 \equiv Y_2 + \frac{1}{2}[Z_3 + Z_4 - \mathrm{Re}\,(Z_5 e^{-2i\theta_{23}})]v^2$. These equations exhibit multiple solutions (modulo π) corresponding to different orderings of the h_k masses. Likewise, the angle θ_{12} is determined from:

$$\tan 2\theta_{12} = \frac{2\cos 2\theta_{13}\;\mathrm{Re}\,(Z_6\, e^{-i\theta_{23}})}{c_{13}\left[c_{13}^2(A^2/v^2 - Z_1) + \cos 2\theta_{13}\;\mathrm{Re}\,(Z_5\, e^{-2i\theta_{23}})\right]}\,. \tag{2.80}$$

For a given solution of θ_{13} and ϕ_6, Eq. (2.80) yields two solutions for θ_{12} modulo π, corresponding to the two possible relative mass orderings of h_1 and h_2.

[9] This procedure differs somewhat from the one presented in section 2.1.3.1. In the latter, the diagonalization of the scalar squared-mass matrix is carried out in a generic basis. The advantage of performing this computation in the Higgs basis is that it allows one to easily identify the (pseudo)-invariant quantities that relate the neutral scalar interaction- and mass-eigenstates.

The neutral Higgs boson masses $M_k \equiv M_{h_k}$ can be expressed in terms of Z_1, Z_6 and the θ_{ij}:

$$M_1^2 = \left[Z_1 - \frac{s_{12}}{c_{12}c_{13}} \operatorname{Re}\left(Z_6\, e^{-i\theta_{23}}\right) + \frac{s_{13}}{c_{13}} \operatorname{Im}\left(Z_6\, e^{-i\theta_{23}}\right) \right] v^2 \,, \tag{2.81}$$

$$M_2^2 = \left[Z_1 + \frac{c_{12}}{s_{12}c_{13}} \operatorname{Re}\left(Z_6\, e^{-i\theta_{23}}\right) + \frac{s_{13}}{c_{13}} \operatorname{Im}\left(Z_6\, e^{-i\theta_{23}}\right) \right] v^2 \,, \tag{2.82}$$

$$M_3^2 = \left[Z_1 - \frac{c_{13}}{s_{13}} \operatorname{Im}\left(Z_6\, e^{-i\theta_{23}}\right) \right] v^2 \,. \tag{2.83}$$

Eqs. (2.79) and (2.81)–(2.83) can be used to obtain [16]:

$$s_{13}^2 = \frac{(Z_1 v^2 - M_1^2)(Z_1 v^2 - M_2^2) + |Z_6|^2 v^4}{(M_3^2 - M_1^2)(M_3^2 - M_2^2)} \,, \qquad c_{13}^2 s_{12}^2 = \frac{(Z_1 v^2 - M_1^2)(M_3^2 - Z_1 v^2) - |Z_6|^2 v^4}{(M_2^2 - M_1^2)(M_3^2 - M_2^2)} \,, \tag{2.84}$$

and

$$\sin 2\theta_{12} = \frac{2\,|Z_6| v^2 \cos\phi_6}{c_{13}(M_2^2 - M_1^2)} \,, \qquad \tan 2\phi_6 = \frac{\operatorname{Im}\left(Z_5^* Z_6^2\right)}{\operatorname{Re}\left(Z_5^* Z_6^2\right) + \dfrac{|Z_6|^4 v^2}{M_3^2 - Z_1 v^2}} \,. \tag{2.85}$$

These results uniquely determine the invariant angles (modulo π) for a given h_k mass ordering.

Using Eqs. (2.73) and (2.76), one obtains the following U(2)-covariant expression for the scalar fields in a generic basis in terms of mass-eigenstate fields:

$$\Phi_a = \begin{pmatrix} G^+ \widehat{v}_a + H^+ \widehat{w}_a \\ \dfrac{v}{\sqrt{2}} \widehat{v}_a + \dfrac{1}{\sqrt{2}} \displaystyle\sum_{k=1}^{4} \left(q_{k1} \widehat{v}_a + q_{k2} e^{-i\theta_{23}} \widehat{w}_a \right) h_k \end{pmatrix} , \tag{2.86}$$

where $h_4 \equiv G^0$ and the $q_{k\ell}$ have been given in Eq. (2.77).

2.3.4 Higgs boson couplings

The gauge boson–Higgs boson interactions are governed by the following interaction Lagrangians:

$$\begin{aligned} \mathscr{L}_{VVH} = {} & \left(g m_W W_\mu^+ W^{\mu -} + \frac{g}{2c_W} m_Z Z_\mu Z^\mu \right) \operatorname{Re}\left(q_{k1}\right) h_k \\ & + e m_W A^\mu (W_\mu^+ G^- + W_\mu^- G^+) - g m_Z s_W^2 Z^\mu (W_\mu^+ G^- + W_\mu^- G^+) \,, \end{aligned} \tag{2.87}$$

$$\begin{aligned} \mathscr{L}_{VVHH} = {} & \left[\tfrac{1}{4} g^2 W_\mu^+ W^{\mu -} + \frac{g^2}{8c_W^2} Z_\mu Z^\mu \right] \operatorname{Re}\left(q_{j1}^* q_{k1} + q_{j2}^* q_{k2}\right) h_j h_k \\ & + \left[e^2 A_\mu A^\mu + \frac{g^2}{c_W^2} \left(\tfrac{1}{2} - s_W^2\right)^2 Z_\mu Z^\mu + \frac{2ge}{c_W} \left(\tfrac{1}{2} - s_W^2\right) A_\mu Z^\mu \right] (G^+ G^- + H^+ H^-) \\ & + \left\{ \left(\tfrac{1}{2} e g A^\mu W_\mu^+ - \frac{g^2 s_W^2}{2c_W} Z^\mu W_\mu^+ \right) (q_{k1} G^- + q_{k2}\, e^{-i\theta_{23}} H^-) h_k + \text{h.c.} \right\} , \end{aligned} \tag{2.88}$$

$$\begin{aligned} \mathscr{L}_{VHH} = {} & \frac{g}{4c_W} \operatorname{Im}\left(q_{j1} q_{k1}^* + q_{j2} q_{k2}^*\right) Z^\mu h_j \overleftrightarrow{\partial_\mu}\, h_k + \frac{ig}{c_W} \left(\tfrac{1}{2} - s_W^2\right) Z^\mu (G^+ \overleftrightarrow{\partial_\mu}\, G^- + H^+ \overleftrightarrow{\partial_\mu}\, H^-) \\ & - \tfrac{1}{2} g \left\{ i W_\mu^+ \left[q_{k1} G^- \overleftrightarrow{\partial^\mu}\, h_k + q_{k2} e^{-i\theta_{23}} H^- \overleftrightarrow{\partial^\mu}\, h_k \right] + \text{h.c.} \right\} , \\ & + ie A^\mu (G^+ \overleftrightarrow{\partial_\mu}\, G^- + H^+ \overleftrightarrow{\partial_\mu}\, H^-) \end{aligned} \tag{2.89}$$

where $s_W \equiv \sin\theta_W$, $c_W \equiv \cos\theta_W$ and there is an implicit sum over the repeated indices $j,k = 1,\ldots,4$ (with $h_4 = G^0$). Since $e^{-i\theta_{23}}H^-$ is an invariant field, Eqs. (2.87)–(2.89) are indeed U(2)-invariant.

Likewise, one can work out the cubic and quartic Higgs boson self-couplings [16]:

$$\begin{aligned}
\mathscr{L}_{3h} = &-\tfrac{1}{2}v\,h_jh_kh_\ell\Big[q_{j1}q_{k1}^*\,\mathrm{Re}\,(q_{\ell1})Z_1 + q_{j2}q_{k2}^*\,\mathrm{Re}\,(q_{\ell1})(Z_3+Z_4) + \mathrm{Re}\,(q_{j1}^*q_{k2}q_{\ell2}Z_5\,e^{-2i\theta_{23}}) \\
&\qquad + \mathrm{Re}\,\Big([2q_{j1}+q_{j1}^*]q_{k1}^*q_{\ell2}Z_6\,e^{-i\theta_{23}}\Big) + \mathrm{Re}\,(q_{j2}^*q_{k2}q_{\ell2}Z_7\,e^{-i\theta_{23}})\Big] \\
&-v\,h_kG^+G^-\Big[\mathrm{Re}\,(q_{k1})Z_1 + \mathrm{Re}\,(q_{k2}\,e^{-i\theta_{23}}Z_6)\Big] - v\,h_kH^+H^-\Big[\mathrm{Re}\,(q_{k1})Z_3 + \mathrm{Re}\,(q_{k2}\,e^{-i\theta_{23}}Z_7)\Big] \\
&-\tfrac{1}{2}v\,h_k\Big\{G^-H^+\,e^{i\theta_{23}}\Big[q_{k2}^*Z_4 + q_{k2}\,e^{-2i\theta_{23}}Z_5 + 2\,\mathrm{Re}\,(q_{k1})Z_6\,e^{-i\theta_{23}}\Big] + \mathrm{h.c.}\Big\}\,, \qquad (2.90)
\end{aligned}$$

and

$$\begin{aligned}
\mathscr{L}_{4h} = &-\tfrac{1}{8}h_jh_kh_lh_m\Big[q_{j1}q_{k1}q_{\ell1}^*q_{m1}^*Z_1 + q_{j2}q_{k2}q_{\ell2}^*q_{m2}^*Z_2 + 2q_{j1}q_{k1}^*q_{\ell2}q_{m2}^*(Z_3+Z_4) \\
&+2\,\mathrm{Re}\,(q_{j1}^*q_{k1}^*q_{\ell2}q_{m2}Z_5\,e^{-2i\theta_{23}}) + 4\,\mathrm{Re}\,(q_{j1}q_{k1}^*q_{\ell1}^*q_{m2}Z_6\,e^{-i\theta_{23}}) + 4\,\mathrm{Re}\,(q_{j1}^*q_{k2}q_{\ell2}q_{m2}^*Z_7\,e^{-i\theta_{23}})\Big] \\
&-\tfrac{1}{2}h_jh_kG^+G^-\Big[q_{j1}q_{k1}^*Z_1 + q_{j2}q_{k2}^*Z_3 + 2\,\mathrm{Re}\,(q_{j1}q_{k2}Z_6\,e^{-i\theta_{23}})\Big] \\
&-\tfrac{1}{2}h_jh_kH^+H^-\Big[q_{j2}q_{k2}^*Z_2 + q_{j1}q_{k1}^*Z_3 + 2\,\mathrm{Re}\,(q_{j1}q_{k2}Z_7\,e^{-i\theta_{23}})\Big] \\
&-\tfrac{1}{2}h_jh_k\Big\{G^-H^+\,e^{i\theta_{23}}\Big[q_{j1}q_{k2}^*Z_4 + q_{j1}^*q_{k2}Z_5\,e^{-2i\theta_{23}} + q_{j1}q_{k1}^*Z_6\,e^{-i\theta_{23}} + q_{j2}q_{k2}^*Z_7\,e^{-i\theta_{23}}\Big] + \mathrm{h.c.}\Big\} \\
&-\tfrac{1}{2}Z_1G^+G^-G^+G^- - \tfrac{1}{2}Z_2H^+H^-H^+H^- - (Z_3+Z_4)G^+G^-H^+H^- - \tfrac{1}{2}Z_5H^+H^+G^-G^- \\
&-\tfrac{1}{2}Z_5^*H^-H^-G^+G^+ - G^+G^-(Z_6H^+G^- + Z_6^*H^-G^+) - H^+H^-(Z_7H^+G^- + Z_7^*H^-G^+), \qquad (2.91)
\end{aligned}$$

where there is an implicit sum over the repeated indices j, k, ℓ, $m = 1,2,3,4$ (with $h_4 = G^0$). Using Eq. (2.74) and noting that the combinations $Z_5e^{-2i\theta_{23}}$, $Z_6e^{-i\theta_{23}}$ and $Z_7e^{-i\theta_{23}}$ are U(2)-invariant quantities, it follows that the cubic and quartic Higgs boson self-couplings are also U(2)-invariant.

Expressions for the cubic and quartic Higgs self-couplings in the CP-violating 2HDM have also been obtained in terms of generic basis parameters in [15, 47, 161], and an application of these results to the CPX scenario [111] of the minimal supersymmetric extension of the Standard Model (MSSM) is given in Section 3.6. Indeed, the effective Lagrangian of the MSSM Higgs sector *is* a general CP-violating 2HDM when one-loop radiative corrections (which are sensitive to supersymmetry-breaking effects and new CP-violating phases) are taken into account. The relative simplicity of the Higgs self-couplings given in Eqs. (2.90) and (2.91) illustrates the power of the basis-independent techniques.

The Higgs couplings to quarks are governed by the Yukawa Lagrangian given in Eq. (2.46) In terms of the quark mass-eigenstate fields, Eq. (2.46) can be expressed in U(2)-covariant form:.[10]

$$-\mathscr{L}_{\rm Y} = \overline{Q}_L\widetilde{\Phi}_{\bar{a}}\eta_a^U U_R + \overline{Q}_L\Phi_a\eta_{\bar{a}}^{D\,\dagger}D_R + \mathrm{h.c.}\,, \qquad (2.92)$$

where $\widetilde{\Phi}_{\bar{a}} \equiv i\sigma_2\Phi_{\bar{a}}^*$, and $\eta_a^U \equiv (V_L^U\Gamma_1V_R^{U\,\dagger}\,,\, V_L^U\Gamma_2V_R^{U\,\dagger})$ and $\eta_a^D \equiv (V_R^D\Delta_1V_L^{D\,\dagger}\,,\, V_R^D\Delta_2V_L^{D\,\dagger})$. We employ the standard notation: $\psi_{R,L} \equiv P_{R,L}\psi$ with $P_{R,L} \equiv \frac{1}{2}(1\pm\gamma_5)$. The unitary matrices $V_{L,R}^U$ and $V_{L,R}^D$ relate the quark interaction-eigenstate and quark mass-eigenstate fields via the bi-unitary transformations of Eq. (2.47). One can rewrite Eq. (2.92) in terms of Higgs basis scalar fields:

$$-\mathscr{L}_{\rm Y} = \overline{Q_L}(\widetilde{\boldsymbol{H}}_1\kappa^U + \widetilde{\boldsymbol{H}}_2\rho^U)U_R + \overline{Q}_L(\boldsymbol{H}_1\kappa^{D\,\dagger} + \boldsymbol{H}_2\rho^{D\,\dagger})D_R + \mathrm{h.c.}\,, \qquad (2.93)$$

[10] To obtain the Higgs couplings to leptons, let $Q \to L$ and $D \to E$, and omit U (right-handed neutrinos are not included).

where

$$\kappa^Q \equiv \widehat{v}_{\bar{a}}^* \eta_a^Q = \sqrt{2} M_Q / v \,, \qquad \rho^Q \equiv \widehat{w}_{\bar{a}}^* \eta_a^Q \,. \tag{2.94}$$

Under a U(2) transformation, κ^Q is invariant, whereas ρ^Q is a pseudo-invariant that transforms as:

$$\rho^Q \to (\det U) \rho^Q \,. \tag{2.95}$$

By construction, κ^U and κ^D are proportional to the (real non-negative) diagonal quark mass matrices, as indicated in Eq. (2.50). That is, we have chosen the unitary matrices V_L^U, V_R^U, V_L^D and V_R^D such that M_D and M_U are diagonal matrices with real non-negative entries. In the general 2HDM, the ρ^Q are arbitrary complex 3×3 matrices.

In order to determine the interactions of the Higgs (and Goldstone) bosons with the quark mass eigenstates, one can bypass the intermediate step involving the Higgs basis by inserting Eq. (2.86) into Eq. (2.92) to obtain:

$$\begin{aligned} -\mathscr{L}_Y = {} & \frac{1}{v} \overline{D} \left\{ M_D (q_{k1} P_R + q_{k1}^* P_L) + \frac{v}{\sqrt{2}} \left[q_{k2} \, [e^{i\theta_{23}} \rho^D]^\dagger P_R + q_{k2}^* \, e^{i\theta_{23}} \rho^D P_L \right] \right\} D h_k \\ & + \frac{1}{v} \overline{U} \left\{ M_U (q_{k1} P_L + q_{k1}^* P_R) + \frac{v}{\sqrt{2}} \left[q_{k2}^* \, e^{i\theta_{23}} \rho^U P_R + q_{k2} \, [e^{i\theta_{23}} \rho^U]^\dagger P_L \right] \right\} U h_k \\ & + \left\{ \overline{U} \left[K [\rho^D]^\dagger P_R - [\rho^U]^\dagger K P_L \right] D H^+ + \frac{\sqrt{2}}{v} \, \overline{U} \left[K M_D P_R - M_U K P_L \right] D G^+ + \text{h.c.} \right\} , \end{aligned} \tag{2.96}$$

where $k = 1, \ldots 4$. Since $e^{i\theta_{23}} \rho^Q$ and $[\rho^Q]^\dagger H^+$ are U(2)-invariant, it follows that Eq. (2.96) is a basis-independent expression of the Higgs-quark interactions.

The Higgs-quark couplings are generically CP-violating as a result of the complexity of the q_{k2} and the fact that the matrices $e^{i\theta_{23}} \rho^Q$ are not generally Hermitian or anti-Hermitian. Consequently, the neutral Higgs bosons (h_1, h_2 and h_3) are typically states of indefinite CP quantum number (whereas $h_4 \equiv G^0$ is always a pure CP-odd state). Basis-independent conditions for the CP-invariance of the neutral Higgs boson couplings to quark pairs are obtained by requiring that Eq. (2.75) is satisfied and [16]:

$$Z_5 [\rho^Q]^2 \,, \;\; Z_6 \rho^Q \,, \;\; \text{and} \;\; Z_7 \rho^Q \quad \text{are Hermitian matrices} \qquad (Q = U, D) \,. \tag{2.97}$$

In this case, the only remaining source of CP-violation in the 2HDM is the unremovable phase in the CKM matrix K that enters via the charged current interactions mediated by either $W^\pm$ or $H^\pm$ exchange.

The Higgs-quark couplings also generate Higgs-boson-mediated flavor-changing neutral currents at tree-level by virtue of the fact that the ρ^Q are not diagonal (in the quark mass basis). Thus, for a phenomenologically acceptable theory, the off-diagonal elements of ρ^Q must be small.

2.3.5 Conclusions

In the most general (CP-violating) 2HDM, physical observables do not depend on the choice of scalar field definitions (or basis). Employing the U(2) freedom of field redefinitions, one can write down the Higgs couplings of the 2HDM in a form that is manifestly basis independent. The U(2)-invariant forms for the Higgs boson couplings have been explicitly presented in this paper. In particular, the parameter $\tan\beta$, which depends on the choice of basis, does not appear in any of the Higgs boson (or Goldstone boson) couplings. In specialized versions of the 2HDM, additional theoretical assumptions are introduced that may implicitly select a preferred basis. For example, one can impose a discrete symmetry on the Lagrangian that takes a simple form in some particular basis. The type-I and type-II models discussed in Section 2.1.4.2 provide examples of such a scenario. In this case, $\tan\beta$ is promoted to a physical parameter, and one can express $\tan\beta$ directly in terms of U(2)-invariant quantities [14–16].

The basis-independent formalism provides a powerful approach for connecting physical observables that can be measured in the laboratory with fundamental invariant parameters of the 2HDM. This will permit the development of two-Higgs doublet model-independent analyses of data in Higgs studies at the LHC, ILC and beyond.

2.4 Symmetries of 2HDM and CP violation

Ilya F. Ginzburg and Maria Krawczyk

This contribution is based on the results published in [15] and some new results that have recently been obtained. The main aspects of the results of [15] are included in Section 2.1. Here we present alternative treatments of some problems and add new results, some of which were reported in [162].

The spontaneous electroweak symmetry breaking (EWSB) via the Higgs mechanism is described by the Lagrangian

$$\mathcal{L} = \mathcal{L}_{gf}^{SM} + \mathcal{L}_H + \mathcal{L}_Y \quad with \quad \mathcal{L}_H = T - V\,. \tag{2.98}$$

Here $\mathcal{L}_{gf}^{SM}$ describes the $SU(2) \times U(1)$ Standard Model interaction of gauge bosons and fermions, $\mathcal{L}_Y$ describes the Yukawa interactions of fermions with Higgs scalars and $\mathcal{L}_H$ is the Higgs scalar Lagrangian. Higgs potential. In our calculations we use the 2HDM Higgs potential as specified in Eq. (2.1); however, we insert explicit negative signs in the terms proportional to m_{11}^2 and m_{22}^2 terms. In this latter convention, if $m_{12}^2 = 0$ then EWSB is generated for positive values of m_{11}^2 and m_{22}^2. The most general renormalizable kinetic term is

$$T = (D_\mu\phi_1)^\dagger(D^\mu\phi_1) + (D_\mu\phi_2)^\dagger(D^\mu\phi_2) + \Big[\varkappa(D_\mu\phi_1)^\dagger(D^\mu\phi_2) + h.c.\Big]\,. \tag{2.99}$$

2.4.1 Reparametrization group

The "flavor" basis transformations discussed in Section 2.1 are described by a unitary group give by the direct product of the 3-parameter $SU(2)$ reparametrization (RPa) group and a $U(1)$ group, describing an overall phase freedom of the Lagrangian. This entire group operates on the space of fields while the RPa group operates also in the space of Lagrangians (with coordinates given by its parameters). The parameters of the Lagrangian can be determined in principle from measurements only with an accuracy up to the RPa freedom. All observable quantities (at least in principle) are invariants of the RPa group (IRPa). These are, for example, masses of observable Higgs bosons, i.e. eigenvalues of the mass matrix, and eigenvalues of the Higgs-Higgs scattering matrices. The transformations $\phi_k \to e^{-i\rho_k}\phi_k$ form a rephasing transformation (RPh) group, which is a subgroup of the RPa group with a single parameter $\rho = \rho_2 - \rho_1$.

The method described in Section 2.1 allows one to obtain a large series of (generally not independent) IRPa's [37]. An alternate method is based on the irreducible representations of SU(2) RPa group as discussed [19]. In this paper some basic objects, related to these irreducible representations, were determined: 3 scalars A^k, 2 vectors L_i and M_i and tensor a_{ij} $(i,\, j = x,\, y,\, z)$. After a simple reorganization of scalars A^k, we get

$$A^I = \lambda_1 + \lambda_2 + 2\lambda_3,\quad A^{II} = \lambda_3 - \lambda_4,\quad A^{III} = m_{11}^2 + m_{22}^2\,, \tag{2.100a}$$

$$(L_x, L_y, L_z) = \frac{1}{\sqrt{2}}\,(-Re(\lambda_6 + \lambda_7),\ \ Im(\lambda_6 + \lambda_7),\ -(\lambda_1 - \lambda_2)/2)\,, \tag{2.100b}$$

$$(M_x, M_y, M_z) = \frac{1}{\sqrt{2}}\left(Re\; m_{12}^2,\ -Im\; m_{12}^2,\ (m_{11}^2 - m_{22}^2)/2\right)\,, \tag{2.100c}$$

$$a_{ij} = \frac{1}{2}\begin{pmatrix} Re\;\lambda_5 - b & -Im\;\lambda_5 & Re\,(\lambda_6 - \lambda_7) \\ -Im\;\lambda_5 & -Re\;\lambda_5 - b & Im\,(\lambda_7 - \lambda_6) \\ Re\,(\lambda_6 - \lambda_7) & Im\,(\lambda_7 - \lambda_6) & 2b \end{pmatrix}, \tag{2.100d}$$

with $b = (\lambda_1 + \lambda_2 - 2\lambda_3 - 2\lambda_4)/6$. Introducing the vectors $L_i^I = a_{ij}L_j$ and $L_i^{II} = a_{ij}L_j^I$, a complete set of 11 independent invariants of RPa transformations can be naturally chosen as follows

$$\begin{gathered} I_1 = A^I,\quad I_2 = A^{II}\,,\quad I_3 = L_iL_i, \\ I_4 = Tr(a^2) \equiv Tr\,(a_{ij}a_{jk})\,,\quad I_5 = Tr(a^3) = Tr\,(a_{ij}a_{jk}a_{k\ell})\,, \\ I_6 = a_{ij}L_iL_j \equiv L_iL_i^I\,,\quad I_7 = \varepsilon_{ijk}L_iL_j^IL_k^{II}\,, \\ I_8 = A^{III}\,,\quad I_9 = M_iM_i\,,\quad I_{10} = L_iM_i\,,\ \ I_{11} = \varepsilon_{ijk}L_iL_j^IM_k\,. \end{gathered} \tag{2.101}$$

2.4.2 Z_2 symmetry

The CP violation and the flavour changing neutral currents (FCNC) are absent for a 2HDM Lagrangian with a Z_2 symmetry, which inhibits the $\phi_1 \leftrightarrow \phi_2$ transitions [18]. The Lagrangian is invariant under the interchange $\phi_1 \leftrightarrow \phi_1, \phi_2 \leftrightarrow -\phi_2$ or $\phi_1 \leftrightarrow -\phi_1, \phi_2 \leftrightarrow \phi_2$.

• The case of exact Z_2 symmetry is described by the Lagrangian Eq. (2.98) with potential Eq. (2.1), where $\lambda_6 = \lambda_7 = m_{12}^2 = 0$, and a kinetic term Eq. (2.99) with $\varkappa = 0$.

• In the case of soft violation of Z_2 symmetry, one adds to the Z_2 symmetric Lagrangian a term of operator dimension two, $m_{12}^2(\phi_1^\dagger\phi_2) + h.c.$, with a generally complex m_{12}^2 (and λ_5) parameter. This type of violation respects the Z_2 symmetry at short distances (much shorter than a cut-off $1/M$) to all orders in the perturbative series, i.e. the amplitudes for $\phi_1 \leftrightarrow \phi_2$ transitions disappear at virtuality $k^2 \sim M^2 \to \infty$. That is why we call this a "soft" violation.

Let our physical system be described by the Lagrangian $\mathcal{L}_s$ with an exact or softly violated Z_2 symmetry. The general RPa transformation converts $\mathcal{L}_s$ to a hidden soft Z_2 violating form $\mathcal{L}_{hs}$, with $\lambda_6,\ \lambda_7 \neq 0,\ \varkappa = 0$. The 14 parameters of this type of Lagrangian are constrained since they can be obtained from 9 independent parameters of an initial Lagrangian $\mathcal{L}_s$ (+ 3 RPa group parameters); the nondiagonal $\varkappa$ kinetic term does not arise from the loop corrections. For such a physical system the preferable RPa representation is given by $\mathcal{L}_s$.

The criteria whether the soft Z_2 symmetry of the potential is hidden can be easily obtained from Eq. (2.101) (the invariant condition is provided in [14]). If this case is realized, one can consider the RPa representation with an explicit soft Z_2 symmetry ($\lambda_6 = \lambda_7 = 0$) and with a real λ_5 (this can be achieved by a suitable RPh transformation). In this representation, a_{ij} is a diagonal matrix, and the vector $L_i \equiv (0,\ 0,\ L)$ has only a z-component. Therefore the vectors L_i^I and L_i^{II} also have only z-components. Hence, the invariant $I_7 = 0$. A straightforward calculation gives in addition: $I_3 = L^2$, $I_4 = (\lambda_5^2 + 3b^2)/2$, $I_5 = 3b(b^2 - \lambda_5^2)/4$, $I_6 = bL^2$. Therefore, these four invariants obey the relation $I_5 I_3/I_6 + 3I_4/2 = 3(I_6/I_3)^2$. These relations are written for invariants. Hence, the necessary and sufficient conditions for soft Z_2 symmetry violation are

$$I_7 = 0\,, \qquad I_3^2 I_4 I_6 + (2/3) I_3^3 I_5 - 2I_6^3 = 0\,. \tag{2.102}$$

• In the general case, the terms of an operator of dimension four, with generally complex parameters λ_6, λ_7 and $\varkappa$, are added to the Lagrangian with a softly violated Z_2 symmetry. This case covers both the opportunity of a hidden soft Z_2 symmetry violation and of a true hard violation of the Z_2 symmetry of the Lagrangian, which cannot be transformed to an exact or softly violated Z_2 symmetry form by any RPa transformation. For the true hard violation case, the Z_2 symmetry is broken at both large and short distances in any scalar ("flavor") basis.

The mixed kinetic terms Eq. (2.99) can be eliminated by the nonunitary transformation (rotation + renormalization), e.g.

$$(\phi_1', \phi_2') \to \left(\frac{\sqrt{\varkappa^*}\phi_1 + \sqrt{\varkappa}\phi_2}{2\sqrt{|\varkappa|(1+|\varkappa|)}} \pm \frac{\sqrt{\varkappa^*}\phi_1 - \sqrt{\varkappa}\phi_2}{2\sqrt{|\varkappa|(1-|\varkappa|)}} \right). \tag{2.103}$$

However, in the presence of the λ_6 and λ_7 terms in the potential Eq. (2.1), the renormalization of the quadratically divergent, non-diagonal two-point functions leads anyway to mixed kinetic terms (e.g. from loops with $\lambda_6^*\lambda_{1,3-5}$ and $\lambda_7^*\lambda_{2-5}$). This means that $\varkappa$ becomes nonzero at higher orders in perturbative theory (and *vice versa* a mixed kinetic term generates counterterms with $\lambda_{6,7}$). Therefore all of these terms should be included in Lagrangian on the same footing, i.e. the treatment of the hard violation of Z_2 symmetry without $\varkappa$ terms is inconsistent. (This term does not appear if the parameters λ_i are constrained by the relations given in Eq. (2.102).) In the case of true hard violation of the Z_2 symmetry, the parameter $\varkappa$ is running like the λ parameters. Therefore, the diagonalization of Eq. (2.103) is scale

dependent, and the Lagrangian remains off–diagonal in the fields $\phi_{1,2}$ even at very short distances in any RPa representation. Such a theory seems to be unnatural.

Although we present in [15] and here the relations for the case of hard violation of the Z_2 symmetry at $\varkappa = 0$, the loop corrections create a $\varkappa$ terms and can change the results significantly. Such a treatment of the case with true hard violation of the Z_2 symmetry is as incomplete as in other papers that consider the "most general 2HDM potential". Note, however that there is no consensus whether the parameters $\varkappa$ are independent parameters.

2.4.3 Ground state after EWSB. Criterium for CP conservation

The extrema of the potential define the vacuum expectation values (v.e.v.'s) $\langle\phi_{1,2}\rangle$ of the fields $\phi_{1,2}$ via equations Eq. (2.5), $\partial V/\partial\phi_i|_{\phi_i=\langle\phi_i\rangle} = 0$. The physical reality can be described only by a potential with a ground state obeying the condition for $U(1)$ symmetry of electromagnetism[11]:

$$\langle\phi_1\rangle = \frac{1}{\sqrt{2}}\begin{pmatrix}0\\ v_1\end{pmatrix}, \quad \langle\phi_2\rangle = \frac{1}{\sqrt{2}}\begin{pmatrix}0\\ v_2 e^{i\xi}\end{pmatrix}, \tag{2.104}$$

The rephasing transformation of fields allows one to eliminate the phase difference ξ and leads to the corresponding changes of the coefficients of Lagrangian. This real vacuum Lagrangian is used in [15] and in Section 2.1.

A standard decomposition of the fields $\phi_{1,2}$ in the component fields Eq. (2.20) at $\varkappa = 0$ retains a diagonal form of the kinetic terms for the fields φ_i^+, χ_i, φ_i. The mass-squared matrix for the component fields has a block diagonal form with separate blocks, corresponding to massless Goldstone boson fields, charged Higgs boson fields $H^\pm$ and a 3×3 matrix for the neutral fields Eq. (2.26), for two scalars η_1, η_2 and a pseudoscalar $A = -\chi_1 sin\beta + \chi_2 cos\beta$.

The possible mixing of the scalar and pseudoscalar states, which yields physical Higgs states h_i having no definite CP parity, generates CP violation in Higgs sector. Therefore, a signature for CP conservation in the Higgs sector is given by the zero values of squared-mass matrix elements Eq. (2.26) responsible for this mixing (i.e. $M_{13} = M_{23} = 0$ in the real vacuum basis). The vanishing of M_{13} and M_{23} can be realized if in such a basis m_{12}^2 and $v_1^2\lambda_6 - v_2^2\lambda_7$ (and also λ_5 – see Eq. (2.10)) are real. The set of arbitrary bases can be obtained from the set of real vacuum bases by the rephasing of fields. Therefore the sufficient condition for CP conservation in the Higgs sector can be written in a basis independent form as

$$Im\lambda_5^*(m_{12}^2)^2 = 0\,, \quad Im(\lambda_6^* + \lambda_7^*)m_{12}^2 = 0\,, \quad Im\lambda_6^*\lambda_7 = 0. \tag{2.105}$$

Each of these quantities is not RPa invariant but these forms are very simple. (For the soft Z_2 violating potential, this condition becomes both necessary and sufficient; it is simply: $Im\,\lambda_5^*(m_{12}^2)^2 = 0$, cf. [163]).

The imaginary part of the quantity $v_1^2\lambda_6 - v_2^2\lambda_7$ can be equal to 0 (which is necessary for CP conservation) even for complex λ_6 and λ_7. The RPa transformation from one real vacuum basis to another depends on two independent parameters (3 parameters of a general RPa transformation with one parameter restoring the real basis). One can use these parameters to eliminate the imaginary parts of λ_6 and λ_7 separately. Using in addition Eq. (2.10) one can conclude that in the case of CP violation in the Higgs sector there exists a Higgs basis in which all the coefficients of the potential are real (which is necessary condition for CP conservation).

Generally, these v.e.v.'s can be complex even in the case of a Lagrangian with real parameters. Therefore, the coefficients of the real vacuum Lagrangian can be complex even in the case where all coefficients of the incident Higgs potential are real. Hence, the existence of an RPa representation of the potential with all real coefficients forms a necessary but not a sufficient condition for CP conservation.

[11] Detail analysis of two possible vacuum solutions, including charged vacuum [20], is presented in [162], [15].

The RPa invariant form of this necessary condition is presented in Section 2.1 [38, 40, 164], [14, 37], and with invariants (2.101) in [19].

2.4.4 Tree level unitarity constraints

The quartic terms in the Higgs potential (with λ_i) lead, in the tree approximation, to the s–wave Higgs-Higgs and W_LW_L and W_LH, etc. scattering amplitudes for different elastic channels. These amplitudes should not overcome the unitary limit for this partial wave – that is the tree-level unitarity constraint. Such a constraint was obtained first in [18] for the minimal SM, with one Higgs field. For the 2HDM with soft Z_2 violation and CP conservation, they were derived in [32]. In the general CP nonconserving case, the corresponding constraints were obtained in [34].

Since in the Higgs–Higgs scattering the total hypercharge Y and weak isospin σ are conserved, one can consider separate S matrices, $S_{Y\sigma}$, for the different quantum numbers of the initial state. The unitarity constraint means that the eigenvalues of these $S_{Y\sigma}$ are less than 1 [34], where

$$16\pi S_{Y=2,\sigma=1}=\begin{pmatrix} \lambda_1 & \lambda_5 & \sqrt{2}\lambda_6 \\ \lambda_5^* & \lambda_2 & \sqrt{2}\lambda_7^* \\ \sqrt{2}\lambda_6^* & \sqrt{2}\lambda_7 & \lambda_3+\lambda_4 \end{pmatrix}, \quad 16\pi S_{Y=2,\sigma=0}= \lambda_3-\lambda_4, \tag{2.106a}$$

$$16\pi S_{Y=0,\sigma=1}=\begin{pmatrix} \lambda_1 & \lambda_4 & \lambda_6 & \lambda_6^* \\ \lambda_4 & \lambda_2 & \lambda_7 & \lambda_7^* \\ \lambda_6^* & \lambda_7^* & \lambda_3 & \lambda_5^* \\ \lambda_6 & \lambda_7 & \lambda_5 & \lambda_3 \end{pmatrix}, \tag{2.106b}$$

$$16\pi S_{Y=0,\sigma=0} = \begin{pmatrix} 3\lambda_1 & 2\lambda_3+\lambda_4 & 3\lambda_6 & 3\lambda_6^* \\ 2\lambda_3+\lambda_4 & 3\lambda_2 & 3\lambda_7 & 3\lambda_7^* \\ 3\lambda_6^* & 3\lambda_7^* & \lambda_3+2\lambda_4 & 3\lambda_5^* \\ 3\lambda_6 & 3\lambda_7 & 3\lambda_5 & \lambda_3+2\lambda_4 \end{pmatrix}. \tag{2.106c}$$

The eigenvalues of these matrices can be found as roots of equations of the 3-rd or 4-th degree. It is useful to start the diagonalization from the corners of the above matrices, corresponding to the fixed values of the Z_2 parity. This particular diagonalization transforms $S_{Y\sigma}$ to a form with diagonal elements that are coincident with the eigenvalues found in [32] (for soft Z_2 violation without CP violation) with the sole change of $\lambda_5 \to |\lambda_5|$.

Next, one can use the following observation: For an Hermitian matrix $\mathcal{M} = ||M_{ij}||$ with maximal and minimal eigenvalues Λ_+ and Λ_-, all diagonal matrix elements M_{ii} lie between them, $\Lambda_+ \geq M_{ii} \geq \Lambda_-$. By virtue of this fact, the mentioned corrected constraints from [32] form necessary conditions for unitarity. These constraints are enhanced due to the λ_6, λ_7 terms that govern the hard violation of the Z_2 symmetry.

2.4.5 Couplings to fermions

The general form of Yukawa interaction couples a 3-family vector of the left-handed quark isodoublets Q_L with 3-family vectors of the right-handed field singlets d_R and u_R and Higgs fields ϕ_i Eq. (2.46).

If some fermion field singlet is coupled to both scalar fields ϕ_1 and ϕ_2, the counterterms corresponding to the one-loop propagator corrections to the Higgs Lagrangian contain operators of dimension 4, which violate the Z_2 symmetry in a hard way. They contribute to the renormalization of the parameters $\varkappa$, λ_6 and λ_7. Therefore, to have only a soft violation of Z_2 symmetry (to prevent $\phi_1 \leftrightarrow \phi_2$ transitions at short distances), one demands that [18, 165] each right-handed fermion couples to only one scalar field, either ϕ_1 or ϕ_2. The case $\Gamma_2 = \Delta_1 = 0$ with diagonal Γ_1, Δ_2 corresponds to the well known Model II, while $\Gamma_2 = \Delta_2 = 0$ corresponds to Model I. Note that a general RPa transformation makes these properties of the Lagrangian hidden. The widespread Model II, with many useful relations for it partially obtained in [15] and first collected together there, is described in Section 2.1.

In this analysis we use in principle measurable relative couplings—that is, ratios of the couplings of each neutral Higgs boson h_i to the corresponding SM couplings Eq. (2.41). We present here, for completeness, only the case of model I Yukawa interactions. In this model, all right handed fermions are coupled to one Higgs field, say ϕ_1. The general RPa transformation makes this property hidden, changing simultaneously $\tan\beta$. The parameter β corresponding to the Model I form of the Lagrangian will be labeled with a subscript I. For this form of the Lagrangian we have ($i = 1, 2, 3$):

$$\text{Model I}: \qquad \chi_u^{(i)} = \chi_d^{(i)} \equiv \chi_f^{(i)} = \frac{[R_{i2} - i\cos\beta_I\, R_{i3}]}{\sin\beta_I}. \tag{2.107}$$

In this case, among the methods presented for Model II, only one method succeeds in determining β_I via observable quantities, namely [see Eq. (2.58)]

$$\frac{1}{\sin^2\beta_I} = \sum_{i=1}^{3} (\operatorname{Re}\chi_u^{(i)})^2. \tag{2.108}$$

2.4.6 A natural set of parameters of 2HDM

It is natural to assume that the 2HDM that describes physical reality allows for the existence among the reparametrization equivalent Lagrangians the one in which the fields ϕ_k do not mix at small distances (mixed kinetic term does not appear). This would correspond to the 2HDM with an exact or softly violated Z_2 symmetry. We assume such choice in this section. Besides, it is natural to assume that the CP symmetry in the Higgs sector is violated only weakly at least for the lightest Higgs boson h_1. This assumption together with rephasing invariance offers the basis for the selection of *the natural set of parameters of 2HDM*.

The Eq. (2.30) shows that the CP symmetry for the lightest Higgs boson is violated weakly if and only if $|M'_{13}| \ll |M_A^2 - M_h^2|$. In view of Eq. (2.34), for *the real vacuum Lagrangian* at $\beta + \alpha \neq \pi/2$ this condition can be rewritten in the form

$$v^2 |\operatorname{Im} m_{12}^2| \ll v_1 v_2 |M_A^2 - M_h^2|\,. \tag{2.109}$$

For all other rephasing equivalent Lagrangians, this condition Eq. (2.109) contains both $\operatorname{Im} m_{12}^2$ and $\operatorname{Re} m_{12}^2$. Therefore, for *the natural set of parameters of 2HDM* we require that both $|\operatorname{Im} m_{12}^2|(v^2/v_1v_2)$ and $|\operatorname{Re} m_{12}^2|(v^2/v_1v_2)$ are small for all rephasing equivalent Lagrangians. In the case of soft violation of Z_2 symmetry, the same requirements is transmitted to $\operatorname{Im}\lambda_5$ and $\operatorname{Re}\lambda_5$. Therefore, we define *a natural set of parameters* as follows

$$|\eta|,\ |\lambda_5| \ll |\lambda_{1-4}|\,. \tag{2.110}$$

For the natural set of parameters of the 2HDM, the breaking of the Z_2 symmetry is governed by a small parameter η. Due to the existence of a limit where the Z_2 symmetry holds, a small soft Z_2 violation in the Higgs Lagrangian and the Yukawa interactions also remains small beyond the tree level. In this respect, we use term *natural* in the same sense as in [166]. (Note also that the non-diagonal Yukawa coupling matrices Γ_1 and Δ_2 (leading to FCNCs) are unnatural in this very sense).

In accordance with Eq. (2.26), for the natural set of parameters M_A cannot be too large. This parameter regime is not ruled out by the data; in the CP conserving case see e.g. Section 2.2.1.

2.5 Textures and the Higgs boson-fermion couplings

Justiniano L. Díaz-Cruz, Roberto Noriega-Papaqui and Alfonso Rosado-Sánchez

The 2HDM [8, 167] has a potential problem with flavour changing neutral currents (FCNC) mediated by the Higgs bosons, which arise when one quark of type u or d is allowed to couple to both Higgs doublets. The possible solutions to this problem of the 2HDM involve an assumption about the Yukawa Lagrangian of the model. The specific choices for the Yukawa matrices $\Gamma_{1,2}$ and $\Delta_{1,2}$ define the versions of the 2HDM known as I, II or III, which involve certain mechanism to eliminate the otherwise unbearable FCNC problem or at least to keep it under control. In this paper we are interested in studying the 2HDM-III, where the FCNC problem is ameliorated by assuming a certain texture for the Yukawa couplings. However, the original six-texture ansatz that leads to the popular Cheng-Sher ansatz [168] seems disfavored by current data on the CKM mixing angles. More recently, mass matrices with four-texture ansatz have been considered, and are found in better agreement with the observed data [169,170]. In this paper we investigate how the form of the $ff'\phi^0$ couplings, get modified when one replaces the six-texture matrices by the four-texture one. We also discuss some implications for rare quark and lepton decays, as well as the phenomenology of the Higgs bosons [129].

2.5.1 The fermion sector of the 2HDM-III with four-texture mass matrices

We will assume that both Yukawa matrices $\Gamma_{1,2}$ and $\Delta_{1,2}$ have the four-texture form and are Hermitian; following the conventions of [169], the quark mass matrix is written as:

$$M_q = \begin{pmatrix} 0 & C_q & 0 \\ C_q^* & \tilde{B}_q & B_q \\ 0 & B_q^* & A_q \end{pmatrix}. \tag{2.111}$$

when $\tilde{B}_q \to 0$ one recovers the six-texture form. We also consider the hierarchy:
$\mid A_q \mid \gg \mid \tilde{B}_q \mid, \mid B_q \mid, \mid C_q \mid$, which is supported by the observed fermion masses in the SM.
Because of the hermicity condition, both $\tilde{B}_q$ and A_q are real parameters, while the phases of C_q and B_q, Φ_{B_q,C_q}, can be removed from the mass matrix M_q by defining: $M_q = P_q^\dagger \tilde{M}_q P_q$, where $P_q = diag[1, e^{i\Phi_{C_q}}, e^{i(\Phi_{B_q}+\Phi_{C_q})}]$, and the mass matrix $\tilde{M}_q$ includes only the real parts of M_q. The diagonalization of $\tilde{M}_q$ is then obtained by an orthogonal matrix O_q, such that the diagonal mass matrix is: $\bar{M}_q = O_q^T \tilde{M}_q O_q$. Expanding in powers of $z_f = m_2^f/m_3^f$, where $m_{2,3}^f$ denote the masses for 2^{nd} and 3^{rd} generations, the Yukawa Lagrangian can then be expressed in terms of the mass-eigenstates for the neutral (h^0, H^0, A^0) and charged Higgs bosons $(H^\pm)$. The interactions of the neutral Higgs bosons with the d-type and u-type quarks ($u, u' = u, c, t$ and $d, d' = d, s, b$) are expressed as follows.

$$\begin{aligned}
\mathcal{L}_Y^q &= \frac{g}{2}\bar{D}\left[\left(\frac{m_d}{m_W}\right)\frac{\cos\alpha}{\cos\beta}\delta_{dd'} + \frac{\sin(\alpha-\beta)}{\sqrt{2}\cos\beta}\left(\frac{\sqrt{m_d m_{d'}}}{m_W}\right)\tilde{\chi}_{dd'}\right]D'H^0 \\
&+\frac{g}{2}\bar{D}\left[-\left(\frac{m_d}{m_W}\right)\frac{\sin\alpha}{\cos\beta}\delta_{dd'} + \frac{\cos(\alpha-\beta)}{\sqrt{2}\cos\beta}\left(\frac{\sqrt{m_d m_{d'}}}{m_W}\right)\tilde{\chi}_{dd'}\right]D'h^0 \\
&+\frac{ig}{2}\bar{D}\left[-\left(\frac{m_d}{m_W}\right)\tan\beta\,\delta_{dd'} + \frac{1}{\sqrt{2}\cos\beta}\left(\frac{\sqrt{m_d m_{d'}}}{m_W}\right)\tilde{\chi}_{dd'}\right]\gamma^5 D'A^0 \\
&+\frac{g}{2}\bar{U}\left[\left(\frac{m_u}{m_W}\right)\frac{\sin\alpha}{\sin\beta}\delta_{uu'} - \frac{\sin(\alpha-\beta)}{\sqrt{2}\sin\beta}\left(\frac{\sqrt{m_u m_{u'}}}{m_W}\right)\tilde{\chi}_{uu'}\right]U'H^0 \\
&+\frac{g}{2}\bar{U}\left[\left(\frac{m_u}{m_W}\right)\frac{\cos\alpha}{\sin\beta}\delta_{uu'} - \frac{\cos(\alpha-\beta)}{\sqrt{2}\sin\beta}\left(\frac{\sqrt{m_u m_{u'}}}{m_W}\right)\tilde{\chi}_{uu'}\right]U'h^0 \\
&+\frac{ig}{2}\bar{U}\left[-\left(\frac{m_u}{m_W}\right)\cot\beta\,\delta_{uu'} + \frac{1}{\sqrt{2}\sin\beta}\left(\frac{\sqrt{m_u m_{u'}}}{m_W}\right)\tilde{\chi}_{uu'}\right]\gamma^5 U'A^0.
\end{aligned} \tag{2.112}$$

The corresponding Lagrangian for the charged lepton sector is obtained following a similar procedure, and can be read from [171]. Unlike the Cheng-Sher ansatz, the parameters $\tilde{\chi}_{ff'}$ $(f \neq f')$ are now complex. While the diagonal elements $\tilde{\chi}_{ff}$ are real, the phases in the off-diagonal elements are essentially unconstrained by present low-energy data. These phases modify the pattern of flavour violation (FV) in the Higgs sector. However, because of the Hermiticity of the Yukawa matrices, the three-level CP-properties of h^0/H^0 and A^0 remain valid i.e. the couplings $h^0(H^0)f\bar{f}$ are pure scalar, while the coupling $A^0 f\bar{f}$ is proportional to γ_5. Further, in our prescription the FV couplings satisfy some relations, such as: $|\tilde{\chi}_{\mu\tau}| = |\tilde{\chi}_{e\tau}|$ and $|\tilde{\chi}_{sb}| = |\tilde{\chi}_{db}|$, which simplifies the parameter analysis. Henceforth, we denote $|\tilde{\chi}_{ff'}|$ as $\chi_{ff'}$. On the other hand, by considering the effective Lagrangian for the couplings of the charged leptons to the neutral Higgs fields one can also relate our results with the SUSY-induced 2HDM-III. Thus, our result will cover (for specific choices of parameters) the general expectations for the corrections arising in the MSSM.

2.5.2 Bounds on the FV Higgs parameters

Constraints on the lepton flavour violation (LFV)-Higgs interaction will be obtained by studying LFV transitions, which include the 3-body modes ($l_i \to l_j l_k \bar{l}_k$), radiative decays ($l_i \to l_j + \gamma$), as well as the $\mu - e$ conversion in nuclei. On the other side, constraints on the Higgs boson-quark interaction can be obtained by studying FCNC transitions. In particular, we consider the radiative decay $b \to s\,\gamma$ and the decay $B_s^0 \to \mu^-\mu^+$, which together with LFV bounds derived in [171] constrain the parameter space of 2HDM-III, and determine possible Higgs boson signals that may be detected at future colliders.

2.5.2.1 LFV three-body decays

To evaluate the LFV leptonic couplings, we calculate the decays $l_i \to l_j l_k \bar{l}_k$, including the contribution from the three Higgs bosons (h^0, H^0 and A^0). In particular, for the decay $\tau^- \to \mu^-\mu^+\mu^-$ we obtain the following expression for the branching ratio:

$$\begin{aligned} Br(\tau^- \to \mu^-\mu^+\mu^-) &= \frac{5}{3}\,\frac{\tau_\tau}{2^{12}\,\pi^3}\,\frac{m_\mu^3\,m_\tau^6}{v^4}\,\left\{\frac{\cos^2(\alpha-\beta)\,\sin^2\alpha}{m_{h^0}^4} + \frac{\sin^2(\alpha-\beta)\,\cos^2\alpha}{m_{H^0}^4}\right. \\ &\left. -2\,\frac{\cos(\alpha-\beta)\,\sin(\alpha-\beta)\,\cos\alpha\,\sin\alpha}{m_{h^0}^2\,m_{H^0}^2} + \frac{\sin^2\beta}{m_{A^0}^4}\right\}\,\frac{\chi_{\mu\tau}^2}{\cos^4\beta} \end{aligned} \tag{2.113}$$

here τ_τ corresponds to the life time of the τ lepton (we have also assumed $\chi_{\mu\mu} \ll 1$). Using $Br(\tau^- \to \mu^-\mu^+\mu^-) < 1.9 \times 10^{-7}$ [172], we get an upper bound on $\chi_{\mu\tau}$ ($(\chi_{\mu\tau})_{u.b.}^{\tau\to 3\mu}$) (see Table 2.1).

2.5.2.2 Radiative decay $\mu \to e\gamma$

The B.R. of $\mu^+ \to e^+\gamma$ at one loop level is given by [173]

$$\begin{aligned} Br(\mu^+ \to e^+\gamma) &= \frac{\alpha_{em}\tau_\mu m_e m_\mu^4 m_\tau^4}{2^{12}\pi^4 v^4\cos^4\beta}\,\chi_{\mu\tau}^2\,\chi_{e\tau}^2\,\left\{\frac{\cos^4(\alpha-\beta)}{m_{h^0}^4}\left|\ln\frac{m_3^2}{m_{h^0}^2} + \frac{3}{2}\right|^2\right. \\ &+2\frac{\cos^2(\alpha-\beta)\sin^2(\alpha-\beta)}{m_{h^0}^2 m_{H^0}^2}\left|\ln\frac{m_3^2}{m_{h^0}^2} + \frac{3}{2}\right|\left|\ln\frac{m_3^2}{m_{H^0}^2} + \frac{3}{2}\right| \\ &\left. + \frac{\sin^4(\alpha-\beta)}{m_{H^0}^4}\left|\ln\frac{m_3^2}{m_{H^0}^2} + \frac{3}{2}\right|^2 + \frac{1}{m_{A^0}^4}\left|\ln\frac{m_3^2}{m_{A^0}^2} + \frac{3}{2}\right|^2\right\}. \end{aligned} \tag{2.114}$$

We make use of $Br(\mu^+ \to e^+\gamma) < 1.2 \times 10^{-11}$ [174] to constrain $\chi_{\mu\tau} (= \chi_{e\tau})$ (see Table 2.1).

2.5.2.3 Radiative decay $\tau \to \mu\gamma$

The B.R. of $\tau \to \mu\,\gamma$ at one loop level (assuming $\chi_{\tau\tau} \ll 1$) is given by [173]

$$\begin{aligned} Br(\tau \to \mu\,\gamma) &= \frac{3}{5}\,\frac{\alpha_{em}\,m_\mu\,m_\tau^3}{16\,\pi\,\cos^4\beta}\,\chi^2_{\mu\tau}\,\left\{\frac{\sin^2\alpha\,\cos^2(\alpha-\beta)}{m^4_{h^0}}\,\left|\ln\frac{m_\tau^2}{m^2_{h^0}}+\frac{3}{2}\right|^2\right. \\ &+\frac{\cos^2\alpha\,\cos^2(\alpha-\beta)+\sin^2\alpha\,\sin^2(\alpha-\beta)}{m^2_{h^0}\,m^2_{H^0}}\,\left|\ln\frac{m_\tau^2}{m^2_{h^0}}+\frac{3}{2}\right|\,\left|\ln\frac{m_\tau^2}{m^2_{H^0}}+\frac{3}{2}\right| \\ &\left.+\,\frac{\cos^2\alpha\,\sin^2(\alpha-\beta)}{m^4_{H^0}}\,\left|\ln\frac{m_\tau^2}{m^2_{H^0}}+\frac{3}{2}\right|^2+\frac{\sin^2\beta}{m^4_{A^0}}\,\left|\ln\frac{m_\tau^2}{m^2_{A^0}}+\frac{3}{2}\right|^2\right\}. \end{aligned} \tag{2.115}$$

We constrain $\chi_{\mu\tau}$ by using $Br(\tau \to \mu + \gamma) < 3.1 \times 10^{-7}$ [175, 176] (see Table 2.1).

2.5.2.4 $\mu - e$ conversion

The formulas of the conversion branching ratios for the LFV muon electron process in nuclei at large $\tan\beta$, in the aluminum and lead targets, are approximately given by

$$Br(\mu^- Al(Pb) \to e^- Al(Pb)) \simeq 0.18(2.5) \times 10^{-3}\,\frac{m_e\,m_\mu^6\,m_p^2\,\tan^6\beta\,\cos^2\beta}{2\,v^4\,m^4_{H^0}\,\omega_{capt}}\,\chi^2_{e\mu}, \tag{2.116}$$

where ω_{capt} is the rate for muon capture in the nuclei [177]. $\omega_{capt} = 0.7054 \times 10^6\,s^{-1}$ and $\omega_{capt} = 13.45 \times 10^6\,s^{-1}$ in the Al and the Pb nuclei, respectively [178]. We get an upper bound on $\chi_{e\mu}$ ($(\chi_{e\mu})^{\mu\mathcal{N}\to e\mathcal{N}}_{u.\,b.}$) for Al and Pb (see Table 2.1), by using $Br(\mu^-\mathcal{N} \to e^-\mathcal{N}) < 6.1 \times 10^{-13}$ [179].

2.5.2.5 Radiative decay $b \to s\,\gamma$

We will make an estimation of the contribution due to the FV $ff'\phi^0$ couplings to the standard model branching ratio of $b \to s\,\gamma$ as follows

$$\Delta Br(b \to s\,\gamma) = \Delta\Gamma(b \to s\,\gamma) \times \Big(\sum_{l=e,\mu,\tau}\Gamma(b \to c\,l\,\bar{\nu}_l)\Big)^{-1} \tag{2.117}$$

Such contribution to the branching ratio of $b \to s\,\gamma$ at one loop level is then given by [173]

$$\Delta Br(b \to s\,\gamma) = \frac{\alpha_{em}\,m_s\,m_b^3\,\cos^2(\alpha-\beta)}{16\,\pi\,m^4_{h^0}\,|V_{cb}|^2\,\cos^4\beta}\,\chi^2_{sb}\left|-\sin\alpha+\frac{\cos(\alpha-\beta)}{\sqrt{2}}\,\tilde{\chi}_{bb}\right|^2\,\left|\ln\frac{m_b^2}{m^2_{h^0}}+\frac{3}{2}\right|^2. \tag{2.118}$$

We make use of the good agreement between the experimental value for $Br(b \to s\,\gamma) = (3.3 \pm 0.4) \times 10^{-4}$ and the theoretical value obtained for $Br(b \to s\,\gamma) = (3.29 \pm 0.33) \times 10^{-4}$ in the context of the SM [174] to constrain any new contribution to $Br(b \to s\,\gamma)$, namely $\Delta Br(b \to s\,\gamma) \leq 10^{-5}$, and hence to bound $\chi_{sb}(= \chi_{db})$ (see Table 2.1).

2.5.2.6 $B_s^0 \to \mu^-\mu^+$ decay

The width of the decay $B_s^0 \to \mu^-\mu^+$ at the tree level is given as [180]

$$\Gamma(B_s^0 \to \mu^-\mu^+) = \frac{G_F^2\,\eta^2_{QCD}\,m_B^3\,f_B^2\,m_s\,m_b\,m_\mu^2\,\cos^2(\alpha-\beta)}{128\,\pi\,m^4_{h^0}\,\cos^4\beta}\,\chi^2_{sb}\left|-\sin\alpha+\frac{\cos(\alpha-\beta)}{\sqrt{2}}\,\tilde{\chi}_{\mu\mu}\right|^2, \tag{2.119}$$

where $G_F = 1.16639 \times 10^{-5}\,GeV^{-2}$, $\eta_{QCD} \approx 1.5$, $m_B \simeq 5\,GeV$, and $f_B = 180\,MeV$. We make use of $\Gamma(B_s^0 \to \mu^-\mu^+) < 8.7 \times 10^{-19}\,GeV$ [180, 181] to constrain $\chi_{sb}(= \chi_{db})$ (see Table 2.1).

Table 2.1: Upper bounds on $\chi_{\mu\tau}$, $\chi_{e\mu}$ and χ_{sb} as functions of $\tan\beta$, for $\alpha=\beta$, $\alpha=\beta-\pi/4$, $\alpha=\beta-\pi/3$, taking $m_{h^0}=120$ GeV, $m_{H^0}=300$ GeV and $m_{A^0}=300$ GeV and $\chi_{\mu\mu}=0$ $\chi_{\tau\tau}=0$. Upper bound $(\chi_{e\mu})^{\mu\mathcal{N}\to e\mathcal{N}}_{u.\,b.}$ as a function of $\tan\beta$ for Al, Pb and assuming $m_{H^0}=300$ GeV.

upper bound	$\beta-\alpha$	$\tan\beta=10$	$\tan\beta=20$	$\tan\beta=30$	$\tan\beta=40$	$\tan\beta=50$
$(\chi_{\mu\tau})^{\tau\to 3\mu}_{u.\,b.}$	0	8.1	2.1	9.0×10^{-1}	5.1×10^{-1}	3.3×10^{-1}
	$\pi/4$	1.6×10^{1}	3.8	1.7	9.2×10^{-1}	5.9×10^{-1}
	$\pi/3$	2.5×10^{1}	5.9	2.6	1.5	9.2×10^{-1}
$(\chi_{\mu\tau})^{\mu\to e\gamma}_{u.\,b.}$	0	1.5×10^{-1}	7.4×10^{-2}	5.0×10^{-2}	3.7×10^{-2}	3.0×10^{-2}
	$\pi/4$	1.9×10^{-1}	9.4×10^{-2}	6.3×10^{-2}	4.7×10^{-2}	3.8×10^{-2}
	$\pi/3$	2.2×10^{-1}	1.1×10^{-1}	7.4×10^{-2}	5.6×10^{-2}	4.5×10^{-2}
$(\chi_{\mu\tau})^{\tau\to\mu\gamma}_{u.\,b.}$	0	1.6	4.0×10^{-1}	1.8×10^{-1}	9.9×10^{-2}	6.4×10^{-2}
	$\pi/4$	2.7	6.6×10^{-1}	2.9×10^{-1}	1.7×10^{-1}	1.1×10^{-1}
	$\pi/3$	3.8	9.3×10^{-1}	4.1×10^{-1}	2.3×10^{-1}	1.5×10^{-1}
$(\chi_{e\mu})^{\mu Al\to eAl}_{u.\,b.}$		1.2×10^{-1}	3.1×10^{-2}	1.4×10^{-2}	7.6×10^{-3}	4.9×10^{-3}
$(\chi_{e\mu})^{\mu Pb\to ePb}_{u.\,b.}$		1.4×10^{-1}	3.6×10^{-2}	1.6×10^{-2}	8.9×10^{-3}	5.7×10^{-3}
$(\chi_{sb})^{b\to s\,\gamma}_{u.\,b.}$	0	8.1×10^{-2}	2.1×10^{-2}	9.1×10^{-3}	5.1×10^{-3}	3.3×10^{-3}
	$\pi/4$	1.8×10^{-1}	4.3×10^{-2}	1.9×10^{-2}	1.1×10^{-2}	6.7×10^{-3}
	$\pi/3$	3.9×10^{-1}	8.9×10^{-2}	3.9×10^{-2}	2.2×10^{-2}	1.4×10^{-2}
$(\chi_{sb})^{B^0_s\to\mu\mu}_{u.\,b.}$	0	1.1	2.7×10^{-1}	1.2×10^{-1}	6.6×10^{-2}	4.2×10^{-2}
	$\pi/4$	2.4	5.6×10^{-1}	2.5×10^{-1}	1.4×10^{-1}	8.6×10^{-2}
	$\pi/3$	5.1	1.2	5.0×10^{-1}	2.8×10^{-1}	1.8×10^{-1}

2.5.3 Higgs boson decays in the 2HDM-III

One of the distinctive characteristic of the SM Higgs boson is the fact that its coupling to other particles is proportional to the mass of that particle, which in turn determines the search strategies proposed so far to detect it at future colliders. In particular, the decay pattern of the Higgs boson is dominated by the heaviest particle allowed to appear in its decay products. When one considers extensions of the SM it is important to study possible deviations from the SM decay pattern as it could provide a method to discriminate among the different models [182, 183]. Within the context of the 2HDM-III, not only modification of the Higgs boson couplings are predicted, but also the appearance of new channels with FV, both in the quark and leptonic sectors [129, 184, 185].

To explore the characteristics of Higgs boson decays in the 2HDM-III, we will focus on the lightest CP-even state (h^0), which could be detected first at LHC. The light Higgs boson-fermion couplings are given by Eq. (2.112), where we have separated the SM from the corrections that appear in a 2HDM-III. In fact, we have also separated the factors that arise in the 2HDM-III too. We notice that the correction to the SM result, depends on $\tan\beta$, α (the mixing angle in the neutral CP-even Higgs sector) and the factors $\tilde{\chi}_{ff'}$ that induce FCNC transitions (for $f\neq f'$) and further corrections to the SM vertex. In our analysis, we will include the decay widths for all the modes that are allowed kinematically for a Higgs boson with a mass in the range $80\,GeV < m_{h^0} < 160\,GeV$. Namely, we study the branching ratios for the decays $h^0\to b\bar{b}$, $c\bar{c}$, $\tau\bar{\tau}$, $\mu\bar{\mu}$ and the FV $h^0\to b\bar{s}(s\bar{b})$, $\tau\bar{\mu}(\mu\bar{\tau})$, as well as the decays into pairs of gauge bosons with one real an the other one virtual, i.e. $h^0\to WW^*, ZZ^*$ [8, 167]. Overall, our results show that the usual search strategies to look for the SM Higgs boson in this mass range, may need to be

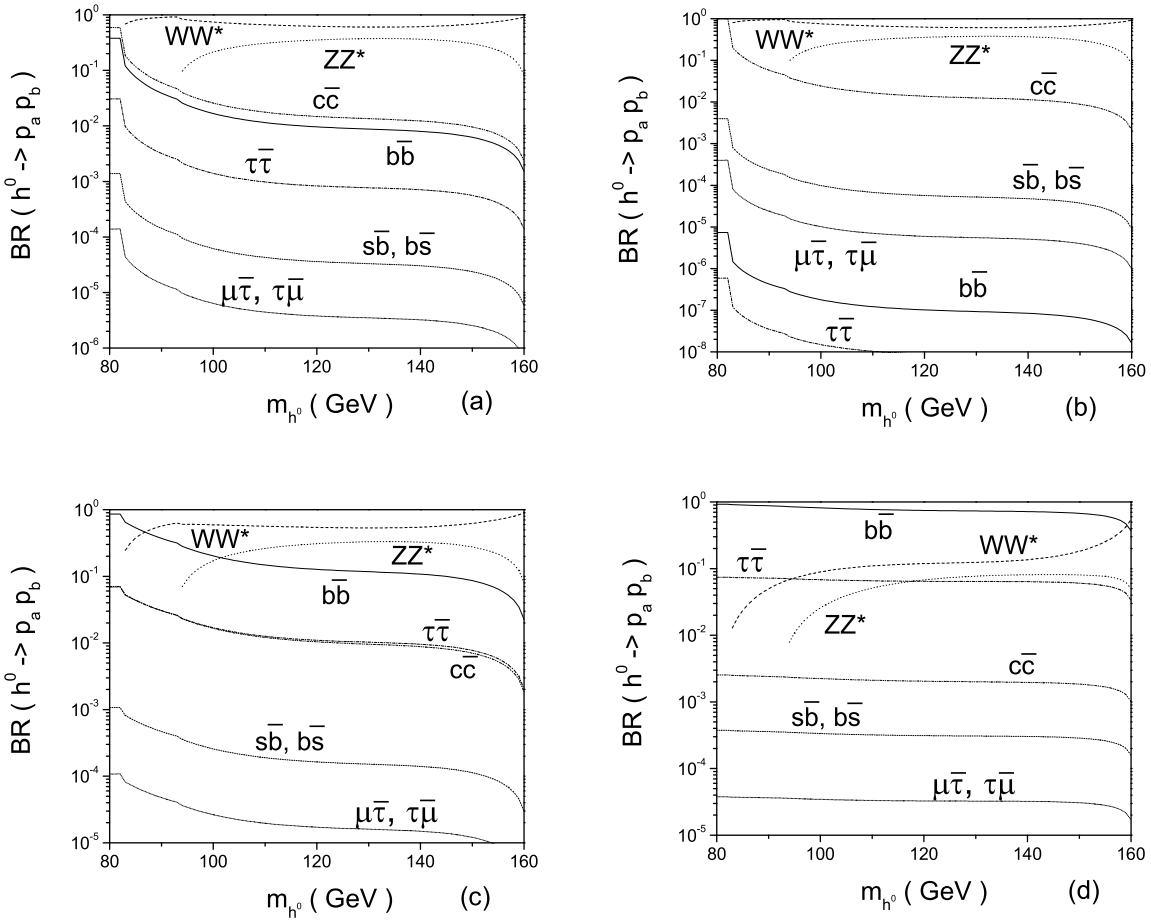

Fig. 2.3: B.R. for all the relevant decay modes that are allowed kinematically for $80\,GeV < m_{h^0} < 160\,GeV$; taking $\alpha = \beta - 3\pi/8$ and assuming $\tilde{\chi}_{ff'} = 0.1$ for $f = f'$ and $f \neq f'$. For: (a) $\tan\beta = 2$; (b) $\tan\beta = 2.61$; (c) $\tan\beta = 5$; (d) $\tan\beta = 15$.

modified in order to cover the full parameter space of the 2HDM-III (see Fig. 2.3).

2.5.4 Conclusions

We have studied in this paper the $ff'\phi^0$ couplings that arise in the 2HDM-III, using a Hermitian four-texture form for the fermionic Yukawa matrix. Because of this, although the $ff'\phi^0$ couplings are complex, the three-level CP-properties of h^0, H^0 (even) and A^0 (odd) remain valid.

We have derived bounds on the parameters of the model, using current experimental bounds on LFV and FCNC transitions. One can say that the present bounds on the couplings $\tilde{\chi}_{ff'}$'s still allow the possibility to study interesting direct FV Higgs boson signals at future colliders.

In particular, the LFV couplings of the neutral Higgs bosons, can lead to new discovery signatures of the Higgs boson itself. For instance, the branching fraction for $h^0 \to \tau\bar{\mu}(\bar{\tau}\mu)$ can be as large as 10^{-5}, while $Br(h \to b\bar{s}(\bar{b}s))$ is also about 10^{-4}. These LFV Higgs modes complement the modes $B^0 \to \mu\mu$, $\tau \to 3\mu$, $\tau \to \mu\gamma$ and $\mu \to e\gamma$, as probes of FV in the 2HDM-III, which could provide key insights into the form of the Yukawa mass matrix sector.

2.6 Electroweak baryogenesis and quantum corrections to the Higgs potential

Shinya Kanemura, Yasuhiro Okada and Eibun Senaha

The connection between cosmology and particle physics is important to understand what the Universe is made of. The baryon asymmetric Universe observed today is one of the outstanding problems in cosmology. The asymmetry is characterized by the ratio of the baryon number density to the entropy density, $n_B/s \sim 10^{-10}$ [186], which remains constant during the expansion of the Universe if there is neither baryon number violation nor entropy production.

In order to construct such baryon asymmetry from the initially baryon symmetric Universe, three ingredients are required [187]: (a) baryon number violation, (b) C and CP violation, and (c) departure from thermal equilibrium. In the electroweak theories, these conditions can in principle be satisfied (*electroweak baryogenesis*). The condition (a) is fulfilled by the sphaleron process in Standard Model at high temperature. The sphaleron is an unstable classical solution of the $SU(2)$ gauge-Higgs system which corresponds to a saddle point connecting different topological vacua. Frequent baryon number violation processes occur near and above the critical temperature by the transition associated with a change of the topological number, which is called the sphaleron process, although it is completely negligible at zero temperature. On the other hand the Standard Model cannot satisfy the other two conditions under the current experimental data. One is that the electroweak phase transition is not first order for experimental lower bounds of the Higgs boson mass, $m_h > 114$ GeV [74], so that the condition (c) cannot be fulfilled. The other difficulty is that the magnitude of the CP violation which is originated from the Kobayashi-Maskawa matrix is too small to generate the sufficient baryon asymmetry during the phase transition. Therefore, the extension of the Standard Model Higgs sector and the additional sources of the CP violation are required. There are many attempts to explain the baryon asymmetry in the extension of the Standard Model. For reviews on electroweak baryogenesis, see Refs. [188–193].

Here, we study electroweak baryogenesis in the two Higgs doublet model [194–203] and the minimal supersymmetric standard model [204–221] focusing on its connections to collider phenomenology. In particular, we discuss relationship between the strength of the first-order electroweak phase transition and the quantum corrections to the trilinear coupling of the lightest Higgs boson [222]. Similar discussions on the Higgs self-coupling in the electroweak baryogenesis scenario can be found in Refs. [223, 224].

First we consider the two Higgs doublet model with the softly-broken discrete symmetry. The Higgs potential at the tree-level is given by Eq. (2.1) with $\lambda_6 = \lambda_7 = 0$. Though m_{12}^2 and λ_5 can be complex, one of the two becomes real by the redefinition of the either Higgs field. As mentioned above, the CP violation plays a crucial role in the generation of the baryon asymmetry. In particular, the difference between the CP violating phase in the symmetric phase and that in the broken phase at finite temperature gives a significant effect on the total amount of the baryon asymmetry. In order to calculate the magnitude of such CP violating phases, the equation of motion for the Higgs bubble wall has to be solved at the critical temperature. In the previous studies, it was found that there is a solution in which the CP violation can enhance only during the phase transition while it can become small at zero temperature enough to escape the experimental constraints of the electric dipole moment [201–203]. Here, we assume such a scenario so that we neglect the CP violating phase as the first approximation. Furthermore, to simplify our analysis we consider the phase transition in the direction of $\langle\Phi_1\rangle = \langle\Phi_2\rangle = (0\ \varphi)^T/2$, which corresponds to $m_1 = m_2,\ \lambda_1 = \lambda_2$, in other words, $\sin(\alpha-\beta) = -1$ and $\tan\beta = 1$ [199–201].

The one-loop contributions to the effective potentials at zero and finite temperatures [225] are respectively given by

$$\mathcal{V}_1(\varphi) = n_i \frac{m_i^4(\varphi)}{64\pi^2}\left(\log\frac{m_i^2(\varphi)}{Q^2} - \frac{3}{2}\right), \quad \mathcal{V}_1(\varphi,T) = \frac{T^4}{2\pi^2}\Big[\sum_{j=\text{bosons}} n_j I_B(a_j^2) + n_t I_F(a_t^2)\Big], \quad (2.120)$$

with

$$I_{B,F}(a_i^2) = \int_0^\infty dx\, x^2 \log\left(1 \mp e^{-\sqrt{x^2+a_i^2}}\right), \quad a_i(\varphi) = \frac{m_i(\varphi)}{T}, \tag{2.121}$$

where $\mathcal{V}_1(\varphi)$ is regularized by using the $\overline{\rm DR}$-scheme, Q is a renormalization scale, $m_i(\varphi)$ is the field dependent mass of the particle i, and n_i is the degree of the freedom of i; i.e., $n_W = 6,\ n_Z = 3$ for gauge bosons ($W^\pm$, Z), $n_t = -12$ for the top quark (t) and $n_h = n_H = n_A = 1,\ n_{H^\pm} = 2$ for the five physical Higgs bosons ($h, H, A, H^\pm$).

Qualitative features of the phase transition can be understood from the effective potential (2.120) by the following high temperature expansion. When $m_\Phi^2 \gg m_h^2,\ M^2$ ($\Phi \equiv H, A, H^\pm,\ M^2 \equiv v^2\eta$), the field dependent masses of the heavy Higgs bosons can be written as $m_\Phi^2(\varphi) \simeq m_\Phi^2\varphi^2/v^2$. At high temperatures, the Higgs potential can be expanded in powers of φ [226, 227].

$$\mathcal{V}_{\rm eff}(\varphi, T) \simeq D(T^2 - T_0^2)\varphi^2 - ET|\varphi|^3 + \frac{\lambda_T}{4}\varphi^4 + \cdots, \tag{2.122}$$

with

$$\begin{aligned}
T_0^2 &= \frac{1}{D}\left(\frac{1}{4}m_h^2 - 2Bv^2\right), && (2.123)\\
B &= \frac{1}{64\pi^2 v^4}\Big(6m_W^4 + 3m_Z^4 - 12m_t^4 + m_H^4 + m_A^4 + 2m_{H^\pm}^4\Big), && (2.124)\\
D &= \frac{1}{24v^2}\Big(6m_W^2 + 3m_Z^2 + 6m_t^2 + m_H^2 + m_A^2 + 2m_{H^\pm}^2\Big), && (2.125)\\
E &= \frac{1}{12\pi v^3}\Big(6m_W^3 + 3m_Z^3 + m_H^3 + m_A^3 + 2m_{H^\pm}^3\Big), && (2.126)\\
\lambda_T &= \frac{m_h^2}{2v^2}\left[1 - \frac{1}{8\pi^2 v^2 m_h^2}\left\{6m_W^4 \log\frac{m_W^2}{\alpha_B T^2} + 3m_Z^4 \log\frac{m_Z^2}{\alpha_B T^2} - 12m_t^4 \log\frac{m_t^2}{\alpha_F T^2}\right.\right.\\
&\qquad \left.\left. + m_H^4 \log\frac{m_H^2}{\alpha_B T^2} + m_A^4 \log\frac{m_A^2}{\alpha_B T^2} + 2m_{H^\pm}^4 \log\frac{m_{H^\pm}^2}{\alpha_B T^2}\right\}\right], && (2.127)
\end{aligned}$$

where $\log\alpha_B = 2\log 4\pi - 2\gamma_E \simeq 3.91,\ \log\alpha_F = 2\log\pi - 2\gamma_E \simeq 1.14$, and γ_E is the Euler constant. The first order phase transition is possible due to the appearance of the cubic term which originates from the bosonic loops at finite temperature. From Eq. (2.122), the critical temperature T_c is expressed by

$$T_c^2 = \frac{T_0^2}{1 - E^2/(\lambda_{T_c} D)}. \tag{2.128}$$

At T_c, the effective potential $\mathcal{V}_{\rm eff}$ has two degenerate minima at

$$\varphi = 0, \qquad \varphi_c = \frac{2ET_c}{\lambda_{T_c}}. \tag{2.129}$$

In order not to wash out the created baryon number density after the electroweak phase transition, we have to require that the sphaleron process should be sufficiently suppressed. The most reliable condition has been obtained from the lattice simulation study [228, 229]. It is expressed as

$$\frac{\varphi_c}{T_c} = \frac{2E}{\lambda_{T_c}} > 1. \tag{2.130}$$

Due to the contributions of the heavy Higgs bosons in the loop, the first order phase transition can be strong enough to satisfy Eq. (2.130). The high temperature expansion makes it easy to see the phase transition analytically. However, it breaks down when the masses of the particles in loops become larger than T_c. In the following, we therefore calculate T_c and φ_c numerically.

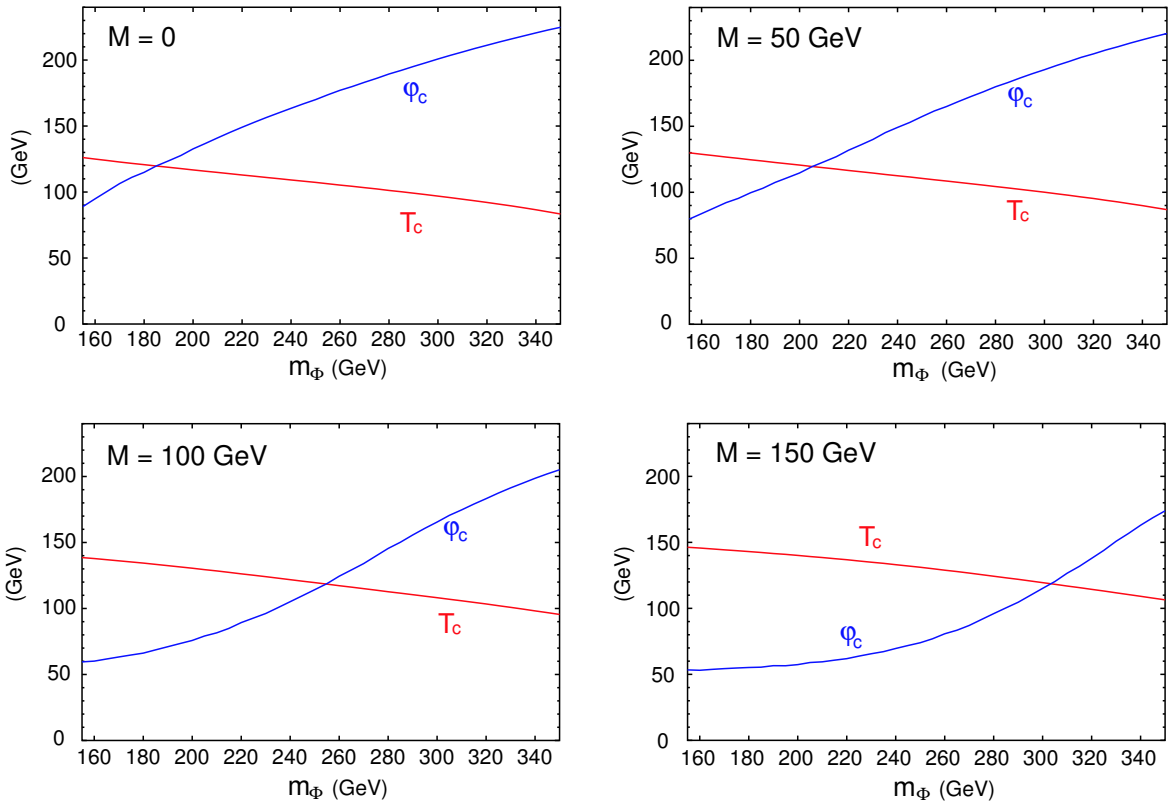

Fig. 2.4: The Higgs vacuum expectation value φ_c at the critical temperature T_c as a function of the heavy Higgs boson mass m_Φ ($m_\Phi = m_H = m_A = m_{H^\pm}$) for $M = 0$, 50, 100 and 150 GeV. Other parameters are fixed as $\sin(\alpha-\beta) = -1$, $\tan\beta = 1$ and $m_h = 120$ GeV.

In order to see phenomenological consequences of our scenario for successful electroweak baryogenesis, we study the trilinear coupling of the lightest Higgs boson (the hhh coupling) at the zero temperature in the parameter region where the phase transition is strongly first order. The leading contribution of the heavy Higgs bosons and the top quark to the hhh coupling can be extracted from the one-loop calculation by [113, 230]

$$\lambda_{hhh}^{\rm eff}(\text{2HDM}) \simeq \frac{3m_h^2}{v}\left[1+\frac{m_H^4}{12\pi^2 m_h^2 v^2}\left(1-\frac{M^2}{m_H^2}\right)^3+\frac{m_A^4}{12\pi^2 m_h^2 v^2}\left(1-\frac{M^2}{m_A^2}\right)^3 + \frac{m_{H^\pm}^4}{6\pi^2 m_h^2 v^2}\left(1-\frac{M^2}{m_{H^\pm}^2}\right)^3 - \frac{m_t^4}{\pi^2 m_h^2 v^2}\right]. \quad (2.131)$$

It is easily seen that the effects of the heavy Higgs boson loops are enhanced by m_Φ^4 ($\Phi = H, A, H^\pm$) when M^2 is zero. These effects do not decouple even in the large mass limit $m_\Phi \to \infty$ and yield the large deviation of the hhh coupling from the Standard Model prediction. In this case, m_Φ is bounded from above by perturbative unitarity ($m_\Phi < 550$ GeV) [31,32,34,231]. We note that when such nondecoupling loop effects due to the extra heavy Higgs bosons are large on the hhh coupling, the coefficient E of the cubic term in Eq. (2.122) becomes correspondingly large. Therefore there is a strong correlation between the large quantum correction to the hhh coupling and successful electroweak baryogenesis.

We calculate the effective potential (2.120) varying the temperature T and determine the critical temperature T_c of the first order phase transition and the expectation value φ_c at T_c. In the plots of Fig. 2.4, T_c and φ_c are shown as a function of the mass of the heavy Higgs boson m_Φ for $M = 0,\ 50,\ 100$

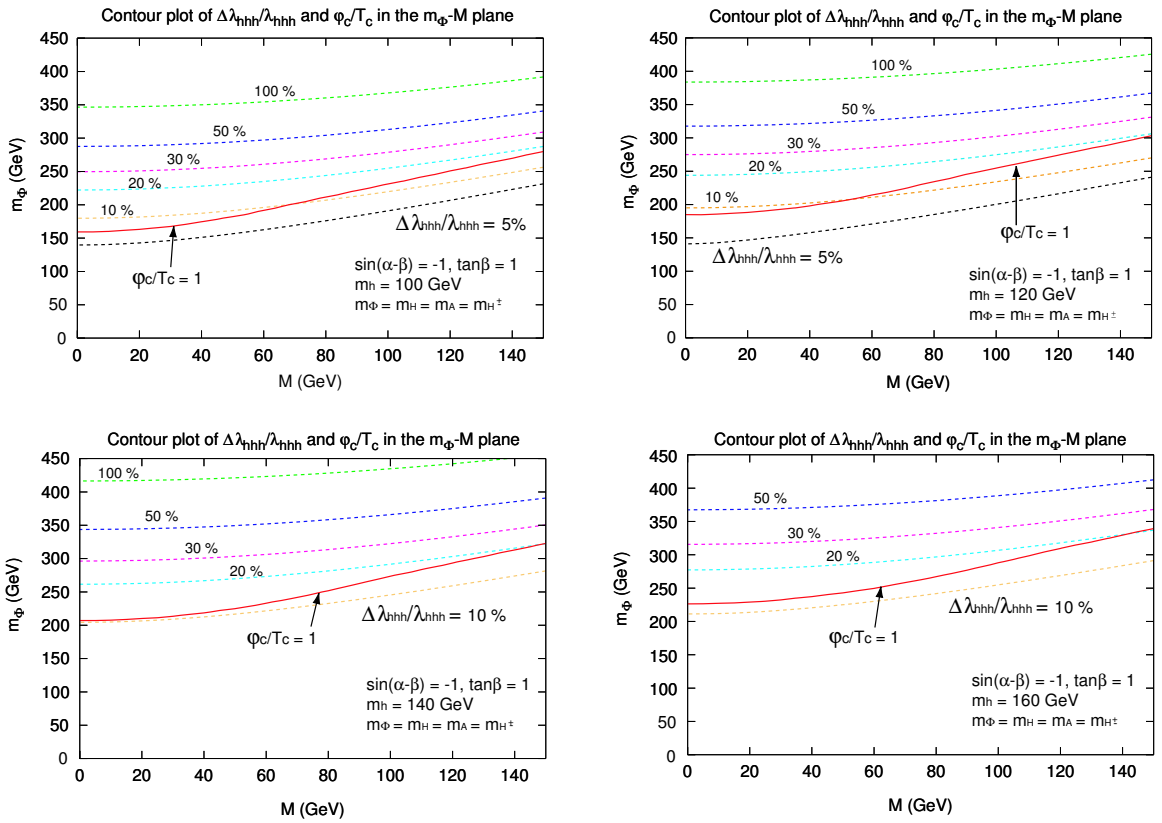

Fig. 2.5: Contours of the radiative correction of the triple Higgs boson coupling constant overlaid with the line $\varphi_c/T_c = 1$ in the m_Φ-M plane for m_h=100, 120, 140 and 160 GeV. Other parameters are the same as those in Fig. 2.4. The above the critical line, the phase transition is strong enough for the successful electroweak baryogenesis scenario.

and 150 GeV. We take $m_h = 120$ GeV. For the heavy Higgs boson mass, we assume $m_H = m_A = m_{H^\pm} (\equiv m_\Phi)$ to avoid the constraint on the ρ parameter from the LEP precision data [232]. We also take into account the ring summation for the contribution of the Higgs bosons to the effective potential at finite temperature to improve our calculation [225, 233–238]. In the case of $M = 0$, it is found that $\varphi_c = T_c \simeq 120$ GeV at $m_\Phi \simeq 185$ GeV, and the condition (2.130) is satisfied for $m_\Phi > 185$ GeV. One can also find that the condition (2.130) can still be satisfied for $M = 150$ GeV, if the masses of the heavy Higgs bosons are greater than about 300 GeV.

In Fig. 2.5, we show the parameter region where the necessary condition of electroweak baryogenesis in Eq. (2.130) is satisfied in the m_Φ-M plane for $m_h = 100,\ 120,\ 140$ and 160 GeV. For $m_h = 120$ GeV, we can see that the phase transition becomes strong enough for successful baryogenesis when the masses of the heavy Higgs bosons are larger than about 200 GeV. For the larger values of M or m_h, the greater m_Φ are required to satisfy the condition (2.130). In this figure we also plot the contour of the magnitude of the deviation in the hhh coupling from the Standard Model value. We define the deviation $\Delta\lambda^{\rm 2HDM}_{hhh}/\lambda^{\rm eff}_{hhh}({\rm SM})$ by $\Delta\lambda^{\rm 2HDM}_{hhh} \equiv \lambda^{\rm eff}_{hhh}({\rm 2HDM}) - \lambda^{\rm eff}_{\rm hhh}({\rm SM})$. We calculated the deviation from the full one-loop results, which give a better approximation than the formula given in Eq. (2.131) [113, 230]. We can easily see that the magnitude of the deviation is significant ($> 10\%$) in the parameter region where electroweak baryogenesis is possible. Such magnitude of the deviation can be detected at future collider experiments [142, 239–241].

Next we discuss a scenario of electroweak baryogenesis in the minimal supersymmetric standard model. The strong first order phase transition can be induced by the loop effect of the light stop in the finite temperature effective potential [204]. We examine the loop effect of the light stop on the hhh

coupling in this scenario. In the following, we only consider the finite and zero temperature effective potentials using high temperature expansion to understand the qualitative feature. As we have done in the case of the two Higgs doublet model, we consider the relationship between the magnitude of the phase transition and the deviation of the hhh coupling from the Standard Model value. The combined result is approximately expressed as

$$\frac{\Delta\lambda_{hhh}(\mathrm{MSSM})}{\lambda_{hhh}(\mathrm{SM})} \simeq \frac{2v^4}{m_t^2 m_h^2}(\Delta E_{\tilde{t}_1})^2, \tag{2.132}$$

where m_h is the one-loop renormalized mass of the lightest Higgs boson and $\Delta E_{\tilde{t}_1}$ is the contribution of the light stop loop to the cubic term in the finite temperature effective potential. From the condition (2.130), the deviation in the hhh coupling from the Standard Model value is estimated to be $\sim 6\%$ for $m_h = 120$ GeV. In the minimal supersymmetric standard model, the condition of the sphaleron decoupling also leads to the large deviation of the hhh coupling from the Standard Model prediction at zero temperature.

In summary, we have discussed electroweak baryogenesis with special emphasis on its connections to the collider phenomenology. If the electroweak phase transition is strong enough for electroweak baryogenesis, the triple Higgs boson coupling can deviate from the Standard Model value. The magnitude of the deviation can be larger than 10% level in the two Higgs doublet model. Such magnitude of the deviation can be detected at future colliders.

2.7 Neutral Higgs bosons with (in)definite CP: decay distributions for $\tau^+\tau^-$ and $t\bar{t}$ final states

Werner Bernreuther, Arnd Brandenburg and Jörg Ziethe

This contribution deals with the question of how to determine the parity, respectively the CP property of a neutral Higgs boson. While the Standard Model Higgs boson is parity-even, SM extensions predict also parity-odd state(s) or, if the (effective) Higgs potential violates CP, states of undefined CP parity with Yukawa couplings both to scalar and pseudoscalar quark and lepton currents. Higgs sector CP violation (CPV) is, especially in view of its potentially enormous impact on the physics of the early universe, a fascinating speculation which can be investigated at the upcoming generation of colliders in several ways. The decays $h \to \tau^-\tau^+$ and/or $h \to t\bar{t}$ are particularly suited, provided that sufficiently large event numbers are available. The analysis presented here is based on the proposals and investigations of [99, 103] for the tau and of [99, 103, 242–245] for the top channel. Other investigations include [101, 246–250].

The following applies to any neutral Higgs boson h_j with *flavor-diagonal* couplings to quarks and leptons f (with mass m_f)

$$\mathcal{L}_Y = -(\sqrt{2}G_F)^{1/2} \sum_{j,f} m_f (a_{jf}\bar{f}f + b_{jf}\bar{f}i\gamma_5 f)\, h_j \ , \tag{2.133}$$

where a_{jf} and b_{jf} are the reduced scalar and pseudoscalar Yukawa couplings, respectively, which depend on the parameters of the scalar potential and on the type of model. In the SM $a_f = 1$ and $b_f = 0$. In models with two Higgs doublets there are three physical neutral Higgs fields h_j in the mass basis. In the type II models the Yukawa couplings to top quarks and τ leptons are (see sections 2.1 and 3.1): $a_{jt} = R_{2j}/\sin\beta$, $b_{jt} = -R_{3j}\cot\beta$, $a_{j\tau} = R_{1j}/\cos\beta$, $b_{j\tau} = -R_{3j}\tan\beta$, where $\tan\beta = v_2/v_1$, and (R_{ij}) is a 3×3 orthogonal matrix that describes the mixing of the neutral spin-zero states. At the Born level only the $\mathrm{CP} = +1$ component of h_j couples to W^+W^- and to ZZ. If Higgs sector CP violation (CPV) is negligibly small then the fields h_j describe two scalar states h, H and a pseudoscalar A. In the

following ϕ denotes, as in section 2.1 above, any of these Higgs bosons. We assume that the differences between the mass of the Higgs particle ϕ under consideration and the masses of the other neutral Higgs states are larger than the experimental resolution.

2.7.1 τ and top spin observables

The observables discussed below for determining the CP quantum number of a neutral Higgs boson in the decay channels $\phi \to \tau^-\tau^+$ and/or $\phi \to t\bar{t}$ may be applied to any Higgs production process. At the LHC this includes the gluon and gauge boson fusion processes $gg \to \phi$ and $q_iq_j \to \phi q_i' q_j'$, respectively, and associated production of a light Higgs boson, $t\bar{t}\phi$ or $b\bar{b}\phi$ with $\phi \to \tau^-\tau^+$. Likewise they can be used in future Higgs search at an ILC, or in Higgs production with envisaged high energetic muon or photon collisions, $\mu^-\mu^+$, $\gamma\gamma \to \phi \to f\bar{f}$. In the following we consider the semi-inclusive reactions

$$i \,\to\, \phi \,+\, X \,\to\, f(\mathbf{k_f}, \alpha) \,+\, \bar{f}(\mathbf{k_{\bar{f}}}, \beta) \,+\, X\,, \tag{2.134}$$

where i is some initial state, $f = \tau^-, t$, $\mathbf{k_f}$ and $\mathbf{k_{\bar{f}}} = -\mathbf{k_f}$ are the 3-momenta of f and $\bar{f}$ in the $f\bar{f}$ zero-momentum frame (ZMF), and α, β are spin labels. We make use of the fact that, at colliders, polarization and spin correlation effects are both measurable and reliably predictable for tau leptons and top quarks.

Let's assume that experiments at the LHC will discover a neutral boson resonance in the channel $gg \to \phi \to \tau^-\tau^+X$. The spin of ϕ may be inferred from the polar angle distribution of the tau leptons. Suppose the outcome of this is that ϕ is a spin-zero (Higgs) particle. One would next like to determine its Yukawa coupling(s), and specifically like to know whether ϕ is a scalar, a pseudoscalar, or a mixture of both, i.e., a state of undefined CP quantum number. For answering this question several CP-even and -odd observables involving the spins of $f, \bar{f}$ apply, and we emphasize that all of them should be used. It was shown in [99] that the correlation resulting from projecting the spin of f onto the spin of $\bar{f}$,

$$\mathcal{O}_1 \,=\, \mathbf{s}_f \cdot \mathbf{s}_{\bar{f}}\,, \tag{2.135}$$

is the best choice for discriminating between a $CP = \pm 1$ state. Here $\mathbf{s}_f, \mathbf{s}_{\bar{f}}$ denote the $f, \bar{f}$ spin operators. This is easy to understand in simple quantum mechanical terms. Consider a reaction $i \to \phi \to f\bar{f}$ where ϕ production and decay factorizes. If ϕ is a scalar ($J^{PC} = 0^{++}$) then $f\bar{f}$ is in a ${}^3P_0$ state, and an elementary calculation yields $\langle \mathbf{s}_f \cdot \mathbf{s}_{\bar{f}} \rangle = 1/4$. If ϕ is a pseudoscalar ($J^{PC} = 0^{-+}$) then $f\bar{f}$ is in a ${}^1S_0$ state and $\langle \mathbf{s}_f \cdot \mathbf{s}_{\bar{f}} \rangle = -3/4$, which is strikingly different from the scalar case. These values do not depend on the mass of ϕ, provided $m_\phi > 2m_f$. For general couplings (2.133) one gets $\langle \mathcal{O}_1 \rangle = (a_f^2\beta_f^2 - 3b_f^2)/(4a_f^2\beta_f^2 + 4b_f^2)$ [99]. In Fig. 2.6 (left) the expectation value $\langle \mathcal{O}_1 \rangle$ is shown for $\phi \to \tau^-\tau^+X$ as a function of the ratio $r_\tau = b_\tau/(a_\tau + b_\tau)$, taking $a_\tau, b_\tau > 0$ for definiteness, for arbitrary Higgs mass $m_\phi \gtrsim 100$ GeV. The figure applies also to $\phi \to t\bar{t}X$ (with $r_\tau \to r_t$) if m_ϕ is markedly above the $t\bar{t}$ threshold. For small t quark velocities β_t the resulting plot is distorted, as compared with Fig. 2.6, between the fixed points 1/4 and -3/4. The QED corrections to this observable, respectively the order α_s QCD corrections in the case of $f = t$ are very small [99].

We note in passing that the CP-even spin-spin correlation in the helicity basis, $\langle (\hat{\mathbf{k}}_\mathbf{f} \cdot \mathbf{s}_f)(\hat{\mathbf{k}}_{\bar{\mathbf{f}}} \cdot \mathbf{s}_{\bar{f}}) \rangle$, is insensitive to the CP quantum number of ϕ [99].

If $\gamma_{CP}^f \equiv -a_f b_f \neq 0$ the Yukawa interactions of ϕ break CP. This leads to CP-violating effects in the reactions (2.134). For an unpolarized initial state i a general kinematic analysis of (2.134) yields the following [103, 243, 245]. If C-violating interactions do not matter in (2.134) then $\mathcal{L}_Y$ (which is C-invariant, but P- and CP-violating) induces two types of CPV effects in the $f\bar{f}$ state: a CP-odd spin-spin correlation and a CP-odd polarization asymmetry which correspond to the observables

$$\mathcal{O}_2 \,=\, \hat{\mathbf{k}}_\mathbf{f} \cdot (\mathbf{s}_f \times \mathbf{s}_{\bar{f}})\,, \quad \mathcal{O}_3 \,=\, \hat{\mathbf{k}}_\mathbf{f} \cdot (\mathbf{s}_f - \mathbf{s}_{\bar{f}})\,. \tag{2.136}$$

Here $\hat{\mathbf{k}}_\mathbf{f} = \mathbf{k_f}/|\mathbf{k_f}|$ in the $f\bar{f}$ ZMF. (A priori two more terms can appear in the squared matrix element of (2.134). They are obtained by replacing $\hat{\mathbf{k}}_\mathbf{f} \to \hat{\mathbf{p}}$ in (2.136), where $\hat{\mathbf{p}}$ is the direction of one of the

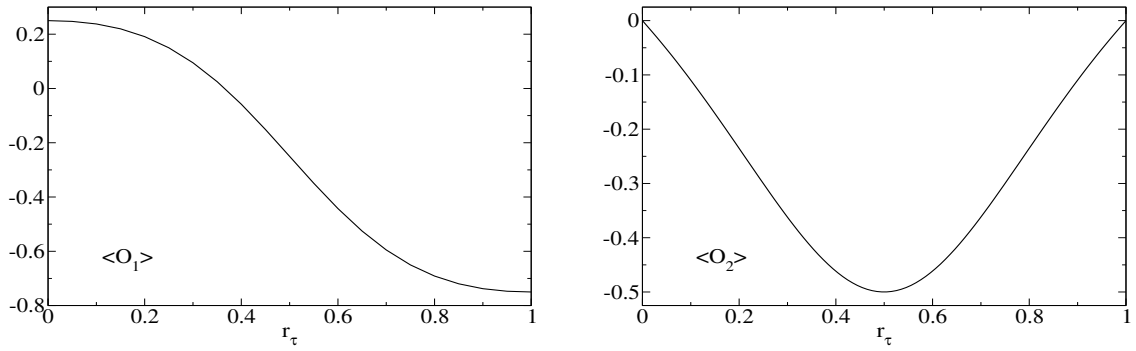

Fig. 2.6: Expectation value of $\langle \mathcal{O}_1 \rangle$ (left) and $\langle \mathcal{O}_2 \rangle$ (right) for $\phi \to \tau^- \tau^+ X$ as a function of r_τ [99].

colliding beams in i. However, for resonant ϕ production only the observables (2.136) are of interest.) The CP-odd and T-odd[12] variable $\mathcal{O}_2$ measures a correlation of the spins of the f and $\bar{f}$ transverse to their directions of flight. A non-zero expectation value is generated already at tree level, $\langle \mathcal{O}_2 \rangle = \gamma_{CP}^f \beta_f / (a_f^2 \beta_f^2 + b_f^2)$ [103], which can be as large as 0.5 in magnitude! In Fig. 2.6 (right) $\langle \mathcal{O}_2 \rangle$ is shown for $\phi \to \tau^- \tau^+ X$ as a function of r_τ, for Higgs masses $m_\phi \gtrsim 100$ GeV. The figure applies also to $\phi \to t\bar{t}X$ (with $r_\tau \to r_t$) for sufficiently heavy ϕ. The QED corrections to this observable, respectively the order α_s QCD corrections in the case of $f = t$, are also very small [99]. The variable $\mathcal{O}_3$ measures an asymmetry in the longitudinal polarization of the f and $\bar{f}$. As it is CP-odd but T-even, a non-zero $\langle \mathcal{O}_3 \rangle$ requires $\gamma_{CP}^f \neq 0$ and a non-zero absorptive part of the respective scattering amplitude. This variable is relevant for heavy Higgs $\to f\bar{f}$, e.g., for $gg \to \phi \to t\bar{t}$ (see below), but not for light Higgs $\to \tau\tau$.

If besides (2.133) and QCD also C-violating interactions (e.g. the standard weak interactions) matter for the reactions (2.134) then there can be, in principle, another CPV effect, namely $\langle \hat{\mathbf{n}} \cdot (\mathbf{s}_f - \mathbf{s}_{\bar{f}}) \rangle \neq 0$ [245]. Here $\hat{\mathbf{n}}$ denotes the normal to the $i \to f\bar{f}$ scattering plane. Below we consider the reactions $gg \to \phi \to f\bar{f}$ within QCD. In this case this CPV polarization effect is absent. This holds true also for reactions (2.134) where the production and decay of ϕ factorizes.

2.7.2 Distributions for the decay products of $\tau^+\tau^-$ and $t\bar{t}$

The polarization and spin-correlation effects (2.135), (2.136) induced in the $f\bar{f}$ sample lead, through the parity-violating weak decays of the τ leptons and top quarks, to specific angular distributions and correlations in the respective final state. We consider here

$$i \to \phi + X \to f(\mathbf{k_f}) + \bar{f}(\mathbf{k_{\bar{f}}}) + X \to a(\mathbf{q_1}) + \bar{b}(\mathbf{q_2}) + X\,, \tag{2.137}$$

where $a, \bar{b}$ denotes a charged particle or a jet from the decays $f \to a + \cdots$, $\bar{f} \to \bar{b} + \cdots$. The 3-momenta of f and $\bar{f}$ in (2.137) refer as above to the $f\bar{f}$ ZMF, while the momenta $\mathbf{q_1}$ and $\mathbf{q_2}$ refer to the f and $\bar{f}$ rest frames, respectively. For $f = \tau, t$ these frames and momenta can be reconstructed using kinematic constraints (c.f., e.g. [115, 251, 252]).

For the tau lepton one may take into account the decay channels $\tau^- \to \pi^-\nu_\tau$, $\rho^-\nu_\tau$, $a_1^-\nu_\tau$, $\ell^-\bar{\nu}_\ell\nu_\tau$, which comprise about 81 % of all tau decays. That is, $B(\tau^-\tau^+ \to a\bar{b}X) \simeq 66$ % for $a, b = \pi, \rho, a_1, \ell$. Here we need to recall only the τ-spin analyzing power of these particles, that is, the coefficient c_a in the distribution $\Gamma_a^{-1} d\Gamma_a / d\cos\theta = (1 + c_a \cos\theta)/2$ of the decay $\tau^- \to a + \cdots$, where $\cos\theta$ is the angle between the τ spin vector and the direction of a in the τ rest frame (c.f., e.g., [252]). They are collected in Table 2.2.

According to the SM the top quark decays into Wb almost 100 % of the time, which leads to the CKM allowed semi- and nonleptonic final states, $t \to b\ell\nu_\ell$, $bq\bar{q}'$, $q\bar{q}'$ = $u\bar{d}$, $c\bar{s}$. Again we need here only

[12] Here T-even/odd refers to a naive T transformation, i.e., reversal of momenta and spins only.

Table 2.2: Spin-analyzing power for tau decays and top quark decays in the SM.

$\tau^- \to$	π^-	ρ^-	a_1^-	ℓ^-
c_a:	1.0	0.46	0.12	-0.33
$t \to$	ℓ^+	b	$j_<$	$j_>$
c_a (LO):	1	-0.41	0.51	0.2
c_a (NLO):	0.999	-0.39	0.47	

Table 2.3: Coefficient D_{ab} in (2.138) for some final states in $\phi \to \tau\tau$.

$\tau\tau \to$	$\pi\pi$	$\rho\rho$	$\ell\ell'$	$\pi\rho$	$\pi\ell$	$\rho\ell$
$\phi\,(0^{++})$:	0.33	0.07	0.04	0.15	-0.11	-0.05
$\phi\,(0^{-+})$:	-1	-0.21	-0.11	-0.46	0.33	0.15

the t-spin analyzing power c_a of particle/jet a in the decay $t \to a + \cdots$. Table 2.2 contains the values of the c_a at tree level (c.f., for instance, [253]) and to order α_s, which were computed for the semi-and non-leptonic decays in [254] and in [255], respectively. For the non-leptonic channels, $j_<$ and $j_>$ denote the least energetic and most energetic non-b jet defined by the Durham clustering algorithm.

Within 2HDMs the decays of the top quark will be mediated also by charged Higgs exchange. However the branching ratio $B(b \to s\gamma)$ implies that H^+ is much heavier than the top quarks, see section 2.2. Thus for the important channel $t \to \ell + \cdots$, $\ell = e, \mu$ the impact of H^+ exchange on the c_ℓ can be neglected. In any case, the results below can be straightforwardly extended if new top decay modes and/or decay mechanisms should be discovered.

The $\cos\theta$ distributions for the antiparticle decays $\bar{f} \to \bar{b} + \cdots$ are proportional to $(1 - c_b \cos\theta)$, assuming CP invariance. Violation of this relation requires that the respective decay amplitude has a CP-violating absorptive part [256]. In 2HMDs the one-loop corrections to the tWb vertex generate such a term [257], but its effect on the c_a of the top quark is negligible in the context of this report.

Let's now come to the analogue of the $\mathcal{O}_i$ at the level of the final states $a, \bar{b}$. The spin correlation $\langle \mathcal{O}_1 \rangle$ leads to a non-isotropic distribution in $\cos\varphi_{ab}$, where $\varphi_{ab} = \angle(\mathbf{q_1}, \mathbf{q_2})$. If no phase space cuts are applied – modulo cuts on the invariant mass $M_{f\bar{f}}$ of the fermion pair – this opening angle distribution is of the form [99, 244]:

$$\frac{1}{\sigma_{ab}} \frac{d\sigma_{ab}}{d\cos\varphi_{ab}} = \frac{1}{2}\left(1 - D_{ab}\,\cos\varphi_{ab}\right)\,, \quad D_{ab} = \frac{4}{3}\,c_a c_b\,\langle \mathbf{s}_f \cdot \mathbf{s}_{\bar{f}} \rangle\,. \tag{2.138}$$

2.7.3 τ decay channels

For $\phi \to \tau\tau$ we have listed in Table 2.3 the coefficients D_{ab} for some of the final states mentioned above. As the charged pion in $\tau \to \pi\nu_\tau$ is the best τ-spin analyzer, this channel discriminates most strikingly between a scalar and a pseudoscalar Higgs boson. In the case of a pseudoscalar ϕ the pion momenta $\mathbf{q_1}$, $\mathbf{q_2}$ are predominantly parallel, while for a scalar ϕ they tend to be antiparallel. As this channel has a small branching ratio, $B(\tau\tau \to \pi\pi) \simeq 0.01$, the other channels also matter.

The analogue of the CP-odd spin observables $\mathcal{O}_{2,3}$ are [99, 245]:

$$Q_2 \,=\, (\hat{\mathbf{k}}_f - \hat{\mathbf{k}}_{\bar{f}}) \cdot (\hat{\mathbf{q}}_2 \times \hat{\mathbf{q}}_1)/2\,, \quad Q_3 \,=\, \hat{\mathbf{k}}_f \cdot \hat{\mathbf{q}}_1 - \hat{\mathbf{k}}_{\bar{f}} \cdot \hat{\mathbf{q}}_2\,, \tag{2.139}$$

where $\hat{\mathbf{k}}_f$ and $\hat{\mathbf{k}}_{\bar{f}} = -\hat{\mathbf{k}}_f$ are defined as above in the $f\bar{f}$ ZMF. Measurement of (2.139) requires the determination of the signs of the charges of a and $\bar{b}$ while this is not necessary for (2.138). The average

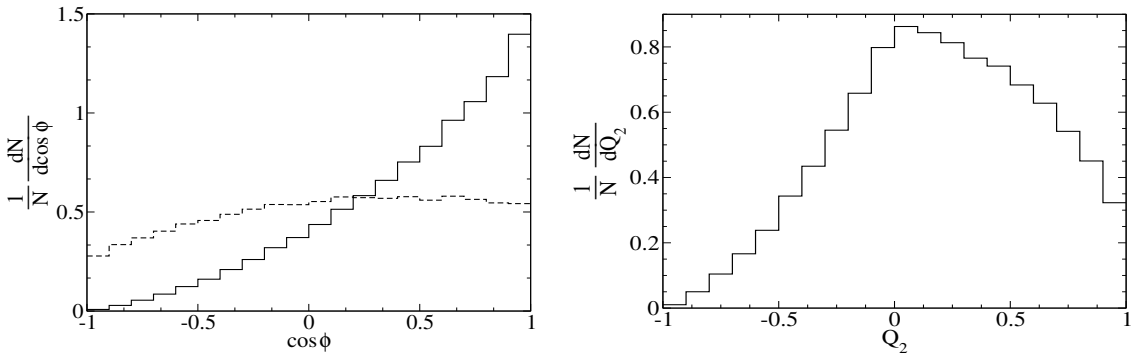

Fig. 2.7: Production of ϕ with m_ϕ= 200 GeV at the LHC via gluon fusion and decay $\phi \to \tau\tau \to \pi\pi$. Left: opening angle distribution for a scalar (dashed) and a pseudoscalar (solid). Right: distribution of Q_2 for a Higgs boson with $a_\tau = -b_\tau$.

of Q_2 should be computed for events (2.137) plus the charge conjugated events $\bar{a}b$, while the average of $\langle Q_3 \rangle$ is to be computed for diagonal channels $a\bar{a}$. Concerning $\mathcal{O}_3$ one may take advantage of larger event samples, as exemplified in the case of top quarks in (2.142) below. Asymmetries corresponding to (2.139) are:

$$A(Q) \;=\; \frac{N_{ab}(Q>0) - N_{ab}(Q<0)}{N_{ab}} \;, \tag{2.140}$$

where N_{ab} is the number of events in the reaction (2.137). They should be experimentally more robust because only the signs of Q_i have to be measured. If no phase-space cuts, besides cuts on $M_{f\bar{f}}$, are imposed then [245]

$$\begin{aligned} \langle Q_2 \rangle_{ab} \;&=\; \frac{4}{9} c_a c_b \, \langle \mathcal{O}_2 \rangle \;, \quad \langle Q_3 \rangle_{aa} \;=\; \frac{2}{3} c_a^2 \, \langle \mathcal{O}_3 \rangle \;, \\ A(Q_2) \;&=\; \frac{9\pi}{16} \langle Q_2 \rangle_{ab} \,, \quad A(Q_3) \;=\; \langle Q_3 \rangle_{aa} \;. \end{aligned} \tag{2.141}$$

Let's apply Q_2 to $\phi \to \tau\tau$. (As already mentioned above $\langle Q_3 \rangle$ is in general small in this channel.) The observable Q_2 measures the distribution of the signed normal vector of the plane spanned by $\mathbf{q_1}, \mathbf{q_2}$ with respect to the τ^- direction of flight. If $\gamma_{CP}^\tau \neq 0$ then this distribution is asymmetric. If ϕ were an ideal mixture of a CP-even and -odd state, $|a_\tau| = |b_\tau|$, the asymmetry corresponding to Q_2 would take the value $|A(Q_2)| = 0.4$ in the $\pi\pi$ and $|A(Q_2)| = 0.06$ in the $\rho\ell$ channel, etc. Notice that the sign of $\langle Q_2 \rangle_{ab}$ resp. of $A(Q_2)$ measures the relative sign of the Yukawa couplings a_τ and b_τ.
How are these results modified by cuts? We have analyzed this for the production of a Higgs boson ϕ via gluon fusion at the LHC, and we report here only on the $\pi\pi$ channel: $gg \to \phi \to \tau^-\tau^+X \to \pi^-\pi^+X$. Backgrounds are due to the irreducible $Z \to \tau\tau$ and the $t\bar{t}$, $b\bar{b}$ and $W + jet$ processes (c.f., for instance, [115, 258]). We apply the cuts $E_T^{a,b} \geq 40$ GeV, $|\eta|$ <2.5. We take m_ϕ = 200 GeV and require 120 GeV $\leq M_{\tau\tau} \leq$ 280 GeV. Figure 2.7 (left) shows the opening angle distribution for a scalar ($b_\tau = 0$) and a pseudoscalar ($a_\tau = 0$) state. Because of the applied cuts the shapes of the distributions differ from (2.138), but the two cases are, nevertheless, clearly distinguishable. One can use $D_{ab} \equiv -3\langle \cos\varphi_{ab} \rangle$ as an unbiased estimator. We get $D_{\pi\pi} = -0.32$ (scalar) and -1.37 (pseudoscalar), which is to be compared with the respective values of Table 2.3. Thus only a few $\pi\pi$ events are required to decide whether ϕ is essentially a parity-even or -odd state. With (2.139) one can further check whether or not ϕ is a CPV mixture. In Fig. 2.7 (right) the distribution of Q_2 is plotted for the case of a Higgs boson with "maximal" CPV in its couplings to tau leptons, $a_\tau = -b_\tau$. This gives $\langle Q_2 \rangle_{\pi\pi} = 0.19$, which is a bit below the "no-cut" value 2/9, obtained from (2.141). We estimate that about 45 $\pi\pi$ events would establish this as a 5 σ effect. The opening angle distribution and Q_2 can be evaluated in analogous fashion for the other tau decay channels which should, of course, also be taken into account to accumulate statistics.

2.7.4 Top decay channels

Finally we discuss heavy Higgs bosons ϕ with mass $m_\phi > 2m_t$ that strongly couple to top quarks. Of particular interest here is the case of a pseudoscalar, as $A \not\to W^+W^-, ZZ$ in lowest order, or a heavy scalar with strongly suppressed couplings to the weak gauge bosons. If $\tan\beta$ is of order 1, the top-quark Yukawa coupling(s) will be large and $\phi \to t\bar{t}$ is the dominant decay mode. For the investigation of the CP nature of ϕ with the observables (2.138) and (2.139), (2.140) in this mode the dilepton and the lepton + jets channels are suitable which, for $\ell = e, \mu$, comprise about 4/81 and 8/27, respectively, of all $t\bar{t}$ decays in the SM. In order to search for a longitudinal polarization asymmetry $\mathcal{O}_3$ it is useful to divide the lepton + jets sample into two classes: $\mathcal{A}: \; t\bar{t} \to \ell^+ + \cdots$, and $\bar{\mathcal{A}}: \; t\bar{t} \to \ell^- + \cdots$. For these events one can use [245]

$$\mathcal{E} \; = \; \langle \hat{\mathbf{k}}_f \cdot \hat{\mathbf{q}}_1 \rangle_{\mathcal{A}} - \langle \hat{\mathbf{k}}_{\bar{f}} \cdot \hat{\mathbf{q}}_2 \rangle_{\bar{\mathcal{A}}} \tag{2.142}$$

and a further asymmetry involving the above triple correlation.

For reactions (2.137) where ϕ production and decay factorizes to good approximation we get the following [99]: If no phase space cuts are applied – modulo cuts on $M_{t\bar{t}}$ – the opening angle distribution is of the form (2.138) with $D_{\ell\ell'} = 1.33\langle \mathbf{s}_t \cdot \mathbf{s}_{\bar{t}} \rangle$ in the dilepton channel and $D_{\ell j_<} = 0.66\langle \mathbf{s}_t \cdot \mathbf{s}_{\bar{t}} \rangle$ in the lepton + jets channel if $j_<$ is used as top-spin analyzer in the non-leptonic top decay modes. The expectation value of $\mathcal{O}_1$ was given above and takes the values 0.25 and -0.75 for a P-even and -odd Higgs boson ϕ, respectively. In addition the formulae (2.141) apply. For a CPV Higgs boson a non-zero $\langle Q_3 \rangle$ and $\mathcal{E}$ are generated by the one-loop QCD corrections. With about 4000 $\phi \to t\bar{t}$ events the CP nature of ϕ could be established, in this ideal situation, for a large range of the coupling ratio r_t with 5 σ sensitivity when (2.138), (2.141), and (2.142) are used in combination [99].

At the LHC the main production reaction is expected to be gluon fusion, for which these results do not apply. The amplitude of $g\,g \to \phi \to t\bar{t} \to \text{final state}$ interferes with the amplitude of the QCD-induced non-resonant $t\bar{t}$ background, $g\,g \to t\bar{t} \to \text{final state}$, and this interference is not negligible, even in the vicinity of $\sqrt{s} \sim m_\phi$, because the resonance is not narrow. The interference generates a peak-dip structure in the $t\bar{t}$ invariant mass distribution $M_{t\bar{t}}$ [244, 259]. Statistically significant signals are possible in the mass range 350 GeV $\lesssim m_\phi \lesssim$ 500 GeV, depending on the strength of the Yukawa couplings and on the width of ϕ [115, 244, 251, 259]. Needless to say, this is a difficult channel which requires very good $M_{t\bar{t}}$ resolution and a precise knowledge of the background contributions to the $M_{t\bar{t}}$ distribution[13].

If experiments will find a signal of a heavy neutral spin-zero boson ϕ in the $t\bar{t}$ channel, the above observables can of course be used in this case, too, to investigate its CP properties. The opening angle distribution (2.138) was investigated in [244] in the dilepton channel with the irreducible $t\bar{t}$ background included. This background dilutes the striking difference between the shapes of the distributions for a scalar and a pseudoscalar ϕ exhibited above. It depends critically on the Yukawa couplings, mass, and width of ϕ whether or not a statistically significant effect is obtained. In order to preserve the discriminating power of this distribution it should be determined only for events with $M_{t\bar{t}} = m_\phi - \Delta$, where Δ is of the order of 40 GeV [244]. For the $t\bar{t}$ background the distribution (2.138) was computed to NLO QCD in [261].

CPV (resonant and non-resonant) ϕ exchange at one loop was computed for $q\bar{q}, gg \to t\bar{t}$ within 2HDM in [103, 243] and confirmed by [118, 262]. The expectation values of the observables (2.139), (2.140), and (2.142) were analyzed in [245] for the dilepton and the lepton + jets channels. When evaluated for events with $M_{t\bar{t}} = m_\phi - \Delta$ it was found that CP effects of a few percent are possible. Observables composed of final state momenta in the laboratory frame yield smaller CP effects [243]. In [263] the CP asymmetry $\Delta_{LR} = [N(t_L\bar{t}_L) - N(t_R\bar{t}_R)]/(\text{all}\, t\bar{t})$, which corresponds to $\langle \mathcal{O}_3 \rangle$, was computed within 2HDM for light ϕ exchange in $q\bar{q}, gg \to t\bar{t}$ production, and found to be $\Delta_{LR} \sim 0.1\,\%$.

Heavy Higgs production by weak gauge boson fusion at the LHC or at an ILC should also be an

[13] The matrix elements of [244] are contained in the MC generator TOPREX [260].

Table 2.4: $\phi \to \tau\tau$ event numbers N_1 and N_2 required to determine the CP-even and -odd correlation D_{ab} and $\langle Q_2\rangle_{ab}$ with 3 σ significance, as a function of $r_\tau = b_\tau/(a_\tau + b_\tau)$.

r_τ	0	0.1	0.2	0.5	0.6	0.7 – 1.0	
N_1:	9×10^3	10^4	1.2×10^4	1.2×10^4	3×10^3	10^3	
r_τ:	0.15	0.2	0.3	0.4 – 0.6	0.7	0.8	0.85
N_2 :	1.2×10^4	6×10^3	3×10^3	1.5×10^3	3×10^3	6×10^3	1.2×10^4

option to explore the $t\bar{t}$ decay channel. If high-energetic left- and right-circularly polarized photon beams will be available in the future then the respective production cross sections $\gamma\gamma \to \phi$ can be measured, and a difference would constitute a clean signal of Higgs sector CPV [109]. For unpolarized $\gamma\gamma$ collisions, the reactions $\gamma\gamma \to \phi \to \tau\tau$, $t\bar{t}$ may be employed to investigate the CP nature of ϕ. In [149] CP observables were analyzed and computed within 2HDM for the ℓ + jets final states of the $\phi \to t\bar{t}$ channel.

2.7.5 Conclusions

In conclusion we have discussed, for $\phi \to \tau\tau$ and $\phi \to t\bar{t}$, a set of observables for determining the CP parity of a neutral Higgs boson ϕ and, in particular, for investigating whether or not there is CPV in the Higgs sector. The τ decay channel is clearly most suited to explore the nature of a light or heavy ϕ, and the above correlations and asymmetries, applied in combination to the various charged final states, should provide powerful tools already at the LHC. Table 2.4 summarizes our results for the τ decay mode: N_1 and N_2 are the $\phi \to \tau\tau$ event numbers required to measure the CP-even and -odd correlation D_{ab} and $\langle Q_2\rangle_{ab}$ with 3 σ significance as a function of $r_\tau = b_\tau/(a_\tau + b_\tau)$, using the τ decay channels discussed above. The numbers apply to light and heavy ϕ. The opening angle distribution (2.138) is sensitive in the ranges $0 \le r_\tau \lesssim 0.2$ (scalar-like ϕ) and $0.7 \lesssim r_\tau \le 1.0$ (pseudoscalar-like ϕ). Assuming that at least 10^4 $\phi \to \tau\tau$ events will be recorded at the LHC, Higgs sector CP violation can be established if the ratio of the Yukawa couplings lies in the range $0.2 \lesssim r_\tau \lesssim 0.8$.

At the LHC a heavy ϕ is expected to be observable in the $t\bar{t}$ channel only under favorable circumstances, i.e., for a restricted parameter range of various SM extensions. We found that the CP-odd correlations and asymmetries (2.141), (2.142), applied to the dilepton and lepton + jets channels and evaluated in appropriate mass bins, deviate from zero with $\gtrsim 3$ σ for a Higgs boson with mass in the range 300 GeV$\lesssim m_\phi \lesssim$ 500 GeV and reduced Yukawa couplings $|a_t b_t| \gtrsim 0.1$. In any case the above observables may be applied to dileptonic and single-lepton $t\bar{t}$ events, irrespective of a significant resonance signal. Moreover, if $\phi \to t\bar{t}$ should be seen at a future high luminosity e^+e^- and/or photon collider the variables above will also show their discriminating power.

2.8 CP-violating top Yukawa couplings in the 2HDM

Wafaa Khater and Per Osland

The Two-Higgs-Doublet Model is a simple extension of the Standard Model that can provide additional CP violation [1, 36, 264–266]. However, the model is rather constrained, it is not a priori obvious that the allowed parameter regions provide CP violation that could be of experimental interest at the LHC. The top Yukawa coupling is of particular interest, since it will become accessible at the LHC. It is interesting to establish how the Higgs sector can be explored via this coupling.

The process

$$pp \to t\bar{t} + X \tag{2.143}$$

has been studied in considerable detail [263, 267], in particular by Bernreuther and Brandenburg [243,

245] who identified the different kinematical structures appearing in the CP-violating part of the interaction, and evaluated them in a generic Two-Higgs-Doublet Model.

At very high energies, the dominant contribution to the process (2.143) is from the gluon-gluon initial state,

$$gg \to t\bar{t} \tag{2.144}$$

as indicated in Fig. 2.8. Also, among various observables proposed by Bernreuther and Brandenburg, we focus [118] on one that requires the decay to electrons (or muons):

$$t \to l^+\nu_l b, \quad \bar{t} \to l^-\bar{\nu}_l\bar{b}. \tag{2.145}$$

In the process of producing $t\bar{t}$ via gluon fusion, the CP violation can arise at the one-loop level, via neutral Higgs exchange involving the t and $\bar{t}$ lines, provided the top Yukawa coupling exhibits both scalar and pseudo-scalar terms as given in Eq. (2.146). Such a coupling induces correlations among the t and $\bar{t}$ momenta and their spins. The most interesting of these correlations are the CP-odd ones which are transferred to the t and $\bar{t}$ decay products, e.g., to the energies and momenta of the electron and the positron.

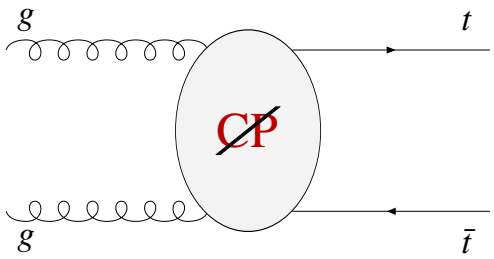

Fig. 2.8: The underlying $g + g \to t + \bar{t}$ reaction.

A necessary condition for having CP-violating Yukawa couplings, is that the mass matrix corresponding to the three neutral Higgs bosons not be block diagonal in the weak basis, i.e., in terms of the real and imaginary parts of the doublet fields Φ_1 and Φ_2. In the notation of [118] (see also section 2.1), this requires one or more among λ_5, λ_6 and λ_7 to be complex. The simplest case is to take λ_5 to be complex. Actually, the model considered in [118] takes $\lambda_6 = \lambda_7 = 0$. The Z_2 symmetry is thus respected by the quartic terms, and Flavour-Changing Neutral Couplings are naturally suppressed [18].

The resulting model can be parameterized in different ways. Let the top Yukawa coupling for a particular Higgs boson H_j be written as

$$H_j t\bar{t}: \qquad [a + i\gamma_5\tilde{a}] \qquad (j = 1, 2, 3) \tag{2.146}$$

or as

$$\frac{m_t}{v}\left[g_L\frac{1-\gamma_5}{2} + g_R\frac{1+\gamma_5}{2}\right]. \tag{2.147}$$

Then, a crucial quantity is the asymmetry between the left- and right-handed parts of the coupling

$$\gamma_{CP} = -a\tilde{a} = -i\,\frac{m_t^2}{4v^2}(g_L^2 - g_R^2). \tag{2.148}$$

In the Model II for Yukawa couplings, where only Φ_2 couples to up-type quarks, and only Φ_1 to down-type quarks, the couplings a and $\tilde{a}$ are simply given in terms of elements of the rotation matrix that diagonalizes the mass-squared matrix $\mathcal{M}^2$ of the neutral Higgs bosons. This rotation matrix R is defined in (2.27) and (2.28). Relative to the SM coupling, the Yukawa couplings can then be written as

$$H_j t\bar{t}: \qquad \frac{1}{\sin\beta}\,[R_{j2} - i\gamma_5\cos\beta R_{j3}], \tag{2.149}$$

with R the rotation matrix as defined in (2.28)

Unless the couplings are suppressed, the dominant contribution to the CP violation will come from diagrams involving exchange of the *lightest* Higgs boson, H_1. According to the above discussion, this contribution will be proportional to $R_{12}R_{13}\cos\beta/\sin^2\beta$. Thus, in order to maximize the CP violation in $t\bar{t}$ production, we are interested in low values of $\tan\beta$, and large values of $|R_{12}R_{13}|$. The latter requirement means large $|\sin\alpha_1|$ and large $|\sin 2\alpha_2|$.

2.8.1 A CP-violating observable

Among various CP-violating observables proposed by Bernreuther and Brandenburg, the quantity

$$A_1 = E_+ - E_- \tag{2.150}$$

was found to be rather promising [118]. Here, E_+ and E_- are the energies of the positron and electron of Eq. (2.145), defined in the laboratory frame.

In order to have a significant observation, the expectation value $\langle A_1\rangle$ must compare favourably with the statistical fluctuations, which behave like $\sqrt{N}$, where N is the number of events. In order to assess this, it is convenient to consider the "signal to noise" ratio [243],

$$\frac{S}{N} = \frac{\langle A_1\rangle}{\sqrt{\langle A_1^2\rangle - \langle A_1\rangle^2}}. \tag{2.151}$$

The analytical expression for $\langle A_1\rangle$ is entirely determined by the coefficients of the CP-odd correlations between the momenta and the spins of the $t\bar{t}$ pair [268]. This explicitly shows that the CP-violation originating at the production level of the top pair manifests itself in the kinematics of their decay products.

2.8.2 Results

One can specify the Two-Higgs-Doublet Model in terms of the potential, plus additional parameters. We found it convenient to follow a different approach. In order to more easily identify regions of large CP violation, we take as input parameters those which are more directly related to the observables. Thus, we take the angles of the rotation matrix and the lowest masses as part of the input:

$$\text{Input:}\quad \tan\beta,\quad \alpha_1,\quad \alpha_2,\quad \alpha_3,\quad M_1,\quad M_2,\quad M_{H^\pm},\quad \mathrm{Re}\, m_{12}^2. \tag{2.152}$$

With this input, the mass of the heaviest Higgs boson, M_3, is determined, as well as the coefficients of the potential, λ_1, λ_2, λ_3, λ_4, and λ_5.

CP violation requires the mass-squared matrix not to be block diagonal. This, in turn, requires $\sin\alpha_2 \neq 0$, and/or $\sin\alpha_3 \neq 0$. However, only a small part of the 8-dimensional parameter space (2.152) yields viable models, when various physical constraints are taken into account. The constraints are of different kinds, the most important of which are: (i) the potential must satisfy positivity and unitarity (constraints most easily expressed in terms of the λs), (ii) the spectrum must be compatible with the LEP searches (which essentially constrains a function of the lightest Higgs mass and its coupling to the Z boson), and (iii) the charged Higgs must be compatible with constraints from direct searches at LEP [232] and $b \to s\gamma$ [83].

For a range of parameters, with the lightest Higgs mass of the order of 100 to 150 GeV, $\tan\beta = 0.5$ and the charged Higgs mass at 300 GeV, the "signal-to-noise" ratio was found to be of the order of 10^{-3}. Thus, a number of semileptonically decaying $t\bar{t}$ events in excess of 10^6 will be required in order to measure a significant CP-violating signal, for "optimal" parameters. This should be possible, after a few years of running at high luminosity [269, 270].

We note from Eqs. (2.148) and (2.149) that in the limit of three degenerate Higgs masses, the CP violation in the top Yukawa coupling vanishes, due to the orthogonality of the rotation matrix R. Also,

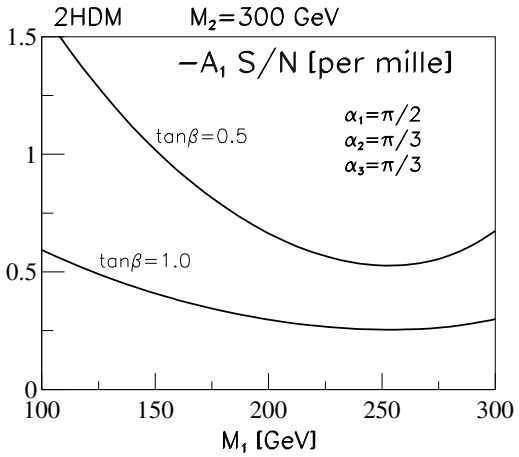

Fig. 2.9: Sensitivity of A_1 vs. lightest Higgs mass, M_1, for $M_2 = 300$ GeV, $M_3 = 500$ GeV, $M_{H^\pm} = 500$ GeV (from [271]).

due to the constraints inherent in the model (with $\lambda_6 = \lambda_7 = 0$), if two of the Higgs boson masses approach each other ($M_1 \to M_2$ or $M_2 \to M_3$) then also the third one will approach this value, and the CP violation will again vanish. Thus, "large" CP violation is only possible if one Higgs boson is fairly light, and the other two are heavy and non-degenerate.

In a recent update of this study [271], more constraints have been imposed on the model. As a result, the allowed regions of the parameter space shrink, and the detection of CP violation within the 2HDM thus becomes more challenging than found earlier, see Fig. 2.9.

2.9 Higgs CP measurement via $t\bar{t}\phi$ partial reconstruction at the LHC

Justin Albert, Mikhail Dubinin, Vladimir Litvin, and Harvey Newman

In the Standard Model, if the Higgs mass is below 140 GeV, the "golden" channels $\phi \to ZZ^* \to 4\ell$ and $\phi \to WW^* \to 2\ell 2\nu$ have small branching fraction, thus the mode $\phi \to \gamma\gamma$ begins to become more favorable for discovery. However, the latter does not, in general, encode information on Higgs properties such as CP and spin. In order for information on Higgs CP and spin to be obtained from such decays, the Higgs must be produced in association with two or more particles, such as $b\bar{b}$ or $t\bar{t}$. From an angular analysis of such processes, one can obtain information, in a model-independent way, on the Higgs spin and CP [272].

We consider here the process $gg \to t\bar{t}\phi$. This process has a relatively small cross-section in the SM (see the left plot of Fig. 2.10), however it has comparatively quite low background. In order to increase the size of the sample of $t\bar{t}\phi$ events, we reconstruct just one of the t *or* $\bar{t}$, *but not both*, *i.e.* a **partial reconstruction** of $t(\bar{t})\phi$, as compared with a **full reconstruction** of *both* the t *and* $\bar{t}$, as well as the Higgs. For an efficiency for top reconstruction of 20%, partial reconstruction increases the efficiency, relative to full reconstruction, from $(20\%)^2 = 4\%$ to $2 * 20\% - (20\%)^2 = 36\%$, nearly an order of magnitude. This could potentially introduce backgrounds of the form $t\phi + X$, however events that contain both top and Higgs are dominated by $t\bar{t} + X$, so this technique does not add significant irreducible background.

One may use both $\phi \to \gamma\gamma$ and $\phi \to b\bar{b}$ channels for this process. We consider here the $gg \to t(\bar{t})\phi, \phi \to \gamma\gamma$ channel, which has less background, although a far lower branching fraction, than $\phi \to b\bar{b}$. We select the $\phi \to \gamma\gamma$ in a similar manner as for the CMS inclusive $\phi \to \gamma\gamma$ analysis [273], and then

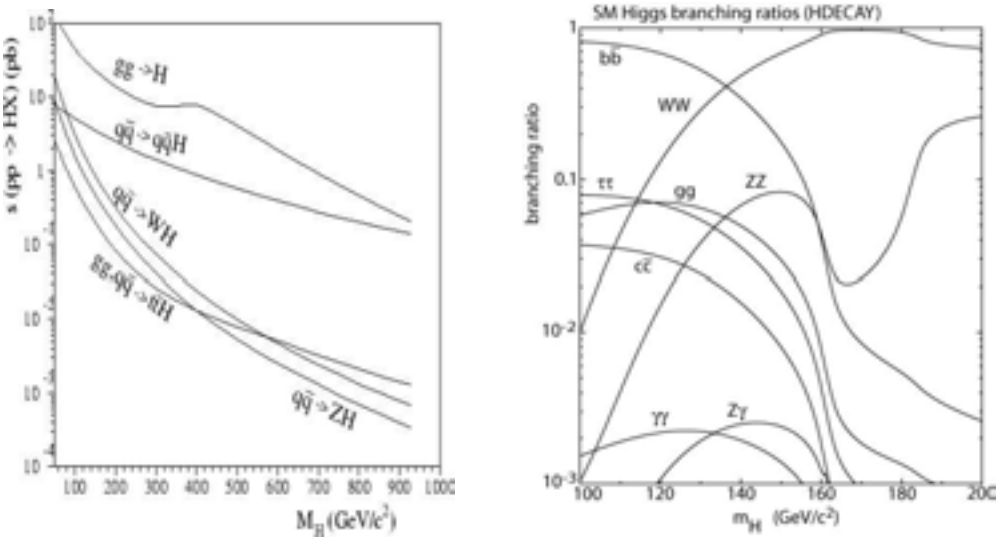

Fig. 2.10: Standard Model cross-sections (left) of processes containing a Higgs at the LHC as a function of Higgs mass, and branching fractions (right) of the Higgs, again as a function of Higgs mass.

add to that a top, reconstructed as a b-tagged jet and a high-p_T (> 40 GeV) lepton. The events themselves, and thus the background channels, are a subset of the inclusive $\phi \to \gamma\gamma$ analysis. Backgrounds are dominated in this case by $t\bar{t}\gamma\gamma$, $b\bar{b}\gamma\gamma$, and $Z\gamma\gamma$ processes. As Higgs discovery and mass measurement would likely be performed by the inclusive Higgs analysis prior to this analysis to determine Higgs spin and CP, a selection on the Higgs mass can dramatically reduce these main "irreducible" backgrounds.

In order to consider the $gg \to t(\bar{t})\phi$ process, the Yukawa Lagrangian can be divided into CP-even and CP-odd components:

$$\mathcal{L} = \bar{t}(c + id\gamma_5)t\phi, \tag{2.153}$$

where $0 \leq c \leq 1$ parametrizes the CP-even contribution and $d = 1 - c$ parametrizes the CP-odd fraction [272]. In the existing approaches to the MSSM with explicit CP violaton in the Higgs sector [47, 274, 275] the parameters c and d are expressed by means of the matrix elements R_{ij} of the Higgs boson mixing matrix (see Eq. 2.27). For the lightest mass eigenstate h_1 we have $c = k\,(R_{21}\sin\alpha + R_{11}\cos\alpha)$ and $d = -k\,(R_{31}\cos\beta)$ where $k = -m_{top}/(\sin\beta\, v^2)$ and α,β are the standard mixing angles of the CP-even/odd states. However, in the following we are not going to use any particular model of explicit CP-violation but simply consider c and d as the model-independent weights parametrizing the CP-even and the CP-odd components in the Yukawa Lagrangian [272].

Gunion and He define 6 CP-sensitive variables, as follows [272]:

$$\begin{aligned}
a_1 &= \frac{(\vec{p}_t \times \hat{n}) \cdot (\vec{p}_{\bar{t}} \times \hat{n})}{|(\vec{p}_t \times \hat{n}) \cdot (\vec{p}_{\bar{t}} \times \hat{n})|}, \quad a_2 = \frac{p_t^x p_{\bar{t}}^x}{|p_t^x p_{\bar{t}}^x|} \\
b_1 &= \frac{(\vec{p}_t \times \hat{n}) \cdot (\vec{p}_{\bar{t}} \times \hat{n})}{p_t^T p_{\bar{t}}^T}, \quad b_2 = \frac{(\vec{p}_t \times \hat{n}) \cdot (\vec{p}_{\bar{t}} \times \hat{n})}{|\vec{p}_t||\vec{p}_{\bar{t}}|} \\
b_3 &= \frac{p_t^x p_{\bar{t}}^x}{p_t^T p_{\bar{t}}^T}, \qquad\qquad b_4 = \frac{p_t^z p_{\bar{t}}^z}{|\vec{p}_t||\vec{p}_{\bar{t}}|},
\end{aligned} \tag{2.154}$$

where $\hat{n}$ is a unit vector in the $+z$ direction along the collision axis. Using the partial reconstruction technique, the information from the second top momentum must be replaced with the momentum of the reconstructed Higgs (or potentially with the unreconstructed [missing] momentum, or some combination. Here we simply use the momentum of the reconstructed Higgs for the replacement.) As shown

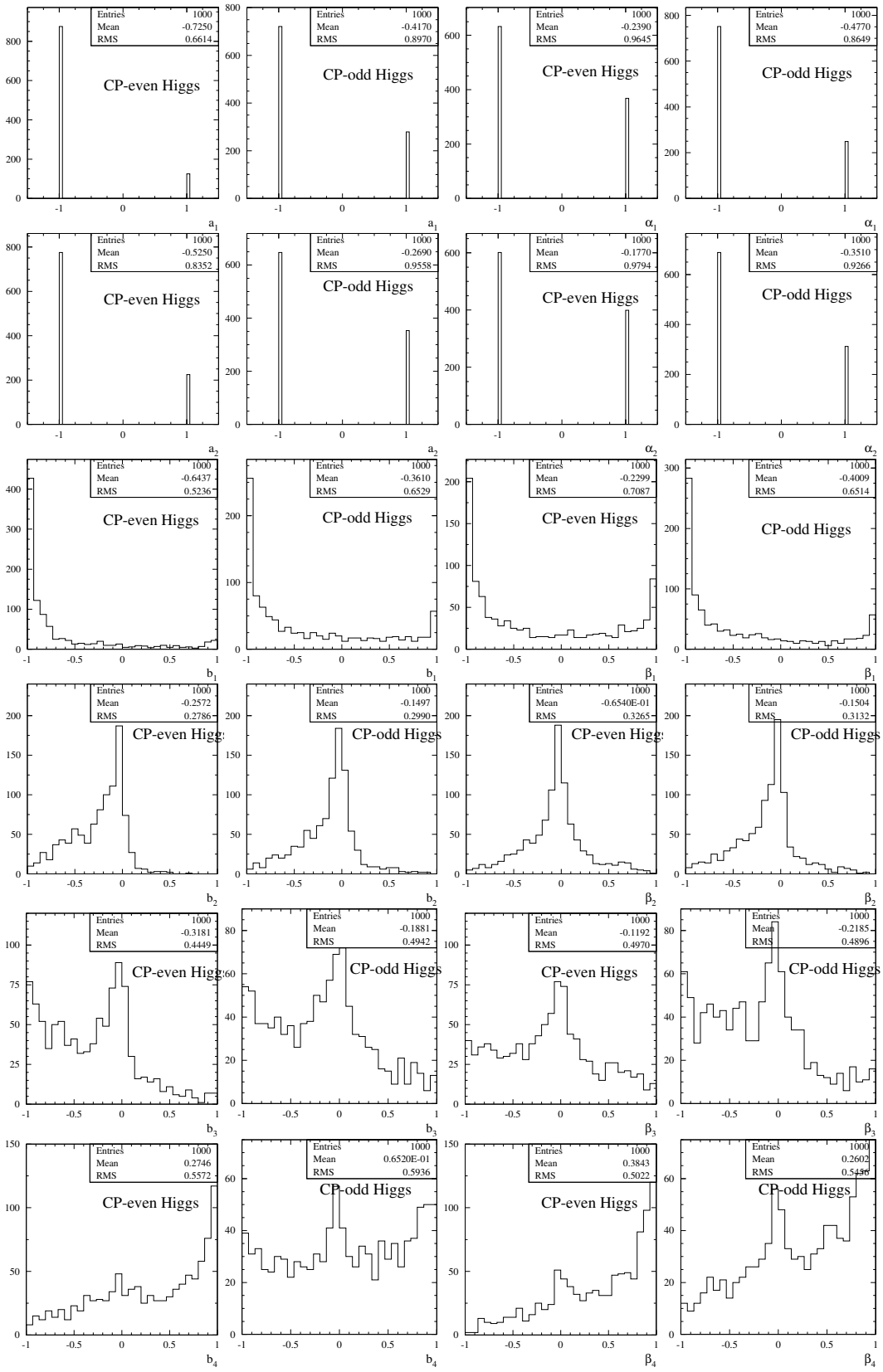

Fig. 2.11: Distributions of (as rows from top) the a_1, a_2, b_1, b_2, b_3, and b_4 variables. Within each row, the leftmost plot shows the distribution for CP-even Higgs full reconstruction, left middle shows CP-odd with full reconstruction, right middle shows CP-even Higgs partial reconstruction, and rightmost shows CP-odd Higgs partial reconstruction.

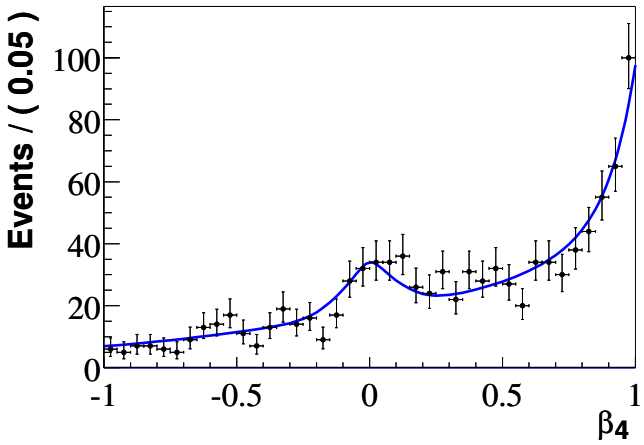

Fig. 2.12: Projection of Higgs CP fit onto the β_4 variable. Monte Carlo data are points with error bars (statistical only). The line shows the projection of the fit to a sum of CP-even and CP-odd components (as well as misreconstructed background).

in Fig. 2.11, the partial reconstruction has a similar overall per-event CP sensitivity to the full reconstruction, along with the much higher efficiencies. We denote the partial-reconstruction versions of the original Gunion-He variables with Greek letters: $(a_i, b_j) \to (\alpha_i, \beta_j)$.

In order to extract the CP-even and CP-odd fractions of the Higgs from reconstructed $t(\bar{t})\phi$ events, we have implemented an unbinned maximum-likelihood fit, combining the information from each of the CP-sensitive variables. For each event i and hypothesis j (CP-even signal, CP-odd signal, background) we define the probability density function (PDF) as

$$\mathcal{P}_j^i = \mathcal{P}_j(\alpha_1^i)\mathcal{P}_j(\alpha_2^i)\mathcal{P}_j(\beta_1^i)\mathcal{P}_j(\beta_2^i)\mathcal{P}_j(\beta_3^i)\mathcal{P}_j(\beta_4^i), \tag{2.155}$$

accounting for correlations between the 6 variables. The likelihood function is

$$\mathcal{L} = \frac{e^{-\sum Y_j}}{N!} \prod_{i=1}^{N} \sum_j Y_j \mathcal{P}_j^i \,, \tag{2.156}$$

where Y_j is the yield of events of hypothesis j and N is the number of events in the sample.

We fit sets of 50, 100, 500, and 1000 partially-reconstructed $t(\bar{t})\phi$ events (corresponding to approximately 40, 80, 400, and 800 fb^{-1} of integrated luminosity respectively), in each case with the ϕ generated as being 50% CP-odd and 50% CP-even. The resulting uncertainties on the CP (*i.e.* parameters c and d of Eq. 2.153) are ± 0.5 for the 50-event case, ± 0.3 for 100 events, ± 0.2 for 500 events, and ± 0.1 for 1000 events. Fig. 2.12 shows a projection of the maximum-likelihood fit onto the β_4 variable, as compared with the data (the points with error bars). The CP-even component has a gentler exponential slope, and smaller central Gaussian fraction, than the CP-odd component for this variable.

To improve measured uncertainties on the Higgs CP and spin, performing a combined analysis of this $gg \to t(\bar{t})\phi,\ \phi \to \gamma\gamma$ channel together with related channels such as $gg \to t(\bar{t})\phi,\ \phi \to b\bar{b}$; $gg \to b(\bar{b})\phi,\ \phi \to \gamma\gamma$; and vector boson fusion Higgs production (for a light Higgs) and $\phi \to ZZ^* \to 4\ell$ and $\phi \to WW^* \to 2\ell 2\nu$ (for a heavier Higgs) is the most promising direction.

2.10 Higgs + 2 jets as a probe for CP properties

Vera Hankele, Gunnar Klämke, and Dieter Zeppenfeld

At the LHC, one would like to experimentally determine the CP nature of any previously discovered (pseudo)scalar resonance. Such measurements require a complex event structure in order to provide the distributions and correlations which can distinguish between CP-even and CP-odd couplings. This can either be done by considering decays, e.g. $H \to ZZ \to l^+l^-l^+l^-$ and the correlations of the decay leptons [93, 119], (see sections 2.12, 2.11 and 2.13), or one can study correlations arising in the production process. Here the azimuthal angle correlations between the two additional jets in Hjj events have emerged as a promising tool [98]. In the following we consider the prospects for using Φjj events at the LHC, where Φ stands for a CP even boson, H, a CP odd state, A, or a mixture of the two. Two production processes are considered. The first is vector boson fusion (VBF), i.e. the electroweak process $qQ \to qQ\Phi$ (and crossing related ones) where Φ is radiated off a t-channel electroweak boson. The second is gluon fusion where Φ is produced in QCD dijet events, via the insertion of a heavy quark loop which mediates $gg \to \Phi + 0, 1, 2$ gluons.

The CP properties of a scalar field are defined by its couplings and here we consider interactions with fermions as well as gauge bosons. Within renormalizable models the former are given by the Yukawa couplings

$$\mathcal{L}_Y = y_f \bar{\psi} H \psi + \tilde{y}_f \bar{\psi} A i\gamma_5 \psi \ , \tag{2.157}$$

where H (and A) denote (pseudo)scalar fields which couple to fermions $f = t,\ b,\ \tau$ etc. In our numerical analysis we consider couplings of SM strength, $y_f = \tilde{y}_f = m_f/v = y_{SM}$. Via these Yukawa couplings, quark loops induce effective couplings of the (pseudo)scalar to gluons which, for (pseudo)scalar masses well below quark pair production threshold, can be described by the effective Lagrangian

$$\mathcal{L}_{\text{eff}} = \frac{y_f}{y_{SM}} \cdot \frac{\alpha_s}{12\pi v} \cdot H\, G^a_{\mu\nu} G^{a\,\mu\nu} + \frac{\tilde{y}_f}{y_{SM}} \cdot \frac{\alpha_s}{16\pi v} \cdot A\, G^a_{\mu\nu} G^a_{\rho\sigma} \varepsilon^{\mu\nu\rho\sigma} \ . \tag{2.158}$$

Similar to the Φgg coupling, Higgs couplings to W and Z bosons will also receive contributions from heavy particle loops which can be parameterized by the effective Lagrangian

$$\mathcal{L}_5 = \frac{f_{\text{e}}}{\Lambda_5}\, H\, \vec{W}_{\mu\nu}\vec{W}^{\mu\nu} + \frac{f_{\text{o}}}{\Lambda_5}\, A\, \vec{W}_{\mu\nu}\vec{W}_{\rho\sigma}\, \frac{1}{2}\varepsilon^{\mu\nu\rho\sigma} \ . \tag{2.159}$$

For most models, one expects a coupling strength of order $f_i/\Lambda_5 \sim \alpha/(4\pi v)$ for these dimension 5 couplings and, hence, cross section contributions to vector boson fusion processes which are suppressed by factors α/π (for interference effects with SM contributions) or $(\alpha/\pi)^2$ compared to those mediated by the tree level HVV $(V = W,\ Z)$ couplings of the SM. However, together with the tree level couplings, the effective Lagrangian of Eq. (2.159) has the virtue that it parameterizes the most general ΦVV coupling which can contribute in the vector boson fusion process $qQ \to qQ\Phi$ and, thus, it is a convenient tool for phenomenological discussions and for quantifying, to what extent certain couplings can be excluded experimentally. Neglecting terms which vanish upon contraction with the conserved quark currents, the most general tensor structure for the fusion vertex $V^\mu(q_1)V^\nu(q_2) \to \Phi$ is given by

$$T^{\mu\nu}(q_1, q_2) = a_1(q_1, q_2)\ g^{\mu\nu} + a_2(q_1, q_2)\ [q_1 \cdot q_2 g^{\mu\nu} - q_2^\mu q_1^\nu] + a_3(q_1, q_2)\ \varepsilon^{\mu\nu\alpha\beta} q_{1\alpha} q_{2\beta} \ . \tag{2.160}$$

Here the $a_i(q_1, q_2)$ are scalar form factors, which, in the low energy limit, are given by the effective Lagrangian of Eq. (2.159). One obtains, e.g. for the $W^+W^-\Phi$ coupling, $a_2 = -2f_e/\Lambda_5$ and $a_3 = 2f_o/\Lambda_5$, while $a_1 = 2m_W^2/v$ is the SM vertex.

The CP-even and CP-odd couplings of Eqs. (2.158,2.159) lead to characteristic azimuthal angle correlations of the two jets in Φjj production processes. Normalized distributions of the azimuthal angle between the two jets, $\triangle\phi_{jj}$, are shown in Fig. 2.13 for vector boson fusion (left panel) and for gluon

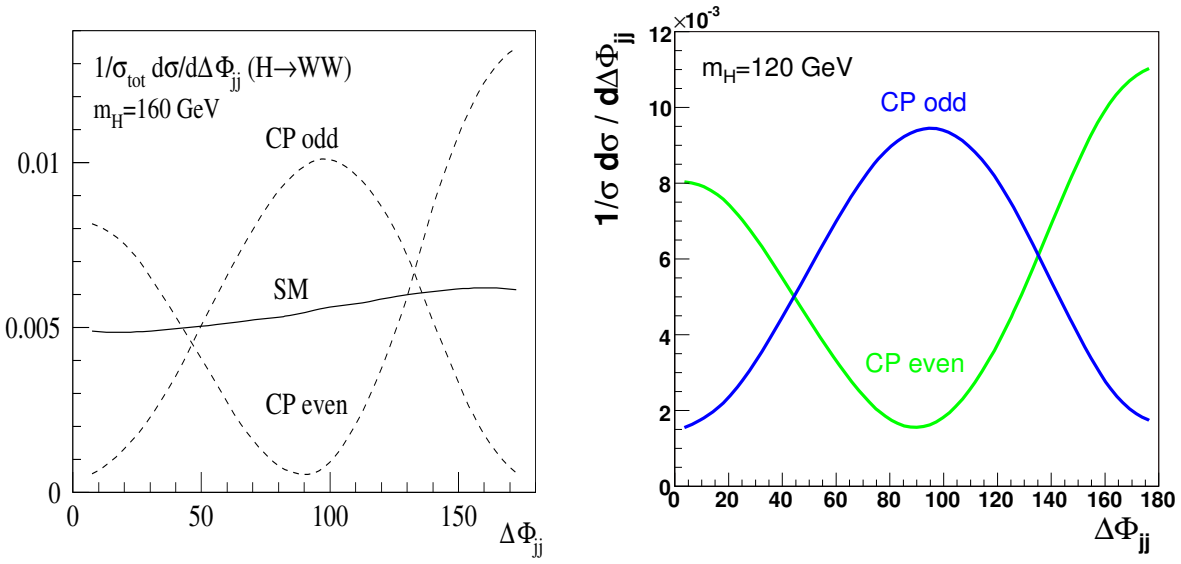

Fig. 2.13: *Left:* Normalized distributions of the azimuthal angle between the two tagging jets, for the $\Phi \to WW \to e\mu\not{p}_T$ signal in vector boson fusion at $m_\Phi = 160$ GeV, from Ref. [98]. Curves, after cuts as in Ref. [276], are for the SM and for single D5 operators as given in Eq. (2.159), i.e. they each assume a single nonzero coupling a_i of Eq. (2.160). *Right:* The same for Higgs production in gluon fusion at $m_\Phi = 120$ GeV. Curves are for CP-even (i.e. SM) and CP-odd Φtt couplings.

fusion processes (right panel) leading to Φjj events: A CP-odd coupling suppresses the cross section for planar events because the epsilon tensor contracted with the four linearly dependent momentum vectors of the incoming and outgoing partons disappears. For a CP-even coupling the dip, instead, appears at 90 degrees [98, 277]. Unfortunately, when both CP-even and CP-odd couplings are present simultaneously, the two $\triangle\phi_{jj}$ distributions simply add, i.e. one does not observe interference effects. The dip-structure which is present for pure couplings is, thus, washed out.

This behavior is demonstrated in Fig. 2.14. For CP-even and CP-odd couplings of the same strength, i.e. $f_e = f_o$, the azimuthal angle distribution is very similar to the SM case. However, in order to test the presence of anomalous couplings in such cases, other jet distributions can be used, e.g. transverse momentum distributions. The $\triangle\phi_{jj}$ distribution is quite insensitive to variations of form factors, NLO corrections and the like [278]. On the other hand, p_T distributions depend strongly on form factor effects. We study these effects for a particular parameterization of the momentum dependence:

$$a_2(q_1, q_2) = a_3(q_1, q_2) \sim M^2 \, C_0 \, (\, q_1, q_2, M \,) \, , \tag{2.161}$$

where C_0 is the familiar Passarino-Veltman scalar three-point function [279]. This ansatz is motivated by the fact that the C_0 function naturally appears in the calculation of one-loop triangle diagrams, where the mass scale M is given by the mass of the heavy particle in the loop. As can be seen in the right panel of Fig. 2.14, even for a mass scale M of the order of 50 GeV the anomalous couplings produce a harder p_T distribution of the tagging jets than is expected for SM couplings. Thus it is possible to experimentally distinguish EW vector boson fusion as predicted in the SM from loop induced $WW\Phi$ or $ZZ\Phi$ couplings by the shape analysis of distributions alone.

Let us now consider the gluon fusion processes where, for Φtt couplings of SM strength, one does expect observable event rates from the loop induced effective Φgg couplings [277]. In order to assess the visibility of the CP-even vs. CP-odd signatures of the azimuthal jet correlations at the LHC, we consider Higgs + 2 jet production with the Higgs decaying into a pair of W-bosons which further decay leptonically, $\Phi \to W^+W^- \to \ell^+\ell^-\nu\bar{\nu}$. We only consider electrons and muons ($\ell = e^\pm$, $\mu^\pm$) in

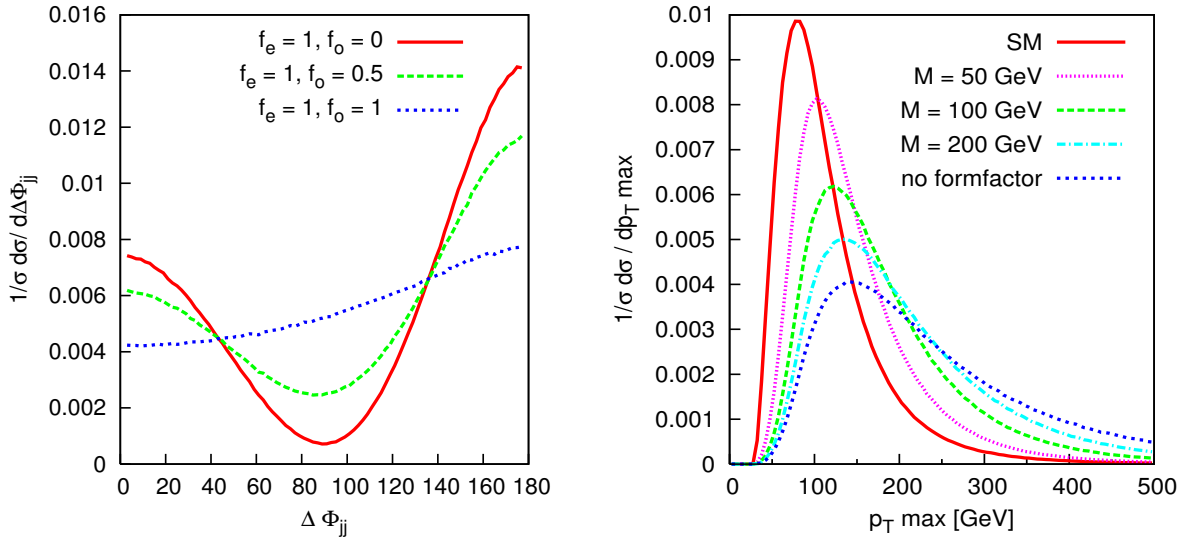

Fig. 2.14: Normalized distributions of the tagging jets in EW vector boson fusion with anomalous couplings and for a Higgs mass of $m_\Phi = 120$ GeV. Typical VBF cuts of $p_{Tj} > 30\,\text{GeV}$, $|\eta_j| < 4.5$, $|\eta_{j_1} - \eta_{j_2}| > 4.0$, $m_{jj} > 600$ GeV are applied. *Left:* Azimuthal angle distribution between the two tagging jets, for different strengths of the operators of Eq. (2.159). *Right:* Transverse momentum distribution of the hardest tagging jet for $f_e = f_o = 1$ and a form factor as in Eq. (2.161). The "no formfactor" curve corresponds to the limit $M \to \infty$, i.e. a constant a_i.

the final state. The Higgs-mass is set to $m_\Phi = 160$ GeV. From previous studies on Higgs production in vector boson fusion [276] the main backgrounds are known to be top-pair production i.e. $pp \to t\bar{t}$, $t\bar{t}j$, $t\bar{t}jj$ [280]. The three cases distinguish the number of b quarks which emerge as tagging jets. The $t\bar{t}$ case corresponds to both bottom-quarks from the top-decays being identified as forward tagging jets, for $t\bar{t}j$ production only one tagging jet arises from a b quark, while the $t\bar{t}jj$ cross section corresponds to both tagging jets arising from massless partons. Further backgrounds arise from QCD induced W^+W^- + 2 jet production and electroweak W^+W^-jj production. These backgrounds are calculated as in Refs. [281] and [282], respectively. In the EW W^+W^-jj background, Higgs production in VBF is included, i.e. the VBF Higgs signal is considered as a background to the observation of Φjj production in gluon fusion. We do not consider backgrounds from Zjj, $Z \to \tau\tau$ and from $b\bar{b}jj$ production because they have been shown to be small in the analyses of Refs. [276, 283].

The inclusive cuts in Eq. (2.162) reflect the requirement that the two tagging jets and two charged leptons are observed inside the detector, and are well-separated from each other.

$$\begin{aligned} p_{Tj} > 30\,\text{GeV}, \qquad |\eta_j| < 4.5, \qquad |\eta_{j_1} - \eta_{j_2}| > 1.0 \\ p_{T\ell} > 10\,\text{GeV}, \qquad |\eta_\ell| < 2.5, \qquad \Delta R_{j\ell} > 0.7 \end{aligned} \tag{2.162}$$

The resulting cross sections for these cuts are shown in Table 2.5. The signal cross section of 121 fb (which includes the branching ratios into leptons) is quite sizeable. The QCD $WWjj$ cross section is about 3 times higher whereas the VBF process reaches $2/3$ of the signal rate. The worst source of background arises from the $t\bar{t}$ processes, with a total cross section of more than 17 pb.
In order to improve the signal to background ratio the following selection cuts are applied:

$$\begin{aligned} p_{T\ell} > 30\,\text{GeV}, \qquad m_{\ell\ell} < 75\,\text{GeV}, \qquad \Delta R_{\ell\ell} < 1.1 \\ m_T^{WW} < 170\,\text{GeV}, \qquad m_{\ell\ell} < 0.5 \cdot m_T^{WW}\,. \end{aligned} \tag{2.163}$$

Table 2.5: Signal rates and background cross sections for $m_\Phi = 160\,\mathrm{GeV}$. Results are given for the inclusive cuts of Eq. (2.162), the additional selection cuts of Eq. (2.163) and b-quark identification as discussed in the text, and with the additional $\Delta\eta_{jj}$ cut of Eq. (2.166) which improves the sensitivity to the CP nature of the Φtt coupling. The events columns give the expected number of events for $\mathcal{L}_{int} = 30\,\mathrm{fb}^{-1}$.

	inclusive cuts	selection cuts		selection cuts + Eq. (2.166)	
process	σ [fb]	σ [fb]	events / $30\,\mathrm{fb}^{-1}$	σ [fb]	events / $30\,\mathrm{fb}^{-1}$
GF $pp \to \Phi + jj$	121.2	39.2	1176	13.1	393
VBF $pp \to W^+W^- + jj$	75.2	20.8	624	17.4	521
$pp \to t\bar{t}$	6832	29.6	888	2.0	60
$pp \to t\bar{t} + j$	9712	56.4	1692	15.6	468
$pp \to t\bar{t} + jj$	1200	8.8	264	3.2	97
QCD $pp \to W^+W^- + jj$	364	15.2	456	3.9	116

Here, the transverse mass of the dilepton-$\not{\vec{p}}_T$ system is defined as [276]

$$m_T^{WW} = \sqrt{(\not{E}_T + E_{T,\ell\ell})^2 - (\vec{p}_{T,\ell\ell} + \not{\vec{p}}_T)^2} \tag{2.164}$$

in terms of the invariant mass of the two charged lepton and the transverse energies

$$E_{T,\ell\ell} = (p_{T,\ell\ell}^2 + m_{\ell\ell}^2)^{1/2}, \qquad \not{E}_T = (\not{p}_T^2 + m_{\ell\ell}^2)^{1/2}. \tag{2.165}$$

In addition to these cuts we make use of a b-veto to reduce the large top-background. We reject all events where at least one jet is identified as a b-jet. Using numbers from Ref. [284], we assume b-tagging efficiencies in the range of $60\% - 75\%$ (depending on b-rapidity and transverse momentum) and an overall mistagging probability of 10% for light partons.
With the selection cuts (2.163) and the b-veto the backgrounds can be strongly suppressed. Table 2.5 shows the resulting cross sections and the expected number of events for an integrated luminosity of $\mathcal{L}_{int} = 30\,\mathrm{fb}^{-1}$. The signal rate is reduced by a factor of 3 but the backgrounds now have cross sections of the same order as the signal. The largest background still comes from the $t\bar{t}$ processes, especially $t\bar{t}+1j$. For $30\,\mathrm{fb}^{-1}$ we get about 1000 signal events on top of 4000 background events. This corresponds to a purely statistical significance of the gluon fusion signal of $S/\sqrt{B} \approx 18$ and a sufficient number of events to analyze the azimuthal jet correlations.

Figure 2.15 shows the expected $\triangle\phi_{jj}$ distribution for $30\,\mathrm{fb}^{-1}$. Plotted are signal events on top of the various backgrounds. An additional cut on the rapidity gap between the jets

$$|\eta_{j_1} - \eta_{j_2}| > 3.0 \tag{2.166}$$

has been applied. It enhances the shape of the distribution that is sensitive to the nature of the Φtt coupling. Clearly visible, the distribution for the CP-even coupling has a slight minimum at $\triangle\phi_{jj} = 90^\circ$ whereas for the CP-odd case there is a pronounced maximum. In order to quantify this, we define the fit-function

$$f(\triangle\phi) = C \cdot (1 + A \cdot \cos 2\triangle\phi + B \cdot \cos\triangle\phi) \tag{2.167}$$

with free parameters A, B, C. The fit is shown as black curves in Fig. 2.15. The parameter A is now a measure for the $\triangle\phi_{jj}$ asymmetry, i.e. whether there is a CP-even or CP-odd Φtt coupling. The fitted values are $A = 0.064 \pm 0.035$ for the CP-even and $A = -0.157 \pm 0.034$ for the CP-odd case, while $A_B = -0.039 \pm 0.040$ for the sum of all backgrounds. Defining a significance s as

$$s = \frac{(A_{S+B} - A_B)}{\Delta A_{S+B}}\,, \tag{2.168}$$

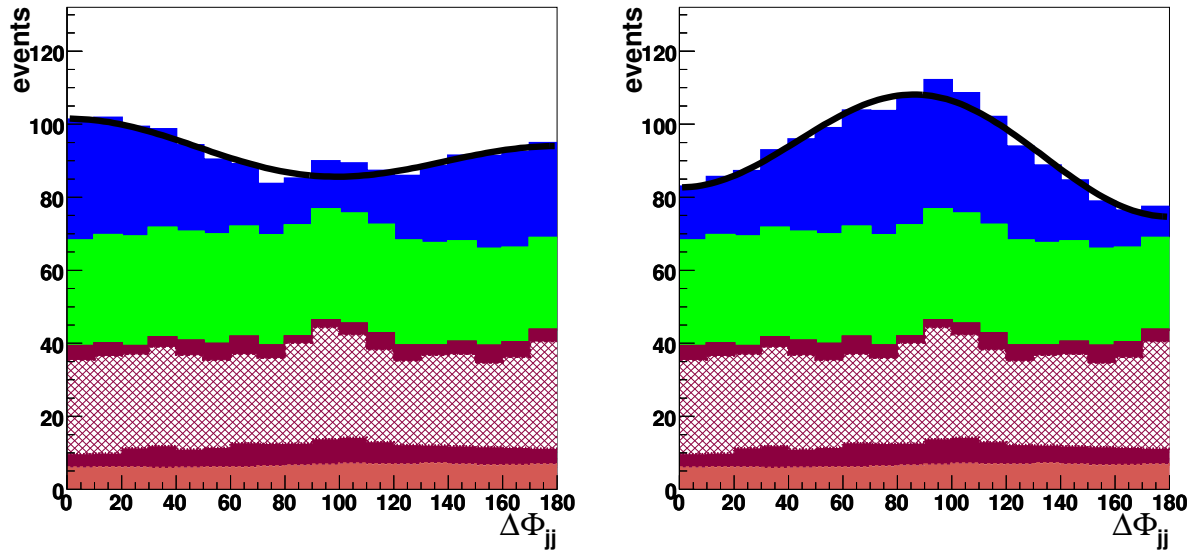

Fig. 2.15: Distribution of the azimuthal angle between the tagging jets in Φjj events for a CP-even (*left*) and a CP-odd (*right*) Φtt coupling. Shown are expected signal and background events per 10 degree bin for $\Phi \to W^+W^- \to \ell^+\ell^-\nu\bar{\nu}$ and $\mathcal{L}_{int} = 30\,\text{fb}^{-1}$ for the cuts of Eqs. (2.162, 2.163, 2.166) and an applied b-veto. Processes from top to bottom: gluon fusion (signal), VBF, $t\bar{t}$, $t\bar{t}j$, $t\bar{t}jj$, QCD $WWjj$. $m_\Phi = 160$ GeV is assumed.

we get $s = 3.0$ and $s = -3.4$ for the CP-even and CP-odd case, respectively. Thus, a distinction of a CP-odd and CP-even Φtt coupling is possible at a 6σ level for the considered process and a Higgs mass of 160 GeV. This implies that, at least for favorable values of the Higgs boson mass, (i) an effective separation of VBF and gluon fusion sources of Φjj events is possible and (ii) the CP nature of the Φtt coupling of Eq. (2.157) can be determined at the LHC.

2.11 CP-violating Higgs bosons decaying via $H \to ZZ \to 4$ leptons at the LHC

Rohini M. Godbole, David J. Miller, Stefano Moretti and Margarete M. Mühlleitner

In this contribution, we study the decay of a Higgs boson to a pair of real and/or virtual Z bosons which subsequently decay into pairs of fermions, $H \to ZZ \to (f_1\bar{f}_1)(f_2\bar{f}_2)$, where f_1 and f_2 are distinguishable. This channel is particularly important at the LHC for Higgs masses $M_H > 2M_Z$, where the Z bosons are produced on-shell, but is also of use for smaller Higgs boson masses where one of the Z bosons must be virtual [285].

To do a model-independent analysis we examine the most general vertex for a spin-0 boson coupling to two Z bosons, including possible CP violation, which can be written as

$$\frac{ig}{m_Z \cos\theta_W}[\, a\, g_{\mu\nu} + b\,(k_{2\mu}k_{1\nu} - k_1 \cdot k_2 g_{\mu\nu}) + c\,\epsilon_{\mu\nu\alpha\beta}k_1{}^\alpha k_2{}^\beta\,], \tag{2.169}$$

with k_1 and k_2 the four-momenta of the two Z bosons, and θ_W the weak-mixing angle, c.f. Eq. (2.63) in the introduction. The form factors b and c may be complex, but since an overall phase will not effect the observables studied here, we are free to adopt a convention where a is real. These form factors can arise from radiative loop corrections or from new physics at the TeV scale, i.e. from higher dimensional operators [98], and may themselves be functions of the momenta. The terms associated with a and b are CP-even, while that associated with c is CP-odd. $\epsilon_{\mu\nu\alpha\beta}$ is totally antisymmetric with $\epsilon_{0123} = 1$. CP violation will be realized if at least one of the CP-even terms is present (i.e. either $a \neq 0$ and/or $b \neq 0$) and c is non-zero. In the following, for the sake of simplicity, we will always assume $b = 0$.

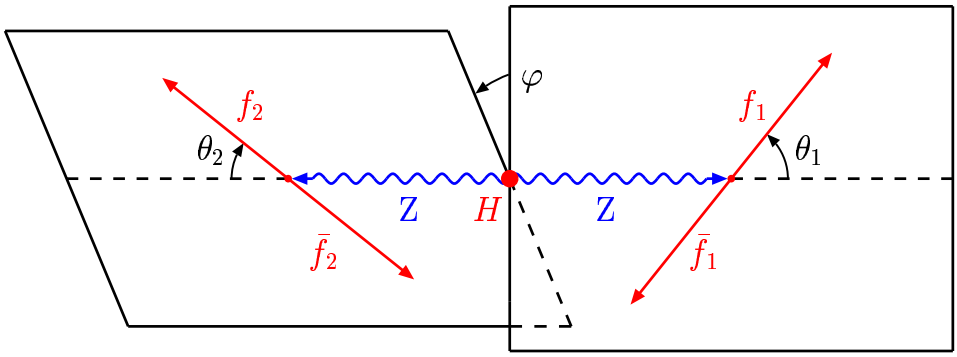

Fig. 2.16: The definition of the polar angles θ_i ($i = 1, 2$) and the azimuthal angle φ for the sequential decay $H \to Z^{(*)}Z \to (f_1\bar{f}_1)(f_2\bar{f}_2)$ in the rest frame of the Higgs boson.

For $b = 0$ this differs from the vertex of Refs. [93, 136] in the CP-odd term by a factor of 2, and differs from that of Refs [119, 286, 287] and section 2.12 in the choice of m_Z as a normalization factor instead of m_H. For further related studies relevant to the LHC also see Refs. [98, 288, 289] and section 2.13; for those relevant to e^+e^- colliders see Refs. [94–97, 134, 151]; for a study at a photon collider see Ref. [147] and section 2.14.

The Standard Model at tree-level is recovered for $a = 1$ and $b = c = 0$, which is obviously CP conserving. Nevertheless, it is interesting to ask if the LHC will be sensitive to any exotic new physics which might provide a CP violating HZZ vertex of this form.

2.11.1 The distributions sensitive to CP violation

In order to fully test for the occurance of CP violation in the HZZ vertex it is helpful to find asymmetries which probe the real and imaginary parts of c. The real part of c is probed by any observable which is CP odd and $\tilde{\mathrm{T}}$ odd (where $\tilde{\mathrm{T}}$ denotes pseudo-time-reversal, which reverses particle momenta and spin but does not interchange initial and final states), while the imaginary part is probed by any observable which is CP odd and $\tilde{\mathrm{T}}$ even. The nonvanishing of the CP$\tilde{\mathrm{T}}$ odd coefficients is related to the presence of absorptive parts in the amplitude [290].

An observable sensitive to $\mathrm{Im}\,(c)$ can be found by looking at the polar angular distributions of the process. We denote the polar angles of the fermions f_1, f_2 in the rest frames of the Z bosons by θ_1 and θ_2 and define,

$$O_1 \equiv \cos\theta_1 = \frac{(\vec{p}_{\bar{f}_1} - \vec{p}_{f_1}) \cdot (\vec{p}_{\bar{f}_2} + \vec{p}_{f_2})}{|\vec{p}_{\bar{f}_1} - \vec{p}_{f_1}||\vec{p}_{\bar{f}_2} + \vec{p}_{f_2}|} \tag{2.170}$$

where $\vec{p}_f$ are the three-vectors of the corresponding fermions with $\vec{p}_{f_1}$ and $\vec{p}_{\bar{f}_1}$ in their parent Z's rest frame but $\vec{p}_{f_2}$ and $\vec{p}_{\bar{f}_2}$ in the Higgs rest frame, see Fig. 2.16. The angular distribution in θ_i ($i = 1, 2$) for a CP-odd state is $\sim (1 + \cos^2\theta_i)$, corresponding to transversely polarized Z bosons, which is very distinct from the purely CP-even distribution proportional to $\sin^2\theta_i$ for longitudinally polarized Z bosons in the large Higgs mass limit [97, 134]. $\mathrm{Im}\,(c) \neq 0$ will introduce a term linear in $\cos\theta_i$ leading to a forward-backward asymmetry. The distribution for $\cos\theta_1$ is shown in Fig. 2.17 for a Higgs mass of 200 GeV and a purely scalar, purely pseudoscalar and CP-mixed scenario. The asymmetry is absent if CP is conserved (for both CP-odd and CP-even states) but is non-zero if $\mathrm{Im}\,(c) \neq 0$ while simultaneously $a \neq 0$. This may then act as a definitive signal of CP violation in this vertex. However, note that this observable requires one to distinguish between f_1 and $\bar{f}_1$.

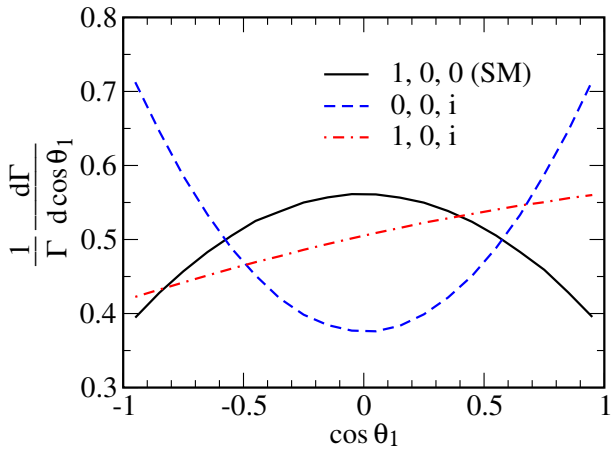

Fig. 2.17: The normalized differential width for $H \to ZZ \to (f_1\bar{f}_1)(f_2\bar{f}_2)$ with respect to the cosine of the fermion's polar angle. The solid (black) curve shows the SM ($a = 1$, $b = c = 0$) while the dashed (blue) curve is a pure CP-odd state ($a = b = 0$, $c = i$). The dot-dashed (red) curve is for a state with a CP violating coupling ($a = 1, b = 0, c = i$). One can clearly see an asymmetry about $\cos\theta_1 = 0$ for the CP violating case.

To quantify this we define an asymmetry by

$$\mathcal{A}_1 = \frac{\Gamma(\cos\theta_1 > 0) - \Gamma(\cos\theta_1 < 0)}{\Gamma(\cos\theta_1 > 0) + \Gamma(\cos\theta_1 < 0)}. \tag{2.171}$$

In the case of no CP violation $\mathcal{A}_1 = 0$, whereas any significant deviation from zero will be a sign that CP is violated. Fig. 2.18 *(left)* shows the value of $\mathcal{A}_1$ for a Higgs mass of 200 GeV as a function of the ratio $\mathrm{Im}\,(c)/a$. The value $\mathrm{Im}\,(c)/a = 0$ corresponds to the purely scalar state whereas $\mathrm{Im}\,(c)/a \to \infty$ to the purely CP-odd case. It is clear from Eq. (2.171) that $\mathcal{A}_1$ is sentitive only to the relative size of the couplings since any factor will cancel in the ratio. We find that the asymmetry is maximal for $\mathrm{Im}\,(c)/a \sim 1.4$ with a value of about 0.077.

In order to get a first rough estimate whether this asymmetry can be measured at the LHC we calculate the significance with which a particular CP violating coupling would manifest at the LHC. In the purely SM case, we assumed that 100 fb^{-1} provide 180 signal events containing $H \to ZZ \to 4$ leptons after cuts to remove background [285] (all production channels). We then divide this number by two to provide an estimate for $H \to ZZ \to e^+e^-\mu^+\mu^-$ (since we need to distinguish the leptons) and scaled this number up to 300 fb^{-1} (i.e. giving 270 events). The number of events for the CP violating case has been obtained by multiplying the number of SM events by the ratio of CP violating to SM cross sections. We are therefore assuming the SM value for the CP even coefficient, i.e. $a = 1$. For simplicity we assume the charge of the particles is unambiguously determined.

Fig. 2.18 *(right)* shows the significance as a function of $\mathrm{Im}\,(c)$, calculated according to $\mathcal{A}_1\sqrt{N}$ where N is the number of expected events. The maximum of the curve is slighlty shifted to higher values of $\mathrm{Im}\,(c)/a$ compared to Fig. 2.18 *(left)* due to the increasing Higgs decay rate with rising pseudoscalar coupling. The curve shows that, even in a best case scenario, the signficance is always less than 3σ, so evidence for CP violation cannot be obtained in this channel without more luminosity. However, since one does not need to distinguish f_2 and $\bar{f}_2$ one could also consider using jets instead of muons, i.e. $H \to ZZ \to l^+l^-jj$, to increase the statistics. This process deserves further study.

To probe $\mathrm{Re}\,(c)$ we require an observable which is CP odd and $\tilde{\mathrm{T}}$ odd, so we choose to define,

$$O_2 \equiv \frac{(\vec{p}_{\bar{f}_1} - \vec{p}_{f_1}) \cdot (\vec{p}_{\bar{f}_2} \times \vec{p}_{f_2})}{|\vec{p}_{\bar{f}_1} - \vec{p}_{f_1}||\vec{p}_{\bar{f}_2} \times \vec{p}_{f_2}|}. \tag{2.172}$$

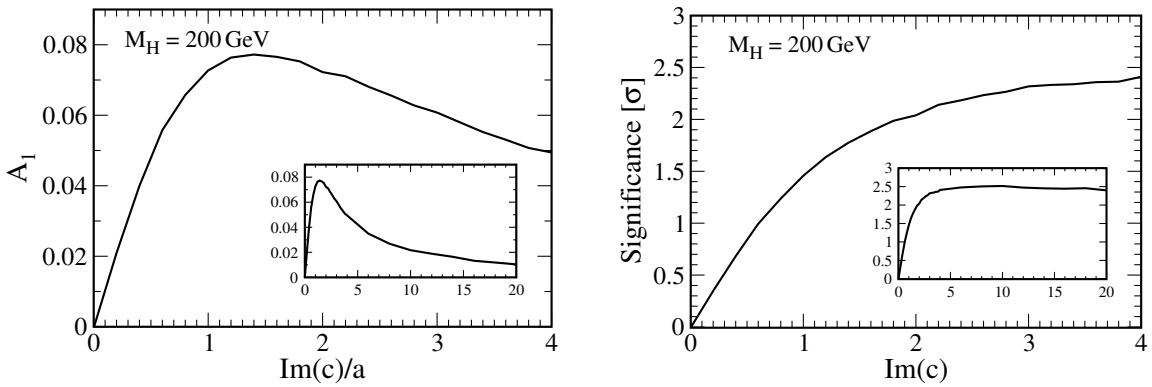

Fig. 2.18: *Left:* The asymmetry given by Eq. (2.171) as a function of the ratio $\mathrm{Im}\,(c)/a$, for a Higgs boson of mass 200 GeV. *Right:* The number of standard deviations the asymmetry deviates from zero as a function of $\mathrm{Im}\,(c)$. The inserts show the same quantities for a larger range of $\mathrm{Im}\,(c)$.

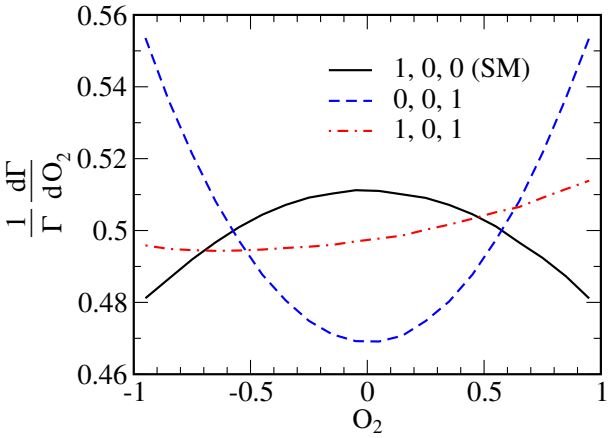

Fig. 2.19: The normalized differential width for $H \to ZZ \to (f_1\bar{f}_1)(f_2\bar{f}_2)$ with respect to the observable O_2 (see text). The solid (black) curve shows the SM ($a = 1$, $b = c = 0$) while the dashed (blue) curve is a pure CP-odd state ($a = b = 0$, $c = 1$). The dot-dashed (red) curve is for a state with a CP violating coupling ($a = 1$, $b = 0$, $c = 1$). Again one sees an asymmetry about zero for the CP violating case.

The dependence of the differential width on this observable is plotted in Fig. 2.19 but while an asymmetry is indeed present, it is very small and will be difficult to see in practice. The corresponding asymmetry is

$$\mathcal{A}_2 = \frac{\Gamma(O_2 > 0) - \Gamma(O_2 < 0)}{\Gamma(O_2 > 0) + \Gamma(O_2 < 0)}, \tag{2.173}$$

which is plotted in Fig. 2.20 *(left)* as a function of $\mathrm{Re}\,(c)/a$. The significance (as calculated for $\mathcal{A}_1$ above) is shown in Fig. 2.20 *(right)*. The significance is always very small, and it is difficult to see how this could provide useful information. In this case one cannot exploit the decay of Higgs bosons to jets since one must also distinguish f_2 and $\bar{f}_2$.

Another distribution sensitive to CP violation is the azimuthal angular distribution $d\Gamma/d\varphi$ where φ denotes the angle between the planes of the fermion pairs stemming from the Z boson decays, cf. Fig. 2.16. Whereas the purely SM case shows a distribution

$$\frac{d\Gamma}{d\varphi} \sim 1 + A\cos\varphi + B\cos 2\varphi, \tag{2.174}$$

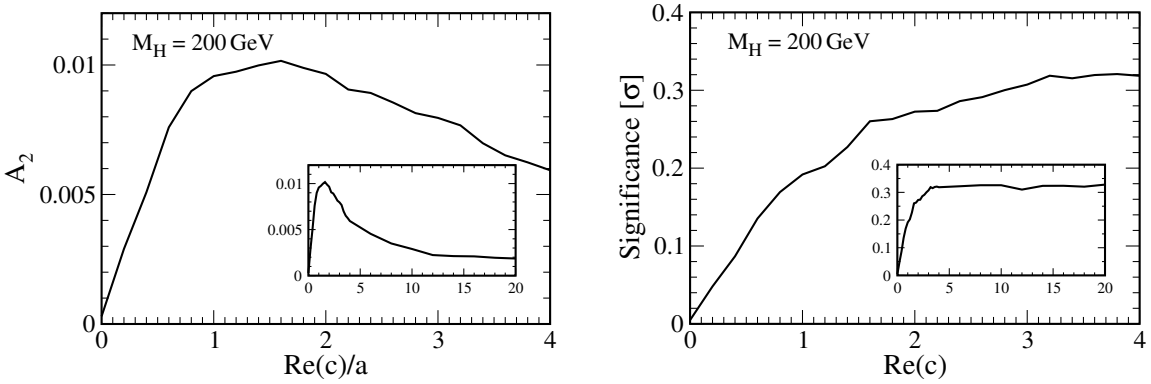

Fig. 2.20: *Left:* The asymmetry given by Eq. (2.173) as a function of the ratio $\mathrm{Re}\,(c)/a$, for a Higgs boson of mass 200 GeV. *Right:* The number of standard deviations the asymmetry deviates from zero as a function of $\mathrm{Re}\,(c)$. The inserts show the same quantities for a larger range of $\mathrm{Re}\,(c)$.

where the coefficients A and B are functions of the Higgs and Z boson mass (see Ref. [93]), in the purely pseudoscalar case

$$\frac{d\Gamma}{d\varphi} \sim 1 - \frac{1}{4}\cos 2\varphi. \tag{2.175}$$

In the CP violating case we must include contributions from both the scalar and pseudoscalar couplings which will alter this behaviour. Knowing the Higgs mass from previous measurements, any deviation from the predicted distribution in the scalar/pseudoscalar case will be indicative of CP violation. This can be inferred from Fig.2.21 which shows the azimuthal angular distribution for $M_H = 200\,\mathrm{GeV}$ in the SM case, for a CP-odd Higgs boson and two CP violating cases. The purely CP-odd curve will always show the same behaviour independently of the value of c since the curves are normalized to unit area. Therefore a special value of c could not fake the flattening of the curve appearing in the CP violating examples. This flattening even leads to an almost constant distribution in φ for the case $c/a = 1$. It should be kept in mind, though, that this method cannot be applied for large Higgs masses where the φ dependence disappears in the SM. One must also beware of degenerate Higgs bosons of opposite CP; since one cannot distinguish which Higgs boson is in which event, one must add their contributions together, possibly mimicking the effect seen above.

This procedure is similar to that of Sections 2.12 and 2.13 where log-likelihood functions were constructed and minimised to extract the coefficients in the vertex or yield exclusion contours.

The next step will be to study in a more realistic simulation how well the φ distribution can be fitted at the LHC and hence to which extent CP violation can be probed in the azimuthal angular distribution.

2.11.2 Summary and Outlook

We have studied the decays of Higgs bosons into a pair of Z bosons, which subsequently decay into leptons, for a general HZZ coupling at the LHC. We examined CP violating asymmetries which probe the real and imaginary couplings of the CP-odd term. We found that the asymmetries produced are small and will not provide evidence of CP violation at the LHC without higher luminosity. However, it may be possible to exploit other channels, such as Higgs decays to leptons and jets, to increase significances. We also examined the dependence on the azimuthal angle between the lepton planes, which is similarly indicative of CP violation. Further studies of this azimuthal angle and the extension to arbitrary higher "Higgs" spin will be the subject of future work.

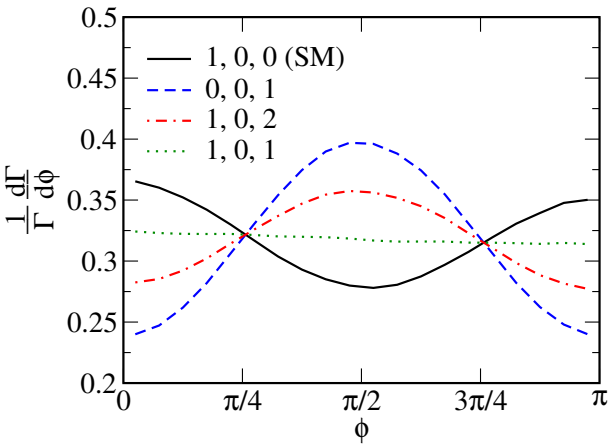

Fig. 2.21: The normalized differential width for $H \to Z^{(*)}Z \to (f_1\bar{f}_1)(f_2\bar{f}_2)$ with respect to the azimuthal angle φ. The solid (black) curve shows the SM ($a = 1$, $b = c = 0$) while the dashed (blue) curve is a pure CP-odd state ($a = b = 0$, $c = 1$). The dot-dashed (red) curve and the dotted (green) curve are for states with CP violating couplings $a = 1$, $b = 0$ with $c = 2$ and $c = 1$, respectively.

2.12 Testing the spin and CP properties of a SM-like Higgs boson at the LHC

Claus P. Buszello and Peter Marquard

To confirm the properties of a Higgs-like particle found at the LHC, we study the angular distributions of the final state particles in the decay $H \to ZZ \to 4\ell$. To this end we consider hypothetical couplings of the Higgs with momentum k to Z bosons with momenta p, q reflecting the different spin/CP states. We use a parametrisation of the couplings as follows

$$\mathcal{L}_{scalar} = \mathbf{X} g_{\mu\nu} + \mathbf{Y} k_\mu k_\nu / m_H^2 + i\mathbf{P}\epsilon_{\mu\nu\rho\sigma} p^\rho q^\sigma / m_H^2 \tag{2.176}$$

for the spin 0 Higgs and

$$\mathcal{L}_{vector} = \mathbf{X}(g_{\rho\mu} p_\nu + g_{\rho\nu} q_\mu) + \mathbf{P}(i\epsilon_{\mu\nu\rho\sigma} p^\sigma - i\epsilon_{\mu\nu\rho\sigma} q^\sigma) \tag{2.177}$$

for the spin 1 case where $\epsilon_{1234} = i$. This parametrisation is discussed in detail in [119]. The scalar couplings in Section 2.11 differ slightly from these by the choice of the masses used to normalize the non-SM contributions. We choose m_H over m_Z as this is more convenient if one wants to use the same parameterisation for HZZ and HWW vertices. We then study the distributions of the final state leptons performing a one and a multi-dimensional analysis.

The analysis presented here is divided in two parts. First, we only consider pure states (i.e all but one of the parameters **X**,**Y** and **P** are zero). The analysis of the feasibility of the exclusion of the pure states is based on a the fast parameterised ATLAS detector simulation [291] . Next, we consider the exclusion of admixtures of the CP-even and CP-odd non-SM contributions. This analysis - detailed in [292] - is the first one that takes all interference terms into account and is based on the same cuts, efficiencies and momentum resolutions as the first part. The event samples for these studies were generated using a new matrix element generator written by the authors implementing the complete couplings including mixtures given above. It generates the decay $H \to ZZ(*) \to 4\ell$ with two on-shell Z bosons in the narrow width approximation above the ZZ-threshold and one on-shell and one off-shell Z below. In the following we give the main results of these analyses. The full results and details can be found in [119, 292]. Another one dimensional analysis of the pure states has also been performed in [93] and a

PYTHIA based study of CP properties at CMS can be found in Section 2.13. A similar analysis can be carried out in other cases, where the Higgs vector boson vertex is present. In fact, in the $ZZ \to 4\ell$ decay the angular correlations are suppressed compared to W decays or $ZZ \to 2\ell 2q$. This makes exploiting WBF and the Higgs decay to W pairs so interesting. In that case, one can use the forward jets and the leptons from the W decay to determine the spin-parity of the Higgs (see e.g. [287] and Section 2.10).

2.12.1 Analysis and results

We study essentially two distributions. One is the distribution of the cosine of the polar angle, $\cos\theta$, of the decay leptons relative to the Z boson. Because the heavy Higgs decays mainly into longitudinally polarised vector bosons the cross-section $d\sigma/d\cos\theta$ should show a maximum around $\cos\theta$ =0. The other is the distribution of the angle ϕ between the decay planes of the two Z bosons in the rest frame of the Higgs boson. This distribution depends on the details of the Higgs decay mechanism. Within the Standard Model, a behaviour roughly like $1 + \beta\ \cos 2\phi$ is expected. This last distribution is flattened in the decay chain $H \to ZZ \to 4\ell$, because of the small vector coupling of the leptons, in contrast to the decay of the Higgs Boson into W pairs or decay of the Z into quarks. The angles under investigation are shown in Fig. 2.16.

I Pure states

The plane-correlation can be parametrised as

$$F(\phi) = 1 + \alpha \cdot \cos\phi + \beta \cdot \cos 2\phi \tag{2.178}$$

In all four cases discussed here, there is no $\sin\phi$ or $\sin 2\phi$ contribution. For the Standard Model Higgs, α and β depend on the Higgs mass while they are constant over the whole mass range in the other cases. The polar angle distribution can be described by

$$G(\theta) = T \cdot (1 + \cos^2\theta) + L \cdot \sin^2\theta \tag{2.179}$$

reflecting the longitudinal or transverse polarisations of the Z boson. We define the ratio

$$R := \frac{L - T}{L + T} \tag{2.180}$$

of transversal and longitudinal polarisation.

Figure 2.22 (left) shows the expected values and errors for the parameter R, using an integrated luminosity of 100 fb^{-1}. It is clearly visible that for masses above 250 GeV the measurement of this parameter allows the various non-SM hypotheses for the spin and CP-state of the "Higgs Boson" considered here to be unambiguously excluded. For a Higgs mass of 200 GeV only the pseudoscalar is excluded. Fig. 2.22 (right) shows the expected values and errors for α and β for a 200 GeV Higgs and an integrated luminosity of 100 fb^{-1}.

The parameter α can be used to distinguish between a spin 1 and the SM Higgs particle, but its use is statistically limited. The same applies to the parameter β. Measuring β, which is zero for spin 1 and > 0 in the SM case, can contribute only very little to the spin measurement even if m_H is in the range where β, in the SM case, is close to its maximum value. Nevertheless, β can be useful to rule out a CP-odd spin 0 particle.

The significance of the parameter α can be improved by exploiting the correlation between the sign of $\cos\theta$ for the two Z Bosons and ϕ. In Fig. 2.23, we plot the parameters separately for $\mathrm{sign}(\cos\theta_1) = \mathrm{sign}(\cos\theta_2)$ and $\mathrm{sign}(\cos\theta_1) = -\mathrm{sign}(\cos\theta_2)$. As can be seen, the difference in α becomes bigger for $J = 1$ and CP-even. For higher masses α and β of the SM Higgs approach 0; thus only α can be used to measure the spin. This is fortunately compensated by the measurement of R.

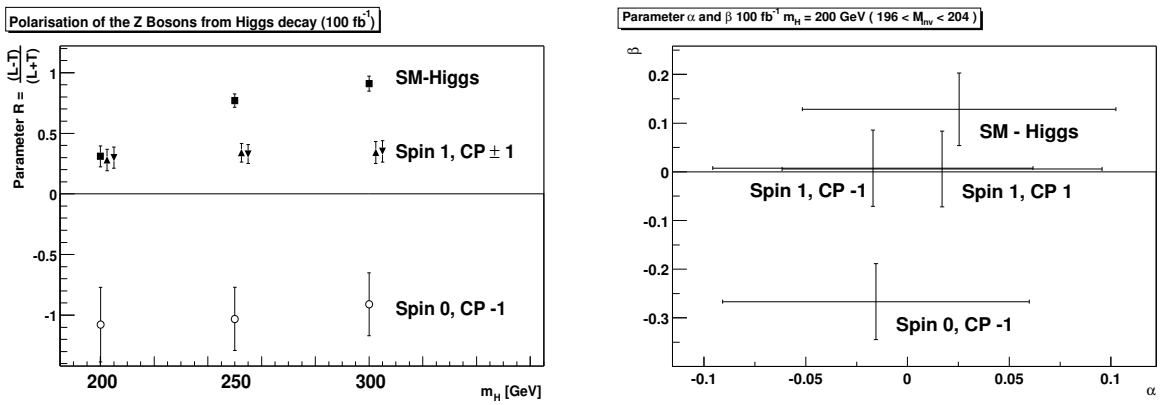

Fig. 2.22: The parameter R for different Higgs massses (left) and α and β (right) for m_H = 200 GeV using 100 fb^{-1}. The error scales with the integrated luminosity as expected.

Fig. 2.25 shows the significance, i. e. the difference of the expected non-SM value and SM value divided by the expected error of the SM Higgs. We add up the significance for α and β for the like-signed und unlike-signed $cos(\theta)$ combinations and plot the resulting significance together with the one from the polar angle measurement in Fig. 2.25 (left). For higher Higgs masses the decay plane angle correlation contributes almost nothing, but the polarisation leads to a good measurement of the parameters spin and CP-eigenvalue. For full luminosity (300 fb^{-1}) the significance can simply be multiplied by $\sqrt{3}$ assuming stable detector performance. This is especially interesting for a Higgs mass of 200 GeV. The spin 1, CP-even hypothesis can then be ruled out with a significance of 6.4σ, while for the spin 1, CP-odd case the significance is still only 3.9σ.
In principle, the same analysis can be done for Higgs masses below the ZZ threshold. In practice this is complicated by the fact, that the cross-section for $H \rightarrow ZZ^*$ is a lot smaller and is further reduced by additional combined impact parameter and isolation cuts needed to suppress the $t\bar{t}$ and $Zb\bar{b}$ backgrounds. Due to this reduction in statistics, the decay plane correlation doesn't yield any useful results, and we limit the discussion to the polar angle and the spin 0 case. Furthermore we will always use an integrated luminosity of 300 fb^{-1}, the maximum foreseen for each of the LHC experiments. We use the number of signal and background events published in the ATLAS TDR [115].
The distortion of the polar angle distribution is sizeable, and we have to introduce a statistical correction. The correction reproducing the SM values properly will not necesarily correct the non-SM values back to the theoretical values. In Fig. 2.24 (left) we present the expected values of R after applying the correction to the distributions. The exclusion significance is shown in Fig. 2.25 (top right).
An additional distribution that is only available below the threshold, is the distribution of the off-shell Z mass. Fig. 2.24 (right) shows this distribution for a Higgs of 150 GeV and the three different spin 0 couplings. The distributions are more robust against the cuts than the polar angle distribution. We generate 300 data samples of the expected number of signal and background events including all cuts for the three different hypothesis, and calculate the χ^2 to the SM-distribution (again after all cuts are applied) for each one of them. The means of these values along with the corresponding confidence levels are plotted against the various Higgs masses in Fig. 2.25.

II Mixed states

In order to measure possible CP-violation in the Higgs to vector boson coupling, we consider the full matrix element including the mixed terms (**PX**, **PY** and **YX**). As in the one dimensional case, we assume the discovery of a signal in the $H \rightarrow ZZ$ channel. Since a significant deviation from the expected number of events would rule out a SM Higgs in a trivial way, we further assume, that the number of events seen is compatible with a SM Higgs. A deviation in the number of events would not allow to

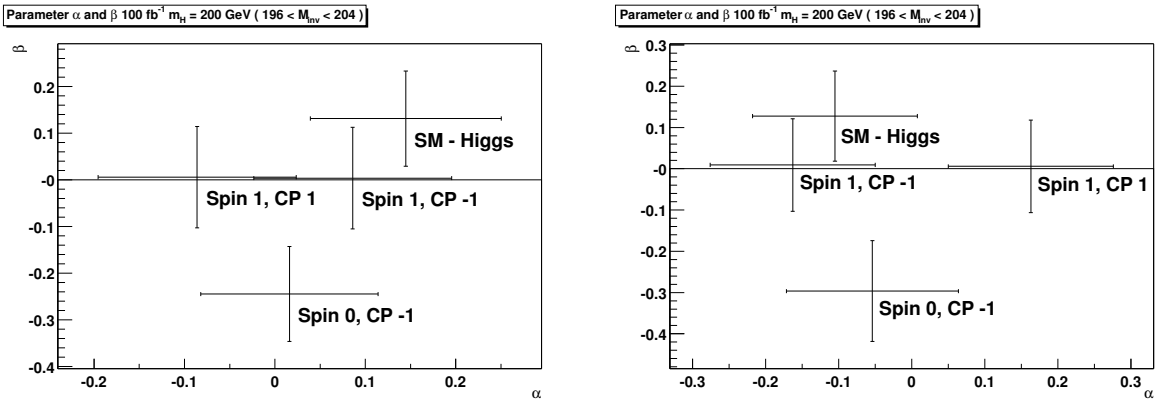

Fig. 2.23: The parameter α depends on the signs of the $\cos(\theta)$ of the two Z bosons. The events where the signs are equal are used for the left plot, those where the signs are different are used for the right plot.

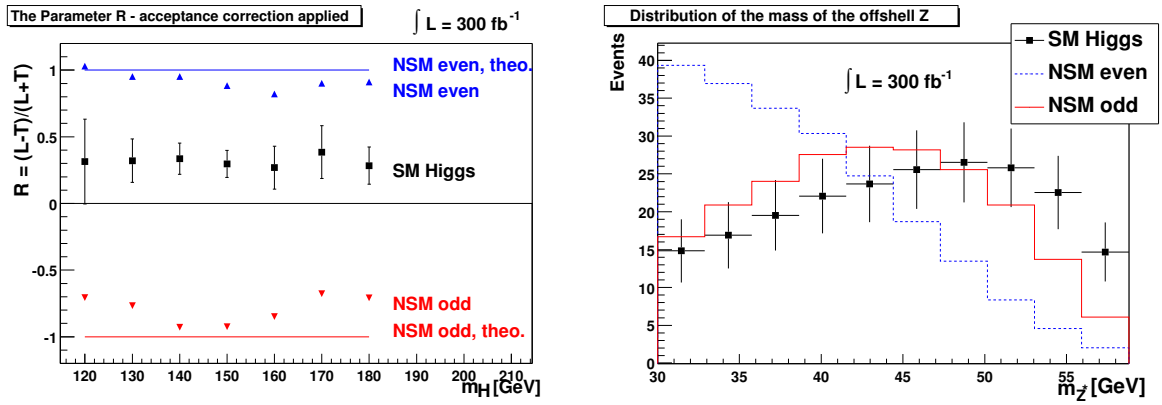

Fig. 2.24: Left: The expected values for the parameter R after reconstruction and signal selection and with a correction for detector effects applied, so that the SM Higgs values are recovered. The errorbars reflect the expected statistical error for the SM case using 300 fb^{-1}. Right: The off-shell Z mass distribution for a 150 GeV Higgs. NSM even refers to states with **Y**=1, **P**=0, **X**=0. NSM odd refers to **Y**=0, **P**=1, **X**=0.

pinpoint the coupling structure anyway, as it would be a possible combination of effects in production and branching ratios. Instead, we use the angular correlations of the decay products to test for small non-SM contributions to the SM coupling. To give a better physical interpretation to the notion of a small coupling, we rescaled $\mathbf{Y}$ and $\mathbf{P}$ to $\mathbf{Y}'$ and $\mathbf{P}'$ such that now for the widths of the pure states $\Gamma_{P'} = \Gamma_{Y'} = \Gamma_X$. The exact scaling factors can be found in Table 2.6. In this study we demonstrate how CP violation in the $H \to ZZ$ coupling could be ruled out. Figure 2.26 and 2.27 show the exclusion significance for **Y'** and **P'** admixtures to an SM Higgs. By turning this around we can interpret a measurement of **P'** and **Y'** outside these boundaries as proof of a non-SM Higgs coupling to vector bosons.

We use the full information from the three fold differential cross-section by constructing the following likelihood function:

$$L(\mathbf{Y},\mathbf{P}) = \sum_{k\in\text{events}} \log \frac{|\mathcal{M}|^2(\phi^k,\theta_1^k,\theta_2^k,\mathbf{P},\mathbf{Y},\mathbf{X}=1)}{\int |\mathcal{M}|^2(\phi,\theta_1,\theta_2,\mathbf{P},\mathbf{Y},\mathbf{X}=1)d\phi d\cos\theta_1 d\cos\theta_2} \tag{2.181}$$

where $|\mathcal{M}|^2$ is the squared matrix element evaluated at leading order. The value of $\mathbf{X}$ is always fixed to the SM value of 1, since we want to measure small contributions from non-standard couplings. By maximising the likelihood we expect to find a value of zero for $\mathbf{P}$ and $\mathbf{Y}$. In order to demonstrate the potential of measuring these parameters with ATLAS we show contour plots of the expected exclusion

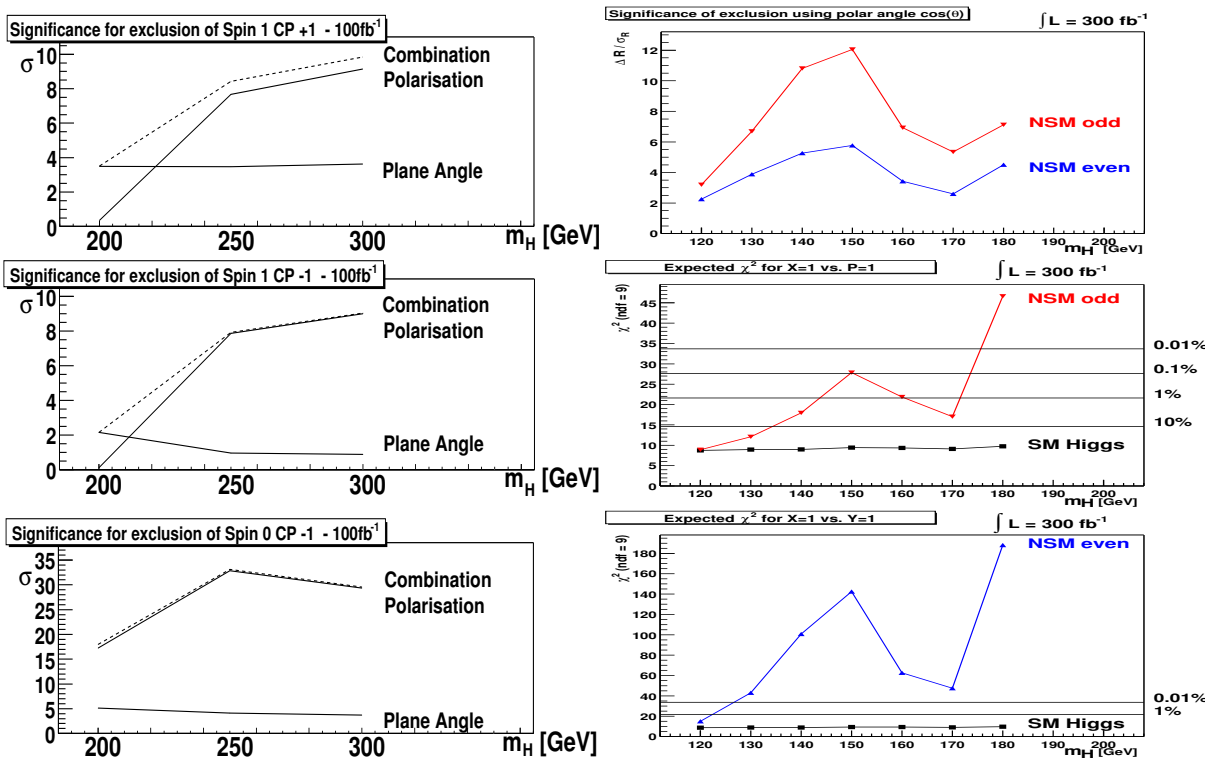

Fig. 2.25: Left: The overall significance for the exclusion of the non standard spin and CP-eigenvalue. The significance from the polar angle measurement and the decay-plane-correlation are plotted separately. Right: The exclusion significance for the non-SM cases for various Higgs masses. The top figure shows the exclusion using the polarisation of the Z. The middle and bottom ones show the exclusion from the distribution of the off-shell Z mass distribution for the pseudoscalar and the scalar non-SM couplings. NSM even refers to states with **Y**=1, **P**=0, **X**=0. NSM odd refers to **Y**=0, **P**=1, **X**=0.

limits (see Fig. 2.26 and 2.27). The full luminosity of 300 fb^{-1} has been used for all plots. The background has been statistically subtracted where the distribution of the background considered in this study was computed with PYTHIA [293]. The distortion of the signal is not negligible, but since the contributions of the non standard model couplings are small the distortions don't vary much. Therefore the expected likelihood distributions are affected only slightly by the detector effects. We do not include any corrections for this effect, which is visible as a small shift of the maximum in positive Y' direction. The plots were achieved by fitting to the whole dataset and as a check to many small samples with the expected number of events (pseudo-experiments). The results from the two methods agree perfectly. A remarkable feature of the contour-plots is the V-form in the $\mathbf{Y} - \mathbf{P}$ plane. This form is understandable, because some combinations of $\mathbf{Y}$ and $\mathbf{P}$ couplings behave very similar to the standard model coupling $\mathbf{X}$. Therefore, neglecting the $\mathbf{Y}$ term in the determination of CP violating contributions could lead to

Table 2.6: Ratio of the roots of the total widths of the pure states for various Higgs masses m_H. These ratios can be used to scale the constants **P** and **Y** such, that the non standard model couplings are of the same strength as the standard model coupling.

$\mathbf{m_H}$ [GeV]	130	140	150	160	170	180	200	250	300
$\sqrt{\frac{\Gamma_Y}{\Gamma_{SM}}}$	0.093	0.106	0.116	0.092	0.106	0.066	0.102	0.284	0.368
$\sqrt{\frac{\Gamma_P}{\Gamma_{SM}}}$	0.106	0.117	0.125	0.123	0.126	0.102	0.146	0.156	0.121

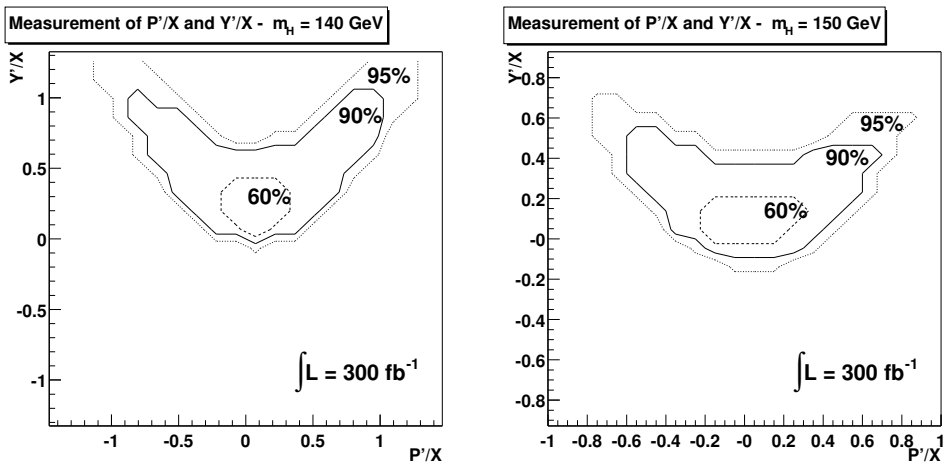

Fig. 2.26: Expected exclusion significance of **P'/X** and **Y'/X** for masses of the Higgs of 140 GeV and 150 GeV. The quality of the measurement is mainly limited by statistics.

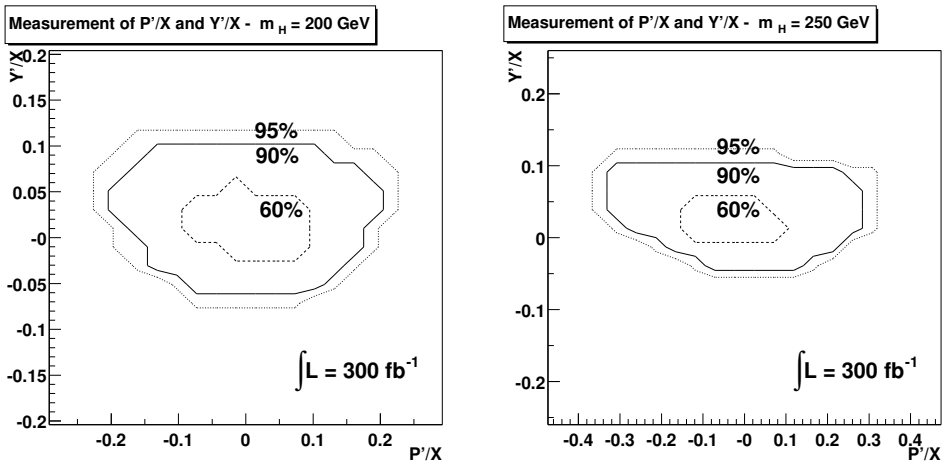

Fig. 2.27: Expected exclusion significance of **P'/X** and **Y'/X** for masses of the Higgs of 200 GeV and 250 GeV. The much higher number of events allows for a much better measurement of the coupling structure above the ZZ threshold.

wrong results.

2.12.2 Conclusions

We have shown with our analyses that the angular correlations of the decay products of the Z bosons can be used to distiguish the SM Higgs-boson from hypothetical particles with different spin and CP quantum numbers. Furthermore, we have demonstrated how and to what extent CP violation in the scalar Higgs decay to Z-pairs can be studied and excluded. The methods discussed work well for a Higgs-boson with a mass above the Z boson pair production threshold. Even small contributions of CP-even and CP-odd non SM couplings can be excluded in this case. Below, the analysis is statistically limited.

2.13 Study of the CP properties of the Higgs boson in the $\Phi \to ZZ \to 2e2\mu$ process in CMS

Michał Bluj

We study a possible measurement of the CP-parity of the Higgs boson Φ at the LHC, using the CMS detector. We consider a „golden channel" $\Phi \to ZZ \to 2e2\mu$ and angular correlations of leptons. The most general ΦVV coupling ($V = W^{\pm}, Z^0$) for a spin-0 Higgs boson looks as follows [93, 119, 288, 294]:

$$\mathcal{C}^{J=0}_{\Phi VV} = \kappa \cdot g^{\mu\nu} + \frac{\zeta}{m_V^2} \cdot p^{\mu} p^{\nu} + \frac{\eta}{m_V^2} \cdot \epsilon^{\mu\nu\rho\sigma} k_{1\rho} k_{2\sigma}, \tag{2.182}$$

where k_1, k_2 are four-momenta of vector bosons V and $p \equiv k_1 + k_2$ is four-momentum of the Higgs boson. In this analysis a simplified version of above ΦVV coupling (Eq. 2.182) is considered with a scalar and a pseudoscalar contributions only (i.e. $\kappa, \eta \neq 0$ and $\zeta = 0$). To study deviations from the Standard Model ΦZZ coupling we take $\kappa = 1$[14]. The differential cross-section for the $\Phi \to Z_1 Z_2 \to (\ell_1 \bar{\ell}_1)(\ell_2 \bar{\ell}_2)$ process consists now of three terms: a scalar one (denoted by H), a pseudoscalar one $\sim \eta^2$ (denoted by A) and the interference term violating CP $\sim \eta$ (denoted by I):

$$d\sigma(\eta) \sim H + \eta\, I + \eta^2 A. \tag{2.183}$$

This way the Standard-Model scalar ($\eta = 0$) and the pseudoscalar (in the limit $|\eta| \to \infty$) contributions could be recovered. It is convenient to introduce a new parameter ξ, defined by $\tan\xi \equiv \eta$, with values between $-\pi/2$ and $\pi/2$. Expressions for H, A and I can be found in article [288].

To study the CP-parity of the Higgs boson we use two angular distributions. The first one is a distribution of the angle φ (called a plane or an azimuthal angle) between the planes of two decaying Zs, in the Higgs boson rest frame[15]. The second one is a distribution of the polar angle θ, in the Z rest frame, between the momentum of the negatively charged lepton and the direction of motion of the Z boson in the Higgs boson rest frame (Fig. 2.16).

2.13.1 MC samples

The Higgs-boson signal samples were generated using `PYTHIA` [295] for three masses of the Higgs boson ($m_\Phi = 200,\ 300,\ 400$ GeV). Generated events were required to contain e^+e^- and $\mu^+\mu^-$ pairs within the detector acceptance region ($p_t^e > 5$ GeV, $|\eta^e| < 2.7$ and $p_t^\mu > 3$ GeV, $|\eta^\mu| < 2.5$). The analysis was performed for the scalar, pseudoscalar and CP-violating states (the latter for $\tan\xi$=$\pm$0.1, $\pm$0.4, $\pm$1, $\pm$4). Samples for the scalar, pseudoscalar and $\tan\xi = \pm 1$ states contain 10 000 events, while each of remaining samples contains 5 000 events. The predicted production cross-sections: σ_Φ, $\sigma_\Phi \cdot BR(\Phi \to 4\ell)$ and $\sigma_\Phi \cdot \epsilon \cdot BR(\Phi \to 4\ell)$, where ϵ is the preselection efficiency for a the signal, are summarized in Table 2.7. We assume the Standard Model cross-section [296] and the Standard Model branching ratio [297] for each value of the ξ parameter (independently on the CP-parity of the Higgs boson). A dependence of the analysis' results on the assumed cross-section is discussed in Section 2.13.4. The following background processes were considered:

Table 2.7: Production cross-sections of the signal. Errors are statistical only.

mass (GeV)	σ_Φ (fb)	$\sigma_\Phi \cdot BR(\Phi \to 4\ell)$ (fb)	$\sigma_\Phi \cdot \epsilon \cdot BR(\Phi \to 4\ell)$ (fb)
200	$17.86 \cdot 10^3$	38.75	7.65 ± 0.09
300	$9.41 \cdot 10^3$	24.03	5.08 ± 0.06
400	$8.71 \cdot 10^3$	20.15	4.45 ± 0.05

[14] The ΦVV coupling with $\kappa = 1$ and arbitrary η is implemented in the `PYTHIA` generator.

[15] The negatively charged leptons were used to fix planes' orientations.

Table 2.8: Production cross-sections and number of used events for background processes. Errors are statistical only.

process	σ_{bkg} (fb)	$\sigma_{bkg} \cdot BR$ (fb)	$\sigma_{bkg} \cdot \epsilon \cdot BR$ (fb)	# events
ZZ/γ^*	$28.9 \cdot 10^3$	730.27	39.75 ± 0.34	20k
$t\bar{t}$	$840 \cdot 10^3$	$87.2 \cdot 10^3$	775.08 ± 4.84	48k
$Zb\bar{b}$	$525 \cdot 10^3$	$9.49 \cdot 10^3$	116.38 ± 3.22	5k

Table 2.9: Selected cross-section for signal and background at chosen stages of the selection. All values in fb; errors are statistical only.

level of selection	signal	background		
		ZZ/γ^*	$t\bar{t}$	$Zb\bar{b}$
selection for $m_\Phi = 200$ GeV				
trigger	6.45±0.09	30.30±0.30	305.04±3.11	81.17±2.69
reco. e^+e^- $\mu^+\mu^-$	5.46±0.08	22.57±0.26	164.04±2.29	32.77±1.73
Zs' mass	3.89±0.07	12.57±0.19	0.09±0.06	<0.03
Φs mass	3.43±0.06	1.84±0.07	<0.02	<0.03
selection for $m_\Phi = 300$ GeV				
trigger	4.34±0.06	30.30±0.30	305.04±3.11	81.17±2.69
reco. e^+e^- $\mu^+\mu^-$	3.74±0.05	22.57±0.26	164.04±2.29	32.77±1.73
Zs' mass	2.69±0.05	7.32±0.15	0.13±0.07	0.05±0.07
Φs mass	2.10±0.04	0.82±0.05	<0.02	<0.03
selection for $m_\Phi = 400$ GeV				
trigger	3.84±0.06	30.30±0.30	305.04±3.11	81.17±2.69
reco. e^+e^- $\mu^+\mu^-$	3.35±0.06	22.57±0.26	164.04±2.29	32.77±1.73
Zs' mass	2.46±0.05	5.35±0.13	0.09±0.06	<0.03
Φs mass	2.02±0.04	0.66±0.05	<0.02	<0.03

1. $ZZ/\gamma^* \to 2e2\mu$ (irreducible background). The leading order cross-section for the $q\bar{q} \to ZZ/\gamma^*$ process calculated using `MCFM` program [298] is equal to 18.7 pb. The next-to-leading order contribution as well as the contribution from the $gg \to ZZ/\gamma^*$ process, with estimated cross-section of about 20% of the $q\bar{q} \to ZZ/\gamma^*$ cross-section at the leading order, was included as a four-lepton-mass dependent K-factor. The K-factor is in average equal to 1.55 in four-lepton-mass range between 30 and 750 GeV, for example K=1.46, 1.66, 1.90 for $m_{4\ell}$=200, 300, 400 GeV, respectively.
2. $t\bar{t} \to W^+W^-b\bar{b} \to 2e2\mu X$. The $t\bar{t}$ cross-section is equal to 840 pb [299].
3. $Zb\bar{b} \to 2e2\mu X$. The $Zb\bar{b}$ cross-section at the next-to-leading order, determined using `MCFM` program [300–302] for $p_t^b > 1$ GeV, $|\eta^b| < 2.5$ and $81 < m_{Z^*} < 101$ GeV, is equal to 525 pb.

The information about the generated background samples are summarized in Table 2.8.
The minimum-bias pile-up events for the low LHC luminosity were added to each signal and background sample.

2.13.2 Selection

We use selection criteria (for four isolated leptons) developed in the Standard-Model Higgs boson searches at CMS for the $H \to ZZ \to 2e2\mu$ process [303]. Values of the selection cuts depend on the Higgs boson mass. The selected cross-section, at chosen stages of the selection, for the signal and the background for three masses of the Higgs boson $m_\Phi = 200,\ 300,\ 400$ GeV are shown in Table 2.9. Fig. 2.28 shows the invariant mass of four reconstructed leptons before and after the off-line selection (i.e. after lepton reconstruction and after cut on two Zs' masses, respectively) for the Higgs boson sig-

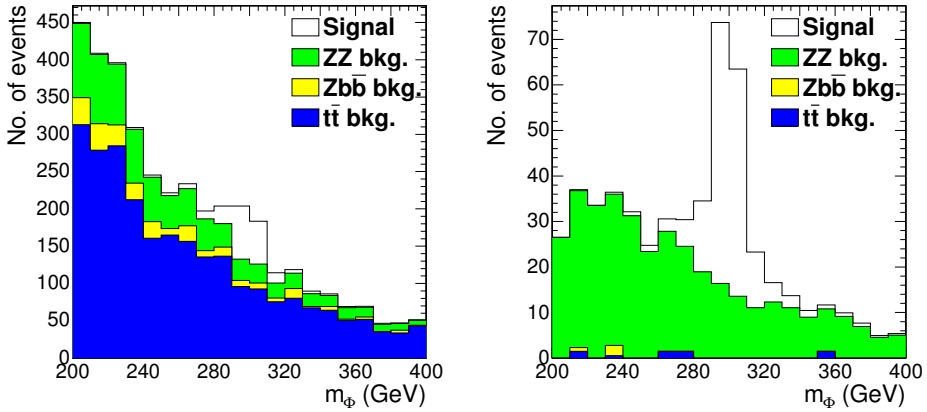

Fig. 2.28: Invariant mass distributions of four leptons before (left) and after (right) the off-line selection (normalized to 60 fb^{-1}). The signal of the Higgs boson with m_Φ=300 GeV (empty histogram) and the background (filled histograms).

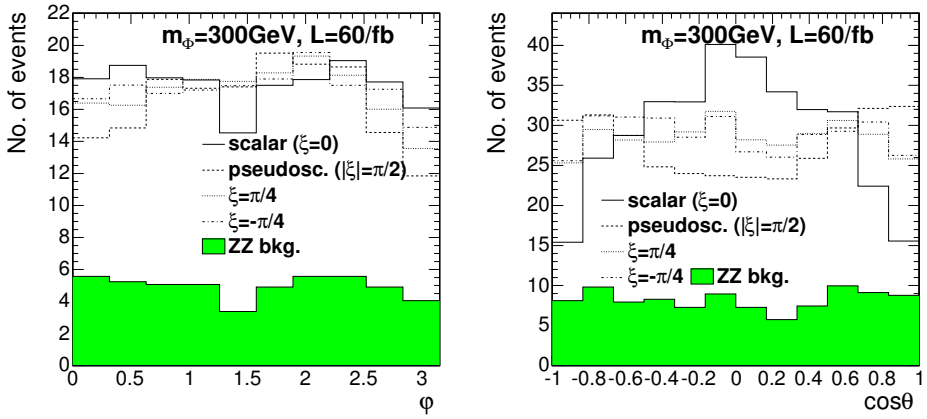

Fig. 2.29: The φ-distributions (left) and the θ-distributions (right) for various values of the parameter ξ after final selection (normalized to 60 fb^{-1}). The signal for m_Φ=300 GeV and $\xi = 0$ (scalar), $\xi = -\pi/4$, $\xi = +\pi/4$ and $|\xi| = \pi/2$ (pseudoscalar), respectively (empty histograms). The ZZ background - filled histogram.

nal, with m_Φ=300 GeV, and for the background. The reconstructed angular distributions after the final selection for the signal (with mass m_Φ=300 GeV) for various values of the parameter ξ, and for the background are shown in Fig. 2.29. Shape of the angular distributions for the background slightly depends on the Higgs-mass-dependent selection. This effect is taken into account in our analysis.

2.13.3 Determination of the parameter ξ

The parameter ξ was determined by maximization of the likelihood function $\mathcal{L}(\xi,R)$, which was constructed, for both the signal and the background, from the angular distributions and invariant mass distribution of four leptons. The function depends on two parameters: ξ describing CP of the Higgs boson, and R describing a fraction of the signal in the data sample. The function has the following form:

$$\mathcal{L}(\xi,R) \equiv 2 \sum_{x_i \in data} \log \mathcal{Q}(\xi,R;\, x_i), \text{ where } \mathcal{Q}(\xi,R;\, x_i) \equiv R \cdot \mathcal{PDF}_S(\xi;\, x_i) + (1-R) \cdot \mathcal{PDF}_B(x_i). \tag{2.184}$$

$\mathcal{PDF}_B(x_i)$ and $\mathcal{PDF}_S(\xi;\, x_i)$ are Probability Density Functions for the background and the signal respectively; $\{x_i\}$ are values of the measured quantities (angles and invariant mass) in the data event i.

They are products of probability densities $\mathcal{P}^M$, $\mathcal{P}^\varphi$, $\mathcal{P}^{\cos\theta_{1,2}}$ of four leptons invariant mass and angles φ and $\cos\theta_{1,2}$ i.e. $\mathcal{PDF} \equiv \mathcal{P}^M\mathcal{P}^\varphi\mathcal{P}^{\cos\theta_1}\mathcal{P}^{\cos\theta_2}$. $\mathcal{P}^M$, $\mathcal{P}^\varphi$, $\mathcal{P}^{\cos\theta_{1,2}}$ are obtained by the Monte Carlo technique, using the normalized histograms of given quantities after the final selection.
A part of the function $\mathcal{Q}$, which describes angular distributions of the signal depends on the parameter ξ. From Eq. (2.183) we obtain:

$$\mathcal{P}(\xi) \equiv (\mathcal{P}_S^\varphi \cdot \mathcal{P}_S^{\cos\theta_1} \cdot \mathcal{P}_S^{\cos\theta_2})(\xi) \equiv (\mathcal{H} + \tan\xi \cdot \mathcal{I} + \tan^2\xi \cdot a^2\mathcal{A})/(1 + a^2\tan^2\xi), \qquad (2.185)$$

where: $\mathcal{H} \equiv \mathcal{P}_H^\varphi \cdot \mathcal{P}_H^{\cos\theta_1} \cdot \mathcal{P}_H^{\cos\theta_2}$ and $\mathcal{A} \equiv \mathcal{P}_A^\varphi \cdot \mathcal{P}_A^{\cos\theta_1} \cdot \mathcal{P}_A^{\cos\theta_2}$ are probability densities obtained by the Monte Carlo technique for the scalar (H) and the pseudoscalar (A), respectively. The parameter a^2 is a (mass dependent) relative strength of the pseudoscalar and scalar couplings. For example a^2=0.51, 1.65, 1.79 for m_Φ=200, 300, 400 GeV, respectively. $\mathcal{I}$ is a normalized product of angular distributions for the CP-violating term. Since $\mathcal{I}$ is not positive, and its integral is equal to zero, it is not possible to simulate it separately. The $\mathcal{I}$ contribution can be obtained indirectly from the combined probability density for the signal with a non-zero value of the parameter ξ. For example by introducing $\mathcal{P}_+ \equiv \mathcal{P}(\pi/4) = (\mathcal{H}+\mathcal{I}+a^2\mathcal{A})/(1+a^2)$ and $\mathcal{P}_- \equiv \mathcal{P}(-\pi/4) = (\mathcal{H}-\mathcal{I}+a^2\mathcal{A})/(1+a^2)$ we have $\mathcal{I} = \frac{1+a^2}{2}(\mathcal{P}_+ - \mathcal{P}_-)$. Finally we obtain:

$$\mathcal{P}(\xi) \equiv [\mathcal{H} + \tan\xi \cdot \frac{1+a^2}{2} \cdot (\mathcal{P}_+ - \mathcal{P}_-) + \tan^2\xi \cdot a^2\mathcal{A}]/(1 + a^2\tan^2\xi). \qquad (2.186)$$

2.13.4 Results

After selection all background contributions but $ZZ/\gamma^* \to 2e2\mu$ are negligible, therefore only such events were used to construct the probability density function for the background. We use the ZZ/γ^* sample containing 15 000 events at the generator level. Signal probability density functions were constructed using samples of scalar Higgs boson (H), pseudoscalar (A) and $\mathcal{P}_+$, $\mathcal{P}_-$ samples, each containing 8 000 events at the generator level. Likelihood functions were constructed independently for three masses of the Higgs boson (m_Φ=200, 300, 400 GeV).

For each value of parameter ξ and for each Higgs-boson mass we made 200 pseudoexperiments for the integrated luminosity $\mathcal{L}$=60 fb^{-1} (3 years of LHC at low luminosity). For each pseudoexperiment we randomly selected events from the signal and background samples to form a test sample[16]. The number of selected events was given by a Poisson probability distribution with mean defined by the process cross-section and the examined luminosity. Then to obtain a value of the parameter ξ, we performed a maximization of the likelihood function $\mathcal{L}(\xi,\mathcal{R})$ for the test sample. The expected and reconstructed values of the parameter ξ (with its uncertainty), obtained for three masses of the Higgs boson are shown in Fig. 2.30.

In our analysis the Standard-Model signal cross-section and branching ratio were used as a reference. However, both of them may change for other Higgs models. An influence of a possible suppression (enhancement) factor C^2 of the Standard Model signal on the reconstructed ξ were studied and we found that its value slightly depends on size of suppression (enhancement). On the other hand, the uncertainty of ξ is approximately $\sim 1/C$ (i.e. it depends on square-root of number of events, what one can expect), namely:

$$\Delta\xi(\xi, C^2) \equiv \frac{\sigma_0(\xi)}{\sqrt{C^2}}. \qquad (2.187)$$

A value of $\sigma_0(\xi)$ (a precision factor) can be determined from the fit. Taking this into account we parametrize a relative error of the difference between ξ and ξ_0 as follows:

$$\frac{\sigma_{|\xi-\xi_0|}(C^2)}{|\xi - \xi_0|} = \frac{\Delta\xi(\xi, C^2)}{|\xi - \xi_0|}. \qquad (2.188)$$

[16] Samples used to select events, contain 2 000 and 5 000 events for the signal and the background, respectively. The samples do not contain events used to construct probability densities for the likelihood function.

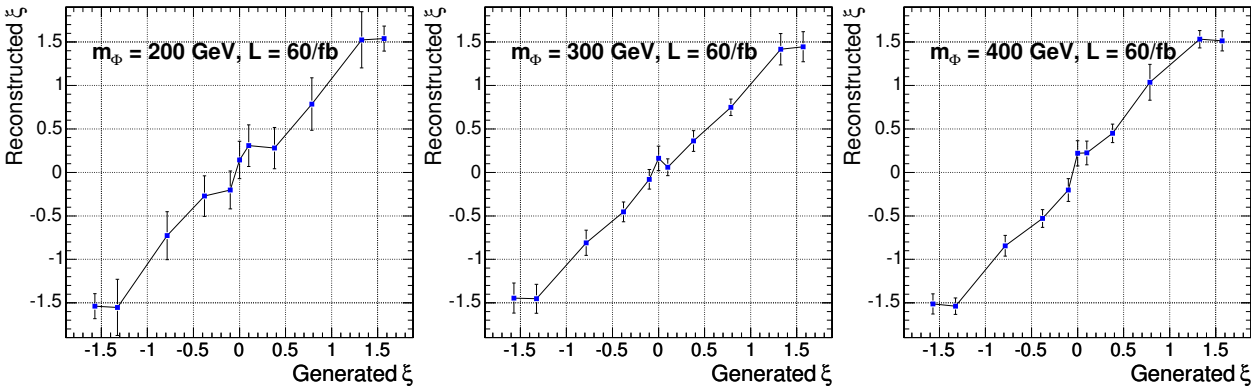

Fig. 2.30: Reconstructed value of the parameter ξ as function of the generated value of the parameter ξ, for $\mathcal{L}$=60 fb^{-1}, for Higgs boson mass m_Φ=200, 300, 400 GeV. Uncertainties correspond to one standard deviation.

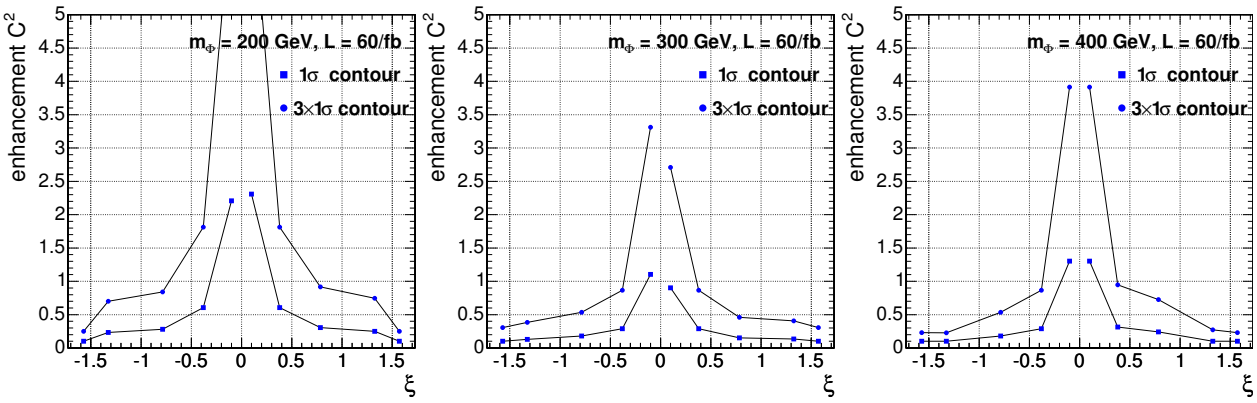

Fig. 2.31: Exclusion contours for scalar Higgs boson as a function of the enhancement factor C^2 for the Higgs boson masses m_Φ=200, 300, 400 GeV (from left to right). Results were obtained for 60 fb^{-1}.

The requirement of exclusion of $\xi \neq \xi_0$ at the level of "N sigmas" could be written as $\sigma_{|\xi-\xi_0|}(C^2) = |\xi - \xi_0|$

$$C^2(N) = N^2 \frac{\sigma_0^2(\xi)}{(\xi - \xi_0)^2}. \tag{2.189}$$

The exclusion contours for N=1, 3 and for $\xi_0 = 0$ (scalar) are shown in Fig. 2.31.

2.13.5 Summary

A possibility of a measurement of the CP-properties of the Higgs boson Φ in the $\Phi \to ZZ \to 2e2\mu$ process at LHC with CMS detector was studied. It was shown that using angular correlations of the Higgs boson decay products (leptons) the measurement of the parameter ξ, describing a general ΦZZ coupling, will be feasible. Precision of this measurement is sufficient for determination of the CP-parity of the Higgs boson, particularly it is sufficient to distinguish scalar from pseudoscalar.

2.14 Higgs-boson CP properties from decays to WW and ZZ at the Photon Linear Collider

Piotr Nieżurawski, Aleksander Filip Żarnecki and Maria Krawczyk

The process of resonant Higgs boson production at the Photon Linear Collider (PLC), due to $h\gamma\gamma$ coupling, is in the Standard Model sensitive to the Higgs boson couplings to both, the gauge-bosons and up-type fermions. Moreover, as the phases of the two dominant contributions to the $\gamma\gamma \to h$ amplitude, from $W^{\pm}$ and top loops, differ, the process turns out to be very sensitive to the possible effects of the CP violation.

In Ref. [304] we performed a realistic simulation of the Standard Model Higgs-boson production at the PLC for W^+W^- and ZZ decay channels, for Higgs-boson masses above 150 GeV. From the combined analysis of W^+W^- and ZZ invariant mass distributions the $\gamma\gamma$ partial width of the Higgs boson, $\Gamma_{\gamma\gamma}$, can be measured with an accuracy of 3 to 8% and the phase of $\gamma\gamma \to h$ amplitude, $\phi_{\gamma\gamma}$, with an accuracy between 30 and 100 mrad. In Ref. [144] we extended this analysis to the generalized Standard Model-like scenario B_h of the Two Higgs Doublet Model II, 2HDM(II), with and without CP-violation. We also considered a general 2HDM (II) with CP violation, and found that only the combined analysis of LHC, ILC and PLC measurements allows for a precise determination of the Higgs-boson couplings and of CP-violating H–A mixing angle [305, 306]. Finally, we considered model with a generic, CP-violating Higgs-boson couplings to vector bosons [93, 136, 307], which leads to different angular distributions for a scalar- and pseudoscalar-type of couplings. From a combined analysis of the invariant mass distributions and angular distributions of the W^+W^- and ZZ decay-products the CP-parity of the observed Higgs state can be determined independently on a production mechanism [147].

In this contribution we summarize selected results of [144, 147, 305, 306], related to the determination of the Higgs-boson CP properties at the PLC.

2.14.1 Event simulation

In analyses we use the `CompAZ` parametrization [308] of the realistic luminosity spectra for a Photon Linear Collider at TESLA [309, 310] and assume that the centre-of-mass energy of colliding electron beams, $\sqrt{s_{ee}}$, is optimized for the production of a Higgs boson with given mass. We consider the mass range between 200 and 350 GeV, where W^+W^- and ZZ decays are expected to dominate. All results presented in this paper were obtained for an integrated luminosity corresponding to one year of the PLC running, as given by [309, 310], i.e. from 600 fb^{-1} for $\sqrt{s_{ee}} = 305$ GeV (optimal beam energy choice for $M = 200$ GeV) to about 1000 fb^{-1} for $\sqrt{s_{ee}} = 500$ GeV (for $M = 350$ GeV).

Analyses described in this work were performed in two steps. In the first step we use samples of events generated with `PYTHIA` 6.152 [295] to estimate selection efficiency, as well as resolutions of the angular variable and of the invariant-mass reconstruction for $\gamma\gamma \to W^+W^-/ZZ$ events, as a function of the $\gamma\gamma$ centre-of-mass energy, $W_{\gamma\gamma}$. We consider the direct vector-bosons production in $\gamma\gamma$ interactions (background) as well as the signal $\gamma\gamma \to h \to W^+W^-/ZZ$ and the interference between the signal and the background. To take into account effects which are not implemented in `PYTHIA` (photon beam polarization, interference term contribution, direct $\gamma\gamma \to ZZ$ production) we exploit the standard method used in various experimental analyses called a reweighting procedure. To each generated event a weight is attributed given by the ratio of the differential cross-section for a vector-boson production in the polarized photon interactions [311–314] to the `PYTHIA` differential cross section for given event. The fast simulation program `SIMDET` version 3.01 [315] is used to model the TESLA detector performance.

For the W^+W^- events only $qq\bar{q}\bar{q}$ decay channel is considered, as without knowing the exact beam-photon energies, which is a case for the Photon Linear Collider, the semileptonic $W^{\pm}$ decays can not be fully reconstructed. For the ZZ events, only $l\bar{l}q\bar{q}$ decay channel is considered, with one Z decaying into e^+e^- or $\mu^+\mu^-$. Selection of the leptonic channel is crucial for a suppression of the

background from the direct $\gamma\gamma \to W^+W^-$ events.

The invariant-mass resolutions obtained from a full simulation of W^+W^- and ZZ events (based on the PYTHIA and SIMDET programs), have been parametrized as a function of the $\gamma\gamma$ centre-of-mass energy, $W_{\gamma\gamma}$. This parametrization can then be used to obtain the parametric description of the expected invariant mass distributions, for $\gamma\gamma \to W^+W^-$ and $\gamma\gamma \to ZZ$ events, avoiding the time consuming event generation procedure. Resolutions expected in the reconstruction of angular variables are very good and the measurement errors can be safely neglected. The measured angular distributions are mainly affected by the detector acceptance and the corresponding selection cuts used in the analysis. The corresponding acceptance corrections have also been parametrized as a function of the relevant angular variables. For arbitrary model, and for arbitrary model parameters, we calculate the expected angular and invariant mass distributions for ZZ and W^+W^- events by convoluting the corresponding cross-section formula with the analytic photon-energy spectra CompAZ [308]. To take into account detector effects, we convolute these distributions further with the function parameterising the invariant-mass resolution and the acceptance function, which takes into account the angular- and jet-selection cuts. This approach has been developed in [304].

2.14.2 Generic model

Following the analysis described in [93,136,307] we consider a generic model with a direct CP violation, i.e. with tensor couplings of a Higgs boson, Φ, to ZZ and W^+W^- given by:

$$\begin{aligned} g_{\Phi ZZ} &= ig\frac{M_Z}{\cos\theta_W}\left(\lambda_H \cdot g^{\mu\nu} + \lambda_A \cdot \varepsilon^{\mu\nu\rho\sigma}\,\frac{(p_1+p_2)_\rho\,(p_1-p_2)_\sigma}{M_Z^2}\right), \\ g_{\Phi WW} &= igM_W\left(\lambda_H \cdot g^{\mu\nu} + \lambda_A \cdot \varepsilon^{\mu\nu\rho\sigma}\,\frac{(p_1+p_2)_\rho\,(p_1-p_2)_\sigma}{M_W^2}\right), \end{aligned} \tag{2.190}$$

where p_1 and p_2 are the 4-momenta of the vector bosons. The λ_H-terms have a structure of the CP-even SM Higgs boson coupling,[17] whereas the one with λ_A corresponds to a general CP-odd coupling for the spin-0 boson. Coefficients λ_H and λ_A can be parametrized by:

$$\begin{aligned} \lambda_H &= \lambda \cdot \cos\Phi_{CP}\,, \\ \lambda_A &= \lambda \cdot \sin\Phi_{CP}\,. \end{aligned} \tag{2.191}$$

The couplings of the Standard Model Higgs boson are reproduced for $\lambda = 1$ and $\Phi_{CP} = 0$ (i.e. $\lambda_H = 1$ and $\lambda_A = 0$). Below we will limit ourselves to $\lambda \approx 1$ and $|\Phi_{CP}| \ll 1$ region, corresponding to a small deviation from the respective Standard Model coupling. However, we do not make any assumptions concerning Higgs-boson couplings to the fermions and we allow for deviations from SM predictions in $\Gamma_{\gamma\gamma}$ and $\phi_{\gamma\gamma}$. Therefore our results do not depend on the Higgs-boson production mechanism and our approach can be considered as a model-independent one.

The angular distributions of the secondary W^+W^- and ZZ decay products turn out to be very sensitive to the CP properties of the Higgs-boson [93, 136, 307]. Angular variables which can be used in the analysis are defined in Fig. 2.32 (see also Fig. 2.16). To test CP-properties of the Higgs-bosons the distributions of the polar angles Θ_1 and Θ_2 as well as the $\Delta\phi$ distribution, where $\Delta\phi$ is the angle between two Z- or two W-decay planes, are used. Here we propose to consider, instead of the two-dimensional distribution in $(\cos\Theta_1, \cos\Theta_2)$, the distribution in a new variable, defined as

$$\zeta = \frac{\sin^2\Theta_1 \cdot \sin^2\Theta_2}{(1+\cos^2\Theta_1)\cdot(1+\cos^2\Theta_2)}\,. \tag{2.192}$$

[17] Other possible CP-even tensor structure, $\sim (p_1+p_2)^\mu (p_1+p_2)^\nu$, give the angular distributions similar to that of the SM Higgs boson and therefore we will not consider this case separately. See also Section 2.12.

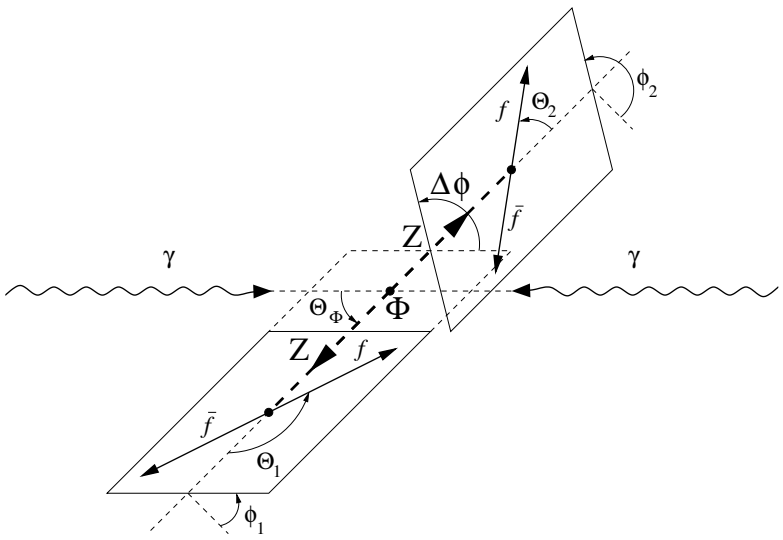

Fig. 2.32: The definition of the polar angles Θ_Φ, Θ_1 and Θ_2, and the azimuthal angles ϕ_1 and ϕ_2 for the process $\gamma\gamma \to \Phi \to ZZ \to 4\ f$. $\Delta\phi$ is the angle between two Z decay planes, $\Delta\phi = \phi_2 - \phi_1$. All polar angles are calculated in the rest frame of the decaying particle.

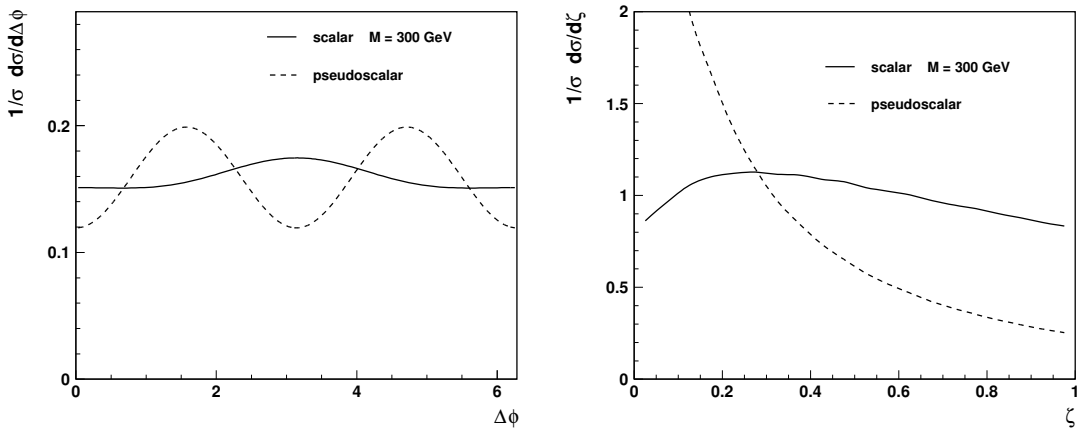

Fig. 2.33: Normalised angular distributions in $\Delta\phi$ (left plot) and ζ (right plot), expected for scalar (solid line) and pseudoscalar (dashed line) Higgs boson decays $H, A \to ZZ \to l^+l^-jj$, for the Higgs boson mass of 300 GeV.

The ζ-variable corresponds to the ratio of the angular distributions expected for the decay of a scalar and a pseudoscalar (in a limit $M_\Phi \gg M_Z$) [93, 136, 307]. It proves to be very useful and complementary to the $\Delta\phi$ variable.

The angular distributions in $\Delta\phi$ and ζ, expected for decays of a scalar H ($\Phi_{CP} = 0$) and a pseudoscalar A ($\Phi_{CP} = \frac{\pi}{2}$) Higgs boson with mass of 300 GeV, $\Phi \to ZZ \to l^+l^-jj$, are compared in Fig. 2.33. Both distributions clearly distinguish between decays of scalar and pseudoscalar Higgs boson; so it's possible to distinguish the CP-even and CP-odd states without taking into account the production mechanism. We point out the usefulness of the ζ distribution.

For the measurement of the $\Delta\phi$ and ζ distributions we introduce an additional cut on the reconstructed ZZ or W^+W^- invariant mass and, for W^+W^- events only, the cut on the Higgs-boson decay angle Θ_Φ, to suppress large background from the nonresonant W^+W^- production. The cuts were optimised for the smallest relative error in the signal cross-section measurement.

The expected precision in the measurements of the $\Delta\phi$- and of the ζ-distributions, for $\gamma\gamma \to ZZ \to l^+l^-jj$ events is illustrated in Fig. 2.34. The reconstructed $\Delta\phi$ values range from 0 to π, since

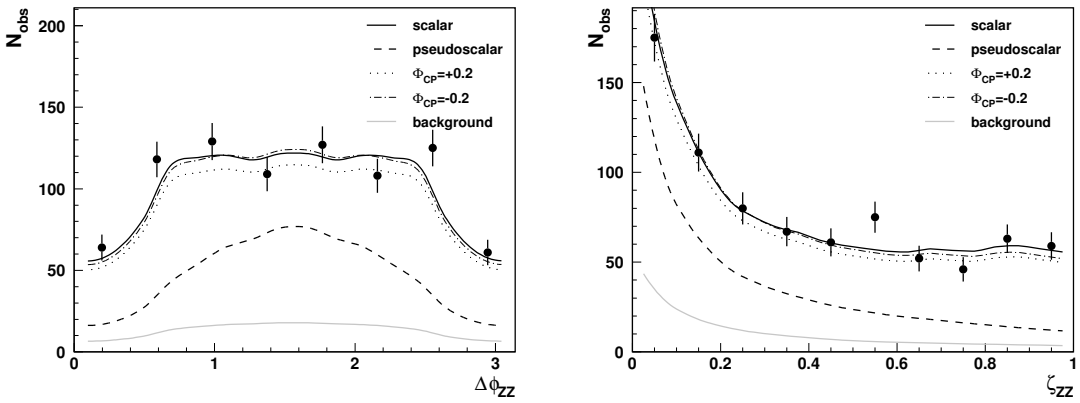

Fig. 2.34: Measurement of the angle $\Delta\phi_{ZZ}$ between two Z-decay planes (left plot) and of the variable ζ_{ZZ} calculated from the polar angles of the $Z \to l^+l^-$ and $Z \to jj$ decays (right plot) for $ZZ \to l^+l^-jj$ events. Error bars indicate the statistical precision of the measurement after one year of PLC running at nominal luminosity, for the scalar Higgs boson with mass of 300 GeV. The solid and dashed lines correspond to the predictions of the model with pure scalar ($\Phi_{CP} = 0$) and pseudoscalar ($\Phi_{CP} = \frac{\pi}{2}$) Higgs-boson couplings, whereas dotted and dash-dotted lines correspond to CP violating couplings with $\Phi_{CP} = \pm 0.2$. The gray line represents the SM background of non-resonant ZZ production.

we are not able to distinguish between quark and antiquark jet. Calculations were performed for the primary electron-beam energy of 152.5 GeV and the Higgs-boson mass of 200 GeV. The results are compared with the expectation for $\Phi_{CP} = 0$ (as in SM) and $\Phi_{CP} = \frac{\pi}{2}$. We see, that even after taking into account the beam spectra, detector effects, selection cuts and background influence, the differences between shapes of the angular distributions for the scalar and pseudoscalar couplings are still significant. Therefore we should be able to constrain Higgs-boson couplings from the shape of the distributions, even if the overall normalisation related to the Higgs-boson production mechanism is not known.

Each of the considered angular distributions discussed above can be fitted with the model expectations, given in terms of the parameters λ and Φ_{CP} describing Higgs-boson couplings to gauge bosons, the parameters $\Gamma_{\gamma\gamma}$ and $\phi_{\gamma\gamma}$ describing the production mechanism, and an overall normalisation. We calculate the expected statistical errors on the parameters λ and Φ_{CP}, from the combined fit to angular distributions measured for the ZZ and W^+W^- decays, and to the invariant mass distributions. Results are shown in Fig. 2.35. The two photon width of the Higgs boson $\Gamma_{\gamma\gamma}$, the phase $\phi_{\gamma\gamma}$ and normalisations of both samples are allowed to vary in the fit, so the results are independent on the production mechanism. One observes that for Higgs-boson masses below 250 GeV, better constrains are obtained from the measurement of W^+W^- events, whereas for masses above 300 GeV smaller errors are obtained from the ZZ events. The error on Φ_{CP} expected from the combined fit is below 50 mrad in the whole considered mass range. The corresponding error on λ is about 0.05.

2.14.3 SM-like Two Higgs Doublet Model

Here we consider the CP violation in the Standard-Model scenario of the 2HDM. This is a generalization of a CP conserving scenario B_h, introduced in [15,63,144]. In the following we consider the CP-violating solution B_h, with a weak CP violation through a small mixing between H and A states.

In this scenario the Yukawa couplings of h ($h \sim h_1$) are equal (up to a sign) to the corresponding SM Higgs-boson couplings. Then, it follows from Eqs. (2.43) and (2.54)–(2.56) that the coupling of h to gauge bosons as well as the corresponding Yukawa and gauge boson couplings of H and A bosons are uniquely determined by $\tan\beta$, as shown in Table 2.10 (for relative couplings). Note that the tensor structure of all couplings is the same as in the Standard Model.

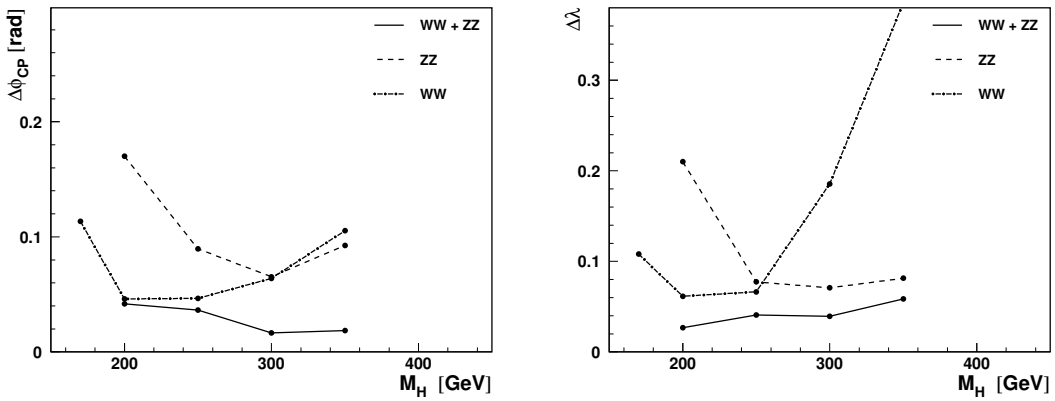

Fig. 2.35: Statistical error in the determination of Φ_{CP} (left plot) and λ (right plot), expected after one year of Photon Linear Collider running, as a function of the Higgs-boson mass M_Φ. Combined fits were performed to the considered angular distributions and invariant mass distributions for ZZ events and W^+W^- events. Results were obtained assuming small deviations from Standard Model predictions, i.e. $\lambda \approx 1$ and $\Phi_{CP} \approx 0$. The two photon width of the Higgs boson $\Gamma_{\gamma\gamma}$, the phase $\phi_{\gamma\gamma}$ and normalisations of both samples are allowed to vary in the fit.

The couplings of the lightest mass-eigenstate h_1 (with mass 120 GeV) are expected to correspond to the couplings of the SM-like h boson, whereas couplings of h_2 and h_3 states can be described as the superposition of H and A couplings. For the relative basic couplings we have:

$$\begin{aligned} \chi_X^{h_1} &\approx \chi_X^h \,, \\ \chi_X^{h_2} &\approx \chi_X^H \cdot \cos\Phi_{HA} \,+\, \chi_X^A \cdot \sin\Phi_{HA} \,, \\ \chi_X^{h_3} &\approx \chi_X^A \cdot \cos\Phi_{HA} \,-\, \chi_X^H \cdot \sin\Phi_{HA} \,, \end{aligned} \tag{2.193}$$

where X denotes a fermion or a vector boson, $X = u,\ d,\ V$ and Φ_{HA} is the $H - A$ mixing angle characterizing a weak CP violation.

We study the feasibility of Φ_{HA} determination from the combined measurement of the invariant-mass distributions[18] in the ZZ and W^+W^- decay-channels for the Higgs-boson mass-eigenstate h_2. From such measurement the $\gamma\gamma$ partial width, $\Gamma_{\gamma\gamma} \times BR(h \to W^+W^-/ZZ)$, and the phase of the $\gamma\gamma h$ amplitude, $\phi_{\gamma\gamma}$, can be extracted. Results obtained for h_2 with mass $M_{h_2} = 300$ GeV are presented in Fig. 2.36, for $M_{h_1} = 120$ GeV and $M_{H^\pm} = 800$ GeV. Error contours (1σ) on the measured deviation from the Standard Model predictions are shown for $\Phi_{HA} = 0$, i.e. when CP is conserved, and for the CP violation with $\Phi_{HA} = \pm 0.3$ rad. Even a small CP-violation can significantly influence the measured

[18]It should be stressed that in the considered case of CP violation via $H - A$ mixing, contrary to the generic model studied in Section 2.14.2, only the invariant mass distributions are sensitive to the mixing angle Φ_{HA}.

Table 2.10: Couplings of the neutral Higgs-bosons to up- and down-type fermions, and to vector bosons, relative to the Standard Model couplings, for the considered solution B_h of the SM-like 2HDM (II).

	h	H	A
χ_u	-1	$-\frac{1}{\tan\beta}$	$-i\,\gamma_5\,\frac{1}{\tan\beta}$
χ_d	$+1$	$-\tan\beta$	$-i\,\gamma_5\,\tan\beta$
χ_V	$\cos(2\beta)$	$-\sin(2\beta)$	0

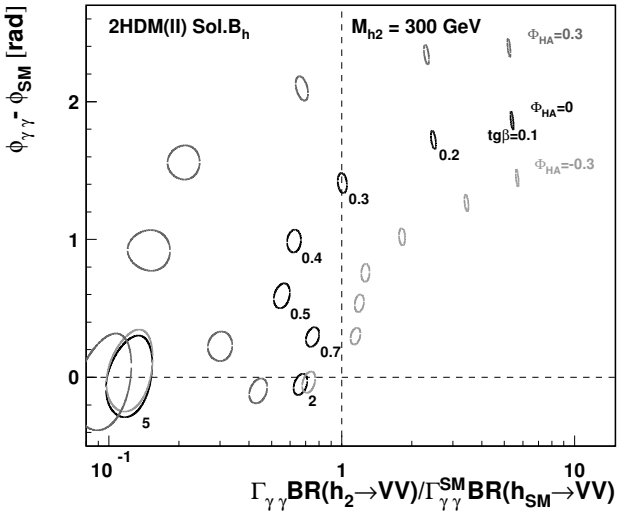

Fig. 2.36: The deviation from the SM predictions for the SM-like 2HDM II (sol. B_h) with CP-violation, for the heavy Higgs-boson h_2 with mass 300 GeV. A light Higgs-boson has mass $M_{h_1} = 120$ GeV. Three values of $H - A$ mixing angle $\Phi_{HA} = -0.3, 0, 0.3$ are considered.

two-photon width and two-photon phase allowing to determine precisely both the CP-violating mixing angle Φ_{HA} and the parameter $\tan\beta$.

As a large sample of events is expected at PLC, especially in the $\gamma\gamma \to W^+W^-$ channel, systematic uncertainties have to be taken into account, as they can significantly influence the final precision. In case of scenario B_h with CP violation, a possible correlations between Φ_{HA} and $\tan\beta$ has to be considered if both parameters are to be constrained from the fit to the data. In this analysis the systematic uncertainties from following sources were considered: the total integrated $\gamma\gamma$ luminosity, shape of the luminosity spectra, energy and mass scale of the detector, reconstructed mass resolution, and in addition the Higgs-boson mass and width from other measurements. In order to take these uncertainties into account we include additional parameters in the fit. Variations of these parameters allow us to account for possible deviations of the invariant-mass distributions, from the nominal model expectation due to the systematic uncertainties.

The total error in the determination of the $H - A$ mixing angle Φ_{HA}, as a function of $\tan\beta$ value, is presented in Fig. 2.37, for four values of heavy Higgs-boson mass M_{h_2}, between 200 and 350 GeV. The simultaneous fit of $\tan\beta$ and Φ_{HA} to the observed W^+W^- and ZZ mass spectra is considered assuming light Higgs-boson mass of 120 GeV, charged Higgs-boson mass of 800 GeV, and no $H - A$ mixing ($\Phi_{HA} = 0$). The error on Φ_{HA} is below ∼100 mrad for $\tan\beta \leq 1$ and increases rapidly for high $\tan\beta$ values.

2.14.4 Two Higgs Doublet Model

In the CP violating 2HDM (II), couplings of the neutral Higgs-bosons to up- and down-type quarks (and leptons), and to vector bosons can be expressed in terms of two mixing angles, α and β, as discussed in Section 2.1.4. In the following we will consider production and decays of the heavy Higgs-boson H. Instead of parameters of the model, angles α and β, we will use its basic relative couplings χ_V^H and χ_u^H, to parametrize cross sections and branching ratios. Moreover, couplings of the other neutral Higgs-bosons h and A are also uniquely defined by χ_V^H and χ_u^H. As in Section 2.14.3 we consider a scenario with a weak CP violation, where the couplings of the lightest mass-eigenstate h_1 correspond to the couplings of h boson, whereas relative couplings of mass-eigenstates h_2 and h_3 can be described as the superposition of H and A couplings (see Eq. 2.193). We study the feasibility of constraining the value of the mixing

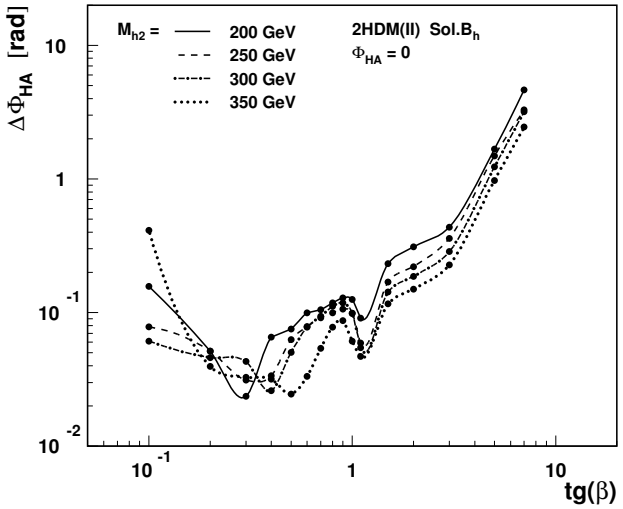

Fig. 2.37: The total error in the determination of the $H - A$ mixing angle Φ_{HA}, as a function of $\tan\beta$ value, for four values of heavy Higgs-boson mass M_{h_2}. The simultaneous fit of $\tan\beta$ and Φ_{HA} to the observed W^+W^- and ZZ mass spectra is considered for the SM-like 2HDM II (sol. B_h), with light Higgs-boson mass of 120 GeV, charged Higgs-boson mass of 800 GeV, and no $H - A$ mixing ($\Phi_{HA} = 0$), Eq. 2.193. Systematic uncertainties related to the luminosity spectra, Higgs boson mass and total width, energy scale and mass resolution are taken into account.

angle Φ_{HA} from the measurements of the heavy Higgs-boson H (i.e. Higgs-boson mass-eigenstate h_2 for $\Phi_{HA} = 0$) production.

The Photon Linear Collider by itself can not uniquely determine the Higgs-boson couplings in case of 2HDM (II) with CP-violation. Therefore, we consider determination of the heavy scalar Higgs-boson properties from the combined analysis of LHC, ILC and Photon Linear Collider data. Fig. 2.38 shows the expected Higgs-boson production rates times the W^+W^-/ZZ branching ratios, at the LHC, ILC and PLC, as a function of χ_V and χ_u. Cross section measurements at these machines are complementary, as they are sensitive to different combinations of the Higgs boson couplings. LHC, ILC and PLC measurements are also complementary in providing an evidence for a weak CP violation, as shown in Fig. 2.39.

An expected h_2 production rates for $h_2 \to W^+W^-/ZZ$ at LHC, ILC and PLC, are shown as a function of χ_u (LHC) or χ_V (ILC and PLC) and the CP-violating $H - A$ mixing angle Φ_{HA}. For $\Phi_{HA} \approx 0$ LHC and ILC measurements weakly depend on the mixing angle Φ_{HA}, as the cross section is dominated by one of the basic couplings, and there is no direct dependence on the coupling phase. At the Photon Linear Collider both couplings as well as their relative phase are important and the cross section is sensitive to the $H - A$ mixing angle (and its sign) even for small Φ_{HA}.

In the simulation of LHC and ILC measurements we use approach similar to the method used for PLC, described in Section 2.14.1. We use results of [316] for the expected invariant mass distribution of the Higgs-boson signal ($pp \to H \to ZZ \to 4l$) and Standard Model background events at LHC, scaled to integrated luminosity of 300 fb^{-1}. For the Higgs-boson production via Higgs-strahlung and WW-fusion at ILC, for $\sqrt{s} = 500$ GeV and the integrated luminosity of 500 fb^{-1}, we use results of [317]. In both cases the signal distributions are obtained from a simple convolution of the Breit-Wigner mass distribution for the Higgs-boson with a detector resolution function. With such an assumption we can scale the SM signal expectations presented in [316, 317] to any scenario of the 2HDM (II).

For each simulated set of the LHC, ILC and PLC data, the Higgs-boson couplings and CP-violating H-A mixing angle were used as the free parameters in the simultaneous fit of the expected distributions

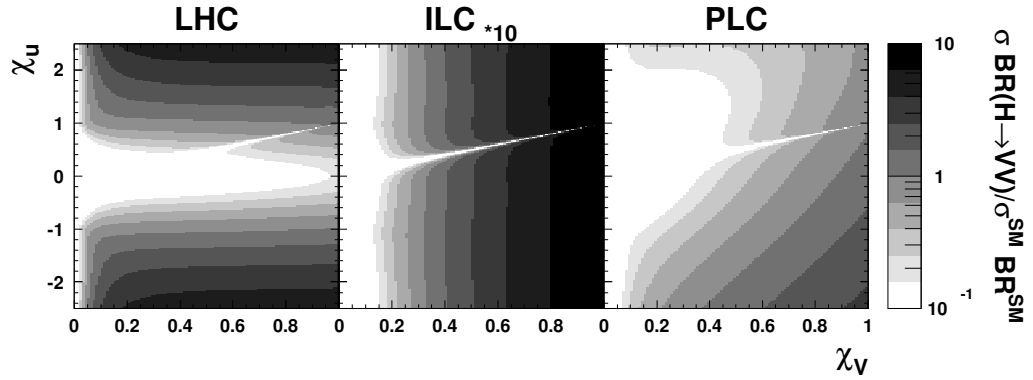

Fig. 2.38: Expected Higgs-boson H production rates times W^+W^-/ZZ branching ratios, relative to SM predictions, as a function of basic relative couplings to vector bosons (χ_V) and up fermions (χ_u). Higgs-boson production at LHC, ILC and PLC is studied for $M_H = 250$ GeV. For ILC the plotted ratio is multiplied by factor 10.

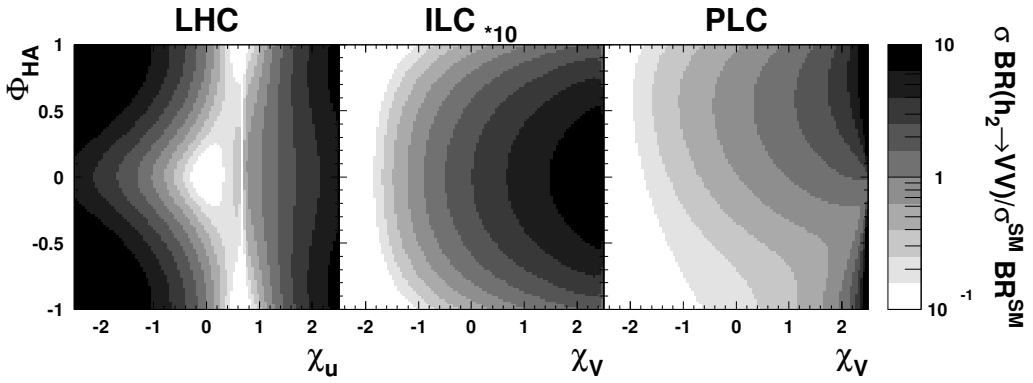

Fig. 2.39: Expected Higgs-boson h_2 production rates times W^+W^-/ZZ branching ratios, relative to SM predictions, as a function of basic relative coupling to vector bosons (χ_V) or up fermions (χ_u), and the $H - A$ mixing angle Φ_{HA}. Higgs-boson production at LHC, ILC and PLC is studied for $M_{h_2} = 250$ GeV. For ILC the plotted ratio is multiplied by factor 10.

to all observed W^+W^- and ZZ mass spectra. To take into account systematic uncertainties additional parameters are added to the fit, as in Section 2.14.3. For LHC we assume 10% systematic uncertainty in the normalization of the background and 20% total systematic uncertainty in the expected signal rate [318]. For ILC the uncertainties in both signal and background normalization are assumed to be 5%. For PLC we take into account 5% uncertainty in the signal and 10% uncertainty in the background normalization, as well as 10% uncertainty in the parameters describing the shape of the luminosity spectra. The Higgs-boson mass is also used as a free parameter in the combined fit, since there will be no other measurements to constrain its value.

In Fig. 2.40 the expected total error on the $H - A$ mixing angle Φ_{HA}, calculated assuming weak CP violation ($\Phi_{HA} \approx 0$), is shown as a function of the couplings χ_V and χ_u, for different heavy Higgs boson masses from 200 to 350 GeV. An average error on Φ_{HA} is about 150 mrad, although in most of the considered parameter space it can be measured with accuracy better than 100 mrad. The corresponding errors on the couplings χ_V and χ_u, averaged over the same parameter range are equal to 0.03 and 0.13, respectively. No significant variations with the Higgs boson mass are observed.

The final step in verifying the coupling structure of the model is the comparison of the direct heavy neutral Higgs boson measurements with constraints on the model parameters resulting from other measurements in the Higgs sector. Assuming no CP violation, constraints on the couplings χ_V^H and

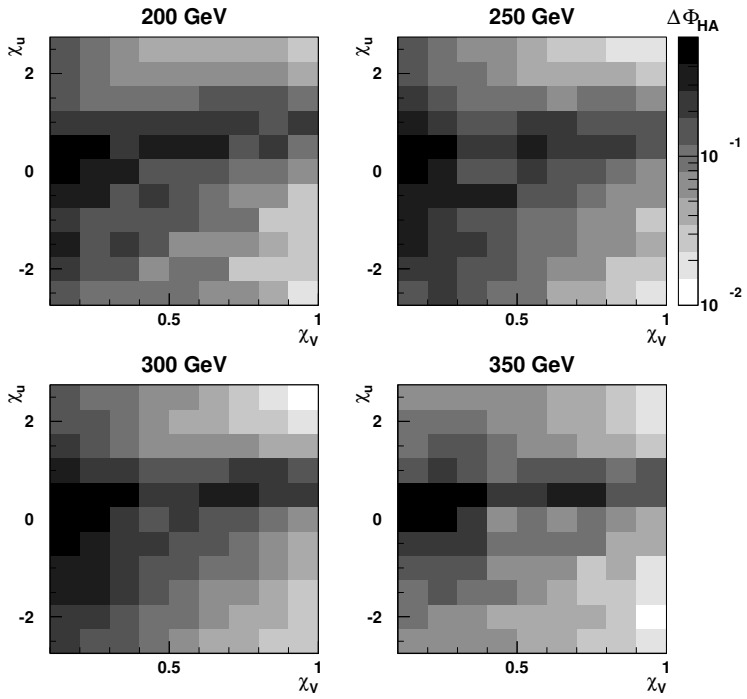

Fig. 2.40: Expected total errors on the $H - A$ mixing angle Φ_{HA}, from combined fit to the invariant mass distributions measured at LHC, ILC and PLC, for $\Phi_{HA} = 0$ and different heavy Higgs boson h_2 masses, as indicated in the plot.

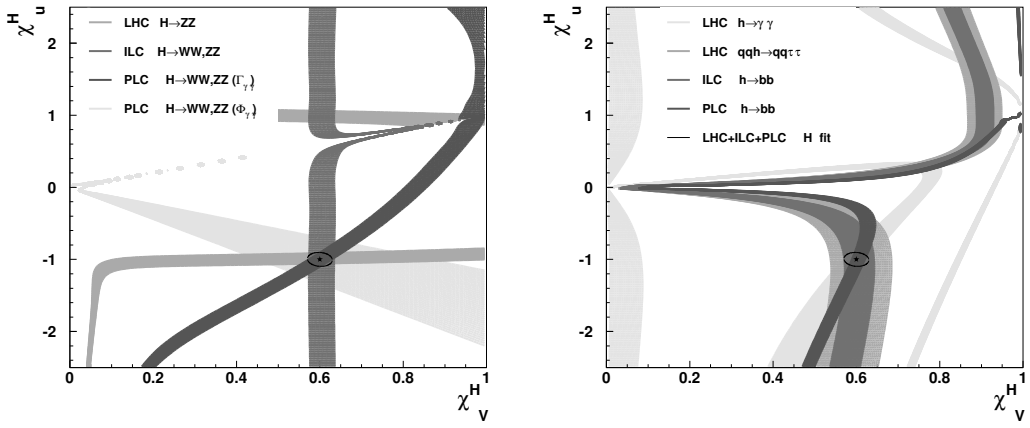

Fig. 2.41: A complementarity of LHC, ILC and PLC measurements in the determination of the 2HDM (II) parameters. Bands show values of the basic heavy Higgs-boson couplings to vector bosons (χ_V^H) and up-type fermions (χ_u^H) consistent (on 1σ statistical error level) with heavy Higgs-boson (left plot) and light Higgs-boson (right plot) measurements at LHC, ILC and PLC, assuming CP conservation. Model with $\chi_V^H = 0.6$, $\chi_u^H = -1$ (star) and H mass of 300 GeV is considered, while the mass of h is set to 120 GeV.

χ_u^H, used to parametrize the model obtained from heavy Higgs-boson (with mass of 250 GeV) and light Higgs-boson (with mass of 120 GeV) measurements at LHC, ILC and PLC, are compared in Fig. 2.41. Measurements of the light Higgs-boson production result in constraints on the H couplings, comparable with the precision of the direct measurements (indicated by the ellipse).

2.14.5 Summary

An opportunity of measuring Higgs-boson CP properties at the Photon Linear Collider has been studied in detail for Higgs boson masses between 200 and 350 GeV, using realistic luminosity spectra and detector simulation. We considered three different models with CP violation. For a generic model with the CP violating Higgs tensor couplings to gauge bosons, the angle describing CP violation can be determined with accuracy of about 50 mrad in a model independent way. In the so called solution B_h of the Standard Model-like 2HDM (II), the $H - A$ mixing angle describing the weak CP violation can be determined to about 100 mrad, for low $\tan\beta$. For the Two Higgs Doublet Model, only the combined analysis of LHC, ILC and PLC measurements allows for the determination of the CP-violating mixing angle Φ_{HA}. In most of the considered parameter space, Φ_{HA} can be measured to better than 100 mrad. Our results demonstrate that the Photon Linear Collider will be an unique place for a precise determination of the CP properties of the neutral Higgs boson.

REFERENCES

[1] T. Lee, Phys. Rev. **D8**, 1226 (1973).

[2] R. Peccei and H. R. Quinn, Phys. Rev. Lett. **38**, 1440 (1977).

[3] P. Fayet, Nucl. Phys. **B78**, 14 (1974).

[4] P. Fayet, Nucl. Phys. **B90**, 104 (1975).

[5] K. Inoue, A. Kakuto, H. Komatsu and S. Takeshita, Prog. Theor. Phys. **67**, 1889 (1982).

[6] R. A. Flores and M. Sher, Ann. Phys. **148**, 95 (1983).

[7] J. F. Gunion and H. E. Haber, Nucl. Phys. **B272**, 1 (1986).

[8] J. F. Gunion, H. E. Haber, G. L. Kane and S. Dawson, *The Higgs Hunter's Guide* (Perseus Publishing, Cambridge, MA, 1990).

[9] M. Carena and H. E. Haber, Prog. Part. Nucl. Phys. **50**, 63 (2003), [hep-ph/0208209].

[10] G. C. Branco, L. Lavoura and J. P. Silva, *CP Violation* (Oxford University Press, Oxford, UK, 1999).

[11] P. Fayet and S. Ferrara, Phys. Rep. **32**, 249 (1977).

[12] H. P. Nilles, Phys. Rep. **110**, 1 (1984).

[13] H. E. Haber and G. L. Kane, Phys. Rep. **117**, 75 (1985).

[14] S. Davidson and H. E. Haber, Phys. Rev. **D72**, 035004 (2005), [hep-ph/0504050].

[15] I. F. Ginzburg and M. Krawczyk, Phys. Rev. **D72**, 115013 (2005), [hep-ph/0408011].

[16] H. E. Haber and D. O'Neil, SCIPP-06/01 (2006), [hep-ph/0602242].

[17] L. Lavoura, Phys. Rev. **D50**, 7089 (1994), [hep-ph/9405307].

[18] S. L. Glashow and S. Weinberg, Phys. Rev. **D15**, 1958 (1977).

[19] I. Ivanov, Phys. Lett. **B632**, 360 (2006), [hep-ph/0507132].

[20] J. Diaz-Cruz and A. Mendez, Nucl. Phys. **B380**, 39 (1992).

[21] J. Velhinho, R. Santos and A. Barroso, Phys. Lett. **B322**, 213 (1994).

[22] P. Ferreira, R. Santos and A. Barroso, Phys. Lett. **B603**, 219 (2004), [hep-ph/0406231].

[23] N. G. Deshpande and E. Ma, Phys. Rev. **D18**, 2574 (1978).

[24] B. M. Kastening, UCLA-92-TEP-22 (1992), [hep-ph/9307224].

[25] S. Nie and M. Sher, Phys. Lett. **B449**, 89 (1999), [hep-ph/9811234].

[26] S. Kanemura, T. Kasai and Y. Okada, Phys. Lett. **B471**, 182 (1999), [hep-ph/9903289].

[27] J. Horejsi, Czech. J. Phys. **47**, 951 (1997), [hep-ph/9603321].

[28] H. A. Weldon, Phys. Rev. **D30**, 1547 (1984).

[29] H. Huffel and G. Pocsik, Z. Phys. **C8**, 13 (1981).

[30] J. Maalampi, J. Sirkka and I. Vilja, Phys. Lett. **B265**, 371 (1991).
[31] S. Kanemura, T. Kubota and E. Takasugi, Phys. Lett. **B313**, 155 (1993), [hep-ph/9303263].
[32] A. G. Akeroyd, A. Arhrib and E.-M. Naimi, Phys. Lett. **B490**, 119 (2000), [hep-ph/0006035].
[33] I. Ginzburg and I. Ivanov, hep-ph/0312374.
[34] I. Ginzburg and I. Ivanov, Phys. Rev. **D72**, 115010 (2005), [hep-ph/0508020].
[35] T. Lee, Phys. Rep. **9**, 143 (1974).
[36] G. C. Branco and M. N. Rebelo, Phys. Lett. **B160**, 117 (1985).
[37] J. F. Gunion and H. E. Haber, Phys. Rev. **D72**, 005002 (2005), [hep-ph/0506227].
[38] F. Botella and J. P. Silva, Phys. Rev. **D51**, 3870 (1995), [hep-ph/9411288].
[39] L. Lavoura and J. P. Silva, Phys. Rev. **D50**, 4619 (1994), [hep-ph/9404276].
[40] G. C. Branco, M. Rebelo and J. Silva-Marcos, Phys. Lett. **B614**, 187 (2005), [hep-ph/0502118].
[41] C. Nishi, hep-ph/0605153.
[42] A. Pilaftsis, Nucl. Phys. **B504**, 61 (1997), [hep-ph/9702393].
[43] S. Choi, J. Kalinowski, Y. Liao and P. Zerwas, Eur. Phys. J. **C40**, 555 (2005), [hep-ph/0407347].
[44] E. Boos, A. Djouadi and A. Nikitenko, Phys. Lett. **B578**, 384 (2004), [hep-ph/0307079].
[45] S. Choi and J. S. Lee, Phys. Rev. **D61**, 015003 (2000), [hep-ph/9907496].
[46] M. Carena, J. R. Ellis, S. Mrenna, A. Pilaftsis and C. E. Wagner, Nucl. Phys. **B659**, 145 (2003), [hep-ph/0211467].
[47] E. Akhmetzyanova, M. Dolgopolov and M. Dubinin, Phys. Rev. **D71**, 075008 (2005), [hep-ph/0405264].
[48] W.-S. Hou, Phys. Lett. **B296**, 179 (1992).
[49] D. Atwood, L. Reina and A. Soni, Phys. Rev. **D55**, 3156 (1997), [hep-ph/9609279].
[50] L. J. Hall and M. B. Wise, Nucl. Phys. **B187**, 397 (1981).
[51] H. E. Haber, G. L. Kane and T. Sterling, Nucl. Phys. **B161**, 493 (1979).
[52] J. F. Donoghue and L. F. Li, Phys. Rev. **D19**, 945 (1979).
[53] H. E. Haber, hep-ph/9501320, in *Physics From the Planck Scale to the Electroweak Scale*, Proceedings of the US–Polish Workshop, Warsaw, Poland, 21–24 September, 1994, edited by P. Nath, T. Taylor, and S. Pokorski (World Scientific, Singapore, 1995), pp. 49–63.
[54] S. Kanemura, T. Kubota and H.-A. Tohyama, Nucl. Phys. **B483**, 111 (1997), [hep-ph/9604381].
[55] P. Ciafaloni and D. Espriu, Phys. Rev. **D56**, 1752 (1997), [hep-ph/9612383].
[56] M. Malinsky, Acta Phys. Slov. **52**, 259 (2002), [hep-ph/0207066].
[57] S. Kanemura and H.-A. Tohyama, Phys. Rev. **D57**, 2949 (1998), [hep-ph/9707454].
[58] J. F. Gunion and H. E. Haber, Phys. Rev. **D67**, 075019 (2003), [hep-ph/0207010].
[59] I. F. Ginzburg, M. Krawczyk and P. Osland, Nucl. Instrum. Meth. **A472**, 149 (2001), [hep-ph/0101229].
[60] M. Krawczyk and D. Temes, Eur. Phys. J. **C44**, 435 (2005), [hep-ph/0410248].
[61] J. F. Gunion, H. E. Haber and J. Wudka, Phys. Rev. **D43**, 904 (1991).
[62] I. F. Ginzburg, M. Krawczyk and P. Osland, hep-ph/0101208.
[63] I. F. Ginzburg, M. Krawczyk and P. Osland, hep-ph/0211371.
[64] J. F. Gunion, B. Grzadkowski, H. E. Haber and J. Kalinowski, Phys. Rev. Lett. **79**, 982 (1997), [hep-ph/9704410].
[65] B. Grzadkowski, J. F. Gunion and J. Kalinowski, Phys. Rev. **D60**, 075011 (1999), [hep-ph/9902308].
[66] A. Djouadi, LPT-ORSAY-05-18 (2005), [hep-ph/0503173].

[67] M. Krawczyk, Acta Phys. Polon. **B35**, 2633 (2004).
[68] V. Telnov, SNOWMASS-2005-PLEN0020 (2005), [physics/0512048].
[69] G. Weiglein *et al.*, Phys. Rep. **246**, 47 (2006), [hep-ph/0410364].
[70] R. M. Godbole *et al.*, CERN-PH-TH-2004-058 (2004), [hep-ph/0404024].
[71] E. Accomando *et al.* [CLIC Physics Working Group], CERN-2004-005 (2004), [hep-ph/0412251].
[72] C. M. Ankenbrandt *et al.*, Phys. Rev. ST Accel. Beams **2**, 081001 (1999), [physics/9901022].
[73] A. Caldwell, J. Phys. **G29**, 1569 (2003).
[74] R. Barate *et al.*, Phys. Lett. **B565**, 61 (2003), [hep-ex/0306033].
[75] J. Abdallah *et al.* (DELPHI Collaboration), Eur. Phys. J. **C44**, 147 (2005), [hep-ex/0510022].
[76] J. Abdallah *et al.* (DELPHI Collaboration), Eur. Phys. J. **C38**, 1 (2004), [hep-ex/0410017].
[77] G. Abbiendi *et al.* (OPAL Collaboration), Eur. Phys. J. **C40**, 317 (2005), [hep-ex/0408097].
[78] G. Pasztor, hep-ex/0605095.
[79] P. Achard *et al.* (L3 Collaboration), Phys. Lett. **B583**, 14 (2004), [hep-ex/0402003].
[80] J. Abdallah *et al.* (DELPHI Collaboration), Eur. Phys. J. **C34**, 399 (2004), [hep-ex/0404012].
[81] ALEPH, DELPHI, L3 and OPAL Collaborations, hep-ex/0107031.
[82] A. Abulencia *et al.* (CDF Collaboration), Phys. Rev. Lett. **96**, 042003 (2006), [hep-ex/0510065].
[83] P. Gambino and M. Misiak, Nucl. Phys. **B611**, 338 (2001), [hep-ph/0104034].
[84] S. Eidelman *et al.,* Eds. (Particle Data Group), *Review of Particle Physics*, Phys. Lett. **B592**, 1 (2004).
[85] Y. Grossman, H. E. Haber and Y. Nir, Phys. Lett. **B357**, 630 (1995), [hep-ph/9507213].
[86] M. Krawczyk, Acta Phys. Polon. **B33**, 2621 (2002), [hep-ph/0208076].
[87] Y.-B. Dai, C.-S. Huang, J.-T. Li and W.-J. Li, Phys. Rev. **D67**, 096007 (2003), [hep-ph/0301082].
[88] Z.-j. Xiao and L.-x. Lu, hep-ph/0605076.
[89] J. P. Idarraga, R. Martinez, J.-A. Rodriguez and N. Poveda, hep-ph/0509072.
[90] P. Chankowski *et al.*, Phys. Lett. **B496**, 195 (2000), [hep-ph/0009271].
[91] K. Cheung and O. C. W. Kong, Phys. Rev. **D68**, 053003 (2003), [hep-ph/0302111].
[92] J. F. Gunion, H. E. Haber and C. Kao, Phys. Rev. **D46**, 2907 (1992).
[93] S. Choi, D. Miller, M. Muhlleitner and P. Zerwas, Phys. Lett. **B553**, 61 (2003), [hep-ph/0210077].
[94] T. Han and J. Jiang, Phys. Rev. **D63**, 096007 (2001), [hep-ph/0011271].
[95] K. Hagiwara, S. Ishihara, J. Kamoshita and B. A. Kniehl, Eur. Phys. J. **C14**, 457 (2000), [hep-ph/0002043].
[96] S. S. Biswal, R. M. Godbole, R. K. Singh and D. Choudhury, Phys. Rev. **D73**, 035001 (2006), [hep-ph/0509070].
[97] K. Hagiwara and M. L. Stong, Z. Phys. **C62**, 99 (1994), [hep-ph/9309248].
[98] T. Plehn, D. L. Rainwater and D. Zeppenfeld, Phys. Rev. Lett. **88**, 051801 (2002), [hep-ph/0105325].
[99] W. Bernreuther, A. Brandenburg and M. Flesch, Phys. Rev. **D56**, 90 (1997), [hep-ph/9701347].
[100] Z. Was and M. Worek, Acta Phys. Polon. **B33**, 1875 (2002), [hep-ph/0202007].
[101] K. Desch, A. Imhof, Z. Was and M. Worek, Phys. Lett. **B579**, 157 (2004), [hep-ph/0307331].
[102] P. Golonka *et al.*, Comput. Phys. Commun. **174**, 818 (2006), [hep-ph/0312240].
[103] W. Bernreuther and A. Brandenburg, Phys. Lett. **B314**, 104 (1993).
[104] V. D. Barger, K. Cheung, T. Han, J. Ohnemus and D. Zeppenfeld, Phys. Rev. **D44**, 1426 (1991).
[105] S. Bar-Shalom, D. Atwood, G. Eilam, R. R. Mendel and A. Soni, Phys. Rev. **D53**, 1162 (1996), [hep-ph/9508314].

[106] J. F. Gunion and J. Pliszka, Phys. Lett. **B444**, 136 (1998), [hep-ph/9809306].

[107] A. Schafer, O. Nachtmann and R. Schopf, Phys. Lett. **B249**, 331 (1990).

[108] A. Bialas and P. V. Landshoff, Phys. Lett. **B256**, 540 (1991).

[109] B. Grzadkowski and J. Gunion, Phys. Lett. **B294**, 361 (1992), [hep-ph/9206262].

[110] J. Alcaraz *et al.* (The LEP collaborations ALEPH, DELPHI, L3, OPAL and The LEP Electroweak Working Group), CERN-PH-EP/2005-051 (2005), [hep-ex/0511027]. For the most recent updates, see: `http://lepewwg.web.cern.ch/LEPEWWG/`.

[111] M. Carena, J. R. Ellis, A. Pilaftsis and C. E. Wagner, Phys. Lett. **B495**, 155 (2000), [hep-ph/0009212].

[112] G. Abbiendi *et al.* (OPAL Collaboration), Eur. Phys. J. **C37**, 49 (2004), [hep-ex/0406057].

[113] S. Kanemura, S. Kiyoura, Y. Okada, E. Senaha and C. Yuan, Phys. Lett. **B558**, 157 (2003), [hep-ph/0211308].

[114] CMS Collaboration, CMS: The electromagnetic calorimeter. Technical Design Report, CERN-LHCC-97-33.

[115] ATLAS Collaboration, ATLAS detector and physics performance. Technical design report, Volume 2, CERN-LHCC-99-15.

[116] J. R. Ellis, J. S. Lee and A. Pilaftsis, Phys. Rev. **D72**, 095006 (2005), [hep-ph/0507046].

[117] J. R. Ellis, J. S. Lee and A. Pilaftsis, Nucl. Phys. **B718**, 247 (2005), [hep-ph/0411379].

[118] W. Khater and P. Osland, Nucl. Phys. **B661**, 209 (2003), [hep-ph/0302004].

[119] C. Buszello, I. Fleck, P. Marquard and J. J. van der Bij, Eur. Phys. J. **C32**, 209 (2004), [hep-ph/0212396].

[120] K. Odagiri, JHEP **03**, 009 (2003), [hep-ph/0212215].

[121] J. F. Gunion and X.-G. He, Phys. Rev. Lett. **76**, 4468 (1996), [hep-ph/9602226].

[122] B. Field, Phys. Rev. **D66**, 114007 (2002), [hep-ph/0208262].

[123] D. K. Ghosh and S. Moretti, Eur. Phys. J. **C42**, 341 (2005), [hep-ph/0412365].

[124] D. K. Ghosh, R. Godbole and D. Roy, Phys. Lett. **B628**, 131 (2005), [hep-ph/0412193].

[125] E. Asakawa, O. Brein and S. Kanemura, Phys. Rev. **D72**, 055017 (2005), [hep-ph/0506249].

[126] K. Y. Lee, D.-W. Jung and H. Song, Phys. Rev. **D70**, 117701 (2004), [hep-ph/0307246].

[127] E. Christova, H. Eberl, W. Majerotto and S. Kraml, Nucl. Phys. **B639**, 263 (2002), [hep-ph/0205227].

[128] E. Christova, H. Eberl, W. Majerotto and S. Kraml, JHEP **12**, 021 (2002), [hep-ph/0211063].

[129] J. L. Diaz-Cruz and J. J. Toscano, Phys. Rev. **D62**, 116005 (2000), [hep-ph/9910233].

[130] G. Bennett *et al.* (Muon $g2$ Collaboration), Phys. Rev. Lett. **92**, 161802 (2004), [hep-ex/0401008].

[131] K. A. Assamagan, A. Deandrea and P.-A. Delsart, Phys. Rev. **D67**, 035001 (2003), [hep-ph/0207302].

[132] J. F. Gunion *et al.*, Phys. Rev. **D38**, 3444 (1988).

[133] S. Heinemeyer *et al.*, SNOWMASS-2005-PLEN0044 (2005), [hep-ph/0511332].

[134] V. D. Barger, K.-m. Cheung, A. Djouadi, B. A. Kniehl and P. M. Zerwas, Phys. Rev. **D49**, 79 (1994), [hep-ph/9306270].

[135] A. Djouadi and B. A. Kniehl, Proc. of Workshop on e^+e^- Collisions at 500 GeV: The Physics Potential, Hamburg, 1993, P.M. Zerwas (Ed.), DESY-93-123C.

[136] D. J. Miller, S. Y. Choi, B. Eberle, M. M. Muhlleitner and P. M. Zerwas, Phys. Lett. **B505**, 149 (2001), [hep-ph/0102023].

[137] M. T. Dova and S. Ferrari, Phys. Lett. **B605**, 376 (2005), [hep-ph/0406313].

[138] B. Grzadkowski, J. Gunion and J. Kalinowski, Phys. Lett. **B480**, 287 (2000), [hep-ph/0001093].

[139] V. Braguta, A. Chalov, A. Likhoded and R. Rosenfeld, Phys. Rev. Lett. **90**, 241801 (2003), [hep-ph/0208133].

[140] J. F. Gunion, B. Grzadkowski and X.-G. He, Phys. Rev. Lett. **77**, 5172 (1996), [hep-ph/9605326].

[141] H.-J. He, S. Kanemura and C. Yuan, Phys. Rev. Lett. **89**, 101803 (2002), [hep-ph/0203090].

[142] A. Djouadi, W. Kilian, M. Muhlleitner and P. M. Zerwas, Eur. Phys. J. **C10**, 27 (1999), [hep-ph/9903229].

[143] R. Belusevic and G. Jikia, Phys. Rev. **D70**, 073017 (2004), [hep-ph/0403303].

[144] P. Niezurawski, A. Zarnecki and M. Krawczyk, JHEP **0502**, 041 (2005), [hep-ph/0403138].

[145] E. Asakawa and K. Hagiwara, Eur. Phys. J. **C31**, 351 (2003), [hep-ph/0305323].

[146] S. Choi, K. Hagiwara and M. Baek, Phys. Rev. **D54**, 6703 (1996), [hep-ph/9605334].

[147] P. Niezurawski, A. Zarnecki and M. Krawczyk, Acta Phys. Polon. **B36**, 833 (2005), [hep-ph/0410291].

[148] G. J. Gounaris, P. Porfyriadis and F. Renard, Eur. Phys. J. **C19**, 57 (2001), [hep-ph/0010006].

[149] H. Anlauf, W. Bernreuther and A. Brandenburg, Phys. Rev. **D52**, 3803 (1995), [hep-ph/9504424].

[150] E. Asakawa, S. Choi, K. Hagiwara and J. S. Lee, Phys. Rev. **D62**, 115005 (2000), [hep-ph/0005313].

[151] R. M. Godbole, S. D. Rindani and R. K. Singh, Phys. Rev. **D67**, 095009 (2003), [hep-ph/0211136].

[152] S. Choi *et al.*, Phys. Lett. **B606**, 164 (2005), [hep-ph/0404119].

[153] M. Battaglia and A. De Roeck, hep-ph/0211207, in *Physics and experiments with future electron–positron linear colliders*, Proceedings of the International Workshop on Linear Colliders (LCWS 2002), edited by J.S. Kang, S.K. Oh, Jeju Island, Korea, 26–30 August 2002, (Korean Physical Society, 2003), pp. 98–104.

[154] A. Ferrari, LC-PHSM-2004-008 (2004).

[155] V. D. Barger, M. Berger, J. Gunion and T. Han, Phys. Rev. Lett. **75**, 1462 (1995), [hep-ph/9504330].

[156] V. D. Barger, M. Berger, J. Gunion and T. Han, Phys. Rep. **286**, 1 (1997), [hep-ph/9602415].

[157] S. Choi and J. S. Lee, Phys. Rev. **D61**, 111702 (2000), [hep-ph/9909315].

[158] E. Asakawa, S. Y. Choi and J. S. Lee, Phys. Rev. **D63**, 015012 (2001), [hep-ph/0005118].

[159] B. Grzadkowski, J. F. Gunion and J. Pliszka, Nucl. Phys. **B583**, 49 (2000), [hep-ph/0003091].

[160] A. Akeroyd and S. Baek, Phys. Lett. **B500**, 142 (2001), [hep-ph/0008286].

[161] M. Dubinin and A. V. Semenov, Eur. Phys. J. **C28**, 223 (2003), [hep-ph/0206205].

[162] I. F. Ginzburg, Acta Phys. Polon. **B37** (2006), [hep-ph/0512102].

[163] C. Froggatt, R. Moorhouse and I. Knowles, Nucl. Phys. **B386**, 63 (1992).

[164] F. J. Botella, M. Nebot and O. Vives, JHEP **01**, 106 (2006), [hep-ph/0407349].

[165] E. Paschos, Phys. Rev. **D15**, 1966 (1977).

[166] G. 't Hooft, Lecture given at Cargese Summer Inst., Cargese, France, 26 August–8 September, 1979.

[167] J. F. Gunion, H. E. Haber, G. L. Kane and S. Dawson, hep-ph/9302272.

[168] T. P. Cheng and M. Sher, Phys. Rev. **D35**, 3484 (1987).

[169] H. Fritzsch and Z.-z. Xing, Phys. Lett. **B555**, 63 (2003), [hep-ph/0212195].

[170] Z.-z. Xing and H. Zhang, J. Phys. **G30**, 129 (2004), [hep-ph/0309112].

[171] J. L. Diaz-Cruz, R. Noriega-Papaqui and A. Rosado, Phys. Rev. **D69**, 095002 (2004), [hep-ph/0401194].

[172] K. Abe *et al.* (Belle Collaboration), Phys. Rev. Lett. **92**, 171802 (2004), [hep-ex/0310029].

[173] D. Chang, W. S. Hou and W. Y. Keung, Phys. Rev. **D48**, 217 (1993), [hep-ph/9302267].

[174] Particle Data Group, K. Hagiwara *et al.*, Phys. Rev. **D66**, 010001 (2002).
[175] B. Aubert *et al.* (BaBar Collaboration), Phys. Rev. Lett. **92**, 121801 (2004), [hep-ex/0312027].
[176] Y. Yusa *et al.* (Belle Collaboration), Phys. Lett. **B589**, 103 (2004), [hep-ex/0403039].
[177] R. Kitano, M. Koike, S. Komine and Y. Okada, Phys. Lett. **B575**, 300 (2003), [hep-ph/0308021].
[178] T. Suzuki, D. F. Measday and J. P. Roalsvig, Phys. Rev. **C35**, 2212 (1987).
[179] W. Molzon, Nucl. Phys. Proc. Suppl. **111**, 188 (2002).
[180] K. S. Babu and C. F. Kolda, Phys. Rev. Lett. **84**, 228 (2000), [hep-ph/9909476].
[181] F. Abe *et al.* (CDF Collaboration), Phys. Rev. **D57**, 3811 (1998).
[182] J. L. Diaz-Cruz and M. A. Perez, Phys. Rev. **D33**, 273 (1986).
[183] E. Barradas, J. L. Diaz-Cruz, A. Gutierrez and A. Rosado, Phys. Rev. **D53**, 1678 (1996).
[184] E. Arganda, A. M. Curiel, M. J. Herrero and D. Temes, Phys. Rev. **D71**, 035011 (2005), [hep-ph/0407302].
[185] A. Brignole and A. Rossi, Phys. Lett. **B566**, 217 (2003), [hep-ph/0304081].
[186] H. V. Peiris *et al.*, Astrophys. J. Suppl. **148**, 213 (2003), [astro-ph/0302225].
[187] A. D. Sakharov, Pisma Zh. Eksp. Teor. Fiz. **5**, 32 (1967).
[188] A. G. Cohen, D. B. Kaplan and A. E. Nelson, Annu. Rev. Nucl. Part. Sci. **43**, 27 (1993), [hep-ph/9302210].
[189] M. Quiros, Helv. Phys. Acta **67**, 451 (1994).
[190] V. A. Rubakov and M. E. Shaposhnikov, Usp. Fiz. Nauk **166**, 493 (1996), [hep-ph/9603208].
[191] K. Funakubo, Prog. Theor. Phys. **96**, 475 (1996), [hep-ph/9608358].
[192] M. Trodden, Rev. Mod. Phys. **71**, 1463 (1999), [hep-ph/9803479].
[193] W. Bernreuther, Lecture Notes Phys. **591**, 237 (2002), [hep-ph/0205279].
[194] N. Turok and J. Zadrozny, Phys. Rev. Lett. **65**, 2331 (1990).
[195] N. Turok and J. Zadrozny, Nucl. Phys. **B358**, 471 (1991).
[196] A. I. Bochkarev, S. V. Kuzmin and M. E. Shaposhnikov, Phys. Rev. **D43**, 369 (1991).
[197] A. E. Nelson, D. B. Kaplan and A. G. Cohen, Nucl. Phys. **B373**, 453 (1992).
[198] P. Huet and A. E. Nelson, Phys. Lett. **B355**, 229 (1995), [hep-ph/9504427].
[199] A. I. Bochkarev, S. V. Kuzmin and M. E. Shaposhnikov, Phys. Lett. **B244**, 275 (1990).
[200] N. Turok and J. Zadrozny, Nucl. Phys. **B369**, 729 (1992).
[201] J. M. Cline, K. Kainulainen and A. P. Vischer, Phys. Rev. **D54**, 2451 (1996), [hep-ph/9506284].
[202] K. Funakubo, A. Kakuto, S. Otsuki, K. Takenaga and F. Toyoda, Prog. Theor. Phys. **94**, 845 (1995), [hep-ph/9507452].
[203] K. Funakubo, A. Kakuto, S. Otsuki and F. Toyoda, Prog. Theor. Phys. **96**, 771 (1996), [hep-ph/9606282].
[204] M. Carena, M. Quiros and C. E. M. Wagner, Phys. Lett. **B380**, 81 (1996), [hep-ph/9603420].
[205] D. Delepine, J. M. Gerard, R. Gonzalez Felipe and J. Weyers, Phys. Lett. **B386**, 183 (1996), [hep-ph/9604440].
[206] J. R. Espinosa, Nucl. Phys. **B475**, 273 (1996), [hep-ph/9604320].
[207] P. Huet and A. E. Nelson, Phys. Rev. **D53**, 4578 (1996), [hep-ph/9506477].
[208] D. Bodeker, P. John, M. Laine and M. G. Schmidt, Nucl. Phys. **B497**, 387 (1997), [hep-ph/9612364].
[209] B. de Carlos and J. R. Espinosa, Nucl. Phys. **B503**, 24 (1997), [hep-ph/9703212].
[210] A. Riotto, Nucl. Phys. **B518**, 339 (1998), [hep-ph/9712221].
[211] A. Riotto, Phys. Rev. **D58**, 095009 (1998), [hep-ph/9803357].

[212] M. Carena, M. Quiros and C. E. M. Wagner, Nucl. Phys. **B524**, 3 (1998), [hep-ph/9710401].

[213] J. M. Moreno, M. Quiros and M. Seco, Nucl. Phys. **B526**, 489 (1998), [hep-ph/9801272].

[214] J. M. Cline and G. D. Moore, Phys. Rev. Lett. **81**, 3315 (1998), [hep-ph/9806354].

[215] J. M. Cline, M. Joyce and K. Kainulainen, JHEP **07**, 018 (2000), [hep-ph/0006119].

[216] M. Carena, J. M. Moreno, M. Quiros, M. Seco and C. E. M. Wagner, Nucl. Phys. **B599**, 158 (2001), [hep-ph/0011055].

[217] M. Carena, M. Quiros, M. Seco and C. E. M. Wagner, Nucl. Phys. **B650**, 24 (2003), [hep-ph/0208043].

[218] K. Funakubo, S. Tao and F. Toyoda, Prog. Theor. Phys. **109**, 415 (2003), [hep-ph/0211238].

[219] H. Murayama and A. Pierce, Phys. Rev. **D67**, 071702 (2003), [hep-ph/0201261].

[220] C. Lee, V. Cirigliano and M. J. Ramsey-Musolf, Phys. Rev. **D71**, 075010 (2005), [hep-ph/0412354].

[221] V. Cirigliano, C. Lee, M. J. Ramsey-Musolf and S. Tulin, hep-ph/0603058.

[222] S. Kanemura, Y. Okada and E. Senaha, Phys. Lett. **B606**, 361 (2005), [hep-ph/0411354].

[223] C. Grojean, G. Servant and J. D. Wells, Phys. Rev. **D71**, 036001 (2005), [hep-ph/0407019].

[224] S. W. Ham and S. K. Oh, hep-ph/0502116.

[225] L. Dolan and R. Jackiw, Phys. Rev. **D9**, 3320 (1974).

[226] G. W. Anderson and L. J. Hall, Phys. Rev. **D45**, 2685 (1992).

[227] M. Dine, R. G. Leigh, P. Y. Huet, A. D. Linde and D. A. Linde, Phys. Rev. **D46**, 550 (1992), [hep-ph/9203203].

[228] G. D. Moore, Phys. Lett. **B439**, 357 (1998), [hep-ph/9801204].

[229] G. D. Moore, Phys. Rev. **D59**, 014503 (1999), [hep-ph/9805264].

[230] S. Kanemura, Y. Okada, E. Senaha and C.-P. Yuan, Phys. Rev. **D70**, 115002 (2004), [hep-ph/0408364].

[231] J. Horejsi and M. Kladiva, hep-ph/0510154.

[232] Particle Data Group, S. Eidelman *et al.*, Phys. Lett. **B592**, 1 (2004).

[233] P. Fendley, Phys. Lett. **B196**, 175 (1987).

[234] M. E. Carrington, Phys. Rev. **D45**, 2933 (1992).

[235] R. R. Parwani, Phys. Rev. **D45**, 4695 (1992), [hep-ph/9204216].

[236] P. Arnold, Phys. Rev. **D46**, 2628 (1992), [hep-ph/9204228].

[237] P. Arnold and O. Espinosa, Phys. Rev. **D47**, 3546 (1993), [hep-ph/9212235].

[238] J. R. Espinosa, M. Quiros and F. Zwirner, Phys. Lett. **B291**, 115 (1992), [hep-ph/9206227].

[239] U. Baur, T. Plehn and D. L. Rainwater, Phys. Rev. **D69**, 053004 (2004), [hep-ph/0310056].

[240] M. Battaglia, E. Boos and W.-M. Yao, Proc. Snowmass 2001, Snowmass Village, CO, 2001, eConf **C010630**, E3016 (2001), [hep-ph/0111276].

[241] Y. Yasui *et al.*, hep-ph/0211047.

[242] W. Bernreuther, T. Schroder and T. N. Pham, Phys. Lett. **B279**, 389 (1992).

[243] W. Bernreuther and A. Brandenburg, Phys. Rev. **D49**, 4481 (1994), [hep-ph/9312210].

[244] W. Bernreuther, M. Flesch and P. Haberl, Phys. Rev. **D58**, 114031 (1998), [hep-ph/9709284].

[245] W. Bernreuther, A. Brandenburg and M. Flesch, hep-ph/9812387.

[246] J. R. Dell'Aquila and C. A. Nelson, Nucl. Phys. **B320**, 86 (1989).

[247] D. Chang, W.-Y. Keung and I. Phillips, Phys. Rev. **D48**, 3225 (1993), [hep-ph/9303226].

[248] M. Kramer, J. H. Kuhn, M. L. Stong and P. M. Zerwas, Z. Phys. **C64**, 21 (1994), [hep-ph/9404280].

[249] B. Grzadkowski and J. F. Gunion, Phys. Lett. **B350**, 218 (1995), [hep-ph/9501339].
[250] D. Atwood, S. Bar-Shalom, G. Eilam and A. Soni, Phys. Rep. **347**, 1 (2001), [hep-ph/0006032].
[251] L. Sonnenschein, Ph.D. thesis, RWTH Aachen, PITHA 01/04 (2001).
[252] A. Stahl, Springer Tracts Mod. Phys. **160**, 1 (2000).
[253] G. Mahlon and S. J. Parke, Phys. Rev. **D53**, 4886 (1996), [hep-ph/9512264].
[254] A. Czarnecki, M. Jezabek and J. H. Kuhn, Nucl. Phys. **B351**, 70 (1991).
[255] A. Brandenburg, Z. G. Si and P. Uwer, Phys. Lett. **B539**, 235 (2002), [hep-ph/0205023].
[256] W. Bernreuther, O. Nachtmann, P. Overmann and T. Schroder, Nucl. Phys. **B388**, 53 (1992).
[257] B. Grzadkowski and J. F. Gunion, Phys. Lett. **B287**, 237 (1992).
[258] S. Abdullin *et al.*, Eur. Phys. J. **C39S2**, 41 (2005).
[259] D. Dicus, A. Stange and S. Willenbrock, Phys. Lett. **B333**, 126 (1994), [hep-ph/9404359].
[260] S. R. Slabospitsky and L. Sonnenschein, Comput. Phys. Commun. **148**, 87 (2002), [hep-ph/0201292].
[261] W. Bernreuther, A. Brandenburg, Z. G. Si and P. Uwer, Nucl. Phys. **B690**, 81 (2004), [hep-ph/0403035].
[262] H.-Y. Zhou, Phys. Rev. **D58**, 114002 (1998), [hep-ph/9805358].
[263] C. R. Schmidt and M. E. Peskin, Phys. Rev. Lett. **69**, 410 (1992).
[264] J. Liu and L. Wolfenstein, Nucl. Phys. **B289**, 1 (1987).
[265] S. Weinberg, Phys. Rev. **D42**, 860 (1990).
[266] Y. L. Wu and L. Wolfenstein, Phys. Rev. Lett. **73**, 1762 (1994), [hep-ph/9409421].
[267] D. Atwood, A. Aeppli and A. Soni, Phys. Rev. Lett. **69**, 2754 (1992).
[268] W. Khater, *Top Quark Pair Production and CP-Violating Higgs Sector*, Ph.D. thesis, University of Bergen (2003).
[269] ATLAS, W. W. Armstrong *et al.*, CERN-LHCC-94-43.
[270] CMS, M. Della Negra *et al.*, CERN-LHCC-92-3.
[271] A. W. E. Kaffas, W. Khater, O. M. Ogreid and P. Osland, hep-ph/0605142.
[272] J. F. Gunion and X.-G. He, Phys. Rev. Lett. **76**, 4468 (1996), [hep-ph/9602226].
[273] The CMS Collaboration, CERN/LHCC 06-001, 4 (2006).
[274] J. S. Lee *et al.*, Comput. Phys. Commun. **156**, 283 (2004), [hep-ph/0307377].
[275] M. Frank, S. Heinemeyer, W. Hollik and G. Weiglein, hep-ph/0212037.
[276] D. L. Rainwater and D. Zeppenfeld, Phys. Rev. **D60**, 113004 (1999), [hep-ph/9906218].
[277] V. Del Duca, W. Kilgore, C. Oleari, C. Schmidt and D. Zeppenfeld, Nucl. Phys. **B616**, 367 (2001), [hep-ph/0108030].
[278] T. Figy and D. Zeppenfeld, Phys. Lett. **B591**, 297 (2004), [hep-ph/0403297].
[279] G. Passarino and M. J. G. Veltman, Nucl. Phys. **B160**, 151 (1979).
[280] N. Kauer, Phys. Rev. **D67**, 054013 (2003), [hep-ph/0212091].
[281] V. D. Barger, T. Han, J. Ohnemus and D. Zeppenfeld, Phys. Rev. **D41**, 2782 (1990).
[282] B. Jager, C. Oleari and D. Zeppenfeld, hep-ph/0603177.
[283] N. Kauer, T. Plehn, D. L. Rainwater and D. Zeppenfeld, Phys. Lett. **B503**, 113 (2001), [hep-ph/0012351].
[284] C. Weiser, CERN-CMS-NOTE-2006-014 (2006).
[285] M. Hohlfeld, ATL-PHYS-2001-004 (2001).
[286] B. Zhang, Y.-P. Kuang, H.-J. He and C. P. Yuan, Phys. Rev. **D67**, 114024 (2003), [hep-ph/0303048].

[287] C. P. Buszello and P. Marquard, hep-ph/0603209.

[288] A. Skjold and P. Osland, Phys. Lett. **B329**, 305 (1994), [hep-ph/9402358].

[289] V. Hankele, G. Klamke and D. Zeppenfeld, hep-ph/0605117.

[290] K. Hagiwara, R. D. Peccei, D. Zeppenfeld and K. Hikasa, Nucl. Phys. **B282**, 253 (1987).

[291] E. Richter-Was, D. Froidevaux and L. Poggioli, ATLFAST 2.0, a fast simulation package for ATLAS, ATL-PHYS-98-131 (1998).

[292] C. P. Buszello, P. Marquard and J. J. van der Bij, hep-ph/0406181.

[293] T. Sjostrand, L. Lonnblad, S. Mrenna and P. Skands, hep-ph/0308153.

[294] J. R. Dell'Aquila and C. A. Nelson, Phys. Rev. **D33**, 101 (1986).

[295] T. Sjostrand *et al.*, Comput. Phys. Commun. **135**, 238 (2001), [hep-ph/0010017].

[296] M. Spira, Fortschr. Phys. **46**, 203 (1998), [hep-ph/9705337].

[297] A. Djouadi, J. Kalinowski and M. Spira, Comput. Phys. Commun. **108**, 56 (1998), [hep-ph/9704448].

[298] J. M. Campbell and R. K. Ellis, Phys. Rev. **D60**, 113006 (1999), [hep-ph/9905386].

[299] M. Beneke *et al.*, hep-ph/0003033.

[300] R. K. Ellis and S. Veseli, Phys. Rev. **D60**, 011501 (1999), [hep-ph/9810489].

[301] J. M. Campbell and R. K. Ellis, Phys. Rev. **D62**, 114012 (2000), [hep-ph/0006304].

[302] J. Campbell, R. K. Ellis and D. L. Rainwater, Phys. Rev. **D68**, 094021 (2003), [hep-ph/0308195].

[303] CMS Collaboration, CMS Physics TDR Volume 2, Physics Performance, CERN/LHCC 2006-021

[304] P. Niezurawski, A. F. Zarnecki and M. Krawczyk, JHEP **11**, 034 (2002), [hep-ph/0207294].

[305] P. Niezurawski, A. Zarnecki and M. Krawczyk, LC-PHSM-2004-035.

[306] P. Niezurawski, A. F. Zarnecki and M. Krawczyk, in preparation.

[307] D. J. Miller, Spin and parity in the HZZ vertex, presented at the ECFA/DESY meeting, Prague, November 2002.

[308] A. F. Zarnecki, Acta Phys. Polon. **B34**, 2741 (2003), [hep-ex/0207021].

[309] V. I. Telnov, Nucl. Instrum. Methods **A355**, 3 (1995).

[310] V. I. Telnov, A code for the simulation of luminosities and QED backgrounds at photon colliders, Second Workshop of ECFA-DESY study, Saint Malo, France, April 2002.

[311] I. Ginzburg and I. Ivanov, Phys. Lett. **B408**, 325 (1997), [hep-ph/9704220].

[312] G. J. Gounaris, J. Layssac, P. I. Porfyriadis and F. M. Renard, Eur. Phys. J. **C13**, 79 (2000), [hep-ph/9909243].

[313] G. Belanger and F. Boudjema, Phys. Lett. **B288**, 210 (1992).

[314] D. A. Morris, T. N. Truong and D. Zappala, Phys. Lett. **B323**, 421 (1994), [hep-ph/9310244].

[315] M. Pohl and H. J. Schreiber, DESY-99-030.

[316] M. Sani, Czech. J. Phys. **55**, B101 (2005).

[317] N. Meyer and K. Desch, Eur. Phys. J. **C35**, 171 (2004).

[318] M. Duhrssen *et al.*, Phys. Rev. **D70**, 113009 (2004), [hep-ph/0406323].